The SWH signalling as a key regulator for the maintenance of NSC quiescence in *Drosophila melanogaster*

A dissertation submitted to the faculty of biology at the Johannes Gutenberg University Mainz in partial fulfilment of the requirements for the degree of

Doctor rerum naturalium (Dr. rer. nat.)

Submitted by:
Rouven Marian Metternich
Born 10.01.1987 in Wolfsburg

Mainz, 21.02.2017

INDEX OF FIGURES

INDEX OF TABLES

ABBREVIATIONS

CNS	Central nervous system
VNC	Ventral nerve cord
NSC	Neural stem cell
MBNB	Mushroom body neuroblast
lNSC	lateral NSC
wt	Wildtype
Ctrl	Control
vNR	Ventral neurogenic region
pNR	Procephalic neurogenic region
AP axis	Anterior-posterior axis
ALH	After larval hatching
SLIF	Slimfast (amino-acid transporter)
TOR	Target of rapamycin
FDS	Fatbody derived mitogen
dILP	*Drosophila* Insulin-like peptide
GMC	Ganglion mother cell
INP	Intermediate neural progenitor
LZ-domain	Leuzine Zipper domain
bHLH-domain	Basic Helix-Loop-Helix domain
RNA	Ribonucleic acid
rRNA	Ribomosal ribonucleic acid
DNA	Deoxyribonucleic acid
cDNA	Complementary DNA
mRNA	Messenger ribonucleic acid
IRES	Internal ribosomal entry site
HSC	Haematopoietic stem cells
MuSC	Muscle stem cells
HFSC	Hair follicle stem cell
GSC	Germ line stem cell
miRNA	Micro ribonucleic acid
RNAi	Ribonucleic acid interference
Dpn	Deadpan

pH3	Phosphohistone H3
pros	Prospero
TGF-ß	Transforming growth factor beta
babo	Baboon
Stat92E	Signal-transducer and activator of transcription protein at 92E
SWH	Salvador/Warts/Hippo signalling pathway
Yki	Yorkie
YAP	Yes-associated protein
TAZ	Transcriptional co-activator with PDZ binding motif
Hpo	Hippo
Wts	Warts
Mst 1/2	Macrophage stimulating 1/2
Lats 1/2	Large tumor suppressor kinase 1/2
Sav	Salvador
Mats	Mob as tumor suppressor
Sd	Scalloped
Hth	Homothorax
Crb	Crumbs
Ed	Echinoid
Ft	Fat
Ds	Dachsous
Ex	Expanded
Kb	Kibra
ban	Bantam
CycE	CyclinE
Mer	Merlin
Tsh	Teashort
D	Dachs
Fj	Four-jointed
Tj	Tight junction
Aj	Adherens junction
FERM-domain	4.1, Ezrin, Radxin, Moesin-domain
3’UTR	3’Untranslated region
PCP	Planar cell polarity

Zyx	Zyxin
FBM	FERM-domain binding motif
LKB1	Liver kinase B1
AMPK	AMP-activated kinase
AMP	Adenosine monophosphate
TEF	Transcriptional enhancer factor
TALE-domain	Transcription activator-like effector
DIAP	*Drosophila* inhibitor of apoptosis protein
HID	Head involution defective
Rpr	Reaper
Ncoa6	Nuclear receptor coactivator 6
Trr	Trithorax related
H3K4	Histone H3 lysine 4
NuRD	Nucleosome remodelling and histone deacetylase
β-Gal	β-Galactosidase
Tgi	Tondu-domain containing growth inhibitor
min	Minutes
g	gram
ng	nanogram
nm	nanometer
L	Liter
ml	Milliliter
h	hour
CO_2	Carbon dioxide
UAS	Upstream activating sequence
CD	Cluster of differentiation
GFP	Green fluorescent protein
PBS	Sodium phosphate buffer
PBL	Phosphate buffer / Lysin
PFA	Paraformaldehyde
PBT	Phosphate buffer / Triton
µl	microliter
dNTP	deoxynucleoside triphosphates
$MgCl_2$	Magnesium chloride

PCR	Polymerase chain reaction
UV-light	Ultraviolet-light
V	Volt
RT	Reverse transcription
FBS	Fetal bovine serum
FACS	Fluorescence activated cell sorting
Pen/Strep	Penicillin / Streptomycin
HEK	Human embryonic kidney cells
IIS	Insulin/Insulin-like growth factor signalling
pAkt	phosphorylated Akt
PKB	Protein kinase B
repo	Reversed polarity
E-cad	E-cadherin
dm	*Drosophila* dimunitive
BMP4	Bone morphogenic protein 4
ErbB-4	Erythroblastic leukemia viral (v-erb-b2) oncogene homolog 4
p73	Tumor protein 73
SMAD	Mothers against decapentaplegic homolog
TBX5	T-box protein 5
Sox9	Sry-related HMG box 9
Upd	Unpaired
JAK-STAT	Janus kinase signal transducer and activator of transcription
MAPK	Mitogen-activated protein kinase
GABA	Gamma-aminobutyric acid

1. Introduction

The central nervous system (CNS) is the most complex organ in the body of every animal. All nervous systems, vertebrate and invertebrate, provide a highly complex system of communication through a network of electrically excitable cells, so called neurons. These cells can appear in a plethora of different shapes and sizes. A key developmental process during the formation of the central nervous system (neurogenesis) is the generation and specification of this variety of neurons and glial cells from neural stem cells (NSCs). The fruit fly *Drosophila melanogaster* is a popular model organism in biology and has been studied for over a century for genetic investigations. All cells, which form the adult CNS of *Drosophila melanogaster* derive from a well-defined set of NSCs. These pluripotent stem cells exhibit two distinct waves of proliferation, one during embryonic and one during larval stages. Between these proliferative episodes the cells pass a resting phase (quiescence). During my thesis work, I attempted to unravel factors or signalling pathways, which are involved in the regulation and maintenance of neural stem cell quiescence.

1.1 Neurogenesis

The presumptive nervous system of the fruit fly *Drosophila melanogaster*, called neuroectoderm, is specified at an early stage during embryonic development. This region consists of ectodermal cells, which have the potential to generate either neural cells or epidermal cells, and is separated into the ventral neurogenic region (vNR), which will form the ventral nerve cord and the procephalic neurogenic region (pNR), which give rise to the central brain (Berger *et al*., 2001; Urbach and Technau 2003). The whole neurogenic region is further subdivided into a precise orthogonal pattern of proneural clusters; within each of these clusters cell-cell interactions will guide one cell into a neural progenitor cell fate while the others will become epidermal cells (Simpson and Carteret, 1990; Cubas *et al*., 1991). These neural stem cells are undifferentiated cells that have the unique ability to produce differentiating daughter cells (neurons and glia) and retain their identity by a process called self-renewal (Knoblich, 2010). Stem cells can exhibit a remarkable proliferative capacity, for example during development or regenerative processes (Knoblich, 2010; Homem and

Knoblich, 2012). Neuroectodermal cells receive the potential to become neural precursors through the expression of proneural genes, mainly genes of the achaete-scute complex. These genes encode DNA binding basic helix-loop-helix transcription factors, which form hetero- and homodimers with each other in order to drive the expression of their target genes. In the next phase one cell of every cluster is singled-out to become a neural stem cell (NSC) and is therefore isolated through a mechanism called lateral inhibition, which is regulated by the neurogenic genes of the Notch signalling pathway. Initially, all the cells in the proneural clusters can express both Notch and Delta but at some point the future NSCs will gain an advantage and exhibit a higher expression of the Notch ligand Delta on its surface and thereby activate Notch signalling in its surrounding cells. This will correspondingly lead to a loss of achaete-scute expression in the neighbouring cells and of the neural potential (Artavanis-Tsakonas and Simpson, 1991; Campos-Ortega, 1993), rendering the presumptive NSC the only neural cell in the proneural cluster. The NSC enlarges and delaminates into the interior of the embryo (Fig. 1A) to form an invariable pattern of about 30 NSCs per hemisegment. A hemisegment is the developmental unit of the nervous system and is the lateral half of a segment (the process of lateral inhibition was reviewed in Beatus and Lendahl, 1998, Rooke and Xu, 1998 and Muskavitch, 1994). Located in between each hemisegment are the CNS midline cells, which consist of a small number of neurons and glial cells (Bossing and Technau, 1994) with specialized functions like axon guidance (Araujo and Tear, 2003) and ventral ectoderm formation (Kim and Crews, 1993; Schweitzer and Shilo, 1997). Once delaminated into the embryo the NSC undergoes stereotypic series of divisions, which are determined according to the time of its delamination from the neuroectoderm, its positional information and through the complex combination of regulatory genes it expresses (Cleary and Doe, 2006; Brody and Odenwald, 2002). In thoracic and abdominal segments this information is nearly the same, that's why NSCs delaminated at the same position in different segments along the anterior-posterior body axis (AP axis) are considered serial homologs. Embryonic NSCs produce all the neurons that shape the larval central nervous system but only about 10% of the cells that form the adult CNS (Prokop and Technau, 1991; Green *et al*., 1993; Truman et al., 2004). After completing their cell-lineages at the end of embryogenesis most of the NSCs in the abdominal regions are removed by apoptosis (White *et al*., 1994). Whereas most cephalic and thoracic NSCs travel through a G_0-like quiescent phase, in which the cell is neither dividing nor preparing to divide. Around four hours after larval hatching (ALH) the larvae start to feed, with the result that the concentration of dietary amino acids is massively increasing in the haemolymph. This rise is sensed by a specialized, hepatic-like

organ called the fat body, via the cationic amino-acid transporter Slimfast (SLIF), which activates the target of rapamycin (TOR) pathway, in turn resulting in the production of a yet unknown fat-body-derived signal (FDS) that is necessary for NSC reactivation and exit from quiescence (Colombani et al., 2003; Sousa-Nunes *et al*., 2011). Furthermore a specialized subpopulation of glial cells proved to be highly relevant for timely NSC reactivation, by translating the FDS into a local activating signal. These glial cells produce and secrete insulin-like peptides (dILPs) that activate the insulin/insulin-like growth factor signalling pathway in NSCs (Chell and Brand, 2010; Sousa-Nunes *et al*., 2011). An initial step during reactivation is the drastic increase in NSC cell size from 4-5µm during quiescence to 10-15µm depending on the type of NSC (Prokop and Technau, 1991; Truman and Bate, 1988). Thus, growth in preparation for cell division is one of the initial hallmarks of NSC reactivation.

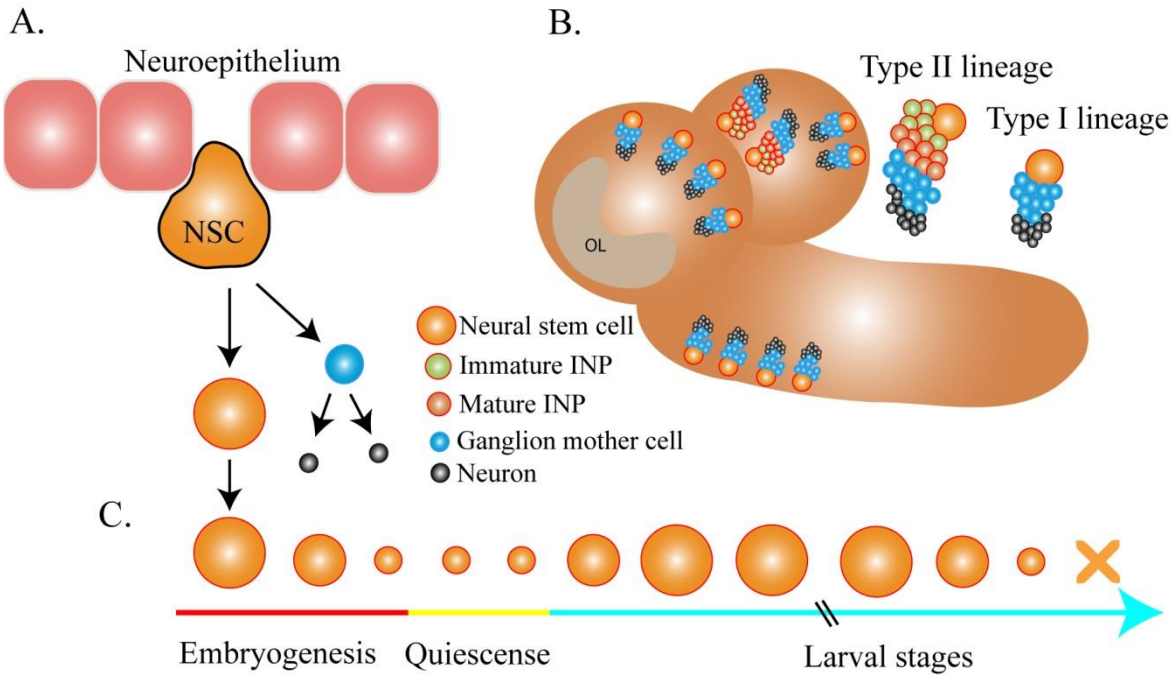

Figure 1: Neurogenesis in *Drosophila melanogaster*. (A) Neural stem cell (NSC, orange) delaminate from the neuroectoderm (bright red) into the *Drosophila* embryo, the division generates a self-renewed NSC (orange) and ganglion mother cell (blue), which divides one more time giving rise to two neurons or glia (black). **(B)** Overview of the *Drosophila* 3rd instar larval central nervous system (CNS), highlighting the main regions of the CNS together with the different NSC types they inherit: the ventral nerve cord (VNC) with its type I NSCs, the central brain lobes with the type I, type II and the optic lobes. **(C)** Time schedule of *Drosophila* NSCs, showing the two periods of proliferation during embryogenesis and larval stages, both phases of mitotic activity are separated by the quiescence phase at the transition between embryonic and larval stages of development. Embryonic NSCs do not re-grow after each division but during the larval development the NSCs do re-grow until they disappear at pupal stages, through apoptosis or terminal differentiation.

The *Drosophila* larval central nervous system was excessively investigated in order to unravel the yet unknown properties of NSCs. In contrast to embryonic NSCs, larval NSCs re-grow after each division to their original size (Fig. 1C) and therefore have the capability to divide hundreds of times and generate huge lineages and thus produce 90% of the cells that form the adult CNS (Homem and Knoblich, 2012). NSC divisions are known to be morphologically as well as molecularly asymmetrical giving rise to an apical cell, which remains a NSC and a smaller basal cell, the ganglion mother cell (GMC). Prior to every division a complex cascade of interactions establishes the apical-basal polarity inside the NSC, which leads to the asymmetric distribution of cell fate determinants. These asymmetrically localized factors specify the differential fates of the two generated daughter cells, for example Numb and Prospero, which are localized at the basal cortex of the dividing NSC, are enriched in the GMC after division (Chia *et al*., 2008; Knoblich, 2010). According to their lineage characteristics and their position in the CNS we are able to distinguish between abdominal and thoracic NSCs in the VNC and between type I, type II, mushroom body, and optic lobe NSCs in the brain lobes of *Drosophila* larvae. The majority of the central brain NSCs is comprised of type I NSCs, which can be found in the anterior as well as in the posterior region of the brain. Compared to that, type II NSCs are located only in the posterior part of the brain. Type I NSCs divide in stereotypic, asymmetric division producing a self-renewed NSC and a smaller neural progenitor cell called GMC, which undergoes a final neurogenic division to generate two daughter cells that exit the cell cycle and differentiate (neurons or glia). On the contrary type II NSCs display a complete different lineage progression, which demonstrate astonishing similarities to the neurogenesis in the mammalian brain, where NSCs act as primary progenitors that amplify the quantity of progeny cells through the formation of secondary progenitors (Fig. 1B) (Bello *et al*., 2008; Homem and Knoblich, 2012). These intermediate neural progenitor cells (INPs) do not express neural differentiation markers, still pass through the cell cycle and exhibit mitotic activity (Bello *et al*., 2008). The divisions of INPs are, contrary to NSC divisions, morphological symmetrical but molecularly asymmetrical, which means that the molecular identity of both daughter cells forces one of them into differentiation whilst the other retains its self-renewing capabilities in order to further amplify the NSC lineage (Bello *et al*., 2008; Li *et al*., 2014). The existence of secondary progenitors in the CNS of *Drosophila melanogaster* suggests that core aspects of neural stem cell biology are broadly conserved between flies and mammals, which clearly prove the necessity of our research in the field of *Drosophila* stem cellbiology.

1.2 Stem cell growth

Stem cells illustrate a unique growth behaviour compared to other cell types. For example most stem cell types re-grow to their original size after each division or they travel through different periods of activation which can be separated by quiescence phases, what goes hand in hand with enormous variations in cellular size (Chell and Brand, 2010; Sousa-Nunes *et al*., 2011; Shin *et al*., 2015). The term cell growth is widely used in the context of cytoplasmic and organelle volume amplification (G1-phase of the cell cycle) and this cellular process depend on a plethora of different growth factors. One factor, which was already widely described as a growth promoting protein is the proto-oncogene Myc (Semsei *et al*., 1989; Hirning *et al*., 1989; Barrios *et al*., 1994). Due to the well-known function of Myc concerning cell growth in various types of cells (Schmidt, 1999), I tried to unravel a potential dependency of quiescent larval NSCs for this growth promoting protein.

1.2.1 The dMyc proto-oncogene

Drosophila Myc (dMyc) is encoded by the *dimunitive* (*dm*) gene and functions as a transcriptional activator that depends on the interaction and dimerization with its binding partner Max (Fig. 2) via their LZ domains (Blackwood and Eisenman, 1991). This heterodimer of dMyc/Max binds to E-box consensus sequences (CACGTG) through their basic Helix-Loop-Helix (bHLH) domain (Amati and Land, 1994; Blackwood *et al*., 1992). dMyc regulates many cellular processes through its transcriptional activity, like proliferation (upregulates cyclins), cell growth (upregulation of ribosomal proteins and rRNA), apoptosis, and stem cell self-renewal (Mateyak *et al*., 1997; Obaya *et al*., 1999; van Riggelen *et al*., 2010; Prendergast, 1999; Varlakhanova *et al*., 2010). Another interesting feature of dMyc is that its mRNA contains a so-called IRES (internal ribosome entry sites), which allows the translation of the mRNA, for example during viral infections when the 5'cap dependent translation is inhibited (Chappell *et al*., 2000). Together with the fact that recent scientific works collected a large body of evidence that up to 15% of all genes are regulated by Myc (Orian *et al*., 2003) leads us to the conclusion that Myc is a critical regulator of the cellular life. Furthermore dMyc is known to regulate organ size by inducing cell competition of juxtaposing cells, by way of example if developmental compartments in *Drosophila* tissues possess cells which are haploinsufficient for dMyc and neighbouring cells which are normal

for the dMyc locus, cells containing less dMyc will be depleted via apoptosis and will not contribute to adult tissues (de la Cova *et al*., 2004; Moreno and Basler, 2004). Due to these important functions of dMyc it becomes obvious that this proto-oncogene needs to be tightly regulated, because even minor changes in cellular Myc levels can cause global effects on the cell.

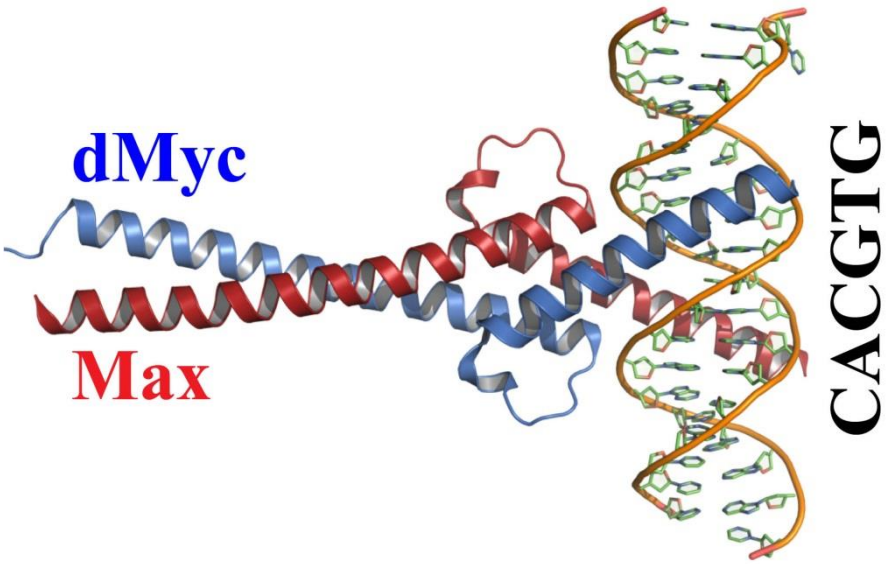

Figure 2: Myc/Max heterodimer binding to DNA. Illustration of a heterodimer formed by dMyc (blue) and its binding partner Max (red) and how it binds to the conserved E-box sequences (CACGTG) on DNA. (From Wikipedia; modified)

1.3 Quiescence

Deregulation of stem cell proliferation can lead to tumour formation or to a premature depletion of the progenitor pool (Cheung and Rando, 2013). Thus, stem cell proliferation has to be tightly regulated according to the cellular or organismal context. In order to meet these requirements NSCs must exert a tight regulation over the proliferative status to produce the adequate number of progeny cells to populate the future CNS. When proliferation is not required, stem cells are maintained in a state of quiescence in the G_0-phase and need to be activated by systemic or local signals (Cheung and Rando, 2013; Coller *et al*., 2006). In late embryonic stages NSCs enter quiescence, which requires intrinsic transcription factors (Tsuij *et al*., 2008; Lai and Doe, 2014). Changes in the physiological condition of the animal, in response to feeding at early larval stages, causes reactivation of NSCs (Britton and Edgar,

1998). The mechanisms regulating quiescence are less well understood. This reversible G_0-like cellular status was thought to be dormant with a minimal basal activity, but recent research that mainly focused on mammalian stem cells suggested that the quiescence is an actively maintained state, which is regulated by diverse signalling pathways that allow rapid reactivation (Shin *et al*., 2015). Furthermore it has been shown that this enormous signalling capability of quiescent NSCs is partly lost after reactivation (Fig. 3), through a significant decrease of the expression of transmembrane molecules, which are required for the responsiveness of these cells to environmental cues (Shin *et al*., 2015). Firstly, quiescent stem cells were identified by two characteristic properties, their low RNA content (Hüttmann *et al*., 2001; Fukada *et al*., 2007) and their lack of cell proliferation markers (Gerdes *et al*., 1984). Further research focused on the transcriptional profiles of different stem cell type's; haematopoietic stem cells (HSCs), muscle stem cells (MuSCs), and hair follicle stem cells (HFSCs). It could be assumed to find out that genes involved in DNA replication and cell cycle progression are downregulated in a non-proliferative phenotype, e.g. cyclin A2, cyclin B1, cyclin E2 and survivin, all of them controlling various aspects of cell cycle progression (Fukada *et al*., 2007; Blanpain *et al*., 2004; Forsberg *et al*., 2010).

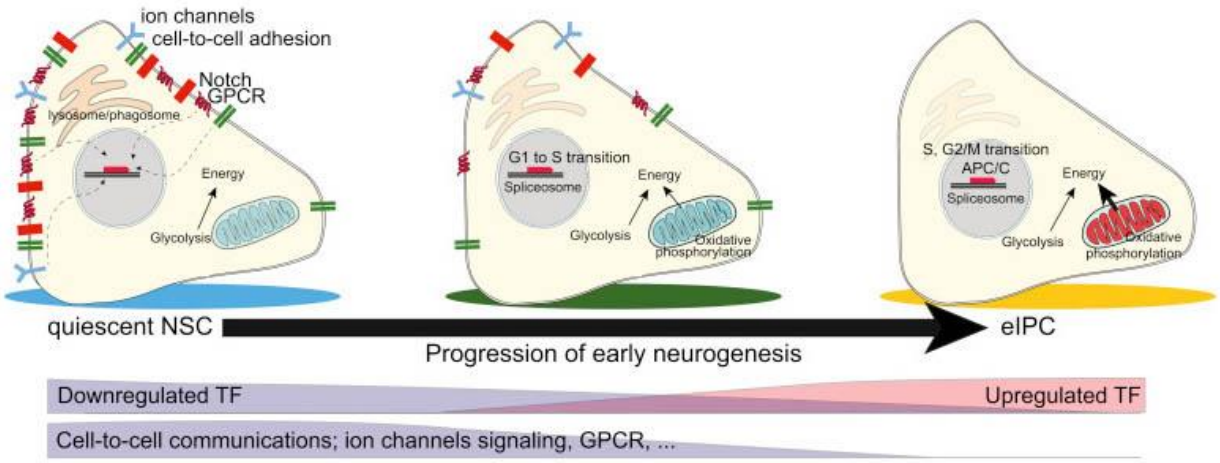

Figure 3: Molecular signatures discriminate between quiescent and reactivated NSCs. Mice adult NSCs (aNSCs) express a huge number of intra- and intercellular signalling molecules (cell adhesion molecules, Notch signalling, ion channels etc.) to precisely sense their local niche during quiescence but this signalling capability is lost after reactivation during the progression of neurogenesis. Quiescence maintaining transcription factors are downregulated upon reactivation and exchanged against a different set of transcription factors. (From Shin *et al*., 2015; modified)

Among the signalling pathways known to contribute to the regulation of stem cell quiescence is for example Notch signalling (Bjornson *et al*., 2012; Mourikis *et al*., 2012), post-transcriptional regulation by miRNAs (Lechmann *et al*., 2012), or signalling pathways, which are necessary to protect the cell from environmental stress (Tothova *et al*., 2007). For the regulation of *Drosophila* NSC quiescence it is known that a certain subpopulation of neighbouring glial cells secrete a glycoprotein (*anachronism*) that keeps NSCs in quiescence, but the precise molecular mechanism remains unknown (Ebens *et al*., 1993). In order to unravel novel factors or signalling pathways involved in the regulation of NSC quiescence in the *Drosophila* CNS I performed a targeted RNAi screen and identified the highly conserved Hippo signalling pathway to play an important role in this important developmental process.

1.4 Salvador/Warts/Hippo signalling pathway

One of the major pathways that control cell proliferation and survival in metazoans is the highly conserved Salvador/ Warts/Hippo signalling pathway (SWH). Recent studies clearly indicate that the SWH signalling pathway is a powerful regulator of organ size and proliferation in *Drosophila* and mammals (Halder and Johnson, 2011; Pan, 2007; Reddy and Irvine, 2008; Zhao *et al*., 2010a, b). The main effector of this pathway is the transcriptional co-activator Yorkie (Yki), Yes-associated protein (YAP)/Transcriptional co-activator with PDZ binding motif (TAZ) in mammals. These proteins bind directly to specific transcription factors after translocation into the nucleus to drive their transcriptional programmes, which promote proliferation and inhibit apoptosis and differentiation (Halder and Johnson, 2011; Reddy and Irvine, 2008). Known target genes of Yki are directly promoting growth (*Bantam* microRNA) (Nolo *et al*., 2006), the cell cycle (Cyclin E) and are inhibiting apoptosis (diap1) (Udan *et al*., 2003; Pantalacci *et al*., 2003). Yki is inhibited via phosphorylation at three specific amino acid residues by a growth-repressing protein complex which is the regulative centre of this signalling pathway and is composed of the two serine/threonine kinases Hippo (Hpo) and Warts (Wts), Mst1/2 and Lats1/2 in mammals (Halder and Johnson, 2011). Both kinases are associated with their individual interaction partners, Salvador (Sav) and Mats, which act as scaffold proteins (Pan, 2007; Zhao *et al*., 2010a). The Hippo kinase activates the Warts kinase, which in turn directly phosphorylates Yki, creating a 14-3-3 binding site that restricts nuclear translocation of Yki (Ren *et al*., 2009). 14-3-3 proteins belong to a conserved family of regulatory proteins that are expressed in every eukaryotic cell. If Hippo/Warts are

inactive, non-phosphorylated Yki enters the nucleus and bind to specific transcription factors like Scalloped (Sd) (Goulev *et al*., 2008; Wu *et al*., 2008) or Homothorax (Hth) (Peng *et al*., 2009) and thereby activates its transcriptional programme promoting cell growth and proliferation. The growth repressive kinases in the centre of this signalling pathway receive regulative input from a plethora of different protein complexes. The regulation especially of the Hpo kinase is complex and involves the adjustment of its enzymatic activity via phosphorylation. Important upstream regulators of the SWH pathway include for example the membrane associated Expanded, Kibra, and Merlin complex (Baumgartner *et al*., 2010; Feng and Irvine, 2007; Genevet *et al*., 2010; Hamaratoglu *et al*., 2006), the sterile 20 kinase Tao (Boggiano *et al*., 2011; Poon *et al*., 2011), the atypical cadherins Fat and Dachsous (Rogulja *et al*., 2008; Bennett and Harvey, 2006; Cho *et al*., 2006; Silva *et al*., 2006; Feng and Irvine, 2007; Tyler and Baker, 2007), the Golgi kinase Four-jointed (Willecke *et al*., 2008) as well as the transmembrane proteins crumbs (Robinson *et al*., 2010), and Echinoid (Yue *et al*., 2012). These regulatory inputs are provided in a combinatorial manner to enable the cell to respond to diverse internal or external cues through the adjustment of the SWH signalling pathway activity.

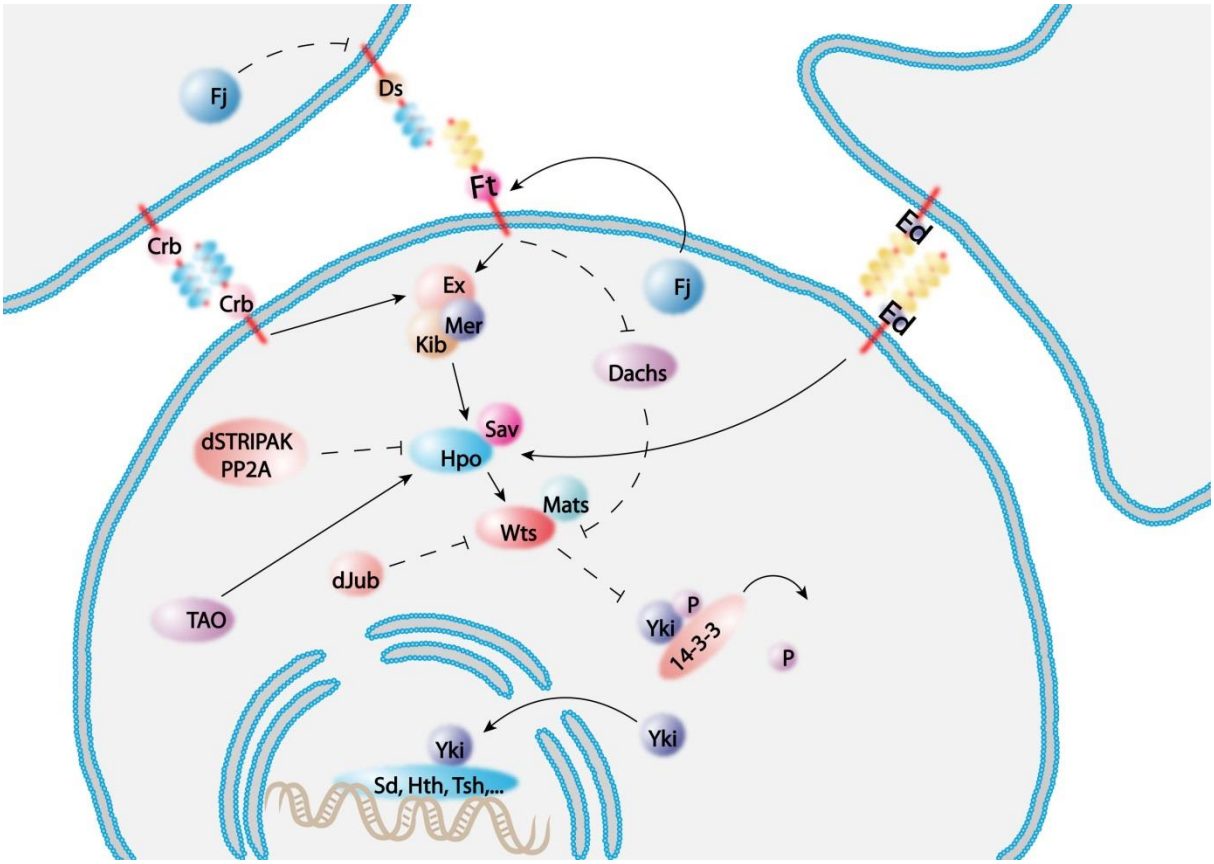

Figure 4: The SWH signalling pathway in *Drosophila melanogaster*. Schematic model of the SWH signalling pathway in *Drosophila melanogaster*. Dotted lines and solid lines indicate inhibition and activation, respectively. Transmembrane proteins like Crumbs (Crb), Echinoid (Ed), Fat (Ft) or Dachsous (Ds) relay extracellular cues to the regulative centres of the SWH pathway. The Expanded (Ex), Kibra (Kb), Merlin (Mer) complex is a main upstream regulation module, which directly acts on the core kinase cascade. The core kinase cascade consists of Hippo (Hpo) and Warts (Wts) together with their interaction partners Salvador (Sav) and Mob as tumour suppressor (Mats). Upon SWH activation Wts/Mats phosphorylates and thereby inactivates the main effector of the pathway Yorkie (Yki), phosphorylated Yki is bound by 14-3-3 proteins. Dephosphorylated Yki translocates into the nucleus, where it interacts with diverse transcription factors like Scalloped (Sd), Homothorax (Hth) or Teashirt (Tsh) to drive its transcriptional programme. Abbreviations of unmentioned proteins: Tao kinase (Tao), Ajuba LIM protein (dJub), Dachs (d), Four-jointed (Fj), dSTRIPAK phosphatase complex.

1.4.1 Upstream regulators

During the last years, research concerning the SWH pathway concentrated and established the highly conserved core kinase cascade, while the upstream factors, which are regulating this developmentally important signalling pathway, are still not completely understood. The majority of the information that was generated on this topic over the past years was found in *Drosophila*. Interestingly many of the regulators of the SWH pathway are well-identified components of tight junctions (TJs), adherens junctions (AJs) and apical-basal polarity protein complexes (Yu and Guan, 2013). The first upstream regulators to be identified were the FERM (F for 4.1, E for Ezrin, R for Radxin, M for Moesin) domain containing proteins Merlin (Mer) and Expanded (Ex) (McCartney *et al*., 2000), it was shown that loss of Merlin and Expanded lead to hyperplasia of the affected tissue. Comparable phenotypes were observed after deletion of the core kinase proteins Hpo, Wts and Sav, in consistence with this co-expression of Ex and Mer led to an activation of the SWH pathway through an increase in Wts phosphorylation (Hamaratoglu *et al*., 2006). Further research identified a third protein that physically interacts with Ex and Mer in order to regulate the SWH pathway, the WW and C2 domain containing protein Kibra (Kib). Together these three proteins activate Wts in a cooperative manner (Baumgartner *et al*., 2010; Genevet *et al*., 2010; Yu *et al*., 2010). Another important step to unravel further upstream regulators of the SWH pathway was the identification of the Fat (Ft)/Dachsous (Ds) system, which is known to be critical in establishing Planar cell polarity (PCP) (Simons and Mlodzik, 2008). The Ft/Ds system was the first transmembrane receptor signalling identified to feed into this pathway, loss of Ft was shown to activate the pathway effector Yki via the inactivation of either Ex or Wts (Bennett and Harvey, 2006; Cho *et al*., 2006; Silva *et al*., 2006; Willecke *et al*., 2006; Feng and Irvine,

2007; Tyler and Baker, 2007). Both Ft and Ds are atypical cadherins, which form heterodimers between neighbouring cells (Cho and Irvine, 2004; Matakatsu and Blair, 2004). This intercellular interaction is strongly regulated by phosphorylation through the Golgi-resident kinase Four-jointed (Fj) (Ishikawa *et al*., 2008). Fat regulates SWH signalling through direct interaction with Ex (Bennett and Harvey, 2006) or through the relocalization of the atypical myosin Dachs (d) to subapical regions, this polarized Dachs in turn promotes the interaction between Wts and Zyxin (Zyx), leading to Wts degradation (Cho *et al*., 2006; Feng and Irvine, 2007; Rauskolb *et al*., 2011). In the search for additional transmembrane molecules regulating the SWH pathway Crumbs (Crb) and Echinoid (Ed) have been identified recently (Chen *et al*., 2010; Grzeschik *et al*., 2010; Ling *et al*., 2010; Robinson *et al*., 2010; Yue *et al*., 2012). During embryogenesis Crb plays a pivotal role in organizing apical-basal polarity (Tepass *et al*., 1990), as transmembrane protein Crb is composed of a long extracellular domain and a short intracellular domain, which consists a FERM-binding motif (FBM) that allows Crb to physically interact with Ex and thereby regulates SWH signalling (Chen *et al*., 2010; Ling *et al*., 2010; Robinson *et al*., 2010). Echinoid on the other hand is an immunoglobulin domain-containing cell adhesion molecule (Bai *et al*., 2001; Wei *et al*., 2005) that has the ability to bind the Hpo interaction partner Sav at AJs and thereby regulating the activity of this pathway. The Ed/Sav interaction depends on the homophilic dimerization between the extracellular domains of two Ed molecules on neighbouring cells (Yue *et al*., 2012). Recently Gailite *et al* introduced a novel mechanism of Yki regulation independently of SWH signalling in the *Drosophila* CNS, through the Liver Kinase B1 (LKB1)/AMP-activated Protein Kinase (AMPK) cascade (Gailite *et al*., 2015). This suggests that a potential energy sensing pathway is controlling cell proliferation in the *Drosophila* CNS. LKB1 is a tumour suppressor kinase, which is involved in a variety of cellular processes like cell polarity, cell proliferation or stress responses (Shackelford and Shaw, 2009), the main phosphorylation target of LKB1 is the AMP-activated protein kinase (AMPK) (Woods *et al*., 2003). AMPK acts as an intracellular energy sensor that is activated by the binding of AMP (Adenosine monophosphate), resulting in conformational changes leading to phosphorylation by LKB1 (Shaw *et al*., 2004). Cell culture experiments with mammalian cells already showed that LKB1 as well as AMPK have the ability to repress YAP function either through modulation of the core kinase cascade or by direct YAP phosphorylation (Mohseni *et al*., 2014; Nguyen *et al*., 2013; DeRan *et al*., 2014).

1.4.2 Downstream Regulators

Diverse studies showed that the main effector of the SWH pathway Yki (Huang *et al*., 2005) is not able to bind to DNA directly, but as a transcriptional co-activator it has the ability to bind to a specific set of transcription factors. Yki translates the activity pattern of the SWH pathway into a distinct transcriptional output, through the interaction with the TEAD/TEF protein Scalloped (Goulev *et al*., 2008; Wu *et al*., 2008; Zhang *et al*., 2008; Zhao *et al*., 2008), the TALE-homeodomain protein Homothorax (Hth), or the zinc finger transcription factor Teashirt (Tsh) (Peng *et al*., 2009). The known target genes regulated by Yki promote cell proliferation as well as cell survival and inhibit apoptosis, for example cells mutant for *hpo* cell-autonomously upregulate the transcription of *cyclin E* and *diap1* (Udan *et al*., 2003; Pantalacci *et al*., 2003; Wu *et al*., 2003; Harvey *et al*., 2003). Cyclin E is a limiting factor for cell cycle progression and S phase entry (Richardson *et al*., 1995) thus making Cyclin E a critical supervisor for cell proliferation. The regulation of cell survival via the inhibition of apoptosis is another characteristic of Yki activity, executed by its transcriptional target DIAP1. This Inhibitor of Apoptosis Protein (IAP) is an E3 ubiquitin ligase that can directly bind to all three pro-apoptotic factors Head involution defective (HID), Reaper (Rpr), or Grim (Vucic *et al*., 1997; Vucic *et al*., 1998) and thereby inhibit apoptosis. Another important target gene is the growth promoting microRNA *bantam*, which was shown to be required for Yki driven tissue overgrowth (Nolo *et al*., 2006). *Bantam* is known to regulate cell number but not cell size or pattern formation in general, so *bantam* overexpressing cells proliferate faster but keep their original size (Hipfner *et al*., 2002; Brennecke *et al*., 2003; Raisin *et al*., 2003). To ensure the tight transcriptional regulation of the SWH pathway target genes, Yki was shown to interact with a plethora of different proteins inside the nucleus. Qing *et al.* identified the Nuclear receptor coactivator 6 (Ncoa6), which is a subunit of the Trithorax related (Trr) histone H3 lysine 4 (H3K4) methyltransferase complex, as an Yki binding partner. This finding for the first time indicated that Yki is involved in the modification of chromatin structure to regulate the expression of its target genes (Qing *et al*., 2014). In addition to Yki's known function as a transcriptional co-activator, Kim *et al.* (2015) showed that the mammalian homologs YAP and TAZ have the ability to influence target gene expression via transcriptional repression. In this study it was shown that YAP/TAZ are actively repressing genes which are anti-proliferative or inducing apoptosis through the recruitment of the nucleosome remodelling and histone deacetylase (NuRD) complex (Kim *et al*., 2015). If there is a comparable mechanism in the *Drosophila* SWH signalling pathway this still has to be shown. The identification of the Tondu-domain containing growth inhibitor (Tgi), which was

shown to bind to Sd in the absence of Yki raised the question whether the main function of Yki is to relieve Sd mediated transcriptional repression rather than activation (Koontz *et al*., 2013). But this question amongst others still has to be answered and for the moment just highlights the complexity of this signalling pathway.

1.4.3 Physiological role of SWH signalling in *Drosophila* and mammals

Noteworthy efforts have been made in order to unravel the physiological functions of the SWH pathway in *Drosophila* as well as in mammals. Recent studies underlined the importance of the SWH pathway core proteins, as loss-of-function mutations lead to significant tissue overgrowth phenotypes in diverse *Drosophila* tissue types (Tapon *et al*., 2002; Harvey *et al*., 2003; Jia *et al*., 2003; Pantalacci *et al*., 2003). The same was reported for the overexpression of the main pathway effector Yki (Huang *et al*., 2005). Furthermore, *Drosophila* larvae that are homozygous mutant for *yki* exhibit massive growth defects and die at approximately 70hrs ALH. This clearly emphasizes the importance of this highly conserved pathway in the regulation of *Drosophila* organ size. Great efforts have been made to elucidate the role of the SWH signalling pathway especially in mammalian organ size regulation. The liver for example is the organ which bears the highest regeneration potential, here it was shown that de-repression of YAP through expression of an constitutively active form (YAP1-S127A) leads to hepatomegaly a four-fold increase in liver size (Camargo *et al*., 2007; Dong *et al*., 2007). The same phenotypes occurred after loss of *Mst1/2* or *Sav1* (Zhou *et al*., 2009; Lu *et al*., 2010; Song *et al*., 2010). All the above results seem to be closely related to stem cell function, because these cells are mainly responsible and necessary for organs to adjust their size, and indeed YAP expression in the intestine and the epidermis was found to be unexceptionally localized within the compartments that comprise the tissue resident stem cells (Camargo *et al*., 2007).

However, whether this is true in *Drosophila* NSCs and whether changes in Yki activity are causative for altering growth and proliferation during normal CNS development remains unclear. In *Drosophila*, the SWH has been implicated in CNS development of the neuroepithelium (Reddy *et al*., 2011; Kawamori *et al*., 2011) and of glial cells (Reddy and Irvine, 2011) in the optic lobe and in cell growth of a specific population of glial cells (subperineural glial cells). However, for central brain NSCs, no function has been attributed to the SWH until now.

2. Aims

In every multi-cellular organism cells need to work together and communicate with each other to control their own activity in response to the signals they receive from the surrounding cells. The same is true for the tight regulation of *Drosophila* NSCs. Due to the fact that there is a huge lack of information concerning the regulation of NSC quiescence between embryonic and larval phases of proliferation; I initiated a screen for known growth regulators and their involvement in this critical process. Two known growth promoting factors proved to play leading roles in this process; namely the proto-oncogene dMyc and the SWH signalling pathway, on which I concentrated during my thesis work. The SWH signalling module is one of the pathways, which are necessary for many tissues to develop correctly. As no detailed analysis of this pathway's role in CNS development has been undertaken, the first aim of my thesis was to describe a potential role in the developing CNS, with a special focus on resting NSCs. The second part of my work focused on the upstream regulation, which is necessary to translate environmental cues (e.g. nutrition) into a specific activity pattern of the SWH pathway. Finally, I concentrated on the NSC specific transcriptional targets of this signalling module.

3. Material and Methods

3.1 Materials

3.1.1 Consumption items

Disposal bags	VWR international GmbH, Darmstadt
Serological pipette 5 ml, 10 ml	Sarstedt, Nümbrecht
Parafilm® M	American National Can Group Inc., Chicago (USA)
Petri dish Ø 90mm Ø 140mm	VWR international GmbH, Darmstadt
Pipette tips 10µl, 200µl, 1000µl	VWR international GmbH, Darmstadt
PP-tubes	Sarstedt, Nümbrecht
Safe lock tubes 1.5ml, 2.0ml	Eppendorf AG, Hamburg
Low Bind Tubes 1.5ml	Eppendorf AG, Hamburg
Disposable Gloves Nitrile	Microflex, Reno (USA)
Cell culture plates (6 well)	Merck Millipore, Billerica (USA)
Rubber policeman	Sigma-Aldrich, St-Louis (USA)
Nunclon® micro well plates (96 well)	Sigma-Aldrich, St-Louis (USA)
Microscope slides	Marienfeld-Superior, Lauda-Königshofen
Coverslips	Marienfeld-Superior, Lauda-Königshofen
Nail polish	COTY Germany GmbH, Mainz
Cell strainer	Becton Dickinson Labware, Franklin Lakes (USA)
96 well plates	Bio-Rad, Hercules (USA)
Optical adhesive covers	Applied Biosystems, Foster city (USA)

3.1.2 Chemicals

Sodium phosphate dibasic (Na_2HPO_4)	Carl Roth GmbH & Co. KG, Karlsruhe
Sodium dihydrogen phosphate (NaH_2PO_4)	Carl Roth GmbH & Co. KG, Karlsruhe
TritonX100 ($C_{14}H_{22}O(C_2H_4O)_n$)	Carl Roth GmbH & Co. KG, Karlsruhe
LysinHCl ($C_6H_{14}N_2O_2 \cdot HCl$)	Sigma-Aldrich, St-Louis (USA)
Sodium hydroxide (NaOH)	Carl Roth GmbH & Co. KG, Karlsruhe
Paraformaldehyde ($OH(CH_2O)_nH$)	Carl Roth GmbH & Co. KG, Karlsruhe
Sodium chloride (NaCl)	Carl Roth GmbH & Co. KG, Karlsruhe

Potassium chloride (KCl)	Carl Roth GmbH & Co. KG, Karlsruhe
Sodium bicarbonate ($NaHCO_3$)	Carl Roth GmbH & Co. KG, Karlsruhe
Glucose ($C_6H_{12}O_6$)	Carl Roth GmbH & Co. KG, Karlsruhe
PIPES ($C_8H_{18}N_2O_6S_2$)	Carl Roth GmbH & Co. KG, Karlsruhe
Magnesium chloride ($MgCl_2$)	Carl Roth GmbH & Co. KG, Karlsruhe
EGTA ($C_{14}H_{24}N_2O_{10}$)	Carl Roth GmbH & Co. KG, Karlsruhe
Glycerol ($C_3H_8O_3$)	Carl Roth GmbH & Co. KG, Karlsruhe
Vectashield®	Vector Laboratories, Inc., Burlingame (USA)
GelRed™	Biotium, Hayward (USA)
LE Agarose ($C_{12}H_{18}O_9$)	Biozym Scientific GmbH, Oldendorf
Glutathione ($C_{10}H_{17}N_3O_6S$)	Sigma-Aldrich, St-Louis (USA)
fetal bovine serum (FBS)	PAA Laboratories, Pasching (Austria)
Tris ($C_4H_{11}NO_3$)	Bio-Rad, Hercules (USA)
Acidic acid (CH_3COOH)	Bio-Rad, Hercules (USA)
EDTA ($C_{10}H_{16}N_2O_8$)	Bio-Rad, Hercules (USA)
Pen ($C_9H_{11}N_2O_4S$)/Strep ($C_{21}H_{39}N_7O_{12}$)	Sigma-Aldrich, St-Louis (USA)

3.1.3 Technical equipment

Power-supply units

- Power Pack HC, Bio-Rad, Hercules (USA)

Refrigerator

- Liebherr Premium, Liebherr International AG, Kirchdorf an der Iller
- Liebherr Comfort, Liebherr International AG, Kirchdorf an der Iller

Magnetic stirrer

- IKAMAG® RCT, Janke und Kunkel GmbH & Co. KG, Staufen i. Br.
- Heidolph MR 3001, Heidolph Instruments Labortechnik, Schwabach

Centrifuges

- Fresco21 centrifuge, Thermo Scientific, Waltham (USA)
- Sigma 3K20, B. Braun, Melsungen
- Micro centrifuge, Carl Roth GmbH + Co. KG, Karlsruhe

Gelchambers

- Wide Mini-Sub® Cell GT, Bio-Rad, Hercules (USA)

Microwave

- MW20 ,TechnoStar, …
- R-201A, Sharp, Osaka (Japan)

Photometers

- NanoDrop® ND2000 Spectrophotometer, Thermo Scientific, Waltham (USA)

Incubators

- WTB Binder GmbH, Tuttlingen
- Friocell, MMM Medcenter Einrichtungen GmbH, München

Thermal cyclers

- X1000 Touch thermal cycler, Bio-Rad, Hercules (USA)
- StepOnePlus,

Vortexer

- Vortex Genie® 2, Scientific industries Inc., New York (USA)
- Whirlmix, Cenco instruments, Breda (NL)

Scales

- Mettler PM4600 DeltaRange, Mettler-Toledo, Columbus (USA)
- EW 1500-2M, Kern und Sohn GmbH, Balingen

Sterile bench

- Steril-VBH, Angelantoni Life Science s.r.l., Massa Martana (Italy)
- BHA 48, Faster, Ferrara (Italy)
- AG Luhmann

Microscopes

- M3B, Wild Heerbrugg, Heerbrugg (Switzerland)
- MS5, Leica Camera AG, Wetzlar
- Axiovert 40CFL, Carl Zeiss AG, Oberkochen
- TCS SP5, Leica Camera AG, Wetzlar
- SZX12, Olympus Deutschland GmbH, Hamburg
- BX50WI, Olympus Deutschland GmbH, Hamburg
- MZ FLIII, Leica Camera AG, Wetzlar

Microplate reader

- Infinite® 1000PRO, Tecan Group, Männedorf (Switzerland)

Heating plate

- Thermomixer comfort, Eppendorf AG, Hamburg

Pipette

- VWR Signature™ Ergonomic Pipettor, VWR international GmbH, Darmstadt

Forceps

- Dumont #55 Mirror Finish, Fine Science Tools GmbH, Heidelberg

FACS Sorter

- FACS ARIA II Flow Cytometer, BD Biosciences, San Jose (USA)

3.1.4 Media and Solutions

Table 1. Media and solutions

0.1M Na_2HPO_4 Na_2HPO_4 8,89g H_2O 600ml	0.1M NaH_2PO_4 1. NaH_2PO_4 6,89g 2. H_2O 500ml
0,1M sodium phosphate buffer (PBS) • 0,1M Na_2HPO_4 500ml • Add X ml 0,1M NaH_2PO_4 with a pH meter until reaches 7.4	0,3 % PBT • X ml 0,1M sodium phosphate buffer • Add 0,3% TritonX100
PBL • LysinHCl 1,8g • H_2O 50ml • Add X ml Na_2HPO_4 with a pH meter until reaches 7.4 Adjust volume to 100ml with 0,1M PBS	8% paraformaldehyde (PFA) • Paraformaldehyde 1.6g • H_2O 50ml • NaOH 140µl Alternate 37°C water bath and vortex until completely solved

Fixation solution (PLP) • PBL 400µl • 8% PFA 400µl	Rinaldini's solution • NaCl 800mg • KCl 20mg • NaH_2PO_4 5mg • $NaHCO_3$ 100mg • Glucose 100mg • H_2O 100ml
Schneider's Medium (suppl.) • fetal bovine serum 100ml • Pen/Strep 20ml • Glutathione 40mg • Schneider's medium 840ml	Dulbecco´s Modified Eagle Medium • fetal bovine serum 50ml • Pen/Strep 5ml • DMEM 500ml
PEM-buffer • 100mM PIPES (pH 6,9) • 1mM EGTA • 1mM $MgCl_2$	Mounting medium • Vectashield® 1ml • 70% Glycerol 1ml
TAE buffer (Bio-Rad #161-0743) • 40mM Tris (pH 7,6) • 20mM Acidic acid • 1mM EDTA	Schneider's medium (Sigma-Aldrich, St-Louis (USA)) Dulbecco´s Modified Eagle Medium (Thermo Scientific, Waltham (USA))

3.1.5 Antibodies

Table 2. Primary antibodies

Antibody	Donor	Dilution	Source
Dpn	guinea pig	1:1000	J. Knoblich
Pros	mouse	1:100	DSHB
Repo	mouse	1:100	DSHB
Dlg	mouse	1:20	DSHB
pH3	mouse	1:1000	CST
ß-Gal	mouse	1:375	Promega

Ex	guinea pig	1:1000	R. Fehon
Tsh	rabbit	1:100	AG Technau
Yki	rabbit	1:400	K. Irvine
CycE	rat	1:500	T. Orr-Weaver
pAkt (S505)	rabbit	1:100	Cell signalling
Ecad	rabbit	1:200	DSHB

Table 3. Secondary antibodies

Antibody	Donor	Dilution	Source
guinea pig-Cy3	Donkey	1:250	Dianova/Jackson
mouse-Alexa647	Donkey	1:500	Invitrogen
rabbit-Alexa647	Donkey	1:500	Invitrogen
rat- Alexa649	Donkey	1:250	Dianova/Jackson

3.1.6 Enzymes

Table 4. Restriction enzymes

Enzymes	Recognition sequence	Reaction buffer	Incubation temperature	Inactivation temperature
SacI	GAGCT ↓ C C ↑ TCGAG	1x or 2x Tango	37°C	65°C for 20 minutes
XhoI	C ↓ TCGAG GAGCT ↑ C	1x red buffer	37°C	80°C for 20 minutes
BglII	A ↓ GATCT TCTAG ↑ A	2x Tango	37°C	No
EcoRI	G ↓ AATTC CTTAA ↑ G	2x Tango	37°C	65°C for 20 minutes

Table 5. Other enzymes

Enzymes	Reaction buffer
Taq polymerase (New England Biolabs Inc.; #M0486S)	20 mM Tris-HCl, 22 mM KCl, 22 mM NH_4Cl, 1.8 mM $MgCl_2$, 5% Glycerol, 0.06% IGEPAL® CA-630, 0.05% Tween® 20, 0.2 mM dNTPs, 1X Xylene Cyanol, 1X Tartrazine, 25 units/ml OneTaq® DNA Polymerase, pH 8.9
Collagenase I (Sigma-Aldrich: C2674)	Optimal pH: 6.0-7.0
Papain (Sigma-Aldrich: P4762)	Optimal pH: 6.0-7.0

3.1.7 Kits

Table 6. Kits

Name	Cat. No.	Company
Cells-to-Ct™ 1 Step TaqMan® Kit	A25603	Thermo Scientific
iScript Advanced cDNA Synthesis Kit for RT-qPCR	**172-5037**	Bio-Rad
iScript™ Universal SYBR® green Supermix	172-5120	Bio-Rad
TaqMan® Gene Expression Assay (*yki*)	4351372	Applied Biosystems
Dual-Luciferase® Reporter Assay System	E1910	Promega
FuGENE® HD transfection reagent	E2311	Promega

3.1.8 Synthesized oligonucleotides/primers

Table 7. Primers for dMyc targets genes

Name	Sequence	T_m
CG1381 FOR	5´-TGTGAGGAGGGCAAAGTTCT-3´	60°C
CG1381 REV	5´-TGTTCCTCGTCGTTCACATC- 3´	60°C
CG5728 FOR	5´-GCGAAAGGCAGAAGTGGTAG- 3´	60°C
CG5728 REV	5´-ACTAGACACACCGGGCAAACG- 3´	60°C
CG6375 FOR	5´-CGAGCAGGGGTACATTGTTT- 3´	60°C
CG6375 REV	5´-TATTTGACGGACATGCAGGA- 3´	60°C
CG6751 FOR	5´-TCTCCTGGACAACTGCTGTG- 3´	60°C
CG6751 REV	5´-GCCATCAAAGTTCCACACCT- 3´	60°C
CG7006 FOR	5´-GAGCGGATTTTGAAGCTGAG- 3´	60°C
CG7006 REV	5´-CGTAGGGCGCCAAGTAGTAG- 3´	60°C

CG7137 FOR	5´-GCACTTTTCCGCAAGGATAG- 3´	60°C
CG7137 REV	5´-GTCGCCAATTATGGCTGTTT- 3´	60°C
CG7845 FOR	5´-GGAGCACGGGATGAGTTTTA- 3´	60°C
CG7845 REV	5´-CACTTATCCCGCCTGTGAAT- 3´	60°C
CG9799 FOR	5´-TTGACAAGCCCTTAGCGACT- 3´	60°C
CG9799 REV	5´-AGGTCATTCAGCTTGGCTGT- 3´	60°C
CG9888 FOR	5´-GCATCTCCGTTGAGACCAAT- 3´	60°C
CG9888 REV	5´-GACACATGCGAGACTGTCGT- 3´	60°C
CG10206 FOR	5´-GAGTGGTACGGTTGGCACTT- 3´	60°C
CG10206 REV	5´-CCTTGACCTTTTCCTCCACA- 3´	60°C
CG10798 FOR	5´-AGCATCACCACCAACAACAA- 3´	60°C
CG10798 REV	5´-GGACCATCGTCCACCATATC- 3´	60°C

Table 8. Yorkie specific primers

Name	Sequence	T_m
YKI FOR_1	5´-ACTACAAAATCTACGCAGTGGGAGG-3´	60°C
YKI REV 1	5´-GGGAAGACGGCGGATTTACAATG-3´	60°C
YKI FOR_2	5´-CCAGCAGCAGCAAATCTTGATGG-3´	60°C
YKI REV 2	5´-GGCCTGTGCGTCATTGAACA-3´	60°C

Table 9. Tgi 3'UTR cloning primers

Name	Sequence	T_m
Megaprimer fwd1	5´-CGTTTAAA**GAATTC**ATGCTGATGTGAACGGAAATTCTTC-3´	62°C
Megaprimer rev1	5´-CACATCAGCAT**GAATTC**TTTAAACGTTAATTGTGTAGTTTG-3´	61°C
Megaprimer 2 fwd	5´-CTGATATAA**CGATCG**TATTGAATATTGATAACGGTTAGCG-3´	62°C
Megaprimer 2rev	5´-CAATATTCAATA**CGATCG**TTATATCAGAAACTTGTAATACAC-3´	60°C

Nucleotides which represent restriction sites are written in bold letters (**G ↓ AATTC**: EcoRI; **CG ↓ ATCG**: PvuI).

3.1.9 Cells

Table 10. Cells

Organism	Strain
Bacteria (*Escherichia coli*)	DH5α
Bacteria (*Escherichia coli*)	JM1
Bacteria (*Escherichia coli*)	XL1
human	HEK293

3.1.10 Vectors

Table 11. Vectors

Name	Size (bp)	Characteristics	Company/ Donator
pmirGLO	7350	Amp^r, Kan/neo^r, PGK promoter, FF luciferase, SV40 poly (A) signal, SV40 promoter, Re luciferase, poly (A) signal	Promega
pEZX-MR04		Amp^r, CMV promoter, eGFP, SV40 poly (A) signal, pUC ori, $PURO^r$	Genecopoeia / AG White
pEGFP-c3	4727	Kan/neo^r, GFP, CMV promoter	AG White
Scramble	5018		AG White
pCR®2.1-TOPO	3931	Amp/neo^r, pUC ori, LacZα, T7 promoter, f1 origin	Thermo Scientific

3.1.11 Computer programmes

Table 12. computer programmes

Name of the programme	Publisher
Microsoft Word	Microsoft Deutschland GmbH
Microsoft Exel	Microsoft Deutschland GmbH
SigmaPlot 11.0	Systat Software Inc.
Adobe Photoshop CS4	Adobe Systems GmbH
Adobe Illustrator CS4	Adobe Systems GmbH
Leica LAS AF Lite	Leica Microsystems
StepOne Software v2.3	Applied Biosystems
I-Control	Tecan Group Ltd.

3.2 Methods

3.2.1 Flies, food, media

3.2.1.1 Fly maintenance

Fly stocks were maintained on a standard food medium containing yeast flakes, soy flour, corn flour, malt extract as well as sugar beets syrup. For solidification agar was added as well as Nipagin and propionic acid for conservation. The fly stocks were maintained at 25°C and transferred to fresh medium containing vials every two weeks. Stocks not currently used for experiments were maintained at 18°C and transferred every three weeks.

3.2.1.2 Apple juice agar

For egg collections, apple juice was solidified with 2% Agar-agar. 1L of commercially available apple juice was mixed with 28g Agar-agar and heated to boiling in a microwave. The mixture was stirred and heated repeatedly until the Agar was completely dissolved. After distributing into vials, the apple juice agar was allowed to cool down and thereby solidify.

3.2.1.3 Fly stocks

Table 13. Fly stocks

Denotation	Genotype	Source
hippo-RNAi	y^1 v^1; P{TRiP.HMS00006}attP2	Bloomington Stock Center
warts-RNAi	y^1 v^1; P{TRiP.HMS00026}attP2	Bloomington Stock Center
crumbs-RNAi	y^1 v^1; P{TRiP.GL00674}attP40	Bloomington Stock Center
14-3-3ζ-RNAi	y^1 v^1; P{TRiP.HM04002}attP2	Bloomington Stock Center
fj-LacZ	w[1118];P{w[+mC]=lacW}fj[9-II]/ CyO,P{ry[+t7.2]=sevRas1.V12} FK1	Bloomington Stock Center
expanded-RNAi	w^{1118}; P{GD12782}v22994	Vienna *Drosophila* Resource Center
kibra-RNAi	P{KK108510}VIE-260B	Vienna *Drosophila* Resource Center
Merlin-RNAi	w^{1118}; P{GD1484}v7161	Vienna *Drosophila* Resource Center
crumbs-RNAi	w^{1118}; P{GD14463}v39177	Vienna *Drosophila* Resource Center
echinoid-RNAi	P{KK106928}VIE-260B	Vienna *Drosophila* Resource Center
hippo-RNAi	P{KK101704}VIE-260B	Vienna *Drosophila* Resource Center

warts-RNAi	P{KK101055}VIE-260B	Vienna *Drosophila* Resource Center
baboon-RNAi	y^1 v^1; P{TRiP.GL00702}attP2	Bloomington Stock Center
stat92E-RNAi	y^1 v^1; P{TRiP.HMS00035}attP2	Bloomington Stock Center
fat-RNAi	y^1 sc^* v^1; P{TRiP.HMS00932}attP2	Bloomington Stock Center
tgi-RNAi	y^1 sc^* v^1; P{TRiP.HMS00981}attP2	Bloomington Stock Center
bantam-Sensor		J. Brennecke
control-sensor		J. Brennecke
lkb1-RNAi	y^1 sc^* v^1; P{TRiP.GL00019}attP2	Bloomington Stock Center
crumbs::GFP		Yang Hong
yki^{B5} mutant	l(2)gl^4 yki^{B5}/CyO	Bloomington Stock Center
ban$^{\Delta 1}$ mutant		J. Knoblich
hpo^{JM1} mutant		N. Tapon
hpo^{KC202} mutant		N. Tapon
dm^4 mutant		Bloomington Stock Center
Dpn::GFP		AG Berger and C. Cabernat
	UAS lines	
UAS-*yki*^{S168A}	w*; P{UAS-yki.S168A.V5}attP2	Bloomington Stock Center
UAS-*crb*	w^*; P{UAS-crb.wt}30.12e	Bloomington Stock Center
UAS-*wts*		N. Tapon/ G.Halter
UAS-*hpo*		N. Tapon/ G.Halter
UAS-*myrPKB*		Bloomington Stock Center
UAS-*dMyc*	w^{1118}; P{UAS-Myc.Z}132	Bloomington Stock Center
	Gal4 lines	
insc-Gal4	*w*; *insc*-Gal4;	AG Berger
repo-Gal4	*w*;; *repo*-Gal4	AG Berger
ase-Gal4	*w*; *ase*-Gal4;	AG Berger
	Balancer line	
4x Balancer	; PM/CyO; CxD/Tm6b	O. Vef

3.2.2 Ectopic gene expression

3.2.2.1 The *Gal4*/UAS system

The *Gal4*/UAS system (Brand and Perrimon, 1993) was utilized for tissue specific overexpression or knockdown of target genes. This expression system consists of two components, which originally derives from the yeast *Saccharomyces cerevisiae* transcriptional machinery: the transcriptional activator Gal4 and its target sequence, the "upstream activating sequence" (UAS) (Fig. 5). The *Gal4* gene is placed under the transcriptional control of an endogenous enhancer on a transposable element (P-element); this P-element is carried by transgenic flies (driver strain or *Gal4*-strain). The second component of this system is carried by so called reporter-strains, which possess several UAS sequences upstream of the transgene of interest. This system allows analysing the function of a specific gene (via overexpression or RNAi) in a tissue or cell type specific manner, at a certain developmental time.

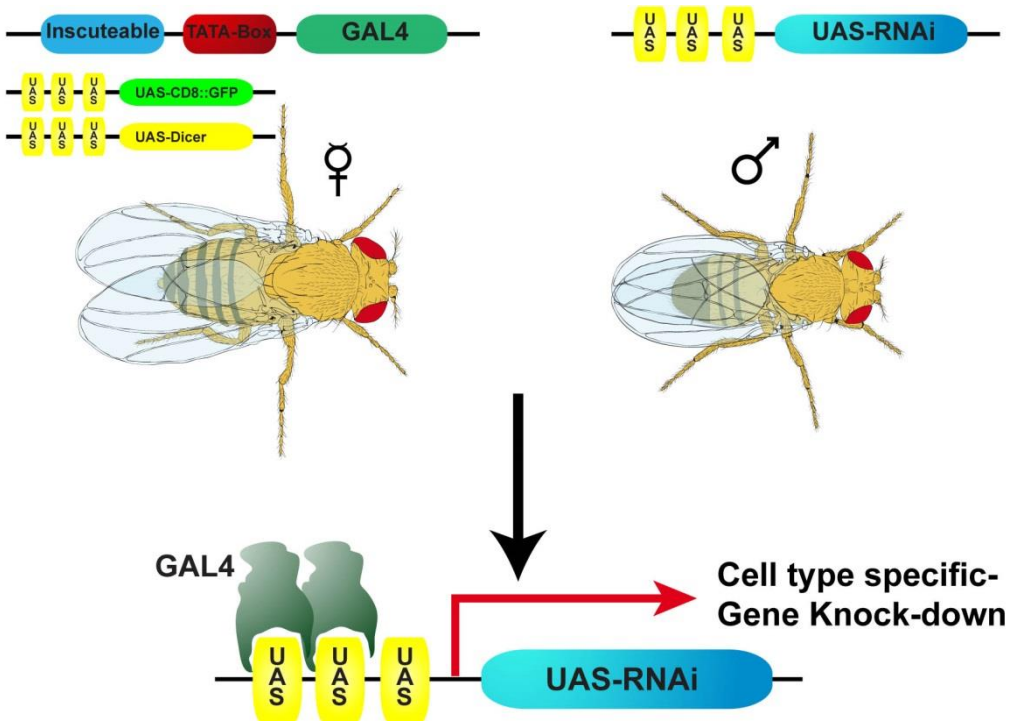

Figure 5: The *insc*Gal4/UAS system. Flies of the *Gal4*-strain express the transcriptional activator Gal4 under the control of a cell type specific enhancer. Female virgins of this *Gal4*-strain are crossed with males of the reporter-strain, which carry the transgene of interest (e.g. a specific RNAi construct) downstream of several UAS sequences. In the progeny of these flies (F1 generation), the Gal4 protein can bind to the UAS sequences and thereby drive the transcription of the transgene of interest. Kindly provided by Dr. C. Berger.

3.2.2.2 Genetic crosses

The majority of the presented fly combinations make use of the UAS-*Gal4* system (Brand and Perrimon, 1993), allowing for tissue specific expression of transgenes. To set up crosses between two different fly strains (driver strain and reporter strain), freshly hatched female virgins of one strain were collected every 3 hours at 25°C. These flies were then crossed to males of the other strain and then allowed to mate for at least three days. The following *Gal4* driver strains were used: *insc*-Gal4>UAS-CD8::GFP driving expression in type I, type II and INPs in the CNS (Betschinger *et al*., 2006; Neumüller *et al*., 2011) and *repo*-Gal4>UAS-CD4::GFP driving expression in all glial cells except of midline glia (Sepp *et al*., 2001). For egg collections these crosses were placed on apple juice agar plates (see 3.2.1.2) overnight, larvae of the wanted genotype were then collected (using the GFP signal) and staged according to the experimental needs.

3.2.3 Immunohistochemistry

3.2.3.1 Preparation and fixation of *Drosophila* larval CNS

Freshly hatched *Drosophila* larvae are referred to as first instar larvae (L1 larvae). Due to the fact that they have already secreted a cuticula, which impairs the access of external agents like fixative or antibodies, they have to be dissected prior to fixation and staining. For this purpose the staged larvae were transferred from the apple agar juice plates into a well containing 1x PBS buffer. Using two forceps the *Drosophila* larvae were opened near the posterior third of the body, the anterior body part was inverted and all tissues except for the CNS were removed. After dissection of the larval CNSs, they were transferred into 0.5ml Eppendorf tubes containing 200µl of 1x PBS. For fixation the PBS was discarded and replaced by the fixation solution (PEM buffer/PBL with 4% PFA), the CNSs were incubated for 30 minutes at room temperature on a shaker. After the CNS's have settled to the bottom of the tube the fixation solution was removed and replaced by PBT, this procedure was followed by 3 washing steps with PBT for 5 minutes at room temperature.

3.2.3.2 Immunofluorescence antibody staining of *Drosophila* CNS

After the washing steps the fixed CNSs were incubated overnight at 4°C in 200µl of PBT containing the primary antibodies of choice (table 2). Afterwards the CNSs were washed 3 times for 5 minutes in PBT and incubated in 200µl of PBT containing the secondary antibodies of choice (see table 3) for 1.5 hours at room temperature on a shaking device. Finally, the CNSs were washed 2 times for 15 minutes in PBT and 2 times in PBS at room temperature before they were mounted in 10µl of the mounting medium Vectashield® and then stored at 4 °C. For analysis of the staining, the CNSs were transferred onto a microscope slide in a drop of Vectashield® and fine dissected; the preparations were covered and sealed with nail polish. The stained preparations were scanned and analysed using fluorescence or a confocal microscope (Leica TCS SP5).

3.2.4 Image acquisition and processing

Confocal images were acquired on a Leica TCS SP5 confocal laser-scanning microscope using 63x glycine immersion objective lens. Images of the fixed samples were acquired at room temperature. All images represent single confocal sections. Images were processed using the Leica LAS AF Lite software, Adobe Photoshop CS4 and Adobe Illustrator CS4. Cell size measurements and pH3-cell counts were conducted using the Leica LAS AF Lite software; statistical analysis was done using SigmaPlot 11.0 and Microsoft Exel.

3.2.5 Polymerase chain reaction (PCR)

The polymerase chain reaction (developed by Kary Mullis) is used to amplify specific DNA fragments of a particular DNA sequence. In this technique the size of the DNA fragment is limited by two oligo-nucleotides (primers), which bind to the 5`- or respectively to the 3`- end of the particular sequence. The polymerase binds these oligo-nucleotides and starts the synthesis of DNA. A conventional PCR reaction requires the following components: oligonucletides (Primer), a heat stable DNA polymerase (*Taq* polymerase), deoxynucleoside triphosphates (dNTP's), magnesium, which is added in form of magnesium chloride ($MgCl_2$),

sulfate anions and the template DNA. The used *Taq* polymerase, isolated from the bacterium *Thermus aquaticus*, has a temperature optimum at around 70°C. Each cycle of the PCR can be subdivided into three main steps. First the denaturation step resulting in separation of the complementary template DNA strands. In the next step, lowering the temperature allows the primers to anneal to the complementary regions in single-stranded DNA template and afterwards the DNA-polymerase can bind to the primer-template DNA hybrid. During the third, the elongation step, the *Taq* polymerase synthesizes a new DNA strand complementary to the DNA template. Every cycle leads to an exponential amplification of the DNA fragment.

3.2.6 Gel electrophoresis

Gel electrophoresis is a technique used to separate DNA molecules in an electric field. The isolation of the different DNA fragments depends on the size and the shape of the molecule, the applied voltage or the qualities of the gel itself. For the electrophoresis we used a 1% agarose gel, agarose is a polysaccharide which is incorporated in electrophoresis buffer (1x TAE), 1 gram in 100ml buffer. The agarose was solubilized by boiling it in the microwave, before heat dissipation 1,25µl of GelRed™ were added. GelRed™ is a dye, which intercalates into the DNA and fluoresces under UV-light. In the next step the agarose gel was covered completely with 1x TAE buffer. DNA loading dye was used in order to visualize the migration of the DNA during the electrophoresis. The applied voltage, used for the separation of DNA molecules, amounts to 80-100V, because nucleic acids are negatively charged they migrate towards the cathode. At the end the agarose gel was analysed with an ultraviolet lamp and pictures from the gel were taken.

3.2.7 cDNA Synthesis for SYBR green based qRT-PCR

The first-strand cDNA synthesis was performed using the iScript Advanced cDNA Synthesis Kit (Bio-Rad, Cat. No. 172-5037). Firstly the following components were added into a novel reaction tube:

5x iScript advanced reaction mix	4µl
iScript advanced reverse transcriptase	1µl
Nuclease-free water	10µl
Total RNA	5µl
Total volume	20µl

The whole reaction mix was incubated in a thermal cycler using the following protocol:

Reverse transcription	30 min at 42°C
RT inactivation	5 min at 85°C

The generated cDNA can be directly used for PCR reactions or can be stored at -20°C.

3.2.8 SYBR green based quantitative Real-Time PCR (qRT-PCR)

This method is used in order to amplify and contemporaneously quantify a specific DNA fragment and is based on the standard polymerase chain reaction. The real time polymerase chain reaction allows us to observe the amount of amplification product generated during the course of the reaction. In order to implement that, this procedure requires a fluorescent reporter that binds the newly formed amplification product to display its presence through fluorescence, namely SYBR Green. SYBR Green is an asymmetrical cyanine dye, which binds preferably to double stranded DNA, this SYBR Green-DNA complex absorbs blue light (λ_{max} = 497 nm) and emits green light (λ_{max} = 520 nm). The fluorescence of this reporter increases together with the quantity of double stranded DNA formed in the course of this procedure. The qRT-PCR experiments were performed in a 96 well format (Bio-Rad; Cat. No.MLL9601). The reaction conditions were as follows: 40 cycles of 95°C for 3 seconds denaturation and 60°C for 30 seconds annealing and extension. The reaction mix was made with 10µl of SYBR Green supermix, 0,1µl forward primer, 0,1µl reverse primer, 10µl cDNA (10ng/µl). All reactions were done in triplicates. The instrument used was the StepOnePlus PCR system from Applied Biosystems and the software utilized for analysis was the StepOne v2.3.

3.2.9 Fluorescence activated cell sorting (FACS)

To purify *Drosophila* NSCs (2h ALH, 24h ALH) via flow cytometry we applied the protocol according to Berger *et al*. (2012). *Drosophila* larvae were collected and washed once in PBS and once in 70% ethanol, finally we dissected the larval brains in supplemented Schneider's medium (10% fetal bovine serum, 2% Pen/Strep, 0.04mg/ml glutathione, Schneider's medium; GIBCO). The brains were collected in 1.5ml Eppendorf tubes and washed twice with Rinaldini's solution (Ceron *et al*., 2006) after the supernatant was discarded 500µl of enzyme cocktail (450µl Rinaldini solution, 1mg/ml collagenase I and papain (Sigma Aldrich)) were added. The samples were incubated for 30 minutes at 30°C and then washed twice with Rinaldini's solution and supplemented Schneider's medium. Finally the tissue was disrupted in 200µl of supplemented Schneider's medium through vigorous pipetting and forced through a cell-strainer FACs tube (BD Falcon).

For NSCs purification via fluorescence the BD Bioscience FACS ARIA II Flow Cytometer was used, the cells were sorted with low pressure according to cell size and fluorescence (GFP intensity). The cells were sorted directly into lysis buffer of the Cells-to-CT™1-Step TaqMan® Kit (see 3.1.7).

3.2.10 Taqman assay

3.2.10.1 RNA isolation and first strand synthesis

The Cells-to-CT™1-Step TaqMan® Kit (Thermo Fisher, Germany, Cat. No. A25603) was used according to the manufacturer's instructions. 1000 NSCs from *Drosophila* larval brains (2h ALH, 24h ALH) were FACs purified (see 3.2.9) and the total RNA was used as a template for the reverse transcription reaction in 50µl volume. After dissection (see 3.2.3.1) the NSCs were immediately sorted into 50µl of lysis solution, mixed gentle through pipetting and incubated at room temperature for 5 minutes. To the samples 5µl of stop solution was added and mixed accurately. The probes were incubated for 2 minutes at room temperature and then stored at -20°C. The reverse transcription reaction was performed as followed: RT step of 50°C for 5 minutes and the inactivation step on 95°C for 20 seconds.

3.2.10.2 Experimental set up

As a template for the Real-time PCR experiments 2µl of the first strand reaction mix were utilized. All the samples to be prepared were processed in parallel. For these experiments the primer probe mix was obtained from Applied Biosystems (Darmstadt, Cat. No. 4351372). The Probe in the primer probe mix from Applied Biosystems had a FAM fluorescent dye at its 5' end and a non-fluorescent quencher in the 3' position. PCR reactions were performed in 96 well plates (Bio-Rad; Cat. No.MLL9601) covered with optical adhesive covers (Applied Biosystems; Cat. No.4311971). The reaction conditions were as follows: 40 cycles of 95°C for 15 seconds denaturation and 60°C for 1 minute annealing and extension. The reaction mix was made with 5µl of TaqMan®1-Step qRT-PCR Mix, 1µl of primer/probe mix, 2µl of Lysate and 12µl of Nuclease-free water. All reactions were done in triplicates. The instrument used was the StepOnePlus PCR system from Applied Biosystems.

3.2.11 Transfection of HEK-293 cells

Transfections were performed in 6 well plates using the FuGENE® transfection reagent (Promega, Cat. No. E2311) according to the manufacturer's instructions. Shortly before transfection $8x10^4$ Human Embryonic Kidney cells (HEK-293) cells were seeded on every required well in 1ml of DMEM medium, containing 1% penicillin/streptomycin mixture and 10% heat inactivated fetal bovine serum (FBS). The cells were incubated under normal growth conditions (37°C and 5% CO_2). On the day of transfection the adequate amount of DNA (pmirGLO constructs 350ng; scramble or pEZX-MR04 (bantam expression) vector 650ng; pEGFP-c3 vector 1000ng) was added to 100µl of culture medium. Then 3µl of the FuGENE® Transfection Reagent were added to the dissolved DNA and mixed thoroughly by pipetting. The following incubation of the samples was performed at 25°C for 20 minutes in order to allow the formation of transfection complexes. For the transfection of the HEK-293 cells the newly formed complexes were added drop-wise onto the cells. Finally to ensure the uniform distribution of the complexes the cultures were gently agitated. The incubation of the cells was performed under normal growth conditions for the appropriate period of time (48h).

3.2.12 Luciferase assay

After transfection and incubation, the cells were washed with 400µl of 1x PBS for 30 seconds three times. Finally the cells were re-suspended in 180µl of 1x PBS and scraped free from the wells with a rubber policeman. The cell suspension was transferred into a novel reaction tube and pipetted in triplicates of 50µl on a 96 well plate. For the measurement of the Firefly Luciferase activity 50µl of the Dual-Glo®Luciferase assay reagent was added to the cells and incubated for 10 min at room temperature in the dark. The Firefly Luciferase activity was measured using a tecan reader. For the measurement of the Renilla Luciferase activity 50µl of the Dual-Glo®Stop and Glo® reagent was added to the cells and incubated for 10 min at room temperature in the dark. The Renilla Luciferase activity was measured using a tecan reader.

3.2.13 Statistics

All the obtained data was analysed with SigmaPlot 11.0 (Systat Software Inc.). Asterisks are used to indicate statistical significance of the presented results (* = $p < 0.05$; ** = $p < 0.01$; *** = $p < 0.005$; ns = $p > 0.05$).
The raw data from all shown statistics can be found in the Supplements (Supl. 8.2).

4. Results

4.1 The role of Salvador/Warts/Hippo signalling in maintaining NSC quiescence in the CNS of *Drosophila melanogaster*

Despite the obvious importance of NSC quiescence for the correct development of the CNS of *Drosophila melanogaster*, only a very general overview of this developmental stage has been provided until now (Chell and Brand, 2010; Sousa-Nunes et al., 2011; Spéder *et al*., 2014; Ebens *et al*., 1993). These studies mainly focused on the exit of NSCs from quiescence and showed that this developmental process is orchestrated by diverse signalling modules, which are unified by a variety of internal and external factors. They identified molecular cues which turned out to be necessary for reactivation of quiescent NSCs, like for example the feeding dependent FDM (see 1.1), which triggers the Insulin signalling in NSCs via glial cells, which translate this organismal signal into a local activating instruction (Chell and Brand, 2010; Sousa-Nunes *et al*., 2011). However, a mechanistic analysis of the maintenance of quiescence and the responsible factors has not been made until now, although it would be an important foundation for further research concerning the regulation of cellular quiescence in *Drosophila* NSCs. Therefore I have performed an RNAi screen to unravel factors which are involved in the regulation of NSC quiescence at early larval stages; in the course of this screen I identified the SWH pathway.

Four approaches were taken during my thesis work in order to gain insight into the role of the highly conserved SWH signalling in the maintenance of NSC quiescence during the development of the central nervous system:

- Identifying the role of SWH signalling pathway core components for the maintenance of NSC quiescence, using *insc*G4 driven gene knockdown, and subsequent comparison of the NSC cell size and the mitotic status in wild type and mutant animals (conducted by myself).
- Analysis of the NSC specific target genes of the SWH pathway using antibody stainings and GFP constructs (conducted by myself).
- Examination of numerous upstream components known to regulate the activity of the SWH pathway, and the developmentally regulated expression pattern of these regulators in NSCs and glial cells, with antibody stainings and GFP constructs (conducted by Kevin Weynans in the course of his master thesis and myself).

- Exposure of a potential negative feedback loop in the regulation of the SWH signalling pathway using the luciferase assay system (conducted by Dr. Thomas Löffler and myself).

The concerted efforts on this part of my work resulted in the publications:

- *Nat. Commun*. 7:10510 doi: 10.1038/ncomms10510 (2016).
- *Cell Cycle* doi:10.1080/15384101.2016.1171653 (2016)

4.2 Targeted mini-screen for factors regulating NSC quiescence and reactivation

In order to identify novel regulators of quiescence and reactivation in *Drosophila* NSCs, I depleted known growth regulators using RNAi-mediated gene knockdown in the NSC specific *insc*GAL4 pattern. I stained NSCs using an antibody against Deadpan (Dpn) and measured the proliferation rate using an antibody against phosphohistone H3 (pH3). Dpn is a transcription factor which is exclusively expressed in NSCs and the mature INPs of the type II lineages, during all larval stages the CNS exhibits a stereotyped pattern of Dpn expression. Histones are highly alkaline proteins that packages and thereby order DNA into structural units and are an important starting point for gene regulation. *Phosphorylation* at a highly conserved serine residue (Ser-10) in the *histone H3* tail is considered to be a crucial event for the onset of mitosis (Crosio *et al*., 2002) on account of this I used this histone modification as a hallmark for proliferation. The first candidates tested for this approach were the transforming growth factor beta (TGF-ß) receptor baboon (babo) and the transcription factor Stat92E, which both caused no growth or reactivation phenotypes in the larval CNS (Fig.6A-C).

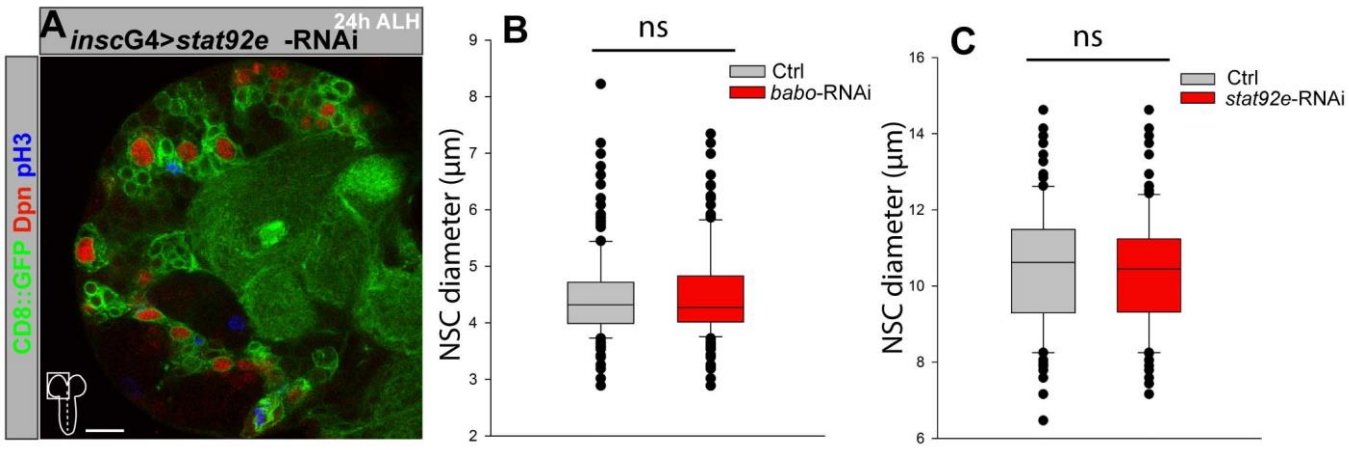

Figure 6: Loss of babo or stat92e causes no reactivation phenotypes in Drosophila NSCs. A) NSC-specific loss (*insc*G4>UAS-CD8:: GFP) of *stat92e* results in naturally reactivated NSCs after 24h ALH. (**B, C)** Quantification of NSC diameters after loss of *babo* (4h ALH) **(B)** and *stat92e* (24h ALH) **(C)**. **(B)** Wild type brains: median 4,5µm (maximum 8µm) n= 150 NSCs (3 brain lobes); *insc*G4>UAS-*babo*-RNAi: median 4,5µm (maximum 7,5µm) n= 156 NSCs (4 brain lobes). **C)** Wild type brains: median 10,5µm (maximum 14,5µm) n= 109 NSCs (3 brain lobes); *insc*G4>UAS-*stat92e*-RNAi: median 10,5µm (maximum 14,5µm) n= 109 NSCs (4 brain lobes).Image is an single confocal section anterior up and scale bar represent 10µm.

Figure 6B and C clearly demonstrate that there is no significant divergence between the NSC cell diameters of *babo* and *stat92e* RNAi larvae and the respective wild type control brains. In the *babo* RNAi background the NSCs display a median cell diameter of 4,5µm at 4h after larval hatching (ALH), what corresponds to the natural size of these cells at this developmental stage (Fig. 6B). A comparable phenotype occurred after loss of the transcriptional activator Stat92E at 24h ALH (Fig. 6C); all NSCs have the same size like the wild type control NSCs, these data led me to the decision that these factors are not involved in the regulation of *Drosophila* NSC quiescence. The next potential factor implicated in NSC regulation I tested was the highly conserved kinase Hippo (*hpo*, see following).

4.2.1 Loss of the SWH signalling pathway core kinases leads to premature reactivation of NSCs

To begin investigations concerning the role of SWH signalling in maintaining NSC quiescence I compared the CNS morphology of wild type (wt) larval brains at 4 hours after larval hatching (ALH) and SWH signalling pathway core kinases (*hpo*, *wts*) knock down brains. At early larval stages, between 0 and 4 ALH, all wt NSCs are still quiescent and morphological small in size (4-5 µm in diameter) and non-proliferative (Fig. 7A, D-F). Exceptions to this rule are the four NSCs of the mushroom body (MBNBs) and one ventrolateral NSC (lNSC) that do not enter quiescence, have a large cell diameter and constantly proliferate (see Figure 7A).

NSC specific loss of the SWH signalling resulting from the knock down of the core kinase hippo induces a dramatic premature increase in NSC cell size from a median of 4.5µm (maximum 6.5µm) in control brains 4h ALH to a median of 7µm (maximum 13µm) in the knock down brains (Fig. 7B, E). I also examined a significant increase in the proliferation rate of the affected tissue due to the loss of SWH signalling in NSCs (Fig. 7D). For the

measurement of the cell sizes I used the membrane bound GFP staining of the *insc*G4>UAS-CD8::GFP driver line. To ensure that this premature growth phenotype is de facto related to loss of SWH signalling I also ablated the second core kinase warts and discovered an intriguing resemblance of the phenotypes. The median NSC diameter in this genetic background was 7µm (maximum 14µm), furthermore the number of actively proliferating NSCs was even higher compared to loss of the Hpo kinase (Fig. 7C, D, F). In order to verify that these observations are not due to an impaired entry into quiescence during late embryonic stages, I generated

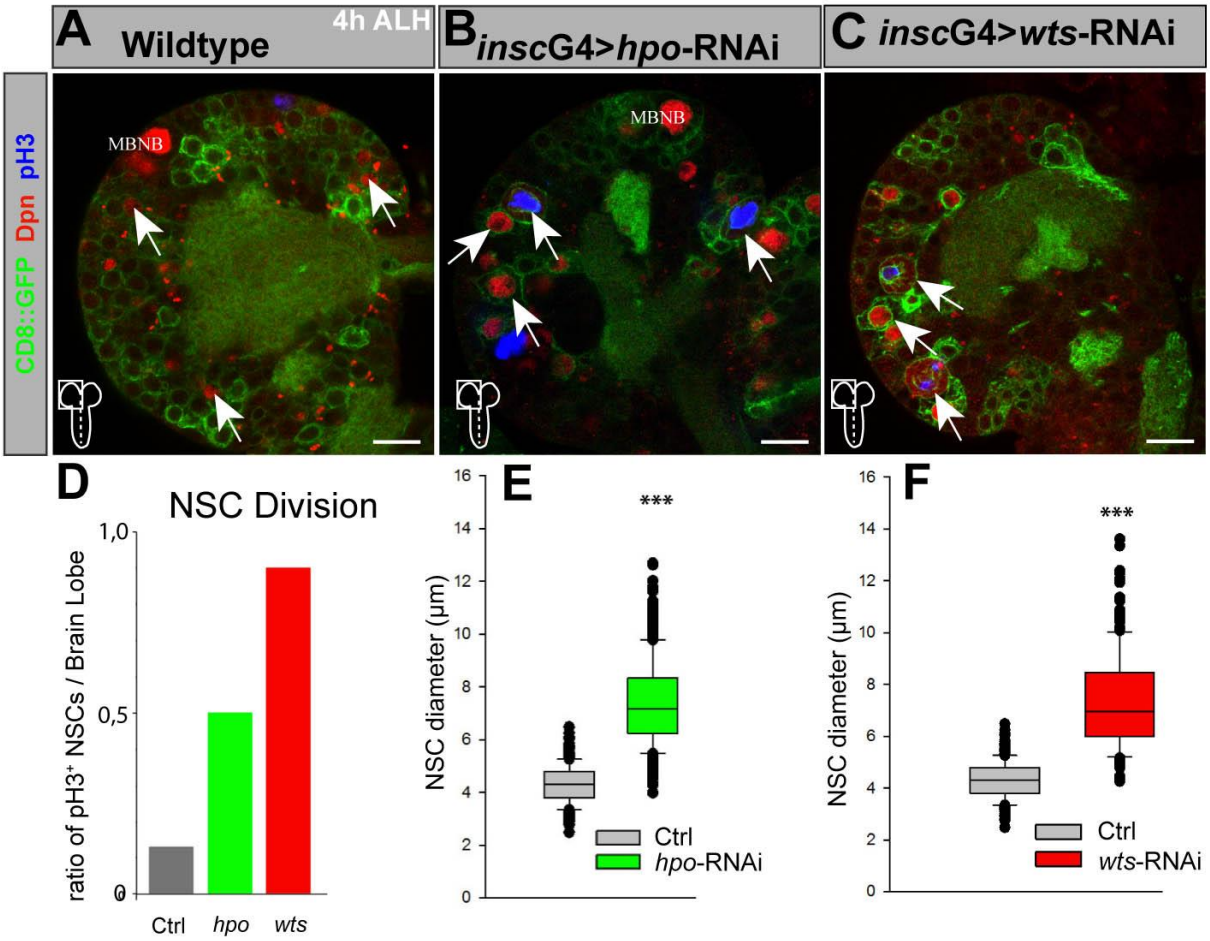

Figure 7: SWH maintains quiescence in larval NSCs. **(A)** Wild type larval brain lobe (*insc*G4> UAS-CD8::GFP) 4h ALH. Quiescent NSCs are small in cell size. Only the NSCs of the mushroom body (MBNB) are big in cell size. No $pH3^+$ NSCs can be observed. **(B-C)** NSC-specific RNAi (*insc*G4>UAS-CD8::GFP and respective construct) of *hippo* (*hpo*)**(B)** and *warts* (*wts*)**(C)** leads to premature cell growth and cell division of NSCs. Arrows depict examples of significantly enlarged NSCs. **(D)** Number of NSCs in mitosis ($pH3^+$) at 4h ALH per brain lobe in wild type (7 brain lobes) and *hpo*-RNAi (11 brain lobes) and *wts*-RNAi (5 brain lobes). **(E-F)** Quantification of the NSC diameters for *hpo* and *wts* RNAi 4h ALH. Wild type brains 4h ALH: median 4,5µm (maximum 7,5µm) n= 355 NSCs (7 brain lobes). **(E)** *insc*G4>*hpo*-RNAi: median 7µm (maximum 13µm) n= 575 NSCs (11 brain lobes). **(F)** *insc*G4>*wts*-RNAi: median 7µm (maximum 14µm) n= 236 NSCs (5 brain lobes). All images are single confocal sections anterior up and scale bars represent 10µm.

a trans-heterozygous *hpo* mutant (*hpo*^{JM1}(Jia *et al*., 2003)/*hpo*^{KC202}(Udan *et al*., 2003)) fly stock and analysed cell size and proliferation rate at two different time points after larval hatching (0-2h ALH and 4h ALH). The *hpo*^{JM1} allele introduces a single amino acid substitution at the conserved residue 181 (G181E), which results in a kinase dead allele. The *hpo*^{KC202} allele on the other hand produces an Hpo protein which is truncated after its kinase domain and is thereby affecting the dimerization domain which is necessary for the interaction with the scaffold protein Sav. Both *hpo* mutant alleles showed similar overgrowth phenotypes in previous studies (Jia *et al*., 2003, Udan *et al*., 2003). In this trans-heterozygous situation the NSCs do not show increased cell diameters or proliferation rates at 0-2h ALH (Fig. 8C, E), revealing an accurate entry into quiescence. Interestingly, these *hpo* trans-heterozygous mutant larvae exhibit a significant increase in cell size at 4h ALH mimicking the reactivation phenotype in *hpo* and *wts* RNAi (Fig. 7E, F) with a median cell diameter of 6,5µm and a maximum diameter of 9,5µm (Fig. 8D, E). To complement these experiments I analysed *Drosophila* stage 17 embryonic brains of *wts* RNAi and found that there is no increase in NSC cell size (Fig. 8A, B). These data equally show that the premature reactivation phenotypes obtained after *hpo* and *wts* RNAi are not due to an impaired entry into quiescence but are rather related to an incorrect maintenance of this cellular status.

To further determine the point at which SWH signalling is needed for normal CNS development I used the GAL4 repressor system Gal80 to restrict the RNAi construct expression to only larval stages. For this temporally controlled RNAi experiment I used the temperature-sensitive Gal80^{ts} mutant, which is active at 18°C but does not repress Gal4 activity at 29°C due to conformational changes (Ma *et al*., 1987; McGuire *et al*., 2004). In these larvae the transcription factor Gal4 is inhibited through its repressor Gal80 in a temperature-sensitive manner during embryonic phases (at 18°C), but an elevation of the temperature to 29°C during larval stages activates the Gal4 driven RNAi expression. The data reveals that the loss of both core kinases exclusively during larval stages is sufficient to prematurely reactivate NSCs at 4h ALH. The median NSC diameter of *hpo*- and *wts*-RNAi exclusively during larval stages is 7µm (maximum 11µm), which resembles the cell growth phenotypes obtained after knock down of these factors during the whole development until dissection (Fig. 8F).

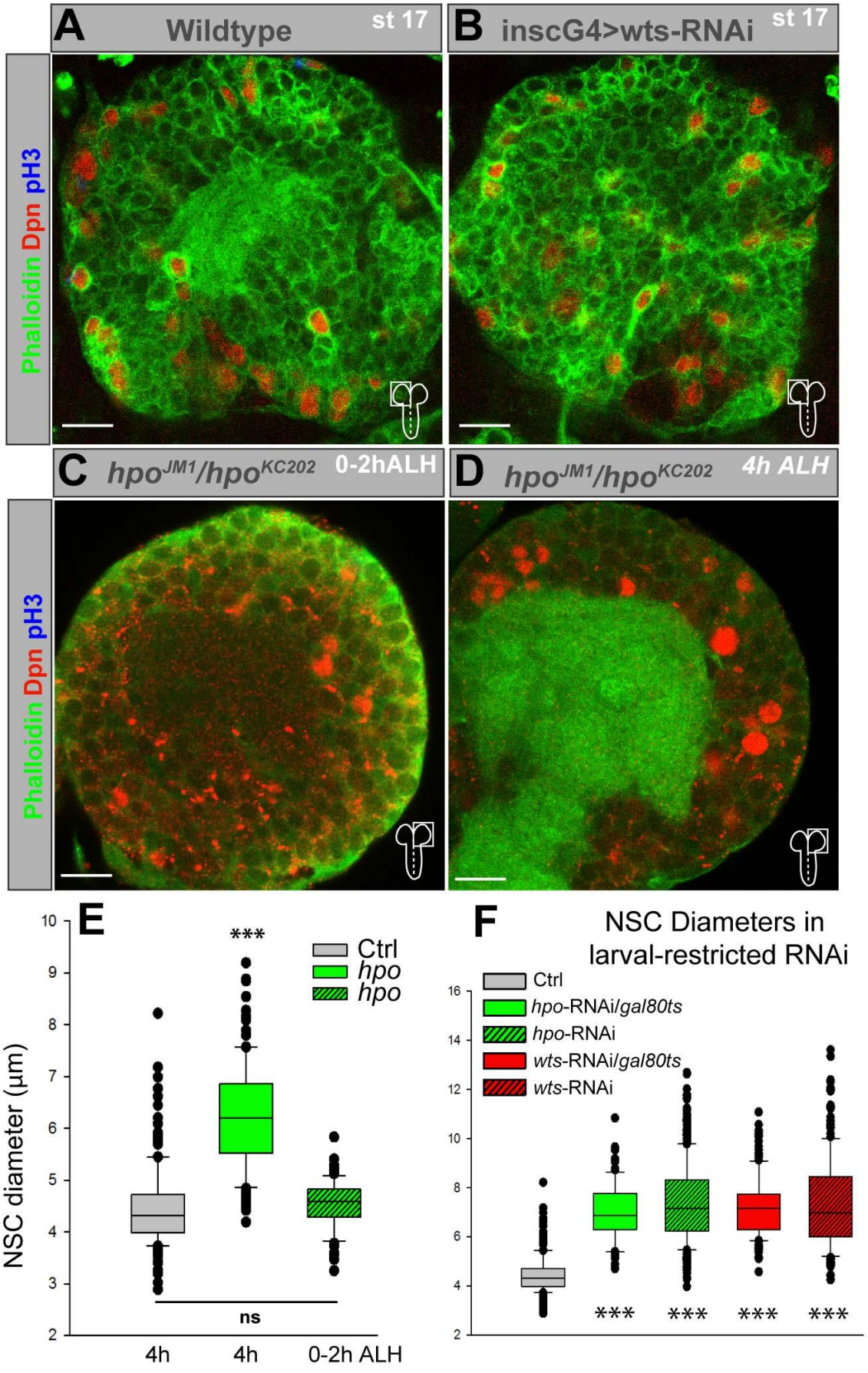
A Wildtype st 17
B inscG4>wts-RNAi st 17
Phalloidin Dpn pH3
C hpoJM1/hpoKC202 0-2hALH
D hpoJM1/hpoKC202 4h ALH
Phalloidin Dpn pH3
E
NSC diameter (µm)
***
Ctrl
hpo
hpo
ns
4h
4h
0-2h ALH
F
NSC Diameters in larval-restricted RNAi
Ctrl
hpo-RNAi/gal80ts
hpo-RNAi
wts-RNAi/gal80ts
wts-RNAi
***
***
***
***

Figure 8: Premature reactivation of NSCs after loss of SWH signalling is not due to impaired entry of quiescence. (A, B) Upon *wts*-RNAi with the *insc*G4>UAS-CD8::GFP driver at 25°C no increase in cell size or mitosis can be observed in NSCs at embryonic stage 17. Entry into quiescence is not impaired. **(C, D, E)** Quantification of NSC diameters in hpo^{JM1}/hpo^{KC202} (*hpo* in figure) trans-heterozygous mutants at 0-2h ALH **(C, E)** and 4h ALH **(D, E)**. **(E, F)** Wild type brains 4h ALH: median 4,5µm (maximum 8µm) n= 150 NSCs (3 brain lobes); hpo^{JM1}/hpo^{KC202} 0-2h ALH: median 4,5µm (maximum 6µm) n= 65 NSCs (2 brain lobes); hpo^{JM1}/hpo^{KC202} 4h ALH: median 6,5µm (maximum 9,5µm) n= 121 NSCs (3 brain lobes). (**F**) Quantification of NSC diameters of larval-restricted RNAi using the $GAL80^{ts}$ system of *hpo* and *wts*. *hpo*-RNAi: median 7µm (maximum 11µm) n= 172 NSCs (8 brain lobes); *wts*-RNAi: median 7µm (maximum 11µm) n= 120 NSCs (10 brain lobes). For comparison *hpo*- and *wts*-RNAi measurements without $GAL80^{ts}$ are added (see Fig. 6). All images are single confocal sections anterior up and scale bars represent 10µm.

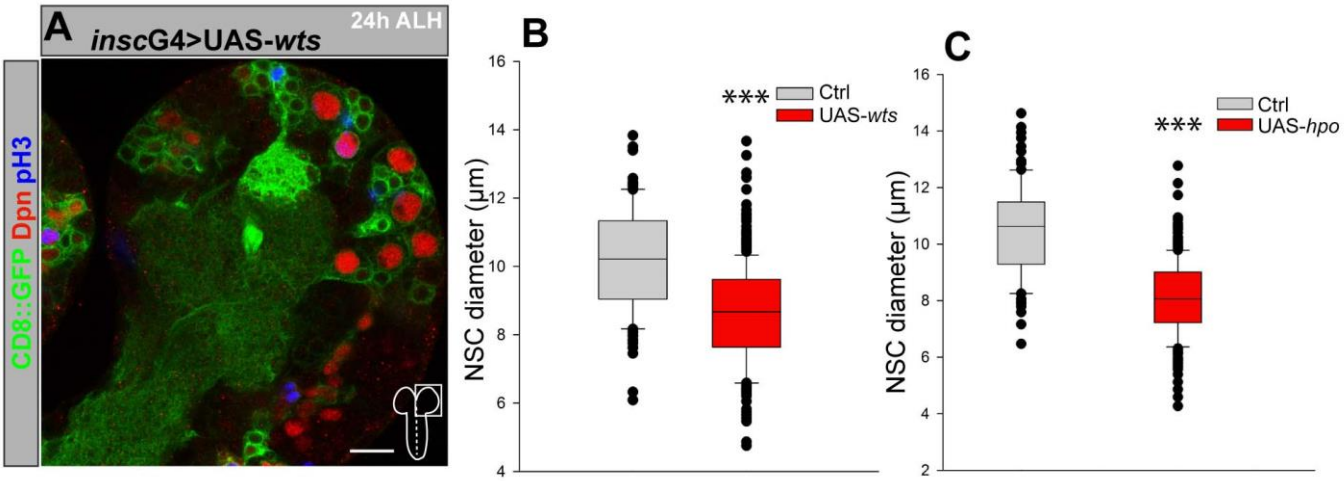

Figure 9: Ectopic expression of Hpo or Wts causes decreased NSC diameters. (A) NSC-specific overexpression (*insc*G4>UAS-CD8::GFP) of *wts* does not prolong quiescence. **(B, C)** Quantification of NSC diameters after *wts* **(B)** and *hpo* **(C)** overexpression. **(B)** Wild type brains 24h ALH: median 10,5µm (maximum 14µm) n= 100 NSCs (3 brain lobes); *insc*G4>UAS-*wts* 24h ALH: median 9µm (maximum 14µm) n= 287 NSCs (6 brain lobes) **(C)** Wild type brains 24h ALH: median 10,5µm (maximum 14µm) n= 109 NSCs (3 brain lobes); *insc*G4>UAS-*hpo* 24h ALH: median 8µm (maximum 13,5µm) n= 311 NSCs (7 brain lobes). Image is single confocal section anterior up and scale bar represent 10µm.

To check whether it is possible to prolong the quiescence phase of NSCs via modulation of the SWH signalling I ectopically expressed the two core kinases of this pathway Hpo and Wts. As can be seen in figure 9 overexpression of both kinases in NSCs does not prolong the quiescence phase of these cells but causes significantly reduced cell diameters at 24h ALH compared to the wild type situation. Control NSCs at 24h ALH have a median cell diameter

of 10,5µm (maximum 14µm), while NSCs with ectopic expression *wts* and *hpo* display a median cell diameter of 8,5µm (maximum 14µm) (Fig. 9B, C).

Taken together these data indicate that the highly conserved SWH signalling pathway is involved in the regulation of NSC quiescence.

4.2.2 Yki is cytoplasmic during quiescence and translocates to the nucleus during reactivation

If the SWH signalling pathway is necessary for maintaining NSC quiescence, the main effector Yki should be phosphorylated and excluded from the nucleus during this resting phase. According to my theory I should observe a translocation of Yki into the nucleus after reactivation. Antibody staining against Yki protein revealed a differential localization in quiescent, nutrition-depend NSCs (cyan clue circles) and in MBNBs (yellow circles) at 4h ALH. In quiescent NSCs Yki is sequestered to the cytoplasm of the cell and there is no nuclear staining at all, whilst the continuously proliferating MBNBs exhibit a strong nuclear staining against Yki already at 4h ALH (Fig. 10A). In contrast, after reactivation at 24h ALH a clear nuclear localization of Yki protein in all NSCs (white circles) can be detected (Fig. 10B). Since *wts*-RNAi caused premature reactivation of NSCs at 4h ALH, I tested for premature nuclear localization of Yki protein in the affected cells. I could monitor an increase in Yki protein levels in the whole CNS as well as a nuclear localization in NSCs that display an increase in cell diameter which are marked with white circles (Fig. 10C). For all pictures the lower panel shows the yki antibody staining in monochrome.

Another crucial factor for the localization of Yki protein is 14-3-3ζ (14–3–3zeta), which is a member of the conserved 14-3-3 family of regulatory proteins that are expressed in every eukaryotic cell. Phosphorylated Yki binds to 14-3-3ζ and is retained in the cytoplasm (Ren *et al*., 2009), therefore I tested whether the loss of this regulatory protein has an impact on NSC reactivation. Indeed I observed premature growth of the NSCs at 4h ALH presumably owing to regulatory defects during the process of Yki localization (Fig. 10D, E). The measured median cell diameter is 6µm (maximum 10,5µm) instead of 4,5µm in the wild type situation (Fig. 10E).

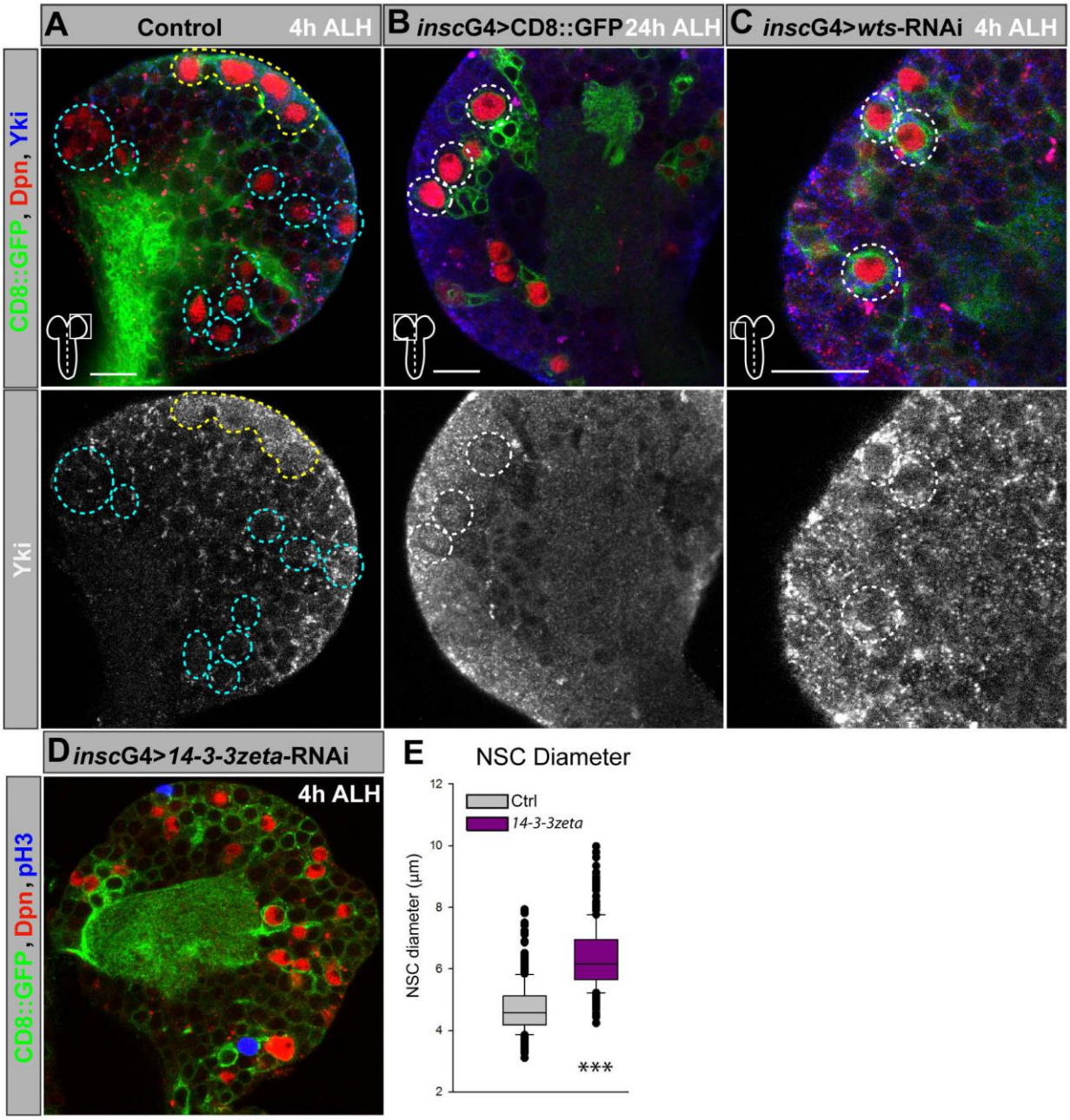

Figure 10: Yorkie is cytoplasmic during quiescence and translocate into the nucleus during reactivation of NSCs. (A-C) Subcellular localization of Yki in quiescent NSC at 4h ALH **(A)** (cyan blue circles, yellow circles show non-quiescent MBNBs), in reactivated NSCs at 24h ALH **(B)** (white circles) and in prematurely reactivated NSCs of *wts*-RNAi at 4h ALH **(C)** (white circles). Lower panels show only the Yki channel in monochrome. Circles depict examples of NSCs. **(D)** NSC-specific RNAi of *14-3-3ζ* leads to premature growth of NSCs at 4h ALH. **(E)** Quantification of NSC diameters in wild type and *14-3-3ζ* RNAi at 4h ALH. Wild type brains 4h ALH: median 4,5µm (maximum 8µm) n= 347 NSCs (7 brain lobes); *insc*G4>*14-3-3ζ* RNAi 4h ALH: median 6µm (maximum 10,5µm) n= 250 NSCs (5 brain lobes). All images are single confocal sections anterior up and scale bars represent 10µm.

In an attempt to quantify the amount of *yki* mRNA transcript levels at the different developmental stages I FACS sorted 1000 NSCs of the larval CNS at two different developmental time points (0-2h ALH and 24h ALH) using flies which carry 3 copies of a

Dpn::GFP construct. For quantification I used the Taqman® gene expression cells-to-Ct technique with *yki* specific primers/probes and showed that there actually is a massive upregulation of *yki* transcript after reactivation at 24h ALH (yellow lines) compared to freshly hatched larvae at 0-2h ALH (red lines) (Fig. 11A). These results show that there is not only a translocation process of Yki in NSCs but also a transcriptional upregulation of this co-activator protein accompanying the reactivation process.

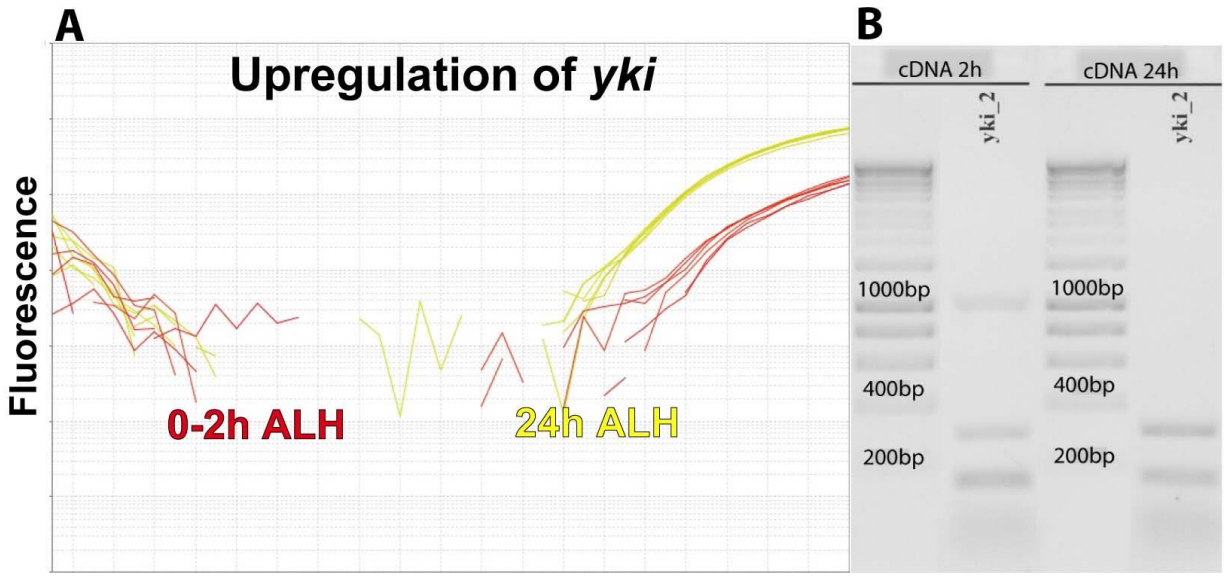

Figure 11: Yki is upregulated after reactivation of larval NSCs. (A) Upregulation of Yki after reactivation. Amplification plot of a Taqman qPCR experiment done with *yki* specific primers/probes on 1000 FACS purified NSCs from 0-2h ALH (red) and 24h ALH (yellow) larval CNS. At 24h ALH there is a significant upregulation of the yki transcript in comparison to the 0-2h ALH sample. **(B)** Existence of two distinct *yki* isoforms. The agarose gel indicates that there are two isoforms of the *yki* gene present in the cDNA of larval brains 2h and 24h ALH; the larger isoform (which runs approximately at 360 bp) seems to be enriched in the 24h old sample.

During the analysis of amplified *yki* transcript from cDNA of whole larval brains on an agarose gel, I found out that there are two distinct isoforms of the *yki* gene, which are present in both the 2h and the 24h old sample. The difference between both isoforms is the third exon (156 bp) of the *yki* gene, which is spliced out in the shorter *yki* variant. The gel further indicates that the long isoform of yki is slightly stronger expressed in the 24h old sample, while the short *yki* splice variant is enriched in the 2h old sample (Fig. 11).

4.2.2.1 Quantification of nuclear and cytoplasmic Yki localization

Considering the fact that Yki can occupy different cellular compartments (cytoplasm, nucleus) in order to fulfil its critical biological function I quantified more closely the ratio of

nuclear versus cytoplasmic Yki at different stages of development, to show that Yki is located in the cytoplasm during quiescence and is mobilized into the nucleus during reactivation. For the realization of the quantification process I measured the pixel intensities of an Yki antibody staining across the cell body (indicated by coloured lines in Fig. 12A, B) of selected NSCs in quiescence (qNSC) or non-quiescent NSCs (lateral NBs and MBNB) at 4h ALH (Fig. 12A) or reactivated NSCs (rNSC) at 24h ALH (Fig. 12B). In order to subdivide the cellular compartments into nucleus and cytoplasm I used an antibody staining against Dpn, the compartment with the highest pixel intensity in the Dpn channel (red) was defined as nuclear, the green channel (Phalloidin::GFP) was used as a membrane marker (outer cell membrane). In quiescent NSCs Yki protein is mainly localized in the cytoplasm of the cell (Fig.12A, C), the pixel intensities for Yki antibody (grey) are very low in the nuclear area (high Dpn, red) and the highest in the cytoplasm (no Dpn). The only exceptions to this rule are the non-quiescent NSCs of the mushroom body and the lateral NSC; they show nuclear localization of Yki already at 4h ALH (Fig. 12A).

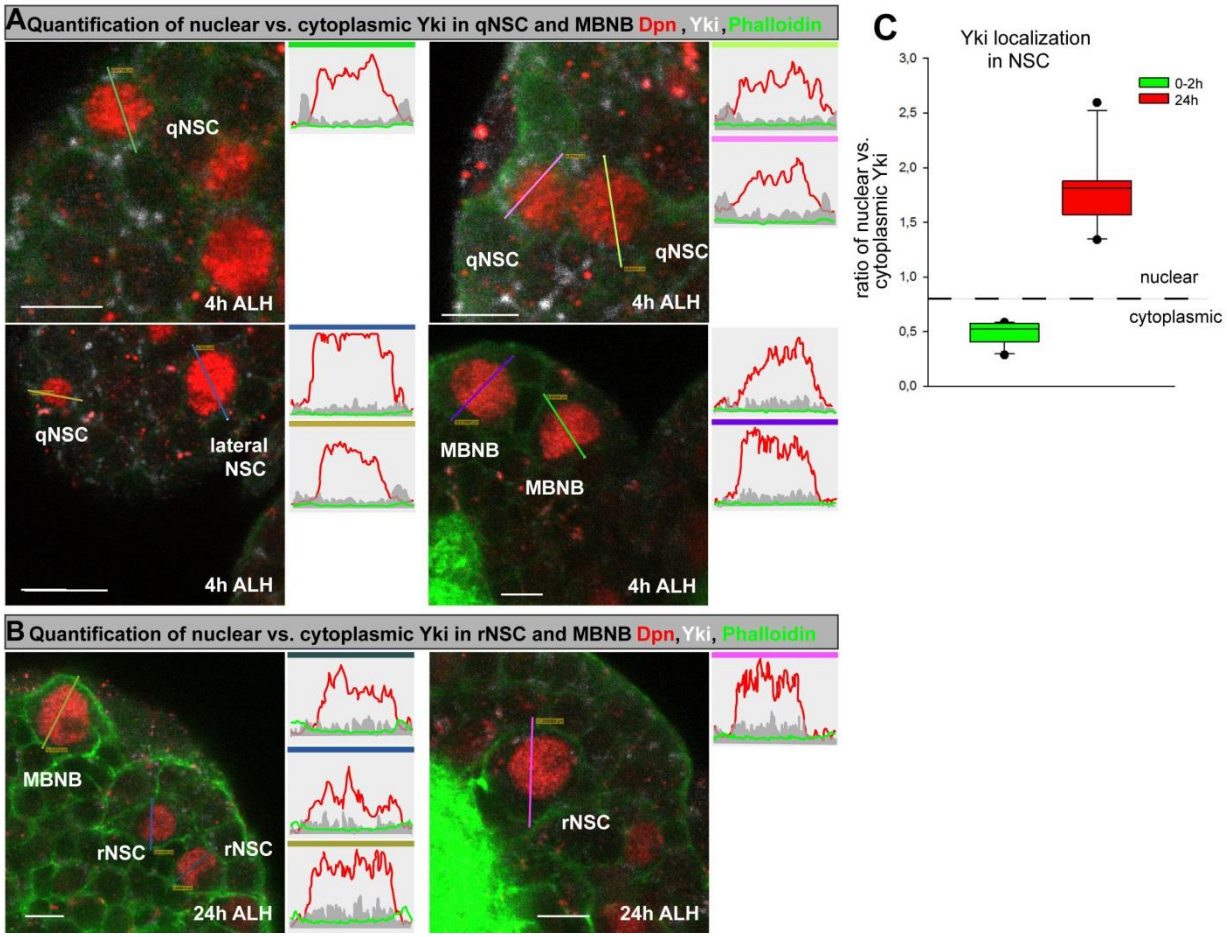

Figure 12: Quantification of the Yki nuclear and cytoplasmic signal in NSCs. (A, B, C) Representative images of measurements of Yki pixel intensities across the cell body (indicated lines) of individual NSCs in quiescence (qNSC) or non-quiescent NSCs (lateral NBs and MBNB) at 4h **(A)** or reactivated NSCs (rNSC) at 24h ALH **(B)**. The schematics to the right of each picture give the intensity measurement of the selected area (line) of each channel, red (Dpn, nucleus), green (Phalloidin, membranes) and dark grey (Yki). See methods for quantification procedure. All images are single confocal sections anterior up and scale bars represent 10µm. **(C)** The statistical analysis of the measured pixel intensities display a shift of the cellular localization of Yki protein from the cytoplasm to the nucleus upon reactivation.

In reactivated NSCs I detected a high pixel intensity of the Yki staining in the nuclei of these cells, indicating a higher concentration of Yki protein in this cellular compartment (Fig. 12B). For the statistical analysis the pixel intensities were averaged for each compartment and the ratio of the means was calculated as a measure for the relative amount of Yki protein per cellular compartment. These data clearly show a shift of Yki cellular localization from the cytoplasm towards the nucleus in reactivated NSCs and a higher proportion of Yki in the cytoplasm of quiescent NSCs (Fig. 12C).

4.2.2.2 Yki is necessary and sufficient for NSC reactivation

To further investigate the dependency of Yki for NSC reactivation I analysed an *yki* null mutation (yki^{B5}) and compared cell growth and proliferation in the mutant situation with wild type larvae (Fig. 13). Homozygous yki^{B5} mutants are embryonically semi-lethal and most larvae die at approximately 48h ALH. Wild type larval NSCs at 48h ALH have been reactivated, the median cell diameter is 11 µm and every NSC generated a huge lineage at this time point due to the fact that these cells are highly proliferative (Fig. 13A, D, E). In contrast to this in the yki^{B5} mutant the NSCs still appear unreactivated and resemble quiescent NSCs with a median cell diameter of 4,5µm and no indication of proliferation (Fig 13B, C, D, E). Another interesting feature of the yki^{B5} mutant is that the Dpn staining of the NSCs is very weak (Fig. 13B; white arrows), also indicating severe developmental problems. The yki^{B5} mutant also harbours a mushroom body specific effect; these non-quiescent NSCs which are proliferative even during the quiescence phase between embryonic and larval phases of development exhibit a growth defect as well. Directly after larval hatching the median cell diameter of the MBNBs is 8,5µm (maximum 10,5µm) but at 48h ALH the median is 13,5µm (maximum 15µm) (Fig. 13F) indicating a newly discovered massive growth of these cells, believed to show a constant cell size due to their continuous proliferation. In the yki^{B5} mutant situation the median cell diameter of the MBNBs is even smaller compared to freshly hatched larvae namely 7,5µm (maximum 9µm) (Fig. 13C, F). A staining against the differentiation

marker prospero (pros) showed that the amount of progeny cells generated by the MBNBs at 48h ALH is noticeably small (violet circles Fig. 13C). In sum these results show a strong dependency between reactivation and the presence of Yki.

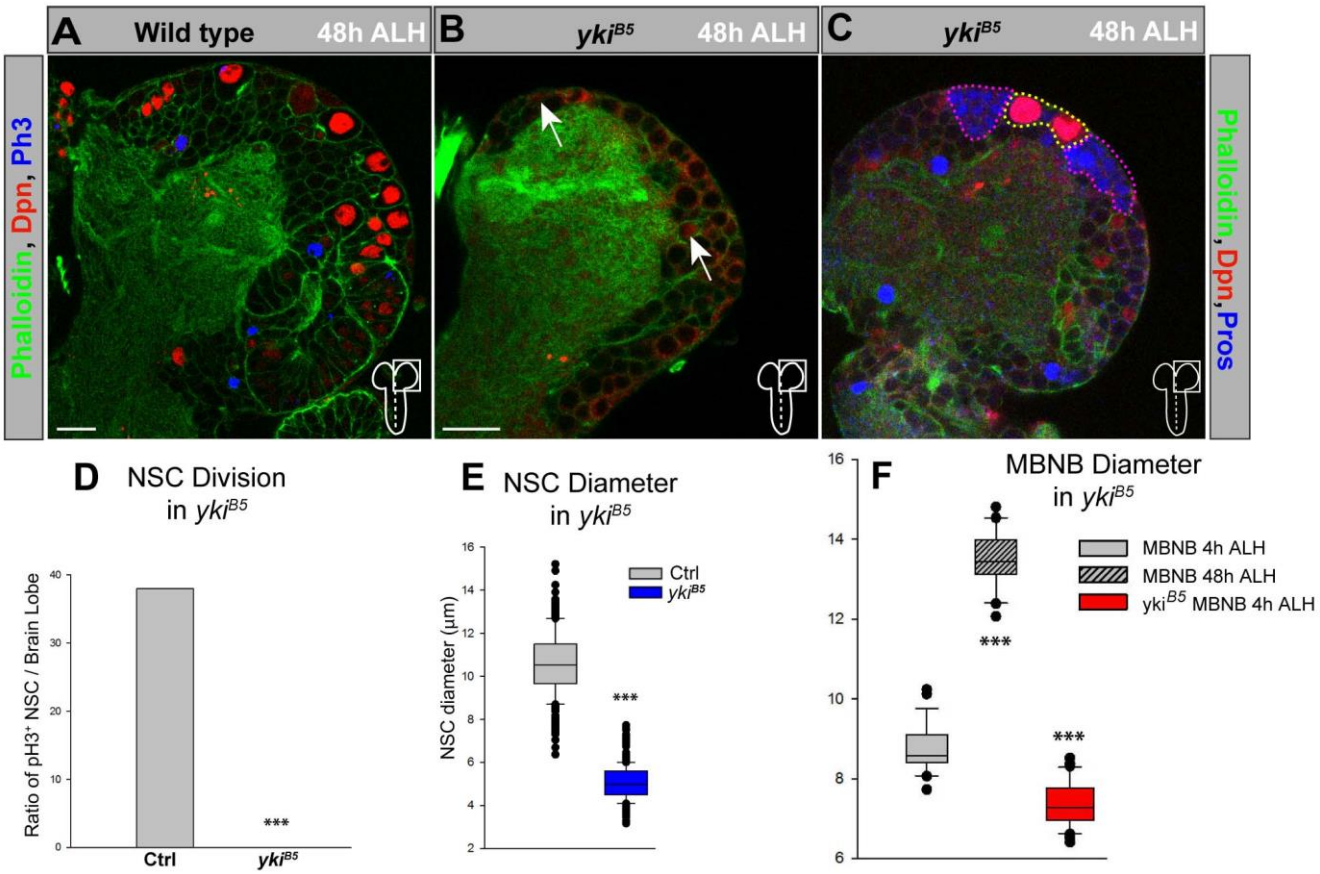

Figure 13: Yki is necessary for reactivation. **(A, B)** NSC growth and proliferation is impaired in *yki*^{B5} deletion mutants **(B)** compared to wild type NSCs at 48h ALH **(A)**. **(C)** NSCs of the MBNB in *yki*^{B5} are smaller and have less Prospero-positive (Pros, blue staining encircled in violet) progeny than compared to wild type brains at 48h ALH. **(D)** Average number of NSCs in mitosis (pH3-positive) at 48h ALH in wild type and *yki*^{B5} deletion mutants. **(E)** Quantification of NSC diameters in *yki*^{B5} deletion mutants at 48h ALH. Wild type brains 48h ALH: median 11µm (maximum 15µm) n= 240 NSCs (5 brain lobes); *yki*^{B5} mutant 48h ALH: median 4,5µm (maximum 8µm) n= 457 NSCs (10 brain lobes). **(F)** Quantification of the cell diameter of NSCs of the mushroom bodies (MBNBs) at 4h ALH, 48h ALH or in *yki*^{B5} mutants at 48h ALH. Wild type brains 4h ALH: median 8,5µm (maximum 10,5µm) n= 28 NSCs (7 brain lobes); Wild type brains 48h ALH: median 13,5µm (maximum 15µm) n= 20 NSCs (5 brain lobes); *yki*^{B5} mutant 48h ALH: median 7,5µm (maximum 8,5µm) n= 40 NSCs (10 brain lobes). All images are single confocal sections anterior up and scale bars represent 10µm.

Next, I tested whether early expression of a constitutively active form of Yki (UAS-*yki*^{S168A}) is sufficient to prematurely reactivate NSCs from quiescence. Serine (Ser) 168 of the Yki protein is a critical phosphorylation site for the Wts kinase and therefore inevitable for the

negative regulation of Yki activity through SWH signalling. Wts-mediated phosphorylation of the Serine (Ser) 168 promotes binding of Yki to 14-3-3 proteins, representing a crucial step for Yki cytoplasmic retention. Expressing a mutant form of Yki in which this Ser residue is changed to alanine (Ala) should abolish this section of Yki regulation (Oh and Irvine, 2008). Indeed, at 4h ALH I observed a significant increase in the NSC cell diameter after ectopic expression of this constitutive active form of Yki with the *insc*G4>UAS-CD8::GFP line (Fig. 14A, B). The median NSC cell diameter was raised from 4,5µm in the wild type situation to 8µm in cells expressing the mutant form of Yki. In order to restrict the overexpression to only larval stages I used the temperature-sensitive GAL4 repressor system GAL80^{ts} and the effect on cellular growth was comparable (Fig. 14B). The median cell diameter was elevated to 7,5µm in diameter.

Therefore I conclude that Yki function is necessary and sufficient for NSC reactivation and initiation of growth and proliferation after quiescence.

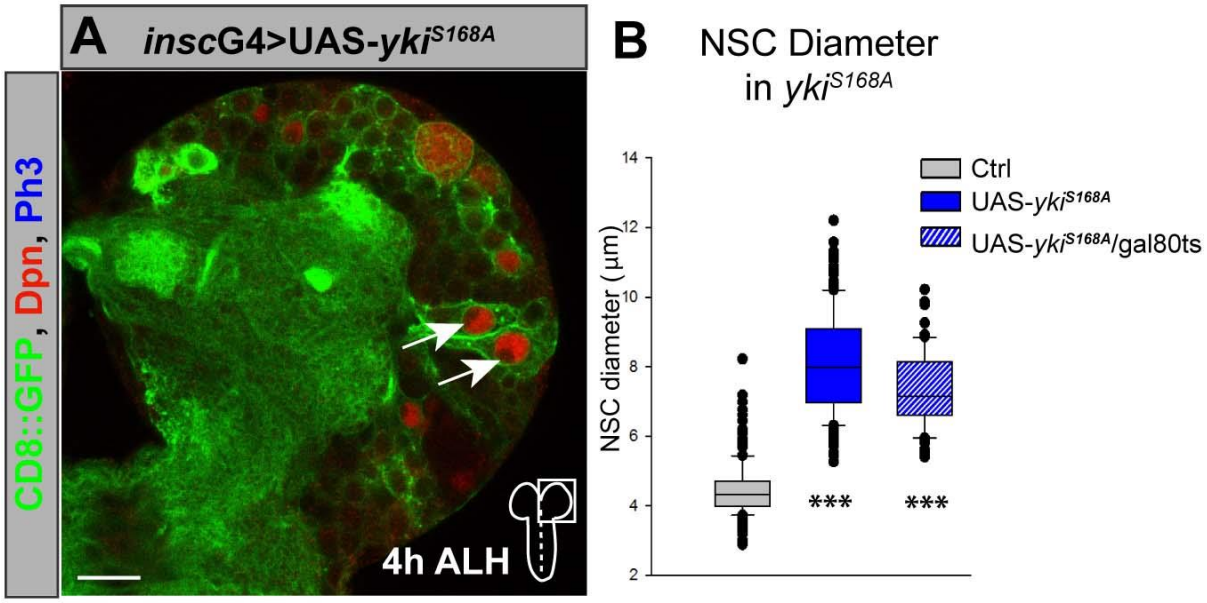

Figure 14: Yki is sufficient for NSC reactivation. **(A)** Expression of *ykiS168A* in NSCs using the *insc*G4>UAS-CD8::GFP driver is sufficient to reactivate NSCs already 4h ALH; significantly enlarged NSCs are marked with white arrows. **(B)** Quantification of NSC diameters in ectopic expression of *insc*G4>UAS-*ykiS168A* at 4h ALH. Wild type brains 4h ALH: median 4,5µm (maximum 8µm) n= 150 NSCs (3 brain lobes); *insc*G4>UAS-*ykiS168A* 4h ALH: median 8µm (maximum 12,5µm) n= 200 NSCs (4 brain lobes); larval restricted (Gal80^{ts}) *insc*G4>UAS-*ykiS168A* 4h ALH: median 7,5µm (maximum 10,5µm) n= 62 NSCs (3 brain lobes). All images are single confocal sections anterior up and scale bars represent 10µm.

4.3 Analysis of NSC specific target genes of the SWH signalling pathway

If Yki is necessary and sufficient for NSC reactivation after quiescence it would be of interest to identify the NSC specific target genes, which are responsible for the obtained phenotypes. Therefore I tested if the expression of the known Yki target genes four-jointed (Fj-lacZ), expanded (Ex), CyclinE, and the microRNA *bantam* correlates with the sub-cellular translocation of Yki during NSC reactivation.

4.3.1 Yki activates the *bantam* microRNA during reactivation

I analysed the expression and activity of the *bantam* miRNA which is known to regulate proliferation and growth (Nolo *et al*., 2006; Brenneke *et al*., 2003; Hipfner *et al*., 2002; Thompson and Cohen, 2006) by using a Green-Fluorescent-Protein (GFP)-sensor system (Brenneke *et al*., 2003). In this sensor system GFP is expressed under the control of a ubiquitous *tubulin* promoter so that the fluorescent protein is expressed in every cell of the organism. In the 3' untranslated region (3'UTR) of the GFP mRNA transcript are diverse binding sites for the *bantam* miRNA, so in every cell the *bantam* miRNA is actively expressed the GFP signal is reduced via the RNAi effect of the miRNA. The loss of GFP expression and thus the activity of *bantam* coincides with the translocation of Yki into the nucleus. The quiescent NSCs in Fig. 15A (0-2h ALH) show strong GFP staining (white circles and magnification) whereas the non-quiescent MBNBs are GFP-negative (yellow circle and magnification). These data are in agreement with the subcellular Yki localization at 0-2h ALH (Fig. 10A; Fig. 11A, C), where I described the nuclear presence of Yki protein in MBNBs.

On the contrary all reactivated NSCs at 24h ALH (Fig. 15B) and 48h ALH (Fig. 15C) exhibit dramatically reduced GFP signals monitoring extensive *bantam* activity (Fig. 15B, C; white circles and magnifications). The right panels show the GFP signal in monochrome and clearly verify my hypothesis that the *bantam* miRNA is activated during reactivation of NSCs through loss of SWH signalling and the translocation of Yki into the nucleus.

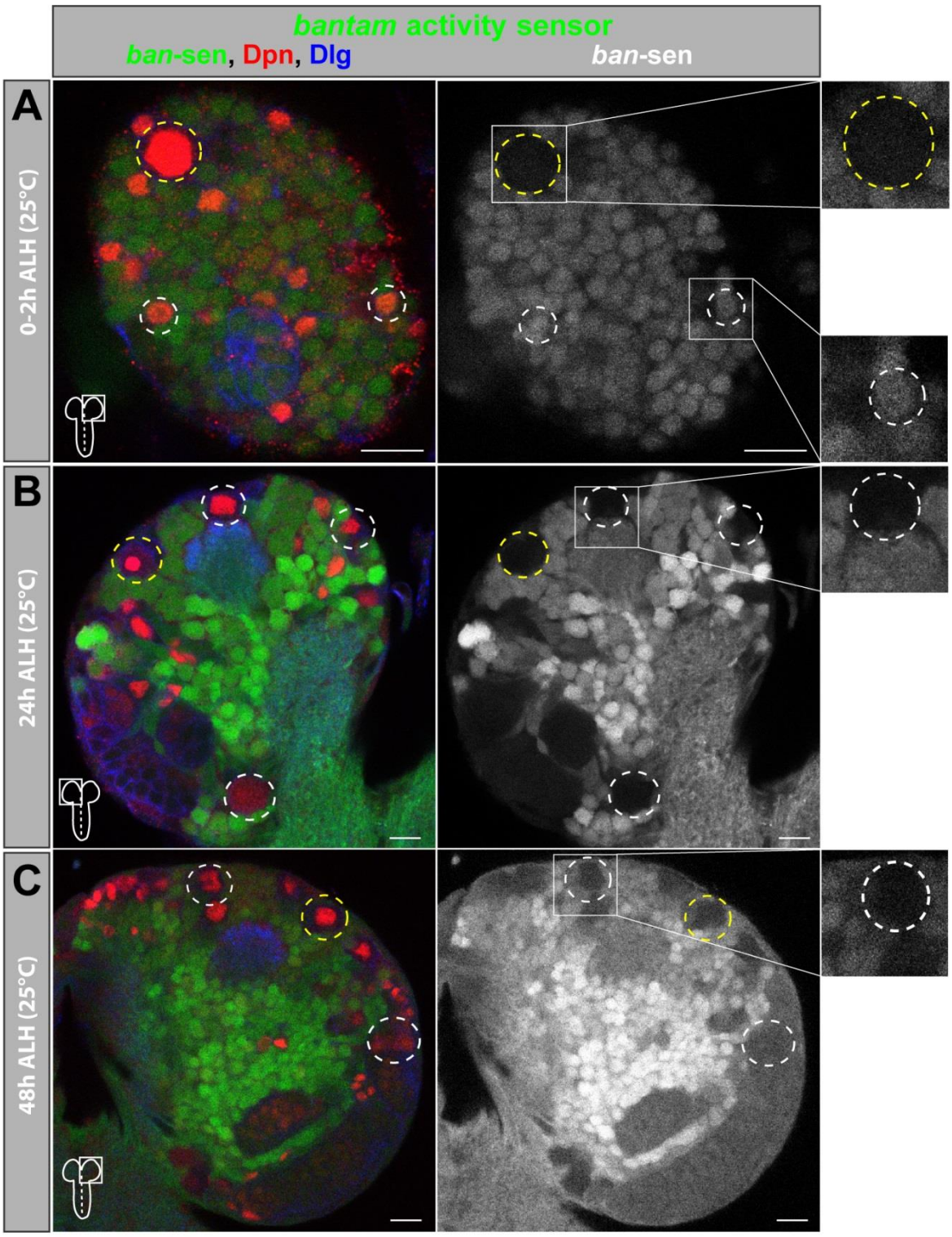

Figure 15: The microRNA *bantam* is expressed upon NSC reactivation. *bantam* (*ban*)-activity sensor in brain lobes at 0-2h **(A)**, 24h **(B)** and 48h **(C)** ALH. Loss of the GFP signal monitors *ban* activity. Quiescent NSCs **(A)** (white circles) do not exhibit active *bantam* (GFP positive), at 0-2h ALH only the MBNB (yellow circles) display a reduction of the GFP signal; whereas reactivated NSCs **(B, C)** (white circles) or the MBNB (yellow circles) have active *ban* and therefore are GFP negative. Right panels and magnifications show GFP channel in monochrome. All images are single confocal sections anterior up and scale bars represent 10µm.

To test if *bantam* is also necessary for NSC reactivation I analysed the *bantam*$^{\Delta 1}$ deletion mutants, lacking ~ 21kb flanking the *bantam* locus (Brennecke *et al*., 2003). The larvae were dissected at 24h ALH and I observed NSC reactivation in the brain, but still there was a dramatically reduced cell size with a median of 6,5µm compared to the wild type situation where I measured a median of 9,5µm. This effect was more intense in the NSCs of the ventral nerve cord (VNC) at 24h ALH, which in *bantam*$^{\Delta 1}$ mutants were indistinguishable from quiescent NSCs in the VNC at 4h ALH. The cell sizes were severely reduced with a median of 4,5µm in diameter in contrast to the wild type larvae which displayed a cell diameter of 8,5µm (Fig. 16A, B, C). In addition to that I statistically analysed separately the mitotic indices of central brain NSCs and VNC NSCs in wild type larvae and the *bantam*$^{\Delta 1}$ deletion mutants. On average there are 13 pH3^{+} NSCs per brain lobe at 24h ALH in the control larvae but only 5 pH3^{+} NSCs in the *bantam* mutant background. In the VNC there are ordinarily 4 pH3^{+} NSCs at 24h ALH and in the mutant VNCs there are no proliferative NSCs at all (Fig. 16D).

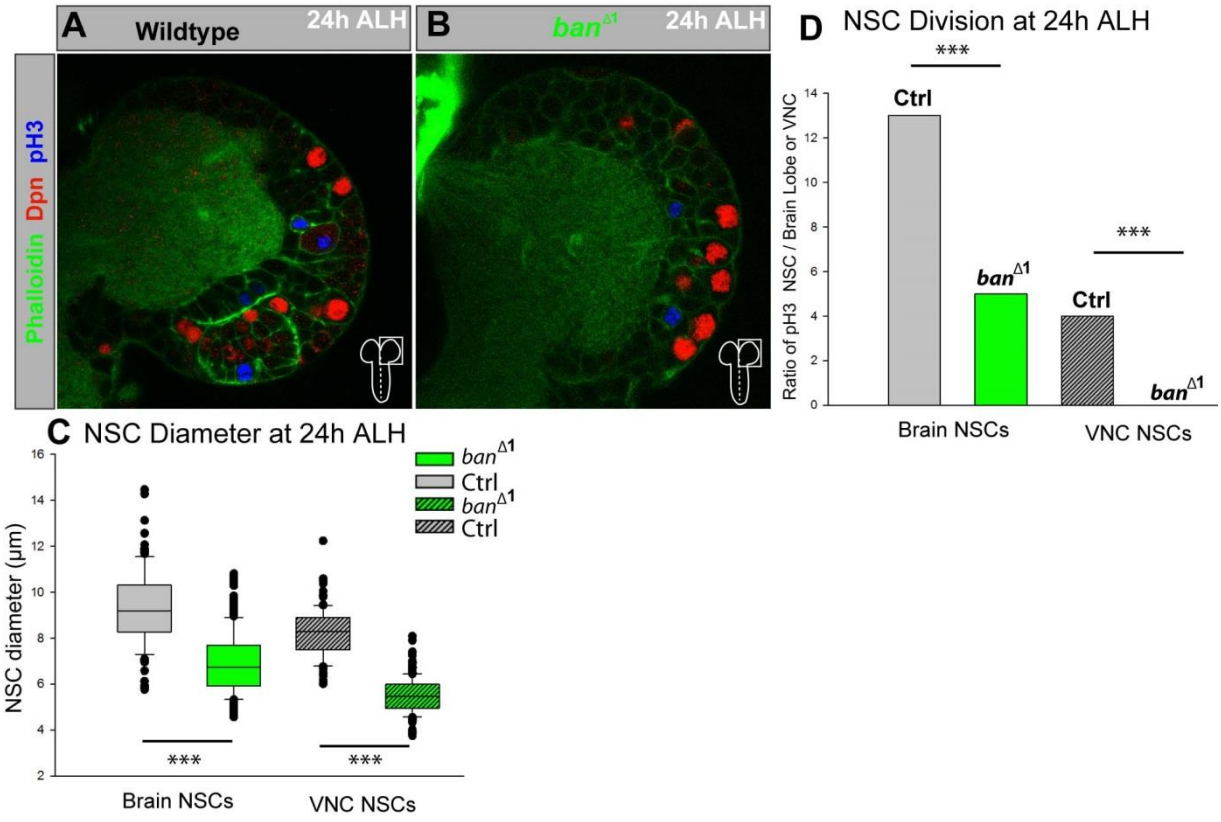

Figure 16: The *bantam* miRNA is necessary for the reactivation of larval NSCs. (A, B) NSC growth and proliferation is decreased in *banΔ*^{1} mutants **(B)** compared to wild type larval brains **(A)** at 24h ALH. Phalloidin-GFP (green) is used as a membrane marker for the measurements of the cell diameters. **(C, D)** Quantification of NSC diameters **(C)** and proliferation **(D)** in *banΔ*^{1} mutants and wild type brains at 24h ALH. Wild type brain 24h ALH: median 9,5µm (maximum 14,5µm) n= 109 NSCs (3 brain lobes); *banΔ*^{1} brain 24h ALH: median 6,5µm (maximum 11µm) n= 319 NSCs (7 brain lobes); wild type VNC NSCs 24h ALH: median 8,5µm (maximum 12µm) n= 109 NSCs (3 VNCs); *banΔ*^{1} VNC NSCs 24h ALH: median 4,5µm (maximum 8µm) n= 253 NSCs (4 VNCs). **(D)** Average number of NSCs in mitosis (pH3-positive) at 24h ALH in wild type of 3 brain lobes and 3 VNCs and *banΔ*^{1} 7 brain lobes and 4 VNCs. All images are single confocal sections anterior up and scale bars represent 10µm.

To show that premature reactivation caused by loss of SWH signalling leads to early activation of the Yki downstream target *bantam*, I combined the *bantam* GFP-sensor system with the *insc*GAL4 driver line. Loss of the core kinase *wts* causes a strongly reduced GFP signal in the affected NSCs at 4h ALH (Fig. 17; white circles) even though there are still some NSCs which show GFP expression (Fig. 17; cyan blue circles) most of the Dpn positive cells are characterized by a strongly reduced GFP signal. The right panel shows the GFP signal in monochrome and emphasises the *bantam* mediated reduction of GFP in the NSCs.

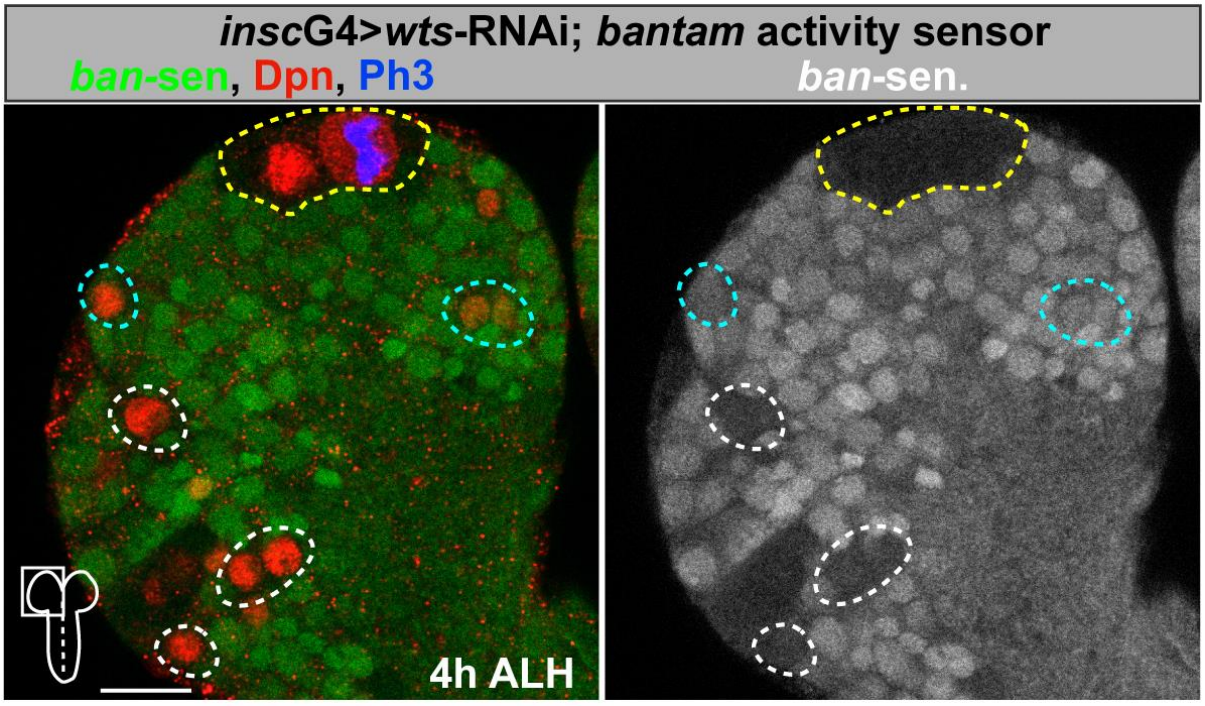

Figure 17: The *bantam* miRNA is expressed after loss of SWH signalling. NSC-specific *wts*-RNAi leads to premature *ban* activity (loss of GFP) in NSCs at 4h ALH. For identifying the NSCs Dpn antibody was used, only Dpn positive cells show a decreased GFP signal (white circles, MBNB are marked with yellow circles), NSCs which are still quiescent and therefore GFP positive are marked with cyan blue circles. All images are single confocal sections anterior up and scale bars represent 10µm.

To further illustrate that the observed growth phenotypes can be attributed to the miRNA *ban* I overexpressed the active form of *ban* in the inscG4 pattern. The larval brains were dissected 4h ALH and stained against Dpn and pH3. The NSCs showed a significant premature growth phenotype with a median cell diameter of 6,5µm, compared to 4,5µm in the wild type control brains (Fig. 18A and B).

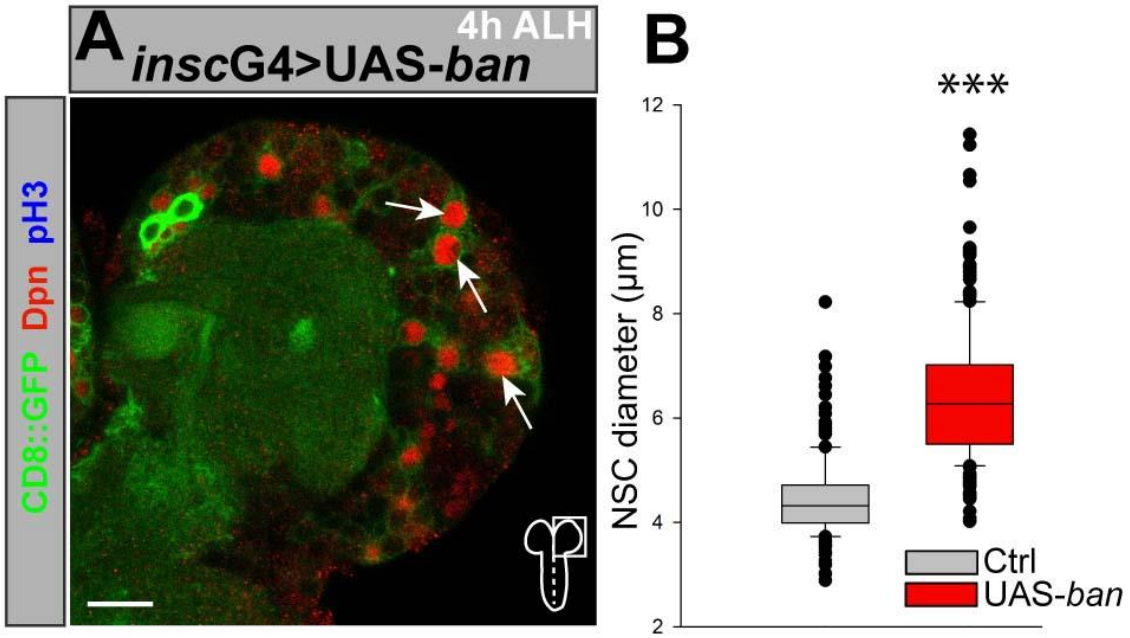

Figure 18: Overexpression of *ban* prematurely reactivates NSCs. (A) Expression of *ban* in NSCs using the *insc*G4>UAS-CD8::GFP driver is sufficient to reactivate NSCs already 4h ALH; significantly enlarged NSCs are marked with white arrows. **(B)** Quantification of NSC diameters in ectopic expression of *insc*G4>UAS-UAS-*ban* at 4h ALH. Wild type brains 4h ALH: median 4,5µm (maximum 8µm) n= 150 NSCs (3 brain lobes); *insc*G4> UAS-*ban* 4h ALH: median 6,5µm (maximum 12µm) n= 250 NSCs (4 brain lobes). All images are single confocal sections anterior up and scale bars represent 10µm.

On these grounds I conclude that *bantam* is an important target of Yki during reactivation of NSCs, whereas this *bantam* mediated growth effect seems to be stronger in the VNC, indicating that other yet unknown Yki targets need to be involved in growth and proliferation of the central brain NSCs.

4.3.2 Yki activates the expression of *Four-jointed* during reactivation

Another protein which is known to be positively regulated by Yki is the golgi resident kinase Four-jointed (Fj). To check whether this protein is also upregulated during NSC reactivation, I used an *fj*-LacZ fly strain to analyse its expression in the larval brain before and after reactivation. Interestingly, the β-Gal staining revealed Fj expression in almost every cell of

the CNS at 4h ALH with the exception of the quiescent NSCs (Fig. 19A; cyan blue circles). The non-quiescent MBNB (yellow circles) exhibit a strong β-Gal staining (Fig 19A; yellow circles) indicating that SWH signalling is an important molecular criterion for the decision between quiescence and non-quiescence. At 48h ALH virtually all NSCs of the CNS are β-Gal positive, the optic lobe NSCs as well as the NSCs of the central brain (Fig. 19B) this demonstrates that *fj* is upregulated during NSC reactivation.

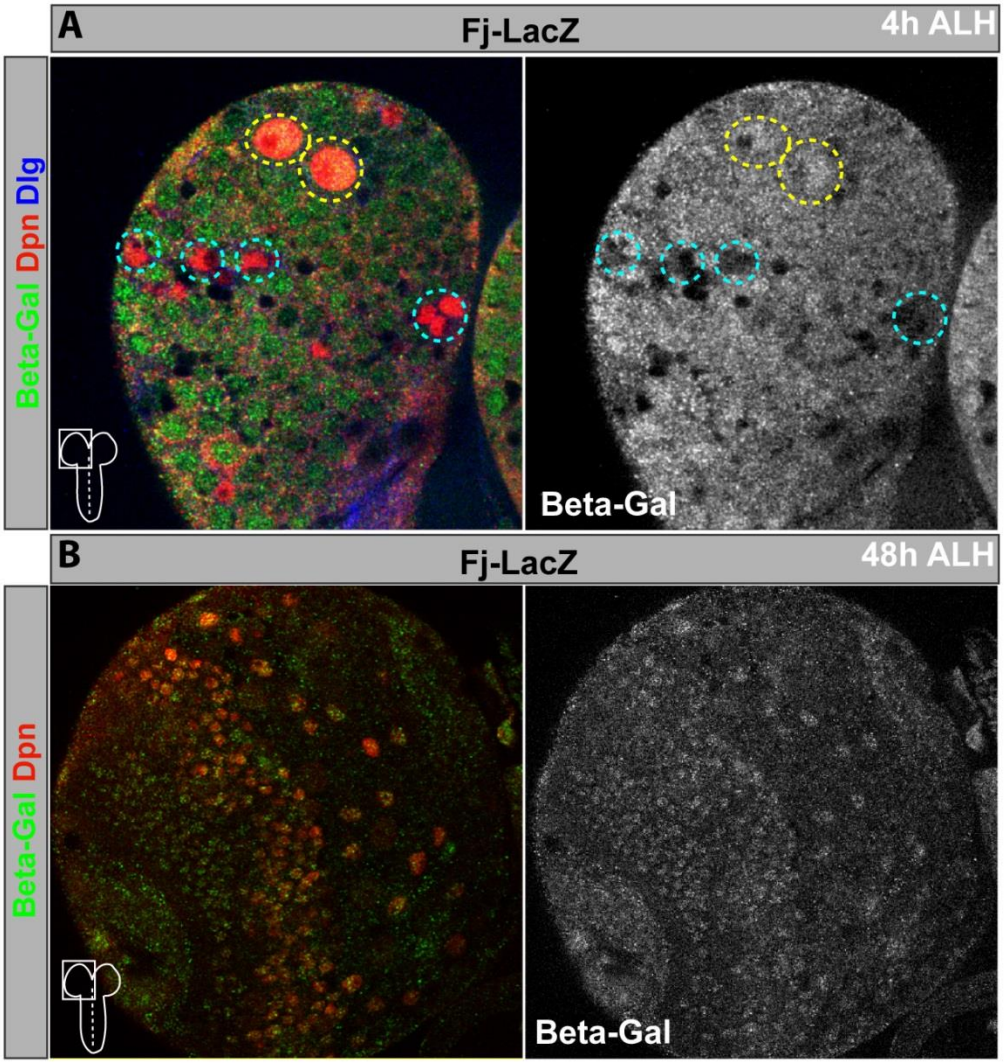

Figure 19: The Yki target Four-jointed is upregulated after reactivation in larval NSCs. (A) Fj-lacZ (green) is expressed in non-quiescent NSCs (MBNB, yellow circles), but not in quiescent NSCs (cyan blue circles) at 4h ALH. **(B)** 48h ALH all NSCs of the larval brain are expressing Fj-lacZ (green). Right panels show the Fj-lacZ staining in monochrome. NSCs are marked with an antibody against Dpn (red). All images are single confocal sections anterior up and scale bars represent 10µm.

4.3.3 Yki activates the expression of *expanded* during reactivation

Next I tested whether the expression of the known Yki target gene *expanded* (*ex*) correlates with the sub-cellular translocation of Yki during NSC reactivation. During quiescence at 4h

ALH there is no specific Ex staining observable in the larval CNS, the right Ex antibody monochrome channel further emphasizes the unspecific staining pattern. Exclusively the non-quiescent MBNB (shown in the inserted magnification) display a distinct, membrane-associated staining pattern against Ex (Fig. 20A). By contrast at 48h ALH all NSCs of the central brain show a massive upregulation of Ex protein (red) (Fig. 20B). The right panel shows the Ex staining in monochrome and highlights the significant NSC specific upregulation of the Yki target Ex after reactivation.

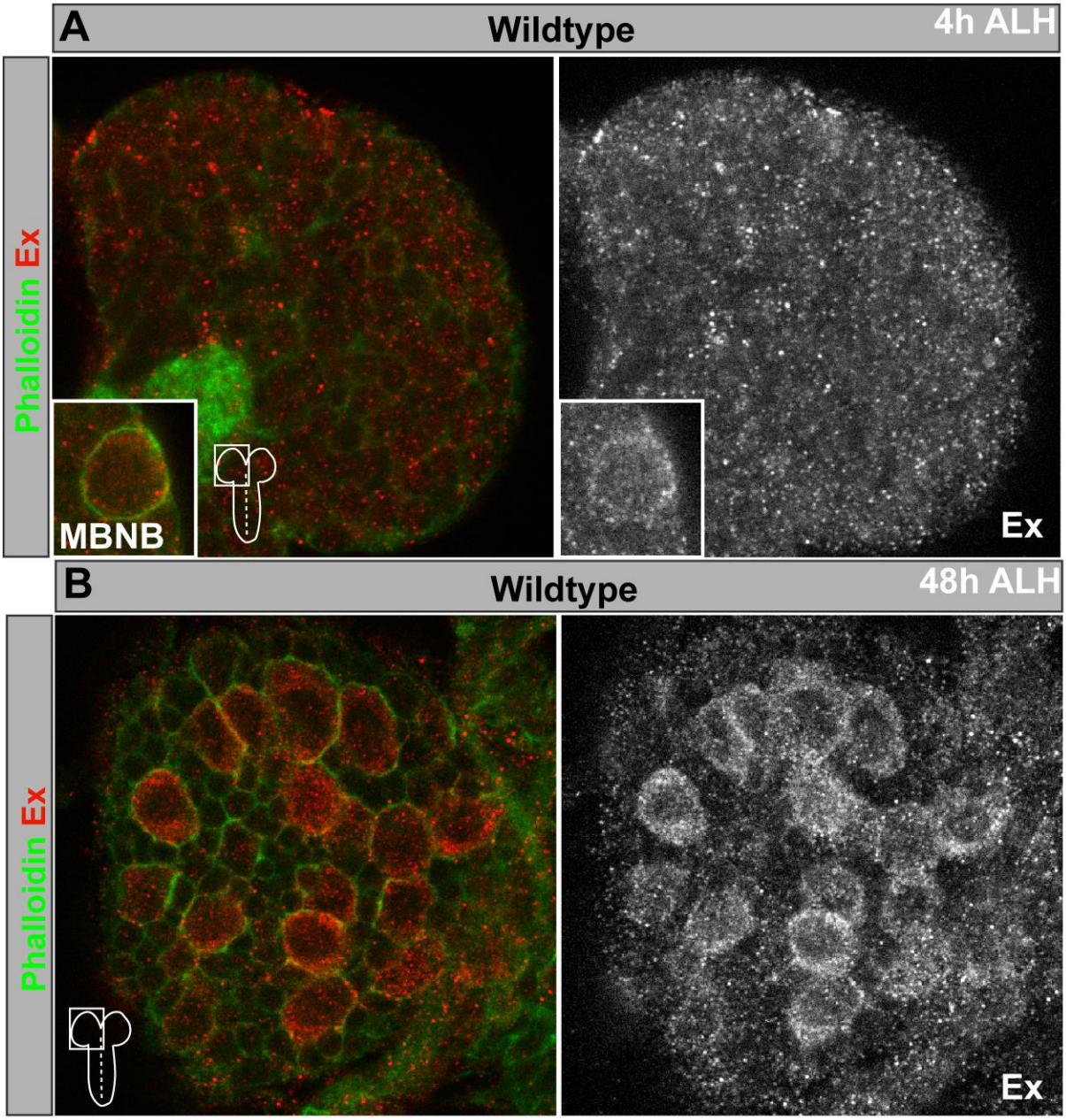

Figure 20: The Yki target *expanded* is upregulated after reactivation in larval NSCs. (A) Expanded (Ex) expression in the larval CNS at 4h ALH. Only weak levels of Ex (red) expression can be observed in the central brain. Inserted magnification shows dorsally located NSC of the mushroom body (MBNB) with an observable Ex expression. **(B)** Ex (red) upregulation in all reactivated NSCs (big cells) of the larval central brain at 48h ALH. Right panels display the Ex antibody channel in monochrome. As a membrane marker I used Phalloidin-GFP. All images are single confocal sections anterior up and scale bars represent 10µm.

4.3.4 Yki activates the expression of *cycE* during reactivation

Another well described target gene of Yki is the S-phase cyclin CycE, so I used the *insc*Gal4>UAS-CD8::GFP driver line to knock down the SWH pathway core kinase Wts in NSCs and stained against CycE. In the wild type situation at 4h ALH there is no distinct CycE signal obtainable (Fig. 21A). One explanation for this is that all members of the cyclin family are expressed periodically during specific time points of the cell cycle; cycE is required for the transition from G1 to S phase (Richardson *et al*., 1995) and can be seen as an important hallmark for cell division which is not occurring during the quiescence phase. In NSCs which are prematurely reactivated due to loss of *wts* there is a significant upregulation of this cell cycle promoting protein (Fig. 21B). The right panels represent the CycE staining in monochrome stating more clearly the enhanced expression of this Yki target after loss of *wts*.

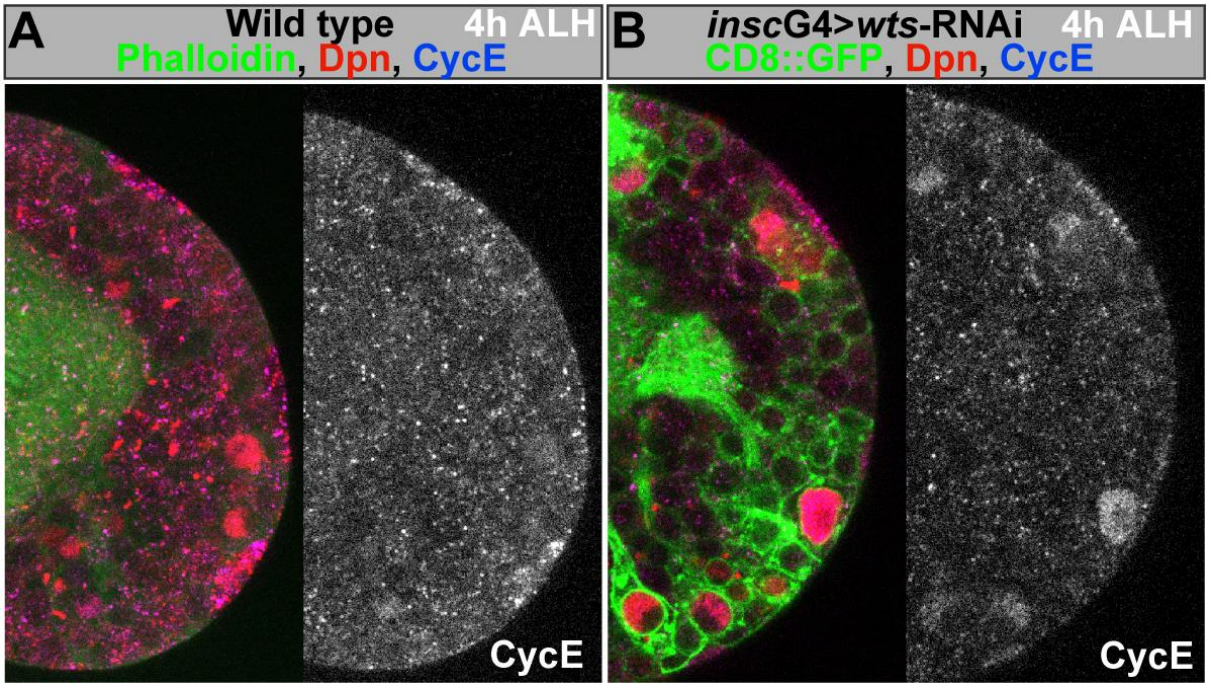

Figure 21: The Yki target *cycE* is upregulated in prematurely reactivated NSCs. (A, B) Upon *wts*-RNAi in NSCs using the *insc*G4>UAS-CD8::GFP driver line CycE is upregulated, NSCs are visualized with an antibody against Dpn (red). **(A)** The G_1 to S-Phase regulator CyclinE (CycE, blue) is weakly expressed in quiescent NSCs at 4h ALH in the wild type situation, as a membrane marker I used Phalloidin-GFP. **(B)** CycE (blue) is upregulated upon *wts*-RNAi in prematurely reactivated NSCs. The right monochrome channels only display the CycE staining. All images are single confocal sections anterior up and scale bars represent 10µm.

4.4 Premature reactivation of NSCs by Hippo signalling depends on the nutritional status

Due to the fact that novel scientific data described a sophisticated cross-talk between the SWH signalling and the Insulin/IGF signalling (IIS) (Straßburger *et al*., 2012), I tried to expose whether there is an molecular interplay between these two well established growth promoting pathways in *Drosophila* NSCs. To translate this idea into action I used the *insc*Gal4 line to down regulate the Wts kinase and stained against phosphorylated Akt (pAkt, PKB), which is a serine/threonine specific protein kinase. Due to the fact that pAkt is an important signalling molecule in the insulin pathway I used it as a read out for IIS signalling. Loss of *wts* indeed resulted in prematurely activated IIS signalling at 4h ALH (Fig 22A, white circles) especially the pAkt monochrome channel displays obviously the IIS pathway activation (white circles = prematurely activated NSCs; yellow circles = MBNB). On the contrary in the wild type situation at 4h ALH there is no NSC (Fig. 22B; cyan blue circles) specific staining pattern obtainable with the pAkt antibody. This can be reasoned by the fact that the Akt kinase is phosphorylated after IIS activation, which in turn is an important criterion for NSC reactivation and does not occur during the quiescence phase (Chell and Brand, 2012).

Because reactivation of NSCs is known to be dependent on a nutritional stimulus and insulin signalling which is relayed from a specialized subpopulation of CNS glial cells (Britton and Edgar, 1998; Chell and Brand, 2012; Sousa-Nunes *et al*., 2011), I tested if premature reactivation upon *wts*-RNAi is depending on nutrition (Fig. 23). Gene knockdown of *wts* in starved larvae resulted in a minor but still significant increase in cell size with a median of 5 µm in diameter (maximum 8µm) compared to *wts* knockdown in well-fed larvae with a median of 7 µm (maximum 11µm) (Fig. 23A, B).

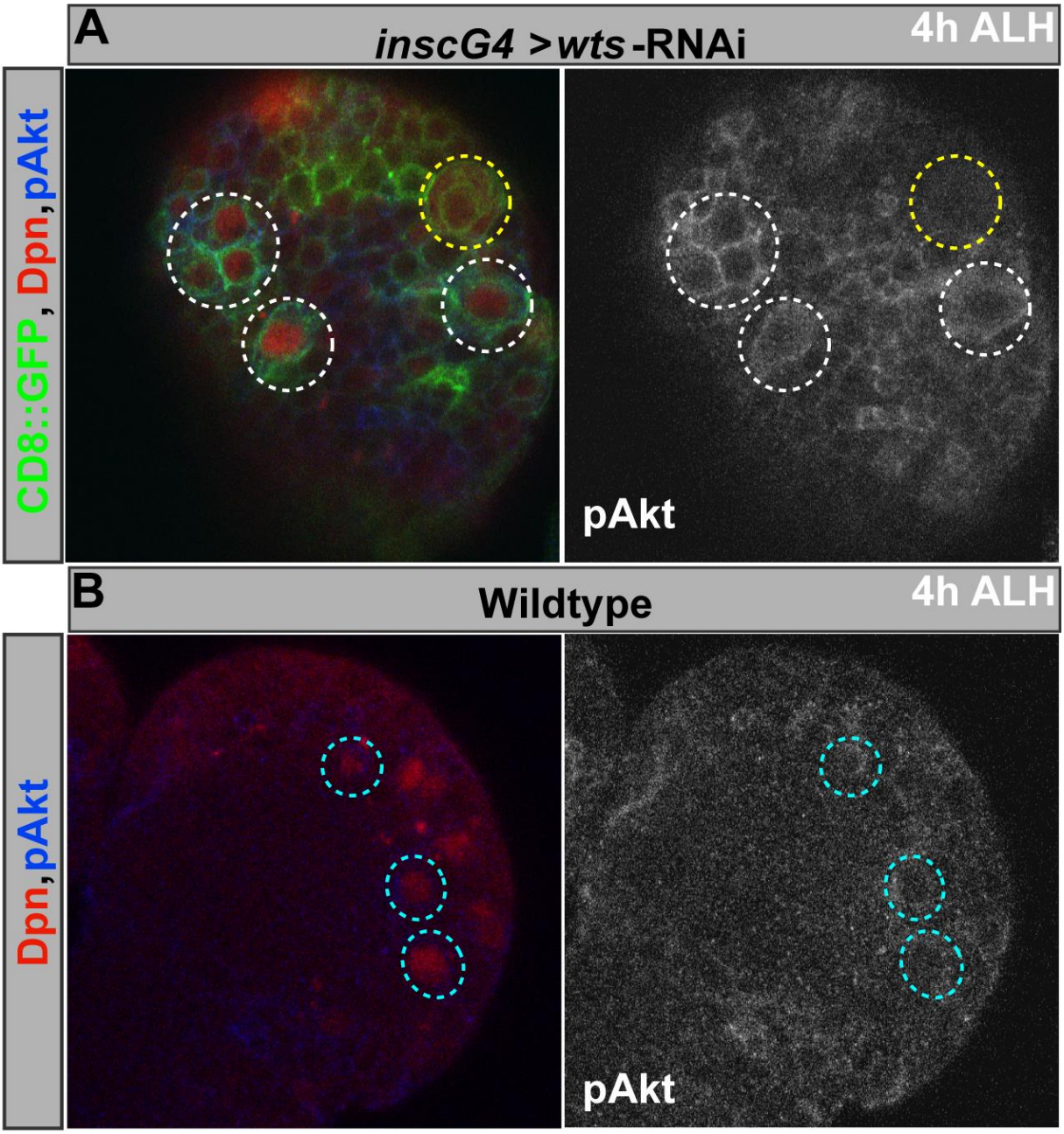

Figure 22: Activation of IIS signalling upon *wts*-RNAi. **(a)** Upon NSC specific *wts*-RNAi (*insc*G4>UAS-CD8::GFP) the prematurely reactivated NSCs (visualized with an antibody against Dpn, red) exhibit a significantly increased staining against pAkt (blue; used as a read-out for IIS signalling) at 4h ALH. Prematurely reactivated NSCs with strong pAkt staining are marked with white circles; MBNB with yellow circle. (**b**) Wild type NSCs at 4h ALH (cyan blue circles) display a low pAkt staining (blue) intensity. All images are single confocal sections anterior up and scale bars represent 10µm.

But despite this growth phenotype I could not detect any pH3-positive NSCs. Thus, the SWH signalling pathway might regulate quiescence and growth initiation of NSCs in parallel to the nutritional response model. This shows sensing of new nutritional resources occurs within the

first 4h ALH and SWH signalling can initiate cell growth, but reactivation even in loss of the SWH depends on the nutritional status of the organism.

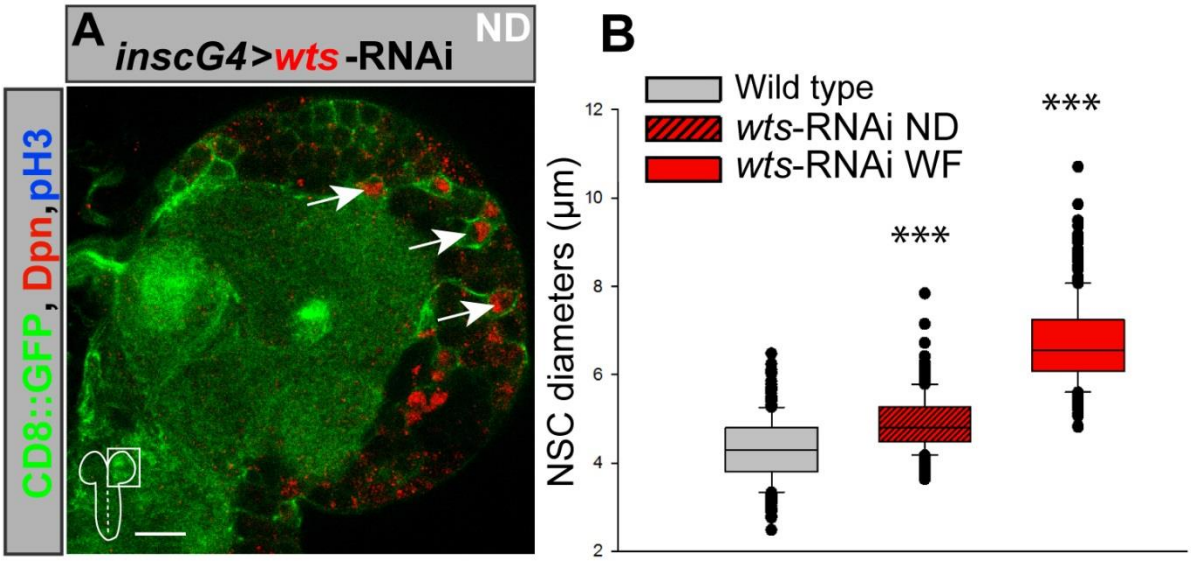

Figure 23: Premature reactivation of NSCs via SWH signalling depends on the nutritional status. (A) NSC-specific RNAi (*insc*G4>UAS-CD8::GFP) of *wts* in nutrition-deprived (ND) larvae leads to only minor reactivation phenotype at 4h ALH. Significantly enlarged NSCs are marked with white arrows. **(B)** Quantification of NSC diameters upon *wts*-RNAi in well-fed (WF) or nutrition-deprived larvae at 4h ALH. Wild type brain 4h ALH: median 4,5µm (maximum 7µm) n= 355 NSCs (7 brain lobes); *insc*G4>*wts*-RNAi ND 4h ALH: median 5µm (maximum 8µm) n= 234 NSCs (5 brain lobes); *insc*G4>*wts*-RNAi WF 4h ALH: median 7µm (maximum 11µm) n= 290 NSCs (6 brain lobes). All images are single confocal sections anterior up and scale bars represent 10µm.

4.4.1 Energy sensing LKB1/AMPK signalling regulates Yki activity in the early larval *Drosophila* CNS

Recent scientific evidence indicates that there are regulative mechanisms of Yki localization which are SWH signalling independent, namely the LKB1/AMPK energy sensing module (Mohseni *et al.*, 2014; DeRan *et al.*, 2014). Gailite *et al.* (2015) showed that loss of Hpo or Wts activity in the central brain does not affect expression of the Yki target gene *expanded* and thereby revealed that LKB1 regulates Yki activity downstream, or in parallel, to SWH signalling in late larval stages. To unravel a potential participation of LKB1/AMPK signalling in Yki regulation at early larval stages during reactivation, I conducted some RNAi experiments against LKB1 at 4h ALH. Using the *insc*G4>UAS-CD8::GFP driver line I was able to show that loss of *lkb1* causes premature reactivation in NSCs at 4h ALH, individual NSCs already started proliferating (Fig. 24A; $pH3^+$ NSC is marked with white arrow). The median NSC diameter in this genetic background is 6µm (maximum 11,5µm) and is therefore

significantly larger compared to the wildtype situation at this developmental time point (median 4,5µm) (Fig. 24B). Due to the fact that the LKB1 kinase seems to be a critical regulator of NSC reactivation through its ability to phosphorylate Yki protein (Gailite *et al*., 2015) I tried to figure out whether it is possible to enhance the obtained NSC growth phenotype by knocking down both kinases which are known to phosphorylate Yki; namely Wts and LKB1. Therefore I combined both RNAi constructs and analysed its effect on NSC reactivation. The double knock down of *lkb1* and *wts* resulted in a slightly more pronounced growth phenotype compared the loss of the individual kinases with a median cell diameter of 7µm (maximum 11µm) (Fig. 24C).

Taken together these results state that the energy sensing LKB1 kinase is necessary for the phosphorylation of Yki protein in the CNS at early larval stages independently of SWH signalling. Rising the question whether there are even more proteins and pathways which play a role in the regulation of the transcriptional co-activator Yki.

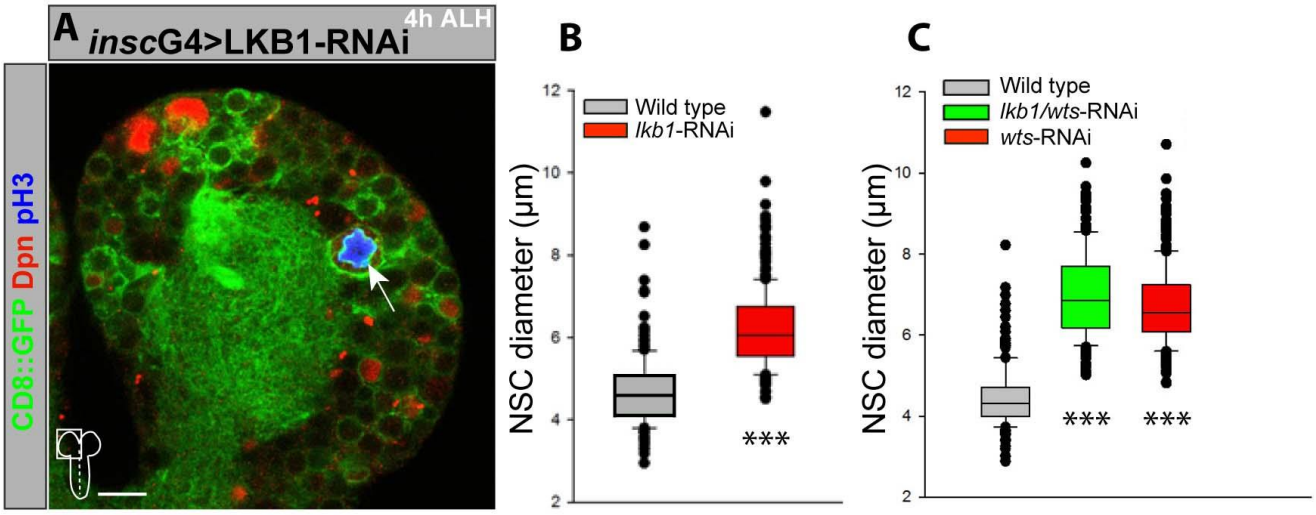

Figure 24: NSC specific loss of the LKB1 kinase leads to premature reactivation. (A) NSC-specific (*insc*G4>UAS-CD8::GFP) RNAi of *liver kinase b1* (*lkb1*) leads to an increase in NSC cell diameter at 4h ALH. Significantly enlarged, $pH3^{+}$ NSC is highlighted by a white arrow. **(B, C)** Quantification of NSC diameters in *lkb1*-RNAi **(B)** and *lkb1/wts*-RNAi **(C)**. **(B)** Wild type brains 4h ALH: median 4,5µm (maximum 8,5µm) n= 150 NSCs (3 brain lobes); *insc*G4>*lkb1*-RNAi 4h ALH: median 6µm (maximum 11,5µm) n= 145 NSCs (3 brain lobes). **(C)** Wild type brains 4h ALH: median 4,5µm (maximum 8,5µm) n= 150 NSCs (3 brain lobes); *insc*G4>*lkb1/wts*-RNAi 4h ALH: median 7µm (maximum 11µm) n=134 NSCs (3 brain lobes); *insc*G4>*wts*-RNAi 4h ALH: median 6,5µm (maximum 11µm) n=290 NSCs (6 brain lobes). Image is single a confocal section anterior up and scale bar represent 10µm.

4.5 Identification of potential NSC specific upstream regulators of the SWH signalling pathway

Signalling pathways that are involved in the regulation of cell growth and proliferation need to be tightly controlled, because dysregulations in these pathways can cause under proliferation and tumour formation. Since I´ve shown that SWH signalling is necessary and sufficient for NSC reactivation and therefore an important regulative counterfoil in CNS development, it is of prime importance to identify CNS specific regulators of this signalling module.

4.5.1 Loss of *ex*, *kib* or *mer* causes premature reactivation of larval NSCs

The first proteins which were shown to regulate the activity of SWH signalling are Expanded, Merlin and Kibra these proteins form a complex in order to regulate this pathway via cooperative activation of the core kinase Wts (Baumgartner *et al*., 2010; Genevet *et al*., 2010; Yu *et al*., 2010). NSC specific loss of each of these proteins using the *insc*G4>UAS-CD8::GFP driver line cause premature reactivation of NSCs at 4h ALH (Fig. 25 A-F). NSCs that exhibit a significantly increased cell diameter are highlighted with white arrows (Fig. 25 A-C). Indeed, the RNAi experiments revealed a similar albeit less pronounced effect in comparison to loss of *hpo* or *wts* but they caused premature cell growth at 4h ALH. The median NSC diameter in *ex*-RNAi was raised to 6µm (maximum 10µm) (Fig. 25D), in *kib*-RNAi to 6µm (maximum 10,5µm) (Fig. 25E) and in *mer*-RNAi to 5,5µm (maximum 9µm) (Fig. 25F).

4.5.2 Loss of *fat* leads to premature reactivation of larval NSCs

The activity of the SWH signalling pathway is known to be controlled by a variety of transmembrane proteins, like the atypical cadherin Fat (ft) that is essential for controlling cell proliferation during development (Halbleib and Nelson, 2006). Fat is described to regulate SWH signalling via two distinct trails either it directly interacts with the FERM domain protein Ex or it mediates the re-localisation of the atypical myosin Dachs (Cho *et al*., 2006;

Feng and Irvine, 2007; Rauskolb *et al*., 2011). Loss of the atypical cadherin ft in NSCs causes premature cell growth at 4h ALH but there is no sign of increased proliferation (no pH3 positive NSCs) (Fig. 26A). Quantification of the cell diameters uncovered a median of 5,5µm

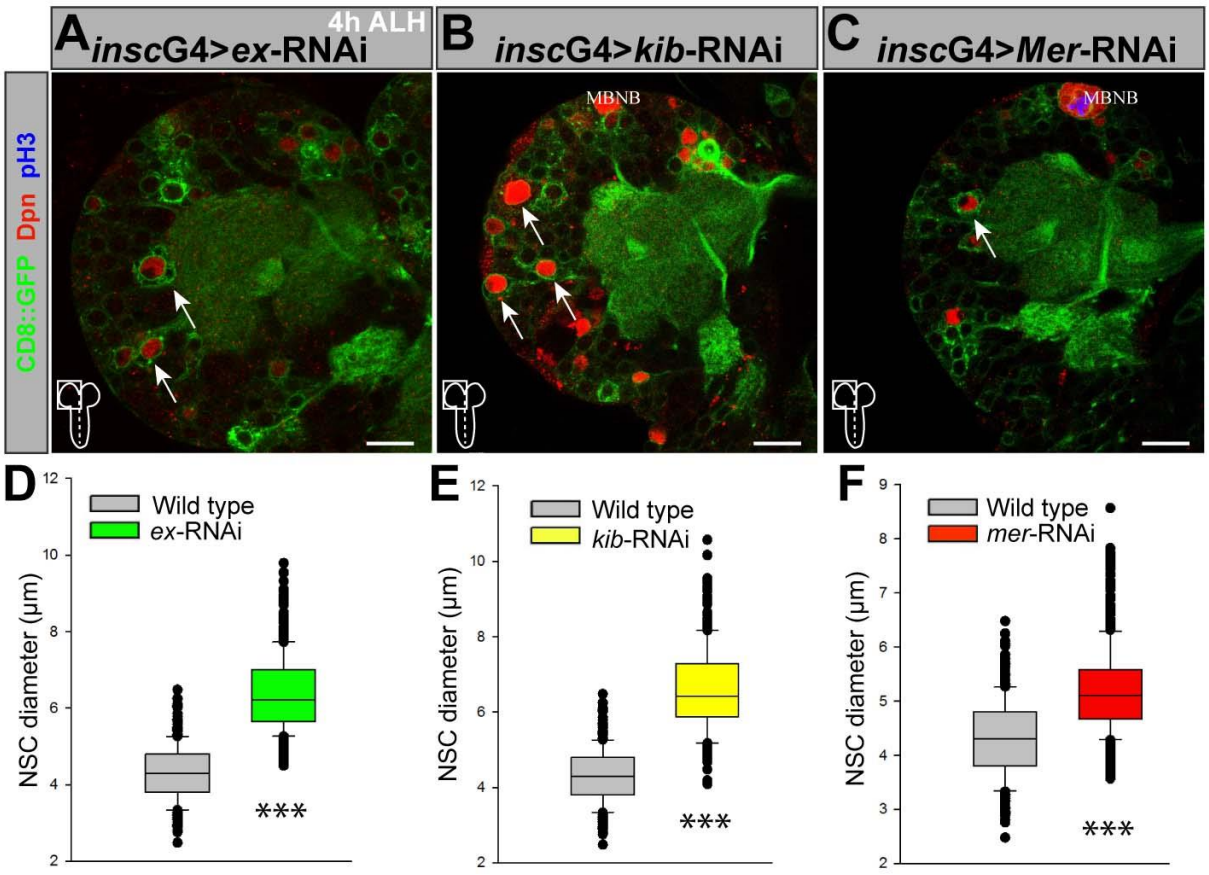

Figure 25: Loss of *ex*, *mer* or *kib* leads to premature reactivation of larval NSCs at 4h ALH. NSC-specific RNAi (*insc*G4>UAS-CD8::GFP) of *expanded* (*ex*)**(A)**, *kibra* (*kib*)**(B)** or *Merlin* (*Mer*)**(C)** leads to premature cell growth of NSCs. Arrows depict examples of NSCs with increased cell diameter. **(D-F)** Quantification of NSC diameters in RNAi mediated knockdown of *ex* **(D)**, *kib* **(E)** and *Mer* **(F). (D-F)** Wild type brains 4h ALH: median 4,5µm (maximum 7µm) n= 150 NSCs (3 brain lobes). **(D)** *insc*G4>*ex*-RNAi 4h ALH: median 6µm (maximum 10µm) n= 400 NSCs (8 brain lobes). **(E)** *insc*G4>*kib*-RNAi 4h ALH: median 6µm (maximum 10,5µm) n= 266 NSCs (5 brain lobes). **(F)** *insc*G4>*Mer*-RNAi 4h ALH: median 5,5µm (maximum 9µm) n= 506 NSCs (10 brain lobes). All images are single confocal sections anterior up and scale bars represent 10µm.

(maximum 9,5µm) (Fig. 26B) and thereby resemble the observed phenotypes of *ex*-, *mer*- and *kib*-RNAi (Fig. 25 A-F). To state that the observed growth defects are related to SWH signalling, I again used the *ban*-sensor system together with the *inscG4* driver, loss of the atypical cadherin *fat* causes a strongly reduced GFP signal in the affected NSCs at 4h ALH (Fig. 26C; cyan blue circles). In sum it becomes obvious that proteins like Ex, Mer, Kib or Ft, which are known to feed into the SWH pathway in diverse tissues also play a central role in the regulation of this signalling module in the larval CNS. Since loss of these proteins lead to premature reactivation of larval NSCs at 4h ALH, due to dysregulations of SWH signalling.

But the effect is lesser pronounced compared to the loss of core components like Hpo or Wts. The pivotal reason for this discrepancy is the mere plurality of upstream regulating factors which act mostly in a redundant manner.

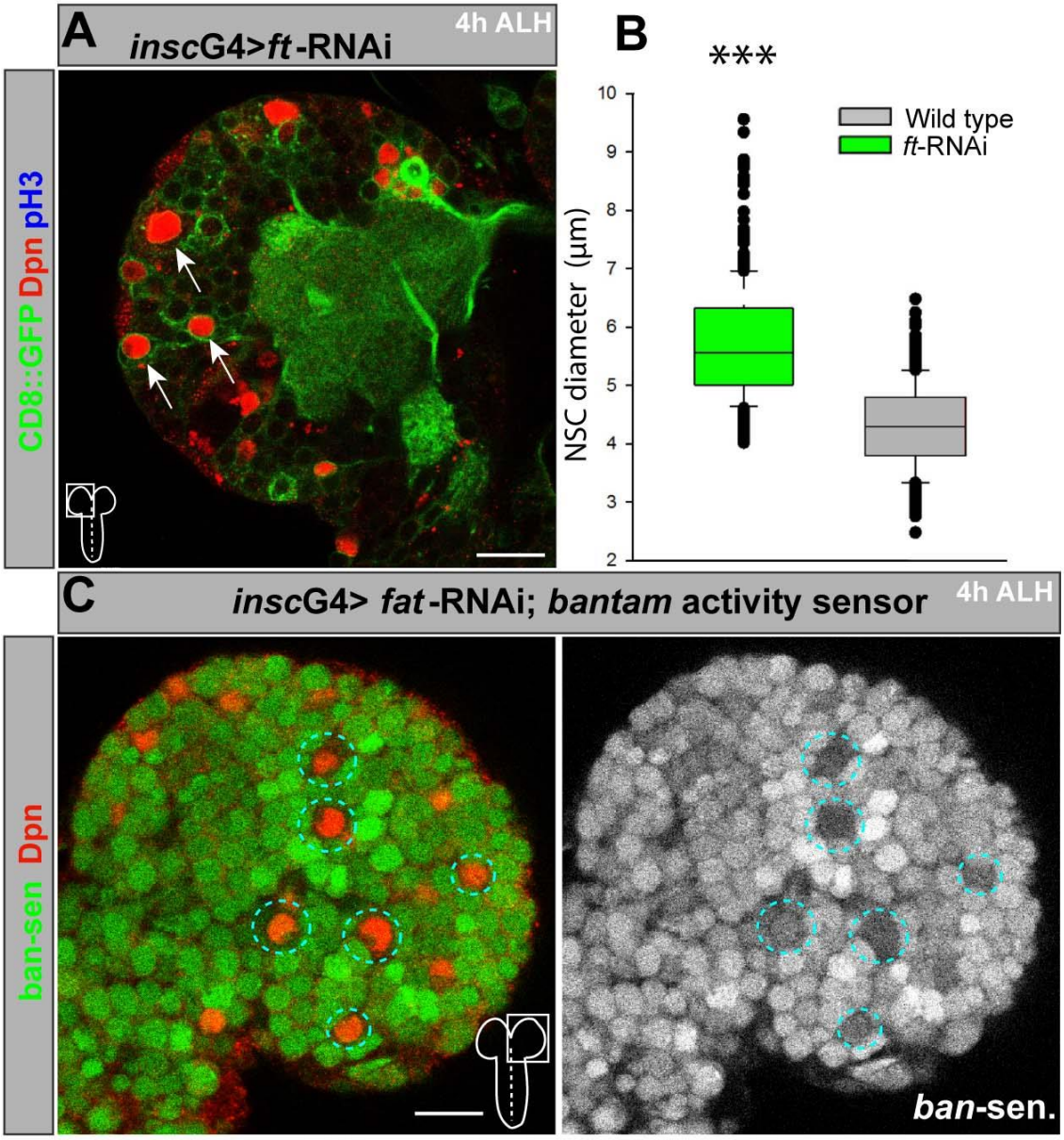

Figure 26: Loss of *fat* leads to premature reactivation of larval NSCs. (A) NSC-specific RNAi (*insc*G4>UAS-CD8::GFP) of *fat* (*ft*) leads to premature cell growth of NSCs. Arrows depict examples of NSCs with increased cell diameter. **(B)** Quantification of NSC diameters in RNAi *fat*-RNAi. Wild type brains 4h ALH: median 4,5µm (maximum 7µm) n= 150 NSCs (3 brain lobes); *insc*G4>*ft*-RNAi 4h ALH: median 5,5µm (maximum 9,5µm) n= 283 NSCs (6 brain lobes). **(C)** NSC-specific *fat*-RNAi leads to premature *ban* activity (loss of GFP) in NSCs at 4h ALH. For identifying the NSCs Dpn antibody was used, only Dpn positive cells show a decreased GFP signal (cyan blue circles); right channel shows the *ban*-sensor in monochrome. All images are single confocal sections anterior up and scale bars represent 10µm.

4.5.3 The transmembrane molecules Crumbs and Echinoid activate SWH signalling during NSC quiescence

I sought to investigate more closely how external signals have the ability to regulate the cell-intrinsic, growth-repressing activity of the SWH signalling pathway during quiescence. Since I've already shown that there is a variety of inter- and extracellular factors known to feed into this pathway to regulate its activity, I tested the transmembrane molecules Crumbs (Robinson *et al*., 2010; Grzeschik *et al*., 2010; Ling *et al*., 2010; Chen *et al*., 2010) and Echinoid (Chang *et al*., 2011; Yue *et al*., 2012) for their role in maintaining NSC quiescence. Both proteins are known to be involved in the regulation of SWH signalling in imaginal discs and other epithelial tissues. When targeting *crb* and *ed* by RNAi using the *insc*G4>UAS-CD8::GFP driver line there is a significant increase in NSC cell size at 4h ALH compared to the wild type situation. After knock down of *crb* the median cell diameter was 6µm (maximum 11µm), the loss of *ed* resulted in a median cell diameter of 6,5µm (maximum 12,5µm) (Figure 27 A-D). Based on these findings it is conceivable that NSC specific SWH signalling is regulated by surrounding cells via cell-cell contacts. Due to the fact that specialized niche glial cells are necessary for NSC reactivation (Chell and Brand, 2010; Sousa-Nunes *et al*., 2011) I further explored the role of niche signalling during NSC quiescence. Stem cells are organized in so called niches, which are specific anatomical regions, where the stem cells reside, but these niches also have functional dimensions and regulate whether and to what extent these cells participate to tissue regeneration, repair or maintenance (reviewed by Scadden, 2006). So I used the same RNAi constructs against *crb* and *ed* and expressed them with a glial specific driver line (*repo*G4>UAS-CD4::GFP) to eliminate the expression of these two transmembrane proteins in glial cells. In point of fact this was sufficient to observe a similar significant but less pronounced increase in NSC cell size (Fig. 27 C-F) compared with the knockdown of *crb* and *ed* in NSCs.

To verify these data I combined the two RNAi constructs against *crb* and *ed,* in order to down regulate both proteins in the same set of cells. The results obtained showed an similar increase in NSC cell size at 4h ALH with the *insc*G4>UAS-CD8::GFP driver, with a median cell diameter of 6µm and a maximum cell diameter of 9µm (Fig. 28A; Fig. 29B). Furthermore antibody stainings against Yki protein in NSCs deficient for *crb* and *ed* displayed obviously nuclear Yki localization at 4h ALH (Fig. 28A; white rectangles). Both magnifications illustrate two prematurely reactivated NSCs with a significant staining against Yki protein inside the nuclear compartment (marked with white circles) stating that the premature growth phenotypes are indeed attributable to loss of SWH signalling. The right panels show the Yki

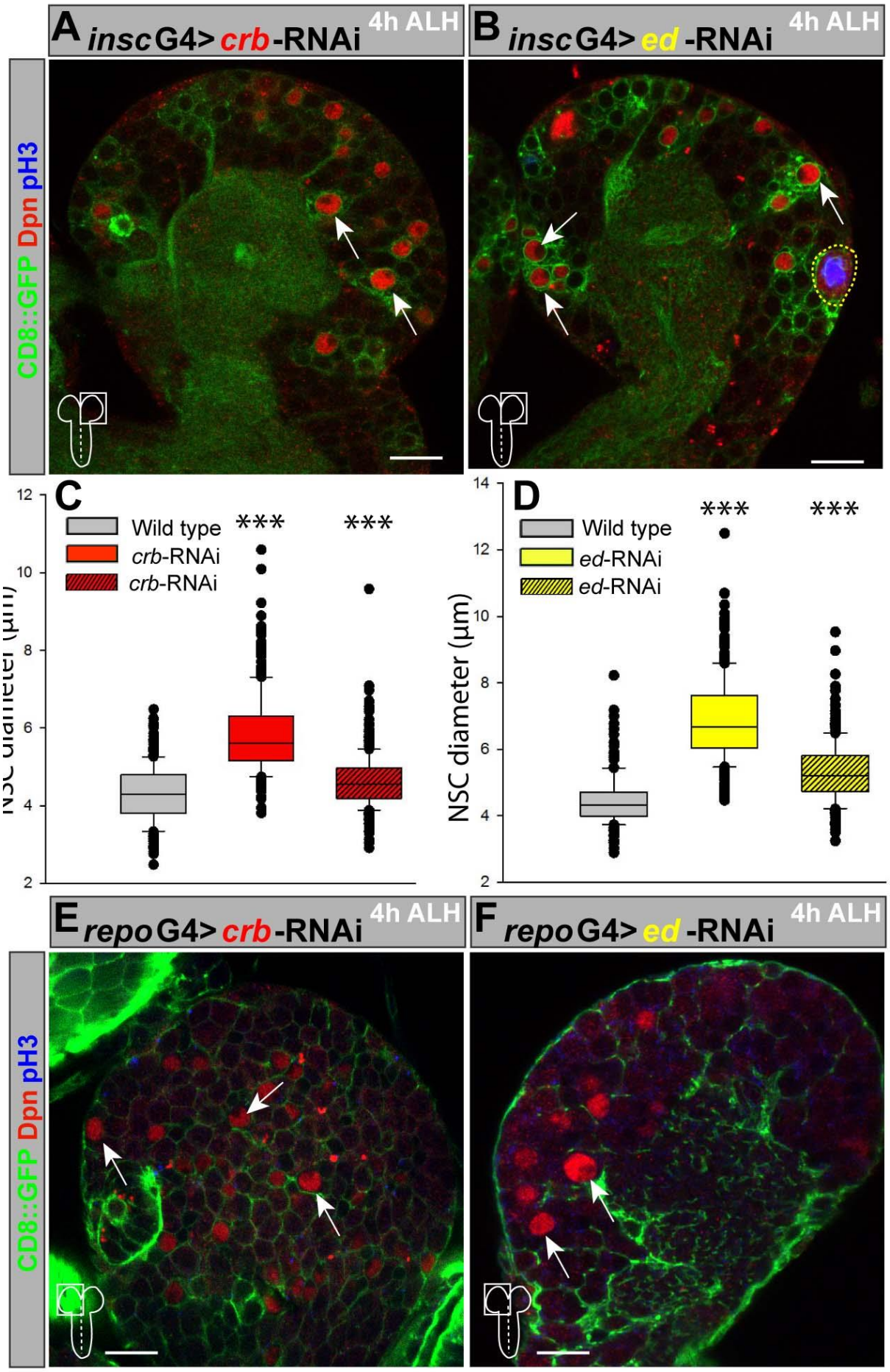
A insc G4> crb -RNAi 4h ALH
B insc G4> ed -RNAi 4h ALH
CD8::GFP Dpn pH3
C
Wild type
crb-RNAi
crb-RNAi
***
***
D
Wild type
ed-RNAi
ed-RNAi
***
***
NSC diameter (µm)
E repo G4> crb -RNAi 4h ALH
F repo G4> ed -RNAi 4h ALH
CD8::GFP Dpn pH3

Figure 27: Crumbs and Echinoid are required in NSCs and glial cells in *cis* and in *trans* to activate SWH signalling during quiescence. (A) NSC-specific (*insc*G4>UAS-CD8::GFP) RNAi of *crumbs* (*crb*) leads to increase in NSC cell diameter at 4h ALH. **(B)** NSC-specific (*insc*G4>UAS-CD8::GFP) RNAi of *echinoid* (*ed*) leads to increase in NSC cell diameter (the lateral non-quiescent NSC is yellow encircled) at 4h ALH. **(C-D)** Quantification of NSC diameters in *crb* **(C)** and *ed* **(D)** RNAi. **(C-D)** Wild type brains 4h ALH: median 4,5µm (maximum 7µm) n= 255 NSCs (5 brain lobes). **(C)** *insc*G4>*crb*-RNAi 4h ALH: median 6µm (maximum 10,5µm) n= 313 NSCs (7 brain lobes); *repo*G4>*crb* RNAi 4h ALH: median 5µm (maximum 10µm) n= 458 NSCs (9 brain lobes). **(D)** *insc*G4>*ed* RNAi 4h ALH: median 6,5µm (maximum 12µm) n= 300 NSCs (6 brain lobes); *repo*G4>*ed* RNAi 4h ALH: median 5µm (maximum 10µm) n= 388 NSCs (7 brain lobes). **(E)** Glial-specific RNAi of *crb* leads to increase in NSC cell diameter at 4h ALH; significantly enlarged NSCs are highlighted with white arrows. Green shows Phalloidin staining (Picture was kindly provided by Kevin Weynans). **(F)** Glial-specific RNAi of *ed* leads to increase in NSC cell diameter at 4h ALH; significantly enlarged NSCs are highlighted with white arrows. Green shows CD4::GFP under the control of *repo*G4 (Picture was kindly provided by Kevin Weynans). All images are single confocal sections anterior up and scale bars represent 10µm.

staining in monochrome. To test potential homophilic interactions of *crb* or *ed* (Letizia *et al*., 2013) I targeted *crb* and *ed* simultaneously in both NSCs and glial cells by RNAi through combining the *insc*G4>UAS-CD8::GFP with the *repo*G4>UAS-CD4::GFP driver line. I observed a slightly increased growth phenotype of NSCs (median of 6,5µm, maximum of 9,5µm) compared with the NSC specific knockdown alone (median of 6µm, maximum of 9µm) (Fig. 29B). Since the growth phenotype in the *crb*/*ed* double knockdown (*insc*G4>UAS-CD8::GFP/*repo*G4>UAS-CD4::GFP) was similar to the NSC specific (*insc*G4>UAS-CD8::GFP) loss of *crb* or *ed* alone I conclude that both *crb* and *ed* act in *trans* (intercellular, between cells) and in *cis* (intracellular, inside a cell) to regulate the activity of the SWH signalling pathway. Knockdown in glial cells (*repo*G4>UAS-CD4::GFP) removes the interaction in *trans* (between glial cells and NSCs) but leaves the interaction in *cis* (on NSCs), thereby producing a less pronounced phenotype (Fig. 27 C-F). Conversely, loss of *crb* or *ed* in NSCs (*insc*G4>UAS-CD8::GFP) or NSC and glial cells (*insc*G4>UAS-CD8::GFP/*repo*G4>UAS-CD4::GFP) simultaneously interrupts both, the interactions in *trans* and in *cis* and accordingly causes more pronounced phenotypes (Fig. 27 A-D; Fig. 28; Fig. 29B). To prove that the obtained NSC specific growth phenotypes caused by knock down of *crb*/*ed* in glial cells can be related to loss of SWH signalling in NSCs, I combined the *bantam*-GFP sensor with a *repo*G4 driver line without CD4::GFP. As can be seen in figure 29A glial specific loss of *crb*/*ed* leads to an enhanced *ban* activity in NSCs (Dpn, red) at 4h ALH, prematurely reactivated NSCs (white circles) display a significant loss of GFP due to *ban* activity. Single NSCs that are still quiescent (cyan blue circles) still exhibit a strong GFP

signal, showing that in these cells SWH signalling is still active and thereby inhibiting the expression of the Yki target *ban*.

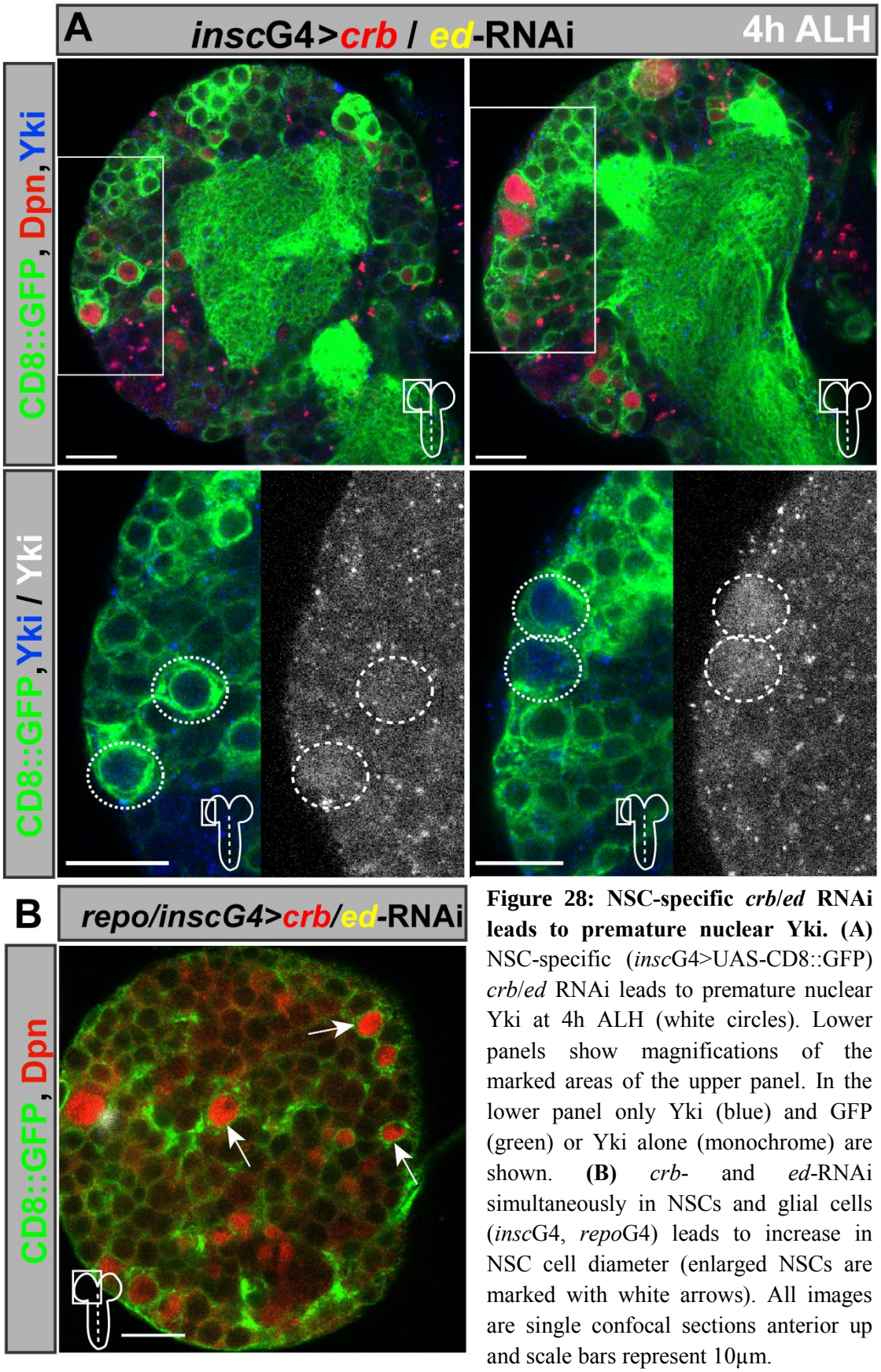

Figure 28: NSC-specific *crb*/*ed* RNAi leads to premature nuclear Yki. (A) NSC-specific (*insc*G4>UAS-CD8::GFP) *crb*/*ed* RNAi leads to premature nuclear Yki at 4h ALH (white circles). Lower panels show magnifications of the marked areas of the upper panel. In the lower panel only Yki (blue) and GFP (green) or Yki alone (monochrome) are shown. **(B)** *crb*- and *ed*-RNAi simultaneously in NSCs and glial cells (*insc*G4, *repo*G4) leads to increase in NSC cell diameter (enlarged NSCs are marked with white arrows). All images are single confocal sections anterior up and scale bars represent 10µm.

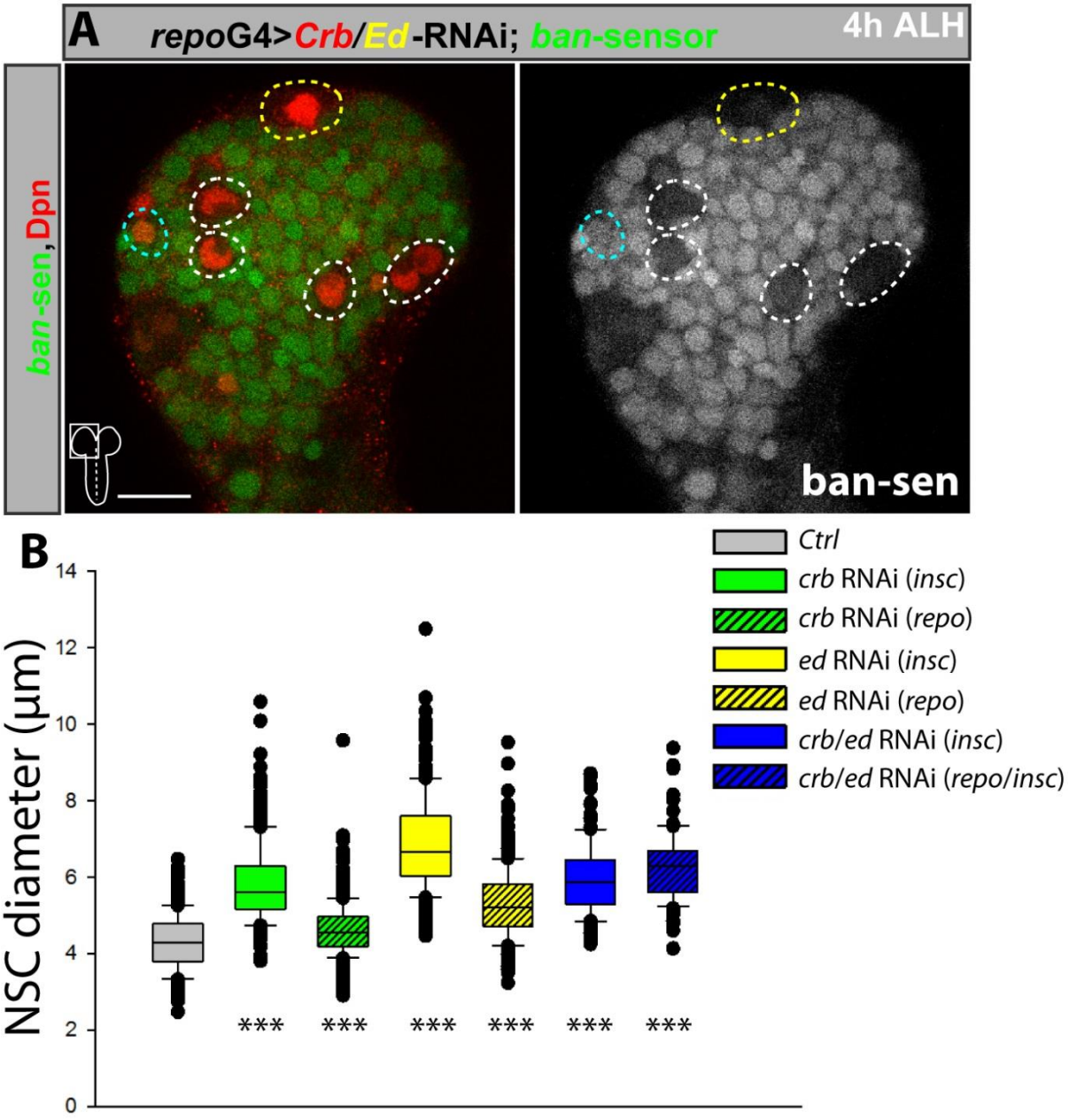

Figure 29: Glial-specific *crb*/*ed* RNAi causes expression of the Yki target *bantam* in NSCs. (A) Glial specific *crb*/*ed* RNAi leads to premature *bantam* activity (loss of GFP in the *bantam* senor system) in NSCs (white circles) at 4h ALH; MBNB is encircled in yellow and a single unreactivated NSC is highlighted in cyan blue. Right panel shows the GFP signal (*ban*-sensor) in monochrome. **(B)** Quantification of NSC diameters at 4h ALH: Wild type brains 4h ALH: median 4,5µm (maximum 7µm) n= 355 NSCs (5 brain lobes); *insc*G4>*crb*-RNAi 4h ALH: median 5,5µm (maximum 10,5µm) n= 313 NSCs (7 brain lobes); *repo*G4>*crb* RNAi 4h ALH: median 5µm (maximum 10µm) n= 458 NSCs (9 brain lobes*); insc*G4>*ed* RNAi 4h ALH: median 6,5µm (maximum 12µm) n= 300 NSCs (6 brain lobes); *repo*G4>*ed* RNAi 4h ALH: median 5µm (maximum 10µm) n= 388 NSCs (7 brain lobes); *insc*G4>*crb/ed*-RNAi 4h ALH: median 6µm (maximum 9µm) n= 183 NSCs (4 brain lobes); *insc*G4; *repo*G4> *crb/ed*-RNAi 4h ALH: median 6µm (maximum 9,5µm) n= 84 NSCs (2 brain lobes). All images are single confocal sections anterior up and scale bars represent 10µm.

The fact that NSCs prematurely reactivate after loss of transmembrane molecules in glia cells consequently shows that SWH signalling in NSCs is at least partly regulated by the surrounding niche glia cells in *trans* via cell contact inhibition.

4.5.3.1 Glial Crumbs expression depends on nutrition

So far Crumbs was thought to be expressed mainly on epithelial cells and its role in NSCs and glial cells was surprising. To further unravel the exact expression pattern of crb, a functional Crumbs::GFP fusion protein was utilized. As shown in figure 30A in Crb::GFP larvae there is a strong GFP signal (lower panel shows the GFP signal in monochrome) at 4h ALH indicating a strong expression of Crb during the quiescence phase on NSCs (red, Dpn) and glial cells (blue, repo). In contrast to that the Crb::GFP expression is strongly down regulated at 24h ALH (Fig. 30A', lower panel shows the GFP signal in monochrome) when the NSCs are reactivated. Interestingly the transcriptional regulation of *crb* in the early phases of CNS development seems to be highly dependent on the nutritional status of the larva, shown in figure 30A''. Nutritional deprivation prolongs NSC quiescence as well as the expression level of Crb::GFP, again the lower panel exhibits the GFP signal in monochrome. Whereas premature reactivation of NSCs through activation of the Insulin-like receptor signalling pathway caused by the overexpression of myristoylated Akt (myrAkt), leads to premature loss of Crb::GFP at 4h ALH (Fig. 30B; the upper panel shows a dorsal section of the larval brain and the lower panel shows a ventral section of the brain, right panels represent the Crb::GFP signal in monochrome). So far my data suggests that cell-contact inhibition between NSCs and glial cells inhibits growth of the quiescent NSCs via activation of SWH signalling. Hence I tested whether Crb::GFP localizes to the contact sites of glial cells and NSCs. Indeed, I could observe a slight accumulation of Crb protein in NSCs towards the contact site with glial cells (Fig. 30C).

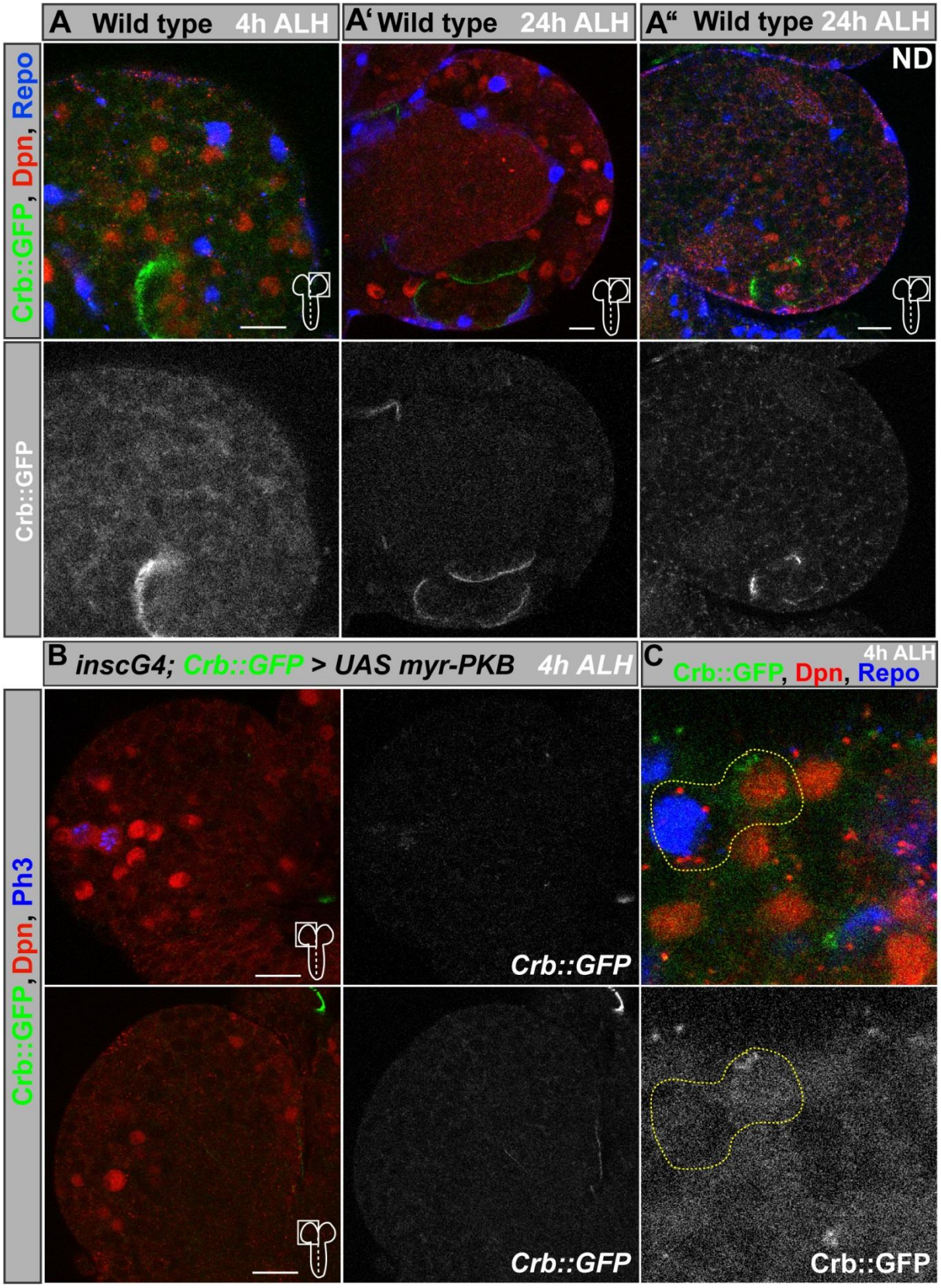
A Wild type 4h ALH
A' Wild type 24h ALH
A" Wild type 24h ALH
ND
Crb::GFP, Dpn, Repo
Crb::GFP
B inscG4; Crb::GFP > UAS myr-PKB 4h ALH
C 4h ALH
Crb::GFP, Dpn, Repo
Crb::GFP, Dpn, Ph3
Crb::GFP
Crb::GFP
Crb::GFP

Figure 30: Crumbs is temporally expressed in glial cells and NSCs; its expression depends on the nutritional status of the organism. (A) Expression of Crb::GFP (fused to the extracellular domain) in glial cells (blue, repo) and NSCs (red, Dpn) at 4h ALH (A), 24h ALH (A') and 24h ALH in nutritional deprivation (ND) (A''). Lower panels show GFP signal in monochrome. Crb is highly expressed during quiescence (4h ALH, A) and is lost after reactivation (24h ALH, A') but persists under nutritional deprivation (ND, 24h ALH, A'') (Pictures were kindly provided by Kevin Weynans). **(B)** Ectopic expression of myristoylated Akt (active form) in NSCs leads to premature reactivation of NSCs (Ph3 (blue) positive NSCs (red, Dpn) and early downregualtion of Crb::GFP). Right panel shows the Crb::GFP signal in monochrome. **(C)** Crb::GFP accumulates at the interface of NSC (red, Dpn) and glial cell (blue, repo) contacts, lower panel shows the Crb::GFP signal in monochrome. All images are single confocal sections anterior up and scale bars represent 10µm.

To prove that NSCs and glial cells indeed form cell-cell contacts, I stained for E-Cadherin (E-cad) to monitor potential adherens junctions (AJ) between these two cell types in the CNS of *Drosophila* larvae. AJs are established by cadherin receptors which form homophilic interactions in *trans* with other cadherins and thereby bridge the neighbouring plasma membrane, so they make an essential contribution to the physical linking of cells (Zhang *et al*., 2009; reviewed by Meng and Takeichi, 2009). As seen in figure 31 there is a massive overlap of the Ecad staining (blue, right panel in monochrome) with the glial plasma membrane (green, *repo*G4>UAS-CD4::GFP). The white circles in the uppermost picture highlight the non-quiescent MBNB at 4h ALH. The Ecad monochrome panel makes it obvious that the staining perfectly matches the GFP signal of the glial membranes indicating the presence of AJ between these cells. The image below shows two quiescent NSCs with equally overlapping stainings of Ecad (blue) and glial membranes (green), these two cells are magnified in the bottom two images (right panels again show Ecad staining in monochrome). Furthermore these figures reveal a complex staining of Ecad in the whole larval CNS at 4h ALH indicating an extensive network of physical interactions between the different cell types of the nervous system, highlighting that the AJ are crucial factors for the morphogenesis and regulation of the CNS development.

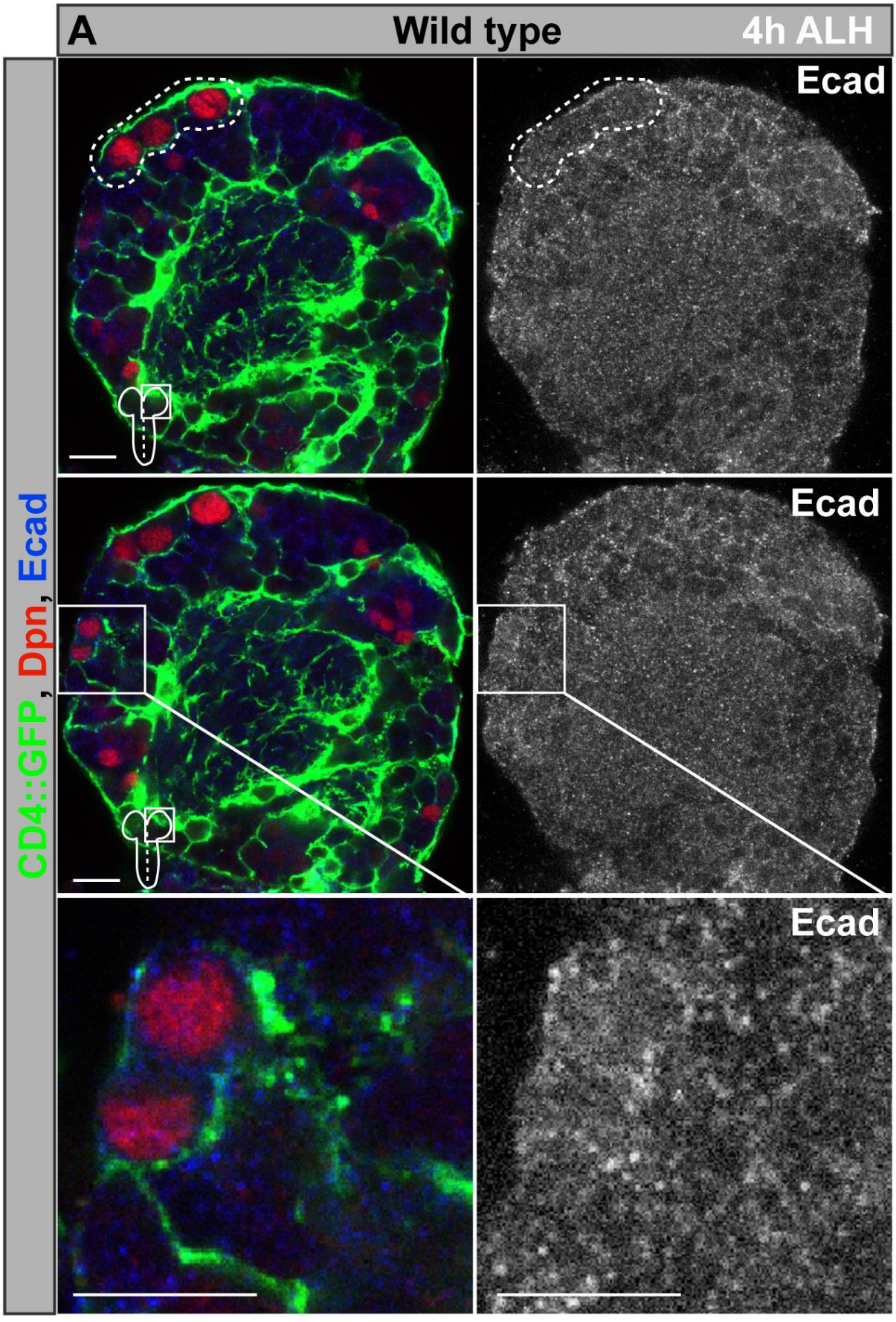
A
Wild type
4h ALH
CD4::GFP, Dpn, Ecad
Ecad
Ecad
Ecad

Figure 31: E-Cadherin unravels adherens junctions between NSCs and glial cells. (A) E-Cadherin (blue, monochrome in right panels) is strongly expressed at the interface between NSCs (red, Dpn) and glial cell membranes (green, CD4::GFP). Magnifications show representative staining of AJs. All images are single confocal sections anterior up and scale bars represent 10µm.

Next I assessed whether the ectopic expression of *crb* or *crb*/*ed* is sufficient to prolong the cellular quiescence of *Drosophila* larval NSCs. Ectopic expression of *crb* caused some problematic phenotypes in the central brain region of the affected larvae, as can be seen in figure 32F. I observed cell clustering of NSCs and a significant increase in the number of MBNBs (Fig. 32F, white circle, lower panel shows the GFP signal in monochrome). Due to the fact that these obstructive conditions were not apparent in the NSCs of the VNC I was able to analyse their growth behaviour and their mitotic index at 24h ALH (Fig. 32 A-E). Ectopic expression of *crb* was not able to completely suppress NSC reactivation in the VNC, but was sufficient to strongly reduce cell growth and proliferation at 24h ALH (Fig.32B, D, E) compared to the wild type situation (Fig.32 A, D, E). Co-expression of *crb* and *ed* had no additive effect on growth suppression, but the proliferation rate was further reduced (Fig. 32 C, D, E).

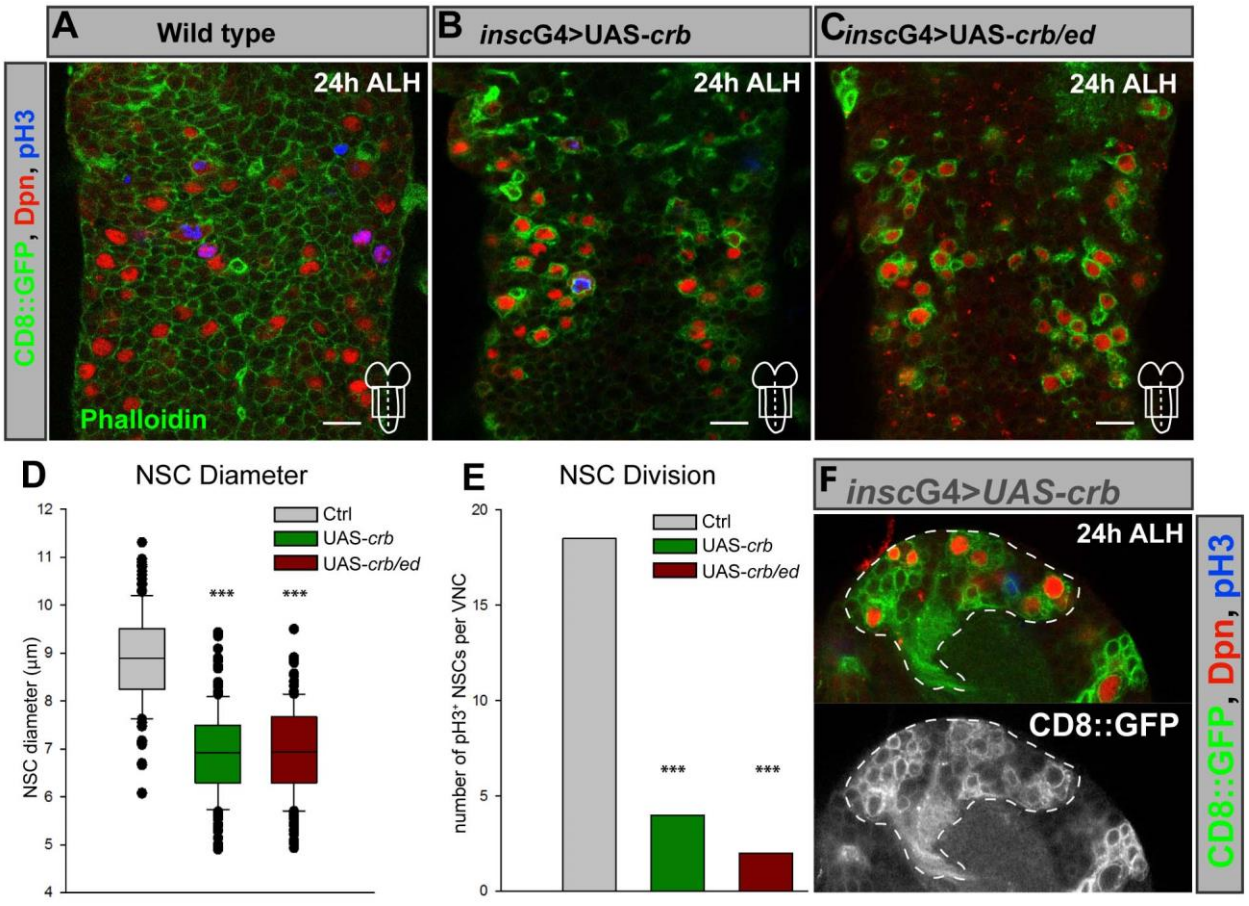

Figure 32:. Ectopic *crb* causes decreased NSC growth and proliferation. (A-C) In comparison to wild type **(A)** prolonged expression in NSCs of *crb* **(B)** or *crb/ed* **(C)** leads to a partial suppression of NSC cell growth and division in ventral nerve cord NSCs at 24h ALH. **(D, E)** Quantification of NSC diameters **(D)** and mitotic index **(E)** in NSC-specific prolonged expression of *crb* or *crb*/*ed* at 24h ALH. **(D)** Wild type VNC NSCs 24h ALH: median 9µm (maximum 11,5µm) n= 129 NSCs (3 VNCs); *insc*G4 >UAS-*crb* 24h ALH: median 7µm (maximum 9,5µm) n= 144 NSCs (3 VNCs); *insc*G4>UAS-*crb/ed* 24h ALH: median 7µm (maximum 9,5µm) n= 165 NSCs (3 VNCs). **(E)** Ratio of NSCs in mitosis ($pH3^+$) per counted VNC at 24h ALH, in the wild type control 3 VNCs, in *insc*G4>UAS-*crb* and in *insc*G4>UAS-*crb*/*ed* 3 VNCs were counted. There is a massive reduction of pH3+ NSCs after ectopic expression of *crb* and *crb/ed*. **(F)** Ectopic expression of *crb* in all NSCs (*insc*G4>UAS-CD8::GFP) leads to an increase in Dpn-positive cells in NSCs of the mushroom bodies (encircled in white) at 24h ALH. Lower panel shows GFP signal in monochrome. All images are single confocal sections anterior up and scale bars represent 10µm.

4.6 Yki discriminates between different populations of NSCs

Next I sought to investigate whether SWH signalling has the capability to discriminate quiescent (nutrition dependent NSCs) from non-quiescent NSCs (MBNB, lNSC) in the CNS of *Drosophila*. Antibody stainings against downstream targets of the SWH signalling pathway revealed a constant expression of Fj-LacZ (Fig. 19), *expanded* (Fig. 20) and the *bantam* miRNA (Fig. 15) in MBNBs and thereby confirm a continuous Yki activity. Stainings against Yki itself displayed its constant nuclear localization in the MBNBs even at 4h ALH (Fig. 10; Fig. 12) whilst the quiescent, nutrition-dependent NSCs showed no nuclear localization of Yki (Fig. 10; Fig. 12). Furthermore I analysed the mitotic indices of non-quiescent MBNBs at 48h ALH under different nutritional conditions (well fed; nutrition deprived) and in the yki^{B5} mutant situation. As shown in figure 33B there is a marked reduction in the proliferative capacity of nutrition deprived and yki^{B5} mutant MBNBs compared to the wild type situation at 48h ALH. The medial number of $pH3^+$ MBNBs per brain lobe is 2,2 in the wild type situation, under nutritional deprivation this value is reduced to 0,1 and in the yki^{B5} mutant background to 0,25 (Fig. 33B). These data reveal that, Yki activity is a necessity for MBNBs to proliferate and that the continuous nuclear localization of Yki is a distinctive feature between quiescent and non-quiescent NSCs in the *Drosophila* CNS.

Another potential possibility of Yki to discriminate between NSC populations is the choice of the nuclear interaction partner, because Yki has the ability to bind to different DNA binding transcription factors; namely Scalloped (Sd), Homothorax (Hth) and Teashirt (Tsh) (Goulev *et al*., 2008; Peng *et al*., 2009). To get a first insight into this I stained against Tsh in *ase*Gal4>UAS-stinger::GFP larval brains at 24h ALH, which drives the expression of GFP only in type I NSCs and the MBNBs but not in the type II lineages. As can be seen in figure

35 expression of the transcription factor Tsh seems to be restricted to the type I NSCs of the larval central brain and is absent in the Type II NSCs (Fig. 35; white circles in the upper panel). The non-quiescent MBNBs also show no Tsh staining (Fig. 35; yellow circles in the lower panel) on the contrary the type I NSCs of the larval central brain exhibit a strong staining intensity against Tsh (Fig. 35; white arrows in the lower panel).

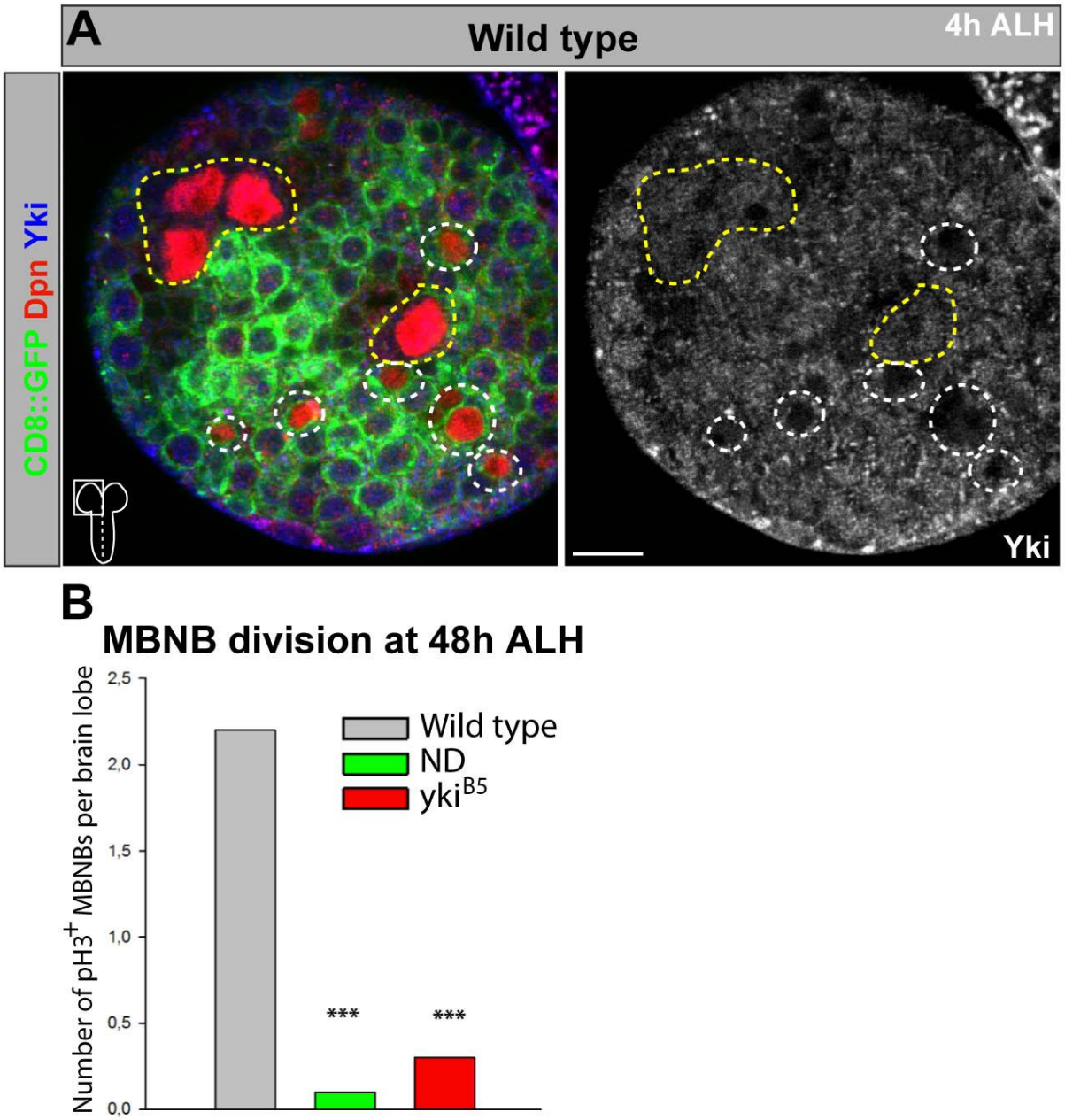

Figure 33: Yorkie activity discriminates between quiescent and non-quiescent NSCs. **(A)** Yki staining in the *insc*G4>UAS-CD8::GFP driver line shows constantly nuclear Yki localization in non-quiescent NSCs (yellow circles) and cytoplasmic localization in quiescent NSCs (white circles) at 4h ALH. Right panel shows the Yki staining in monochrome. **(B)** Quantification of MBNB in mitosis. Ratio of pH3-positive NSCs per brain lobes, counted in 7 well fed wild type brain lobes (grey bar), 5 wild type brain lobes in ND (green bar) and 10 brain lobes in yki^{B5} mutants (red bar). There is a significant reduction of proliferating MBNBs due to loss of Yki in the yki^{B5} mutant. All images are single confocal sections anterior up and scale bars represent 10µm.

The VNC displays a complete different staining pattern for Tsh, a huge number of cells in this part of the CNS show Tsh expression, including the neurons. But equally the majority of NSCs are Tsh positive (Fig. 34; white circles) even though a few NSCs show no Tsh staining (Fig. 34; yellow circle).

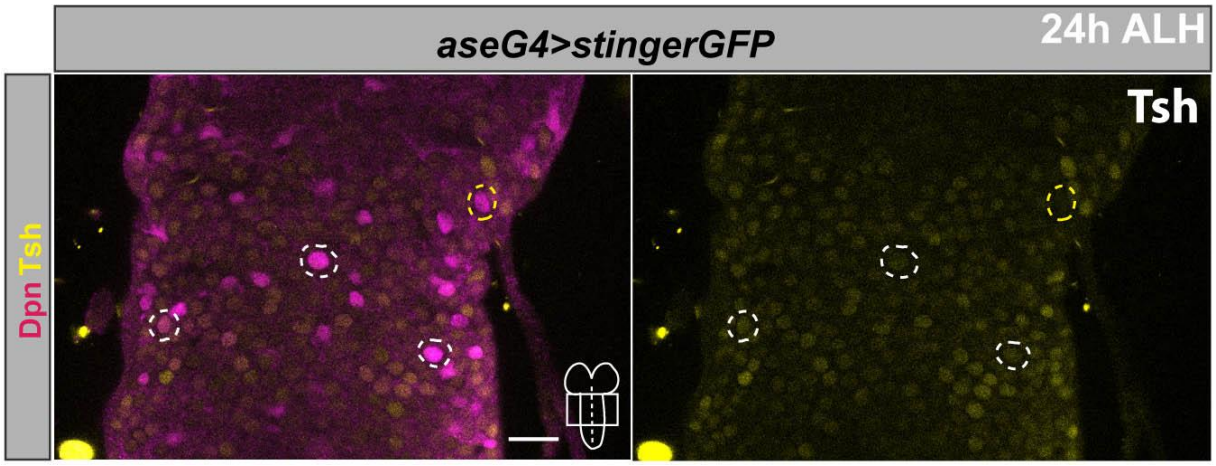

Figure 34: Teashirt is strongly expressed in the VNC. Tsh staining in the aseG4>UAS-stinger::GFP driver line. Tsh is broadly expressed in the thoracic sections of the VNC including the neurons, most NSCs display Tsh expression (white circles), some are Tsh negative (yellow circle). Right panel shows the Tsh staining in monochrome. All images are single confocal sections anterior up and scale bars represent 10µm.

To unravel the importance of the transcription factor Tsh for NSC growth and proliferation I used the *insc*G4>UAS-CD8::GFP driver line to down regulate the expression of Tsh in NSCs. As can be seen in Figure 36 loss of Tsh leads to massive growth defects of the whole CNS. The median cell diameter in the wild type situation at 48h ALH was 12µm (maximum 15,5µm) for central brain NSCs, after loss of Tsh the median cell diameter was reduced to 6,5µm (maximum 10µm) (Fig. 36C).

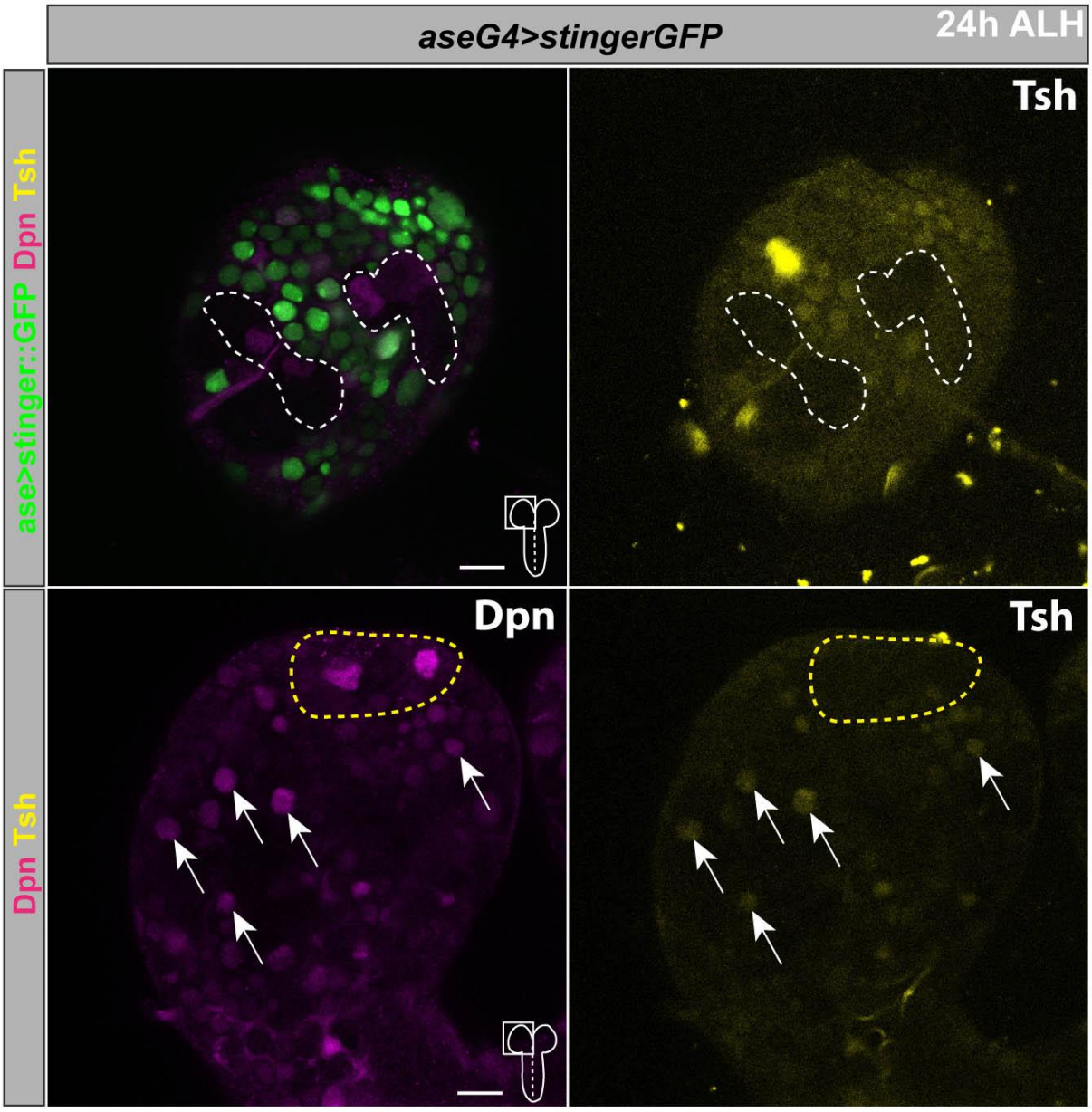

Figure 35: Teashirt is differentially expressed in individual NSCs. Tsh staining in the aseG4>UAS-stinger::GFP driver line shows differential expression of Tsh across the CNS. The type II NSCs show no expression of Tsh (white circles in the upper panel) as well as the MBNBs (yellow circle in the lower panel); only the type I NSCs are Tsh positive (white arrows in the lower panel). The left panels show the Tsh staining in monochrome. All images are single confocal sections anterior up and scale bars represent 10µm.

Taken together these results indicate that Yki has the ability to discriminate between different NSC populations through the cell specific choice of its interaction partner. At least for Tsh I have shown that it is differentially expressed in different NSC populations of the CNS and influences NSC growth and proliferation, what speaks in favour for the hypothesis that the unique combination of cell specific Yki interaction partners play a pivotal role in modulating the transcriptional output of SWH signalling.

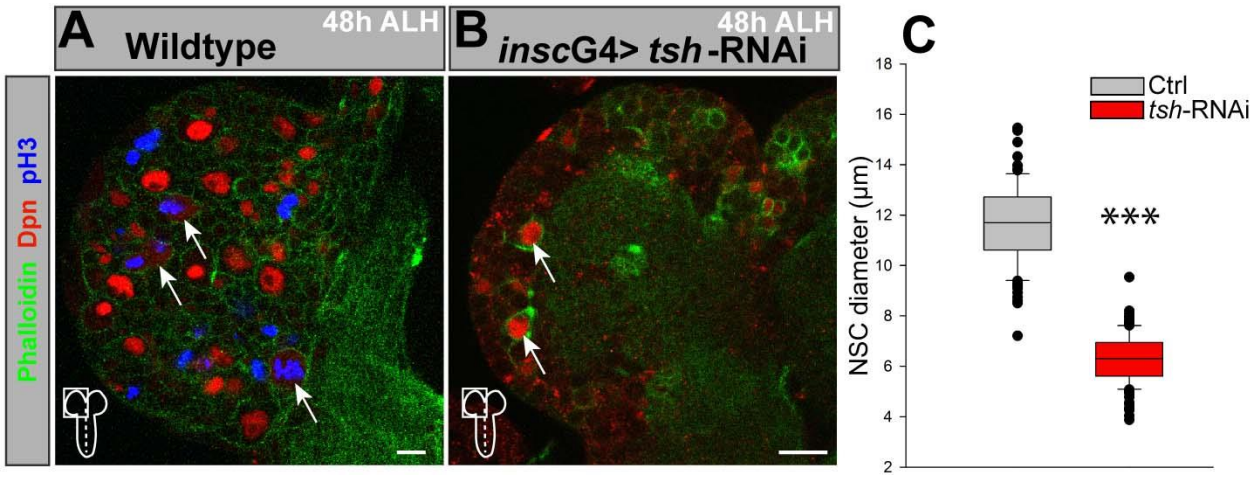

Figure 36: The transcription factor Tsh is necessary for the reactivation of larval NSCs. (A, B) NSC-specific knock-down (*insc*G4>UAS-CD8::GFP) of Tsh is followed by a decreased growth and proliferation of larval NSCs **(B)** compared to wild type larval brains **(A)** at 48h ALH. Phalloidin-GFP (green) is used as a membrane marker for the measurements of the cell diameters. **(C)** Quantification of NSC diameters in *tsh-RNAi* and wild type brains at 48h ALH. Wild type brain 48h ALH: median 12µm (maximum 15,5µm) n= 97 NSCs (2 brain lobes); *tsh*-RNAi brain 48h ALH: median 6,5µm (maximum 10µm) n= 152 NSCs (4 brain lobes). All images are single confocal sections anterior up and scale bars represent 10µm.

4.7 Yki down regulates its own competitor via the *bantam* miRNA

Recently Koontz *et al.* (2013) showed that Yki regulates the expression of its target genes through antagonizing Scalloped (Sd) mediated default repression. Sd is known to be the main interaction partner of Yki in the nucleus (Goulev *et al.*, 2008; Wu *et al.*, 2008; Zhang *et al.*, 2008; Zhao *et al.*, 2008) but during the time Yki is sequestered to the cytoplasm due to active SWH signalling Sd binds to Tgi (Tondu domain containing growth inhibitor). This interaction causes a default repression of its growth promoting target genes. When SWH signalling is inhibited and active Yki protein translocates into the nucleus it displaces Tgi from the Sd binding sites and thus relieving its default repression (Koontz *et al.*, 2013). To figure out whether the transcriptional co-repressor Tgi has an equal role in the regulation of SWH signalling in NSCs I performed an RNAi experiment using the *insc*G4>UAS-CD8::GFP driver line. Indeed NSC specific loss of *tgi* caused premature reactivation visualized through a significant increase in cell diameter compared to the wildtype situation, as seen in figure 37A, B (enlarged NSCs are indicated with white arrows). The median of the affected cells was 6,5µm with a maximum of 12µm (Fig. 37C).

An *in silico* screen identified Tgi as a potential target of the miRNA *ban*, on the basis of two putative *ban* target sites in the 3'UTR of the *tgi* mRNA. This finding raised the question

whether Yki has the ability to down regulate its own competitor through the expression of its target gene *ban* in the sense of a negative feedback loop.

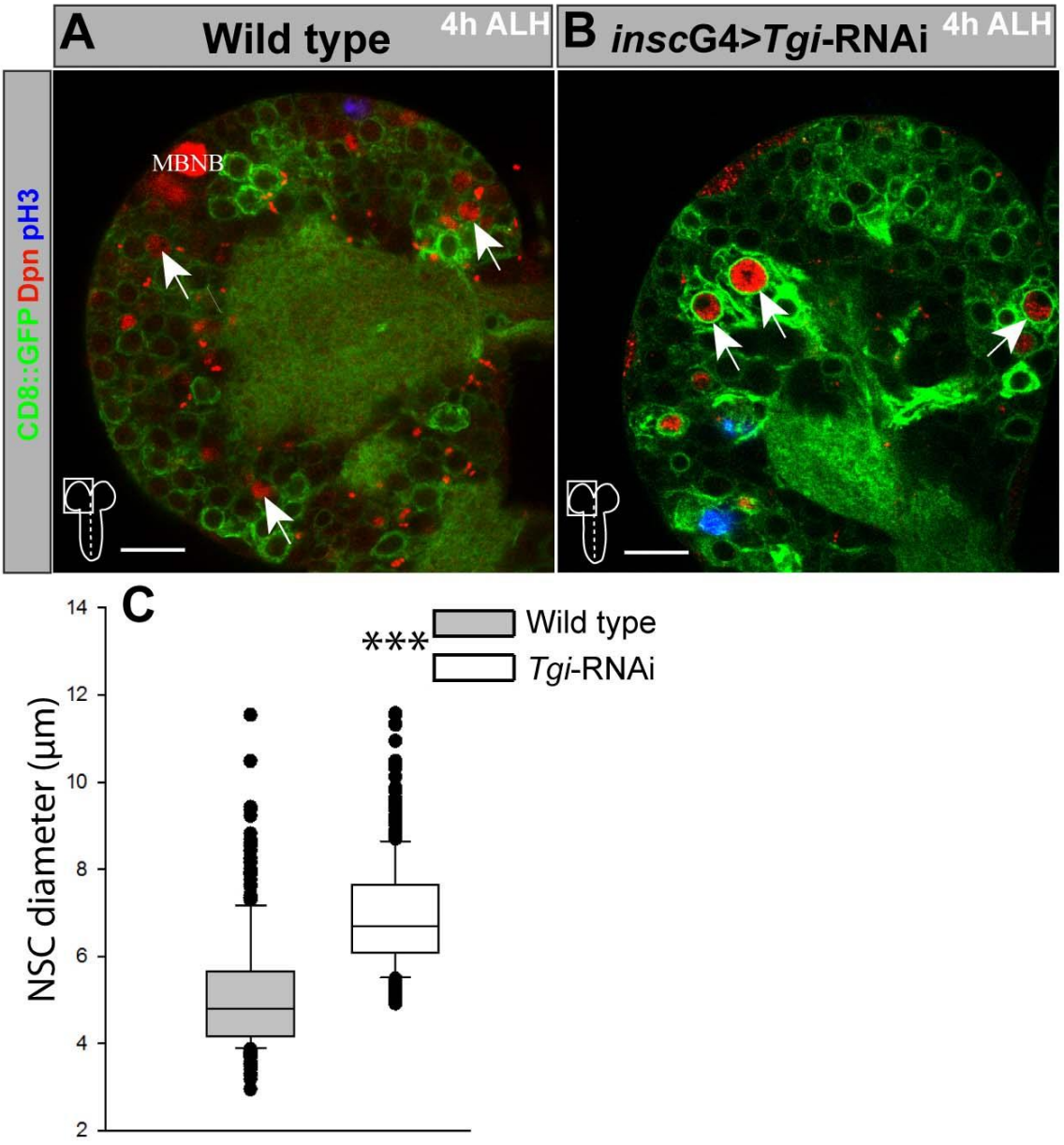

Figure 37: Loss of Tgi in NSCs leads to premature reactivation. (A, B) In comparison to wild type **(A)** loss of *tgi* in NSCs **(B)** leads to premature cell growth of NSCs at 4h ALH; significantly enlarged NSCs are marked with white arrows **(C)** Quantification of NSC diameters at 4h ALH. Wild type brains 4h ALH: median 4,5µm (maximum 12µm) n= 237 NSCs (5 brain lobes); *insc*G4>*tgi*-RNAi 4h ALH: median 6,5µm (maximum 12µm) n= 237 NSCs (4 brain lobes). All images are single confocal sections anterior up and scale bars represent 10µm.

To follow this track Dr. Thomas Löffler designed three different *tgi* 3'UTR constructs bearing different mutations in the distinct, putative binding sites for *ban* (Fig 38A). The first putative *ban* binding site is located at the position 179-185 inside the 3'UTR of *tgi* and has been

replaced by an EcoRI restriction site (Fig. 38A; mutation 1) via megaprimer mutagenesis. The second potential *ban* binding site lies at the position 240-247 inside the 3'UTR of *tgi* and has been replaced by a PvuI restriction site (Fig. 38A; mutation 2). A third *tgi* 3'UTR construct comprises both mutations (mutation 1 and mutation 2) to test for additive effects which may occur when both binding sites are abolished.

For application in a Luciferase assay a wild type *tgi* 3'UTR as well as the three different *tgi* 3'UTR constructs were cloned into the pmirGLO® Dual-Luciferase miRNA Target Expression Vector via the SacI and XhoI restriction sites of the multiple cloning site (MCS). As a positive control the 3'UTR of the known *ban* target head involution defective (HID) was also cloned into this vector system.

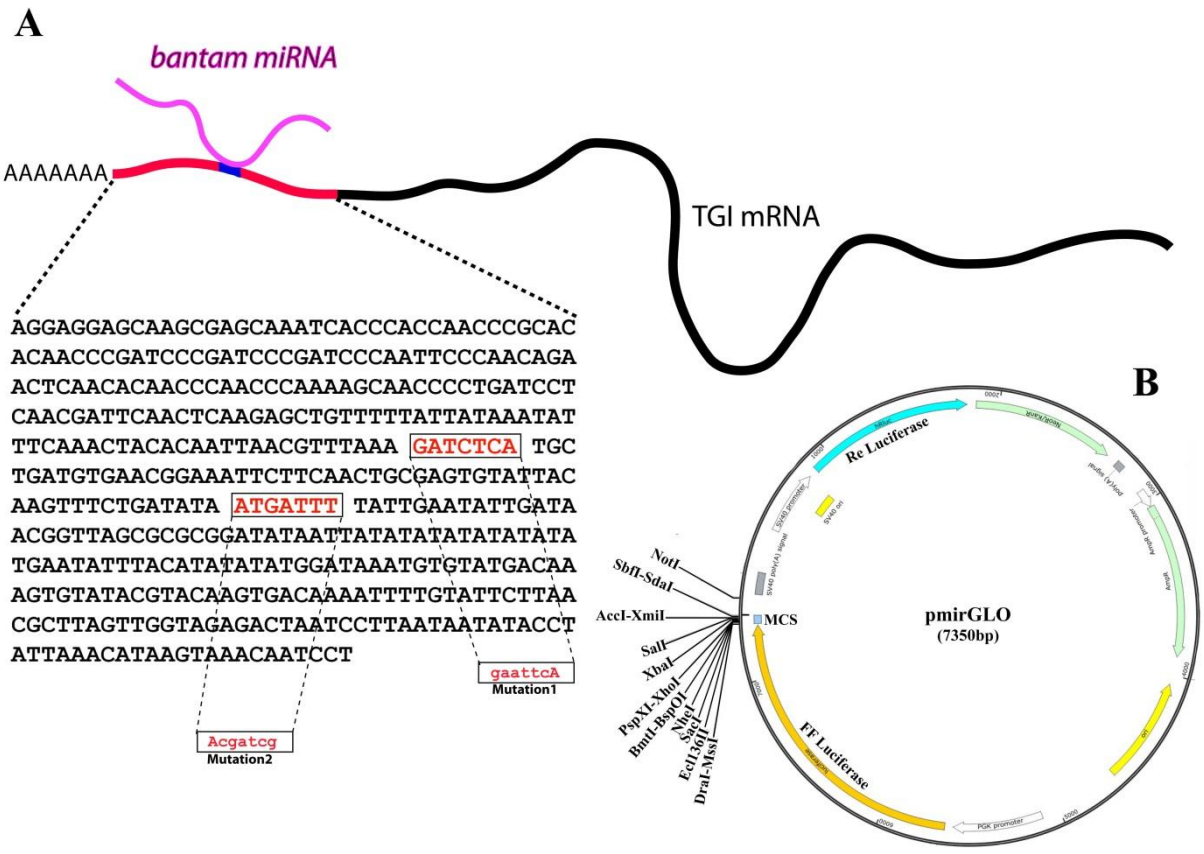

Figure 38: Potential *ban* binding sites in the 3'UTR of Tgi. (A) Schematic representation of the *tgi* mRNA: black = coding region; red = 3'UTR; AAA = polyA tail. The *ban* miRNA is shown in pink as it binds to its potential target sites (blue) in the 3'UTR of *tgi*. In the lower part the nucleotide sequence of the *tgi* 3'UTR is shown, the potential *ban* binding sites are highlighted in red; the boxes illustrate the changed sequences: the first site was replaced by an EcoRI restriction site (mutation1) and the second site was replaced against a PvuI restriction site (mutation2). **(B)** Map of the utilized pmirGLO® Dual-Luciferase miRNA Target Expression Vector and its multiple cloning site (MCS). The vector is equipped with a firefly luciferase under the control of a PGK promoter, a renilla luciferase under the control of a SV40 promoter and ampicillin, kanamycin and neomycin resistance genes. The 3'UTR constructs were cloned into the vector using the restriction sites SacI and XhoI of the MCS.

The five different 3'UTR constructs were individually co-transfected in HEK293 cells together with a *ban* expression vector (pEZX-MR04) and a GFP expression vector as transfection control (Figure 39A). Due to statistical reasons I performed control experiments using a scrambled vector instead of the *ban* expression vector, and the data of the experimental samples was normalized against these control samples. The strongest reduction of the luminescence signal in comparison to the control sample was obtained in cells which were transfected with the 3'UTR of the *hid* gene (with a relative luciferase activity of 0,7), which is a known *ban* target. But expression of the wild type 3'UTR of *tgi* also caused a significant reduction of the luminescence signal (with a relative luciferase activity of 0,8). On the contrary cells which were transfected with the mutated 3'UTR constructs of *tgi* displayed a relative luciferase activity which resembles the control sample (mutation1: 1,05; mutation 2: 1,1; mutation 1 and 2: 1,01) (Figure 39B).

Taken together these data indicates that the *tgi* expression can be negatively regulated through the activity of the *ban* miRNA via RNAi mediated downregulation. To terminally answer this question further experiments have to be done to prove these data.

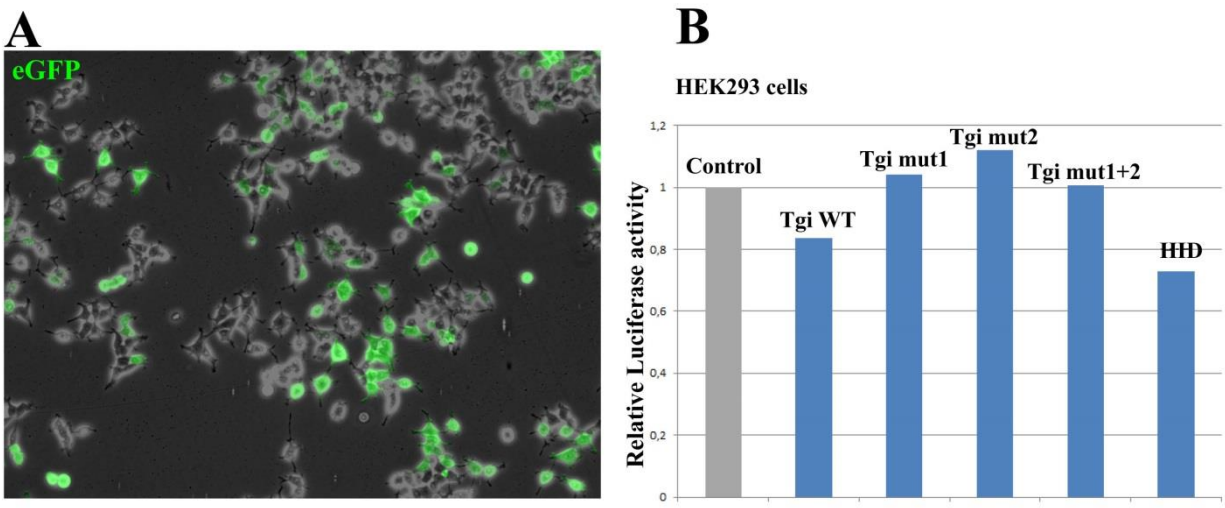

Figure 39: The *ban* miRNA can bind to the 3'UTR of *tgi*. (A) HEK293 cells after transfection, the GFP signal was used as a read-out for the transfection efficiency in all experiments. **(B)** Graphical illustration of the relative luciferase activity of the different 3'UTR constructs (Tgi wt, Tgi mutation 1, Tgi mutation 2, Tgi mutation 1+2 and HID), in comparison to the control samples. Cells which were transfected with the Tgi wt and the HID constructs showed the lowest relative luciferase activity (0,8 and 0,7 respectively), cells which were transfected with the mutated Tgi 3'UTRs displayed luciferase activities that resemble the control sample.

4.8 The role of dMyc for NSC reactivation

4.8.1 The dMyc proto-oncogene is necessary and sufficient for NSC reactivation

At the beginning of my studies concerning the role of dMyc in NSC reactivation after quiescence, I dissected larval brains during early stages of development at 24h ALH in the dm^4 mutant background and compared them with wild type control brains with regards to cellular growth and proliferation. The dm^4 allele represents a null mutation of the *Drosophila dimunitive* (*dm*) gene, lacking the transcriptional start site as well as the first two exons of the gene (Pierce *et al*., 2004). As can be seen in Figure 40A and B the depletion of dMyc causes severe reactivation problems in the CNS. In the dm^4 mutant background no reactivation of the larval NSCs takes place, all NSCs are still quiescent at 24h ALH and not a single one is $pH3^+$, meaning that they are not proliferating (Fig. 40A). The median cell diameter of the wild type control NSCs at this developmental stage is around 11µm (maximum 14µm) and in the dm^4 mutant CNS the measured median is 5µm (maximum 11µm) (Fig. 40B). These data reveal that dMyc is necessary for NSC reactivation.

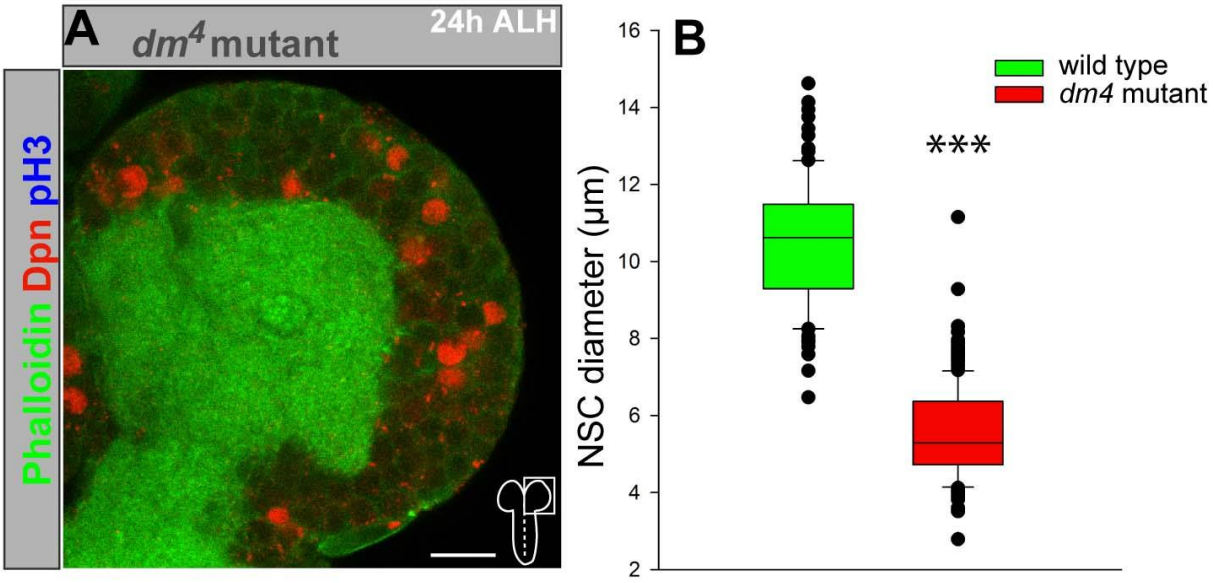

Figure 40: dMyc is necessary for NSC reactivation. **(A)** Depletion of the *dm* locus (*dm*^{4} mutant) causes strong reactivation defects of NSCs; No phosphohistone H3-positive (pH3) NSCs can be observed. **(B)** Quantification of NSC diameters at 4h ALH. Wild type brains 4h ALH: median 11µm (maximum 14µm) n= 109 NSCs (3 brain lobes); *dm*^{4} mutant 4h ALH: median 5µm (maximum 11µm) n= 179 NSCs (4 brain lobes). Image is single confocal section anterior up and scale bar represent 10µm.

To find out whether dMyc is not only necessary but also sufficient for NSC reactivation, I ectopically expressed the dMyc protein in NSCs via the *insc*G4>UAS-CD8::GFP driver line and dissected the larval brains at 4h ALH, during the late quiescence phase. At this developmental time point the NSCs are naturally still small with a median cell diameter of 4,5µm in diameter, but the overexpression of *dmyc* causes a massive premature reactivation (Fig. 41A). The median cell diameter after UAS-dMyc expression was raised to 8µm (maximum 12,5µm) (Fig, 41B) indicating the importance of this protein for the cellular growth of NSCs.

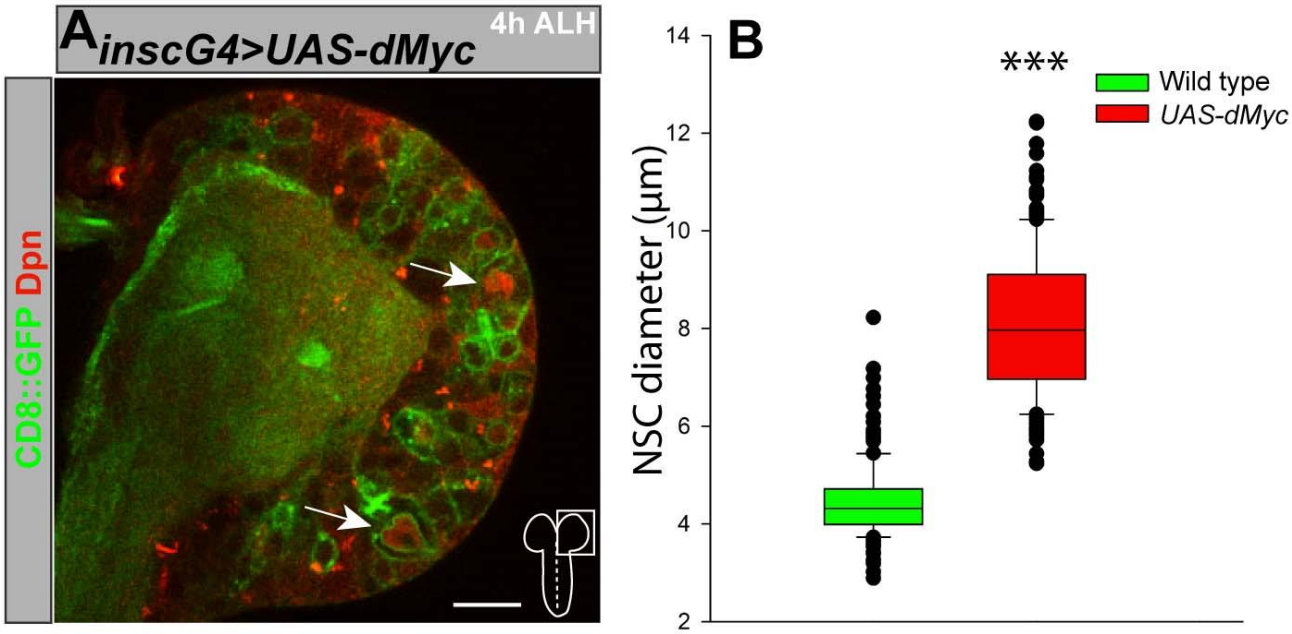

Figure 41: Overexpression of dMyc is sufficient for NSC reactivation. **(A)** NSC-specific overexpression (*insc*G4>UAS-CD8::GFP) of *dmyc* causes premature cell growth of NSCs at 4h ALH; significantly enlarged NSCs are highlighted with white arrows. **(B)** Quantification of NSC diameters at 4h ALH. Wild type type brains at 4h ALH: median 4,5µm (maximum 8µm) n= 150 NSCs (4 brain lobes); *insc*G4>UAS>*dmyc* at 4h ALH: median 8µm (maximum 12,5µm) n= 200 NSCs (5 brain lobes). Image is single confocal section anterior up and scale bar represent 10µm.

4.8.2 Target gene expression of dMyc corresponds to NSC reactivation

To prove that the obtained NSC specific growth phenotypes can to related to dMyc function I analysed the expression levels of known target genes of dMyc. Since Hulf *et al*. (2005) have identified a huge number of genes which showed an upregulation upon dMyc overexpression and decreased expression levels after loss of dMyc (Hulf *et al*., 2005) they assumed that these genes are transcriptional targets of dMyc.

On account of this I initially analysed the expression levels of seven of the described *dmyc* target genes (CG1381, CG5728, CG6375, CG6751, CG7006, CG7137 and CG7845) in quiescent CNSs at 4h ALH and reactivated CNSs at 24h ALH. For this approach I generated cDNA from whole CNSs at the defined time points and used this as a template for the qRT-PCR. As seen in figure 42A the expression levels of all seven *dmyc* target genes which were tested are massively elevated after reactivation at 24h ALH. Especially CG1381 (Ribosomal protein LP0-like) is strongly upregulated, which is a structural component of the large ribosomal subunit and thereby involved in protein biogenesis; a process that is inevitable for cell growth.

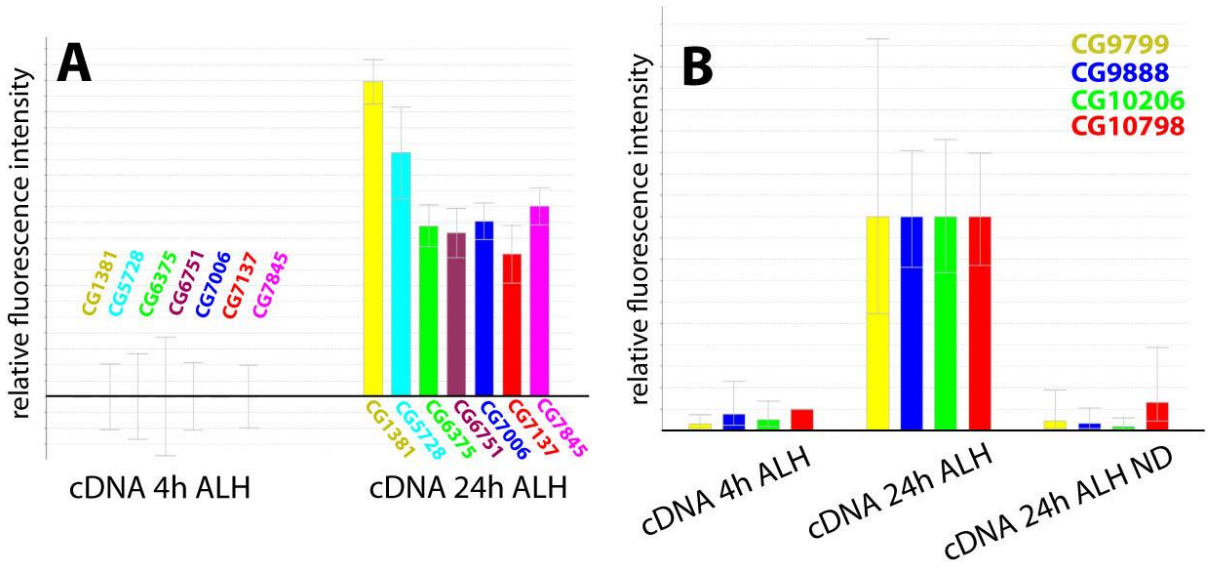

Figure 42: dMyc targets are upregulated upon reactivation of larval NSCs. (A) Significant upregulation of seven dMyc target genes in the CNS of *Drosophila* larvae after reactivation at 24h ALH compared to the quiescent state at 4h ALH. This plot illustrates the relative fluorescent intensity obtained in a qRT-PCR experiment done specific primers against: *CG1381*, *CG5728*, *CG6375*, *CG6751*, *CG7006*, *CG7137* and *CG7845*. For illustrating the transcript amplification between the samples the data was normalized to the cDNA of the 4h old larvae. **(B)** Significant upregulation of *dmyc* and three known target genes in the CNS of *Drosophila* larvae at 4h ALH and 24h ALH; the expression levels after 24h ALH in the nutrition deprived state is comparable to the well fed larvae at 4h ALH. This plot illustrates the relative fluorescent intensity obtained in a qRT-PCR experiment done specific primers against: *CG9799*, *CG9888*, *CG10206* and *CG10798* (*dmyc*). For illustrating the transcript amplification between the samples the data was normalized to the cDNA of the well fed 24h old larvae.

To analyse a putative effect of a prolonged quiescence phase, due to nutritional starvation, on the expression levels of *dmyc* and three chosen target genes, I generated cDNA from well fed larval CNSs at 4h ALH and 24h ALH as well as from larvae which were raised on nutrition deprived media for 24h. Interestingly the qRT-PCR data reveals that the expression levels after 24h of nutritional deprivation resemble the levels at 4h ALH during quiescence, concerning *dmyc* and all three tested target genes (Fig. 42B). To further prove the finding that *dmyc* and its target genes are expressed according to the cellular status I used the same three cDNA samples (4h ALH well fed, 24h ALH well fed and 24h ALH nutrition deprived) and primers against four additional *dmyc* target genes (CG6375, CG7845, CG7137, and CG7006) for a PCR reaction. The PCR products were loaded on a 1% agarose gel and analysed via GelRed staining under UV light, it is obvious that all targets are strongly expressed in the CNS of well-fed larvae after 24h ALH, but the expression levels 4h ALH and 24h ALH under

nutritional deprivation are in a comparable way very low (Fig. 43). These data indicate that all tested dMyc target genes are expressed in the larval CNS and that the obtained expression levels reveal a strong dependency to the nutritional status.

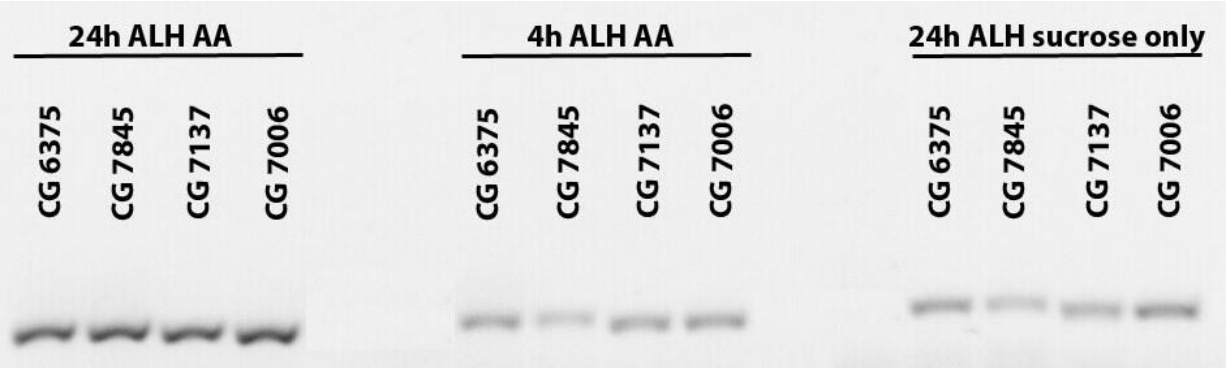

Figure 43: dMyc target genes are differentially expressed according to the nutritional status. The agarose gel highlights the differences in the expression levels of four *dmyc* target genes (CG6375, CG7845, CG7137, and CG7006) in the *Drosophila* larval CNS under different conditions. There is a high expression of these genes after reactivation at 24h ALH in well fed larvae, but the expression levels at 4h ALH and 24h ALH after nutritional deprivation are comparably low.

5. Discussion

One of the major questions in recent biology is how stem cell behaviour is regulated and how the balance between proliferation and quiescence is controlled, since deregulation of the proliferative capacity can lead to tumour formation or premature depletion of the progenitor pool (Knoblich, 2010; Cheung *et al*., 2013). Stem cells are undifferentiated cells and possess the unique ability to generate differentiating daughter cells and at the same moment retain their stem cell identity by a process called self-renewal (Weissmann, 2000). The fruit fly *Drosophila melanogaster* contains diverse tissue resident stem cells during adulthood and several populations of stem cells, which are just transiently present during certain developmental stages (Losick *et al*., 2011). These cells inherit critical functions in animal development, tissue homeostasis, growth and reproduction (Voog and Jones, 2010; Alvarado and Yamanaka, 2014). Stem cells that are necessary for the development of the CNS are called neural stem cells (NSCs) and are formed in the neuroectoderm at early embryonic stages (Urbach and Technau 2003). They pass through two phases of proliferation, one during embryogenesis and the other during larval development; between these highly proliferative stages the NSCs reside in a quiescent phase (Britton and Edgar., 1998; Park *et al*., 2003; Barrett *et al*., 2008). Whereas several seminal publications started to analyse the mechanisms of reactivation (Chell and Brand, 2010; Sousa-Nunes *et al*., 2011) the problem of how quiescence is maintained is currently enigmatic. During my PhD I analysed several known regulators of growth for their capacity to regulate quiescence and could identify the highly conserved SWH signalling module as an important component during this developmental process. During my thesis work, I have made two important findings. The initial one was that the SWH signalling pathway is an important factor for the organ size control of the *Drosophila* CNS during early developmental stages. The functional analysis of various components of the SWH pathway revealed that this signalling module is necessary for the correct maintenance of *Drosophila* NSC quiescence between embryonic and larval stages of development. Using the RNAi technology, I have identified various intracellular and extracellular regulators and downstream targets of SWH signalling in NSCs that play important roles in modulating the activity of this pathway at early larval stages. Further findings provided the evidence that a potential regulative, negative feedback loop exists downstream of SWH signalling, involving the main pathway effector Yki and its nuclear competitor Tgi. The second finding revealed that highly sophisticated niche signalling is necessary for the correct regulation of NSC quiescence. This micro environmental signalling

requires so called niche glial cells, which express the transmembrane proteins Crb and Ed that can act in *trans* and in *cis* to activate the highly conserved SWH signalling pathway in NSCs to maintain quiescence and suppress inappropriate cell growth and proliferation during this developmental stage. Apart from these SWH related findings I showed that the oncogene dMyc is also involved in *Drosophila* NSC growth, through the expression patterns of its target genes. Ectopic expression of dMyc is known to induce premature cell growth due to accelerating cellular mass and the enhanced G1 to S phase transition of the cell cycle (Johnston *et al*., 1999). On the basis of dMycs involvement in such fundamental biological processes it is hard to imagine a molecular mechanism in which dMyc function is not required, for this reason I focused my studies on the SWH signalling pathway and its contribution to NSC growth regulation.

5.1 Maintenance of NSC quiescence depends on niche signalling

In order to orchestrate the complex cellular behaviour according to the status and the requirements of the organism stem cells need to communicate with their surrounding niches. These stem cell niches form highly complex microenvironments, in which the stem cells reside, during development. Stem cell niches in general are highly specialized microenvironments, surrounding the tissue resident stem cells, they interact with these cells to regulate cell fate and proliferation and obtain anatomic as well as functional dimensions (Birbrair and Frenette, 2016; Scadden, 2006). For stem cells it is highly important to integrate the signals from their surrounding microenvironment in order to couple their proliferation and quiescence cycles according to the requirements of the organism. A general characteristic of stem cells is that they directly interact with a multiplicity of different cell types and environmental cues inside their niche to regulate their activity pattern (Llorens-Bobadilla and Martin-Villalba, 2016). These stem cell niches maintain the stemness of these cells and keep them in an undifferentiated state, using specific short-range signalling molecules; these local signals also determine the total number of maintained stem cells and the size of the niche itself. For many specialized stem cell types (e.g. germline stem cells) so-called niche factors are known to regulate the stem cell activity through a complex signalling circuitry (Kiger *et al*., 2001; Kawase *et al*., 2004). These germline stem cells (GSC) in the testis of *Drosophila* are maintained by their juxtaposing hub cells which express the ligand Unpaired (Upd) that in turn activates the Janus kinase signal transducer and activator of transcription (JAK-STAT) signalling in GSCs to maintain their self-renewing capabilities (Kiger *et al*., 2001).

Furthermore there are hierarchies of additional signals which are less well understood but inevitable for maintaining niche integrity like the bone morphogenetic protein (BMP) pathway is needed for the specification of GSCs next to JAK-STAT signalling (Kawase *et al*., 2004). Similar to the neurogenic niche in vertebrates (Bjornsson *et al*., 2015), in insects processes of glial cells enwrap NSCs and thereby form an enclosed chamber known as the trophospongium, which thereby represents the specialized microenvironment of *Drosophila* NSCs (Hoyle, 1986; Dumstrei *et al*., 2003). This trophospongium and is a sponge-like matrix of cortex glial processes. NSC proliferation and the growth of the trophospongium chambers seem to be highly coordinated, so the individual chambers of this superordinate structure contain one NSC and up to 20 neurons (Dumstrei *et al*., 2003). Furthermore it is possible that each individual trophospongium chamber corresponds to one NSC lineage, isolating them from the surrounding lineages and thereby providing a signalling circuitry on an individual basis (Dumstrei *et al*., 2003). It is still not finally proven whether *Drosophila* NSCs also depend on niche signalling, since there is evidence that cultured NSCs undergo asymmetric cell divisions generating a self-renewed daughter cell as well as differentiating progeny (Ceron *et al*., 2006; Homem *et al*., 2013). Furthermore these cells exhibit a highly similar behaviour like their counterparts *in vivo* as they progress through an intrinsically regulated series of transcription factors (temporal transcription factor cascade) (Brody *et al*., 2000) and generate diverse cell types and cell lineages *in vitro* that resemble the *in vivo* lineages in cell number and cell identity (Lüer and Technau, 2009). Conversely, loss of contact to the surrounding epithelium leads to a randomization of the mitotic spindle in isolated embryonic NSCs (Siegrist and Doe, 2006) and loss of the cell adhesion molecule E-Cadherin in niche glial cells compromises the proliferative activity of NSCs (Dumstrei *et al*., 2003). It has been proven that during quiescence and reactivation NSCs exhibit an intense dependency on defined, extrinsic signals derived from the surrounding glial cells. These glial cells have the ability to express and secrete quiescence promoting factors like *anachronism* (Ebens *et al*., 1993) or in response to nutritional signals activating factors like insulin-like growth factors (Chell and Brand, 2010; Sousa-Nunes *et al*., 2011).

During my thesis work I was able to demonstrate the presence of a crosstalk between the niche glial cells and the neural stem cells via Crb and Ed, which activate the SWH signalling in NSCs to repress inappropriate growth and maintain the cellular quiescence of these stem cells. This cellular dialog might also be conserved in mouse aNSCs since Martynoga *et al.* (2013) showed that upon BMP4 induced quiescence *crumbs2* (*CRB2*, *Drosophila crumbs* homologue) is also upregulated in aNSCs. Whether *CRB2* is also expressed in the vertebrate

niche and activates the SWH signalling in NSCs during quiescence still has to be shown. Nevertheless, like vertebrate adult NSCs, *Drosophila* NSCs show different degrees of dependency on niche signalling. During quiescence both NSC populations need extrinsic cues from the surrounding niche to maintain the cellular quiescence (Ding *et al*., 2016; Chell and Brand, 2010; Sousa-Nunes *et al*., 2011; Martynoga *et al*., 2013; Mira *et al*., 2010), whereas during the active, proliferative phase lineage progression seems to be more cell-intrinsically regulated and pre-programmed and to a lesser degree depending on the niche signalling (Lüer and Technau, 2009; Costa *et al*., 2011). These findings were further confirmed by whole transcriptome analysis of murine adult quiescent NSCs. Shin *et al* (2016) revealed molecular signatures of these resting stem cells and showed that a massive expression of genes involved in cell-to-cell communication are a main characteristic of quiescent NSCs. These molecular signatures of adult quiescent NSCs revealed that they heavily depend on glycolysis and fatty acid β-oxidation for energy supply. But even more interesting was that this molecular analysis clearly showed that quiescent NSCs massively communicate with their local microenvironment through various signalling pathways which are globally shut-off after activation. Especially signalling pathways involved in intra- and inter-cellular communication exhibited a marked down-regulation upon activation of these stem cells, e.g. the MAPK signalling pathway, the Notch signalling pathway or the phosphatidylinositol signalling pathway (Shin *et al*., 2016). Many ligands for the detected receptors, including Notch signalling (Pleasure *et al*., 2000), BMP signalling (Lim *et al*., 2000) or GABA signalling (Song *et al*., 2012), are already known to be expressed in the adult NSC niche. These findings further prove that there is strong active cell-to-cell signalling in quiescent NSCs and that these cells are neither dormant nor passive, instead they are actively integrating a plethora of different signals from the niche in order to regulate their activity. Interestingly many of the genes which are involved in the communication between NSCs and their niche exhibit a strongly decreased expression after the activation of these cells, suggesting that the NSCs are losing their ability to respond to the signals of their niche. These data speak in favour of the hypothesis that vertebrate as well as *Drosophila* NSCs do depend on niche signalling in order to harmonize their resting phases with their more cell-intrinsically regulated lineage progression and proliferative phases (Shin *et al*., 2016; Ding *et al*., 2016).

5.2 The role of the SWH pathway in organ size control

Regulation of organ size is one of the major functions of SWH signalling in normal cell physiology. The regulative centre of this signalling module is composed of the two growth-repressive kinases Hpo and Wts, which together with their interaction partners Sav and Mats form a kinase cascade resulting in the phosphorylation mediated inactivation of the transcriptional co-activator Yki. Phosphorylated Yki is bound by the 14-3-3ζ protein (Ren *et al*., 2010) and thereby sequestered to the cytoplasm of the cell, when Yki is dephosphorylated it can translocate into the nucleus to run its transcriptional programme. I have shown that during the quiescence phase this kinase cascade is active and suppresses inappropriate growth and proliferation of NSCs through Yki phosphorylation. Comparable findings in *Drosophila* have already shown that mutations of the SWH core kinases (Hpo and Wts) or the ectopic expression of Yki lead to massive overgrowth of the affected tissues (Tapon *et al*., 2002; Harvey *et al*., 2003; Jia *et al*., 2003; Pantalacci *et al*., 2003; Huang *et al*., 2005). Thus, a similar mechanism of the maintenance of quiescence via growth restriction might exist in adult vertebrate NSCs and indeed a recent molecular study on neural stem cell quiescence revealed that multiple SWH members like Lats2 (Warts homologue) or WWC2 (Kibra homologue) are upregulated in aNSCs, which after BMP4 exposure enter into a quiescence-like status in cell culture (Martynoga *et al*., 2013). Although for the mammalian Yki homolog's YAP and TAZ there is conclusive evidence for their role in organ size control and tumorigenesis which have been shown in cell culture and animal models. In mice overexpression of YAP in the liver leads to an enlarged liver. Interestingly this liver phenotype reverts back when YAP overexpression is switched off and the intracellular YAP level is back to normal (Yimlamai *et al*., 2015; Camargo *et al*., 2007). Similar observations have been shown after loss of *Mst1* and *Mst2* (Song *et al*., 2010). Conversely there is no observable change in the size of other organs like the kidney, the intestines or the lung in *Mst1/2* knockout mice. Taken together these observations speak in favour of the hypothesis that the role of the SWH signalling is strongly dependent on the tissue and cellular context. The results of my thesis work are in accordance with this hypothesis, for example I have shown that Yorkie discriminates between quiescent, nutrition dependent NSCs and non-quiescent NSCs. The activity of the transcriptional regulator Yorkie seems to be a major differentiator between these two populations of NSCs. While quiescent NSCs display active

SWH signalling and thus no nuclear Yorkie, the non-quiescent NSCs show constant nuclear Yki and constant expression of the known Yki target genes Four-jointed and the miRNA *bantam*. Interestingly, in *Drosophila* NSCs I could uncover an essential difference between NSCs in the brain and in the VNC concerning the expression of Yki target genes. In both populations of stem cells Yki activates its well-established target gene *bantam*. Yet, loss of the *bantam* miRNA severely impaired growth and proliferation of the NSCs in the ventral nerve cord, whereas the effects were much less pronounced in the central brain NSCs. These antithetic results are complementary with my observation that the known Yki interaction partner Teashirt (*tsh*) (Peng *et al*., 2009) is differentially expressed in distinct NSCs across the CNS. The non-quiescent MBNBs as well as the type II NSCs do not express this transcription factor, in contrast to the type I NSCs which all demonstrate the presence of Tsh in different levels. Thus, indicating the possibility that Yki interacts with varying combinations of transcription factors among the individual NSCs to differentially regulate the expression of its targets genes in a cell specific manner. Among the transcription factors which are known to interact with Yki are Scalloped (Goulev *et al*., 2008; Wu *et al*., 2008), Homothorax and Teashirt (Peng *et al*., 2009) and through the cell type specific availability of different Yki interaction partners, the SWH signalling pathway is able to fine tune its transcriptional outcome according to the parameters of each cell. The mammalian YAP protein also relies on the association with DNA-binding transcription factors to co-activate its target genes. The members of the TEAD protein family are the major DNA-binding factors for YAP (Chen *et al*., 2010; Li *et al*., 2010). But several other nuclear factors have been identified recently which utilise the interaction domains of YAP to regulate gene expression in different cell types e.g. p73 (Strano *et al*., 2001) or ErbB-4 (Komuro *et al*., 2003). Taken together these data strengthens the assumption that the highly variable and complex interactome of Yorkie/YAP contributes to the cell type specific transcriptional outcome of the SWH signalling in *Drosophila* and mammals.

Alternative splicing is another possible way to further adjust the activity of signalling pathways according to the cellular requirements. During my thesis work I identified two different splice variants of the *yorkie* gene in *Drosophila* NSCs. Both isoforms are detectable during the quiescence phase and after reactivation of these stem cells, but interestingly the shorter isoform seems to be enriched in quiescent NSCs while the longer isoform is more highly concentrated in NSCs after reactivation. Similar is already known from the human YAP gene, which comprises nine exons, generating at least eight alternative splicing variants (Gaffney *et al*., 2012). The mere existence of eight different isoforms suggests that they

execute non-redundant roles within the cell. Indeed, structural differences between the distinct YAP isoforms are associated with altered transcriptional activity and function, concerning e.g. p73 association (Oka *et al*., 2008), ErbB-4 binding (Komuro *et al*., 2003) or angiomotin association (Oka *et al*., 2012). Finch-Edmondson *et al*. (2016) have clearly demonstrated that the varying combination of protein domains in the diverse YAP isoforms permits a huge range of differing transcriptional potencies and abilities to interact with cellular protein partners (Finch-Edmondson *et al*., 2016). Due to the fact that all eight isoforms are expressed as functional proteins *in vivo* and that the differences in transcriptional activity are remarkable, one cannot assume that these YAP isoforms function equivalently. Whether the different *yki* splice variants, I have found in *Drosophila* NSCs display comparable functions as the YAP isoforms in human tissues still has to be elucidated, but the recent data generated in other model organisms are promising.

Apart from these molecular cues, which play a role in NSC reactivation, there are also systemic effects, which play a major role in the regulation of NSC behaviour. NSC reactivation in the *Drosophila* larval CNS for example is known to be dependent on nutrition (Chell and Brand, 2010; Sousa-Nunes *et al*., 2011). Interestingly recent studies revealed that the I/IGF pathway is closely related to the SWH pathway, in a way that I/IGF mediated proliferation is executed partly via Yki/YAP function. Modulation of pAkt results in altered Yki phosphorylation and thereby elevated Yki activity in *Drosophila* wing discs, human NIH-3T3 fibroblasts and HeLa cells (Straßburger *et al*., 2012). In the larval CNS of *Drosophila* I have shown that loss of SWH signalling in NSCs during quiescence results in premature Akt phosphorylation and therefore also activation of the I/IGF pathway. Based on this, one can conclude that these two oncogenic pathways are also functionally interconnected in the larval CNS of *Drosophila*. Taken together this data indicates that SWH signalling and the I/IGF act in parallel to regulate growth initiation of NSCs after quiescence. Another sensor system for the nutritional status of a cell is the LKB1/AMPK pathway, which was also shown to regulate Yki activity independently of SWH signalling. During late larval stages *lkb1* retrains the activity of Yki in central brain and VNC NSCs through the downstream kinase AMPK, which directly phosphorylates and thereby inactivates Yki (Gailite *et al*., 2015). During the early larval quiescence phase loss of *lkb1* causes premature reactivation of NSCs, this evidence suggests that lkb1 is another potent regulator of Yki in NSCs apart from the canonical kinase cascade of SWH signalling.

5.3 SWH signalling in tumorigenesis and cancer

If we combine the important role of SWH signalling in organ size control with the highly complex regulation of the transcriptional outcome, it becomes obvious that a deregulation of this pathway could easily lead to abnormal cell growth with the potential to invade other parts of the body. Indeed it has been shown that YAP and TAZ are able to mediate oncogenic transformations if induced mutations prevent them from binding with members of the TEAD protein family (Chen *et al*., 2010; Zhang *et al*., 2009; Chan *et al*., 2009). Furthermore, ChIP-seq analyses have started to illuminate the transcriptional profile of the YAP/TAZ/TEAD complex and have thereby shown that the majority of their target genes are related to cell cycle progression, regulation of cell migration and extracellular matrix organization (Zanconato *et al*., 2015; Stein *et al*., 2015). In order to promote tumorigenesis YAP and TAZ also interact with other transcription factors, apart from TEADs, like SMADS and TBX5 (Murakami *et al*., 2005; Hiemer *et al*., 2014). It is a general fact that human tumours consists of a multitude of different cell subpopulations, with varying growth and metastatic properties (Visvader and Lindeman, 2008; Kreso and Dick, 2014). So called cancer stem cells are considered the core of each tumour and are defined as the subpopulation of tumour cells that are capable of self-renewal and share the ability to give rise to another tumour. Both YAP and TAZ are known to promote cancer stem cell characteristics (Cordenonsi *et al*., 2011; Basu-Roy *et al*., 2015). By way of example, ectopic expression of a constitutively active TAZ isoform in non-malignant mammary epithelial cells is sufficient to transfer cancer stem cell characteristics to these cells. Vice versa, knockdown of TAZ completely inhibits the self-renewal capabilities and the tumour initiating potential of breast cancer cells. Comparable data is present for the role of YAP in conferring cancer stem cell characteristics. Over expression of YAP is known to confer sphere- and tumour initiating capacity in non-transformed murine esophageal epithelial cells. Mechanistically, it was proven that YAP performs these cancerogenic transformations through the direct upregulation of SOX9 (Song *et al*., 2014). That these reprogramming capabilities of YAP and TAZ are indeed closely associated with cell fate plasticity, has been shown by Panciera *et al*. (2016). Through the ectopic expression of YAP or TAZ in terminally differentiated luminal mammary gland cells, neurons and pancreatic exocrine cells, these cells performed a conversion into cells displaying various characteristics of their corresponding, tissue-specific stem cells (Panciera *et al*., 2016). The fact that there is only a limited availability of normal, somatic stem cells is a

limiting factor for regenerative medicine. The finding that single factors like YAP or TAZ can shape cell plasticity through reprogramming distinct cell types into their tissue-specific stem cells could have massive implications for regenerative medicine and in general for a more profound insight into the still mysterious world of stem cells and the up to date unknown factors which maintain this unique cellular status.

These far-reaching effects of the SWH pathway concerning organ size control, cancer and cellular plasticity prove the importance of deciphering the tight regulation of its activity and the transcriptional outcome. As part of this effort the results of my thesis work shed some light on the involvement of the SWH pathway on the regulation of NSC quiescence.

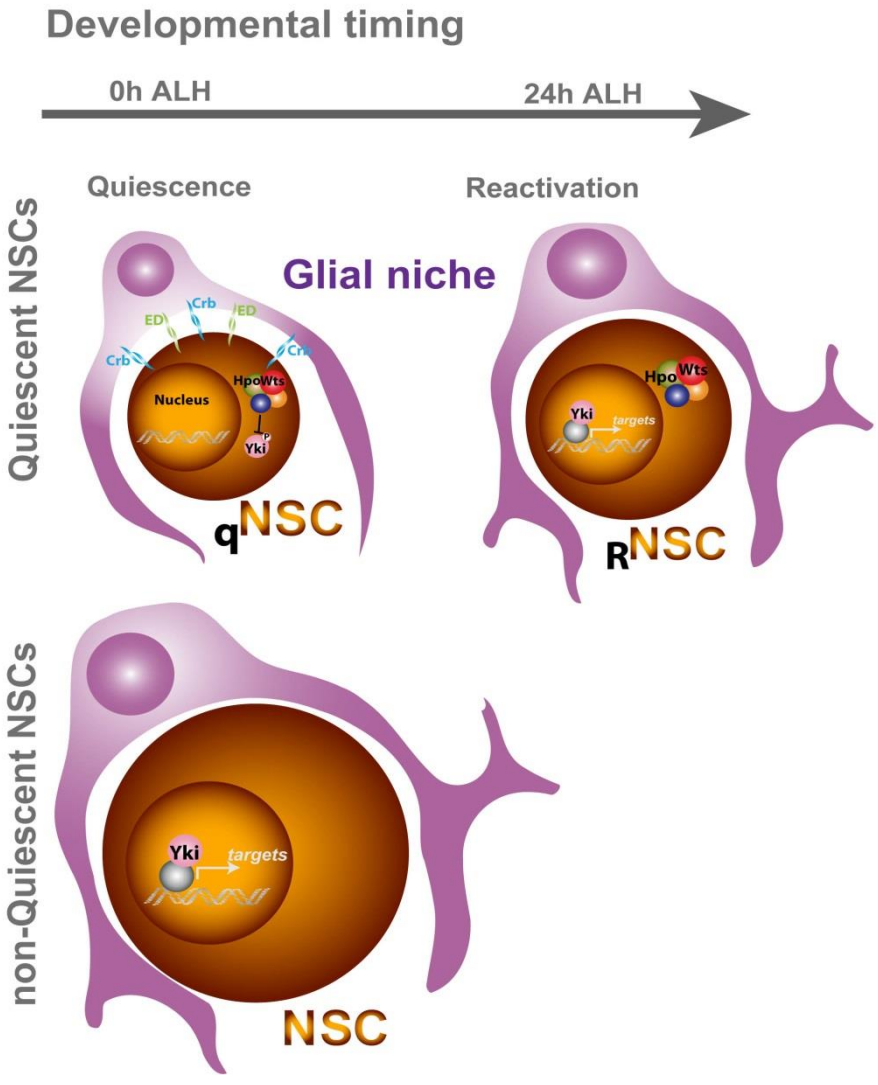

Schematics of Crb and Ed mediated cell contact inhibition of growth via SWH signalling in NSCs. Homophilic interactions of Crb and Ed molecules in *trans* and in *cis* between niche glial cells and NSCs activate the SWH pathway in NSCs. Activated SWH signalling inactivates the transcriptional co-activator Yki and thereby maintains NSC quiescence. In response to nutritional signals Crb and Ed are downregulated in the NSC niche, which inactivates the SWH signalling and activates Yki. Active Yki translocates into the nucleus and starts the transcription of its target genes. Yki is necessary and sufficient for NSC growth and proliferation and is constitutively active in the non-quiescent NSCs of the *Drosophila* CNS (MBNB, lNSC).

6. Conclusions

Taken together these data prompt the conclusion that *Drosophila* NSCs depend on extrinsic cues from the surrounding stem cell niche to tightly control the balance between proliferation and quiescence. The SWH pathway turned out to be a fundamental component for the maintenance of NSC quiescence in the *Drosophila* CNS. During this resting phase the highly conserved signalling pathway inhibits inappropriate growth and proliferation through the regulation of its downstream effector Yorkie. The activity of the SWH pathway is mainly regulated by the stem cell niche dependent expression of the transmembrane molecules Crb and Ed, which are expressed both on NSCs and the niche forming glial cells. The activity of the main effector of this pathway Yki is regulated by a complex network of niche dependent and independent upstream regulators and energy sensing modules. Its transcriptional outcome is, apart from the upstream components, cell type specifically modulated through the varying availability of potential nuclear interaction partners. Therefore, Yorkie/YAP/TAZ emerges as an important regulator of NSC biology and it is therefore of great importance to further identify the precise cellular and molecular mechanisms by which Yorkie/YAP promote growth, proliferation and stem cell identity in neural stem cells.

7. References

- Alvarado AS and Yamanaka S (2014). Rethinking differentiation: Stem cells, regeneration, and plasticity. Cell; 157(1): 110–119. doi: 10.1016/j.cell.2014.02.041
- Amati B, Land H (1994). Myc-Max-Mad: a transcription factor network controlling cell cycle progression, differentiation and death. Curr Opin Genet Dev; 4(1):102-8.
- Araújo S J, Tear G (2003). Axon guidance mechanisms and molecules: lessons from invertebrates. Nat Rev Neurosci; 4(11):910-22.
- Artavanis-Tsakonas S, Simpson P (1991). Choosing a cell fate: a view from the Notch locus. Trends Genet; 7(11-12):403-8.
- Axelrod JD, McNeill H (2002). Coupling planar cell polarity signaling to morphogenesis. ScientificWorldJournal; 2:434-54.
- Badouel C, Gardano L, Amin N, Garg A, Rosenfeld R, Le Bihan T, McNeill H (2009). The FERM-domain protein Expanded regulates Hippo pathway activity via direct interactions with the transcriptional activator Yorkie. Dev Cell; 16(3):411-20. doi: 10.1016/j.devcel.2009.01.010.
- Bai J, Chiu W, Wang J, Tzeng T, Perrimon N, Hsu J (2001). The cell adhesion molecule Echinoid defines a new pathway that antagonizes the Drosophila EGF receptor signaling pathway. Development; 128(4):591-601.
- Barrett AL, Krueger S, Datta S (2008). Branchless and Hedgehog operate in a positive feedback loop to regulate the initiation of neuroblast division in the Drosophila larval brain. Dev Biol.; 317(1):234-45. doi: 10.1016/j.ydbio.2008.02.025.
- Barrios C, Castresana JS, Kreicbergs A (1994). Clinicopathologic correlations and short-term prognosis in musculoskeletal sarcoma with c-myc oncogene amplification. Am J Clin Oncol; 17(3):273-6.
- Barry ER, Morikawa T, Butler BL, Shrestha K, de la Rosa R, Yan KS, Fuchs CS, Magness ST, Smits R, Ogino S, Kuo CJ, Camargo FD (2013). Restriction of intestinal stem cell expansion and the regenerative response by YAP. Nature; 493(7430):106-10. doi: 10.1038/nature11693.
- Basu-Roy U, Bayin NS, Rattanakorn K, Han E, Placantonakis DG, Mansukhani A, Basilico C (2015). Sox2 antagonizes the Hippo pathway to maintain stemness in cancer cells. Nat Commun.; 6:6411. doi: 10.1038/ncomms7411.

- Baumgartner R, Poernbacher I, Buser N, Hafen E, Stocker H (2010). The WW domain protein Kibra acts upstream of Hippo in Drosophila. Dev Cell; 18(2):309-16. doi: 10.1016/j.devcel.2009.12.013.
- Beatus P, Lendahl U (1998). Notch and neurogenesis. J Neurosci Res.; 54(2):125-36.
- Bello BC, Izergina N, Caussinus E, Reichert H (2008). Amplification of neural stem cell proliferation by intermediate progenitor cells in Drosophila brain development. Neural; 3:5. doi: 10.1186/1749-8104-3-5.
- Bennett FC, Harvey KF (2006). Fat cadherin modulates organ size in Drosophila via the Salvador/Warts/Hippo signaling pathway. Curr Biol; 16(21):2101-10.
- Berger C, Urban J, Technau GM (2001). Stage-specific inductive signals in the Drosophila neuroectoderm control the temporal sequence of neuroblast specification. Development; 128(17):3243-51.
- Birbrair A, Frenette PS (2016). Niche heterogeneity in the bone marrow. Ann N Y Acad Sci.; 1370(1):82-96. doi: 10.1111/nyas.13016.
- Bjornson CR, Cheung TH, Liu L, Tripathi PV, Steeper KM, Rando TA (2012). Notch signaling is necessary to maintain quiescence in adult muscle stem cells. Stem Cells; 30(2):232-42. doi: 10.1002/stem.773.
- Bjornsson CS, Apostolopoulou M, Tian Y, Temple S (2015). It takes a village: constructing the neurogenic niche. Dev Cell; 32(4):435-46. doi: 10.1016/j.devcel.2015.01.010.
- Blackwood EM, Eisenman RN (1991). Max: a helix-loop-helix zipper protein that forms a sequence-specific DNA-binding complex with Myc. Science; 251(4998):1211-7.
- Blackwood EM, Lüscher B, Eisenman RN (1992). Myc and Max associate in vivo. Genes Dev; 6(1):71-80.
- Blanpain C, Lowry WE, Geoghegan A, Polak L, Fuchs E (2004). Self-Renewal, Multipotency, and the Existence of Two Cell Populations within an Epithelial Stem Cell Niche. Cell; 118(5):635-48.
- Boggiano JC, Vanderzalm PJ, Fehon RG (2011). Tao-1 phosphorylates Hippo/MST kinases to regulate the Hippo-Salvador-Warts tumor suppressor pathway. Dev Cell; 21(5):888-95. doi: 10.1016/j.devcel.2011.08.028.
- Bossing T, Technau GM (1994). The fate of the CNS midline progenitors in Drosophila as revealed by a new method for single cell labelling. Development; 120(7):1895-906.

- Brennecke J, Hipfner DR, Stark A, Russell RB, Cohen SM (2003). bantam encodes a developmentally regulated microRNA that controls cell proliferation and regulates the proapoptotic gene hid in Drosophila. Cell; 113(1):25-36.
- Brittle AL, Repiso A, Casal J, Lawrence PA, Strutt D (2010). Four-jointed modulates growth and planar polarity by reducing the affinity of dachsous for fat. Curr Biol; 20(9):803-10. doi: 10.1016/j.cub.2010.03.056.
- Britton JS, Edgar BA (1998). Environmental control of the cell cycle in Drosophila: nutrition activates mitotic and endoreplicative cells by distinct mechanisms. Development; 125(11):2149-58.
- Brody T, Odenwald WF (2000). Programmed transformations in neuroblast gene expression during Drosophila CNS lineage development. Dev Biol; 226(1):34-44.
- Brody T, Odenwald WF (2002). Cellular diversity in the developing nervous system: a temporal view from Drosophila. Development; 129(16):3763-70.
- Camargo FD, Gokhale S, Johnnidis JB, Fu D, Bell GW, Jaenisch R, Brummelkamp TR (2007). YAP1 increases organ size and expands undifferentiated progenitor cells. Curr Biol; 17(23):2054-60.
- Campos-Ortega JA (1993). Mechanisms of early neurogenesis in Drosophila melanogaster. J Neurobiol; 24(10):1305-27.
- Cao X, Pfaff SL, Gage FH (2008). YAP regulates neural progenitor cell number via the TEA domain transcription factor. Genes Dev; 22(23):3320-34. doi: 10.1101/gad.1726608.
- Ceron J, Tejedor FJ, Moya F (2006). A primary cell culture of Drosophila postembryonic larval neuroblasts to study cell cycle and asymmetric division. Eur J Cell Biol; 85(6):567-75.
- Chan SW, Lim CJ, Loo LS, Chong YF, Huang C, Hong W (2009). TEADs mediate nuclear retention of TAZ to promote oncogenic transformation. J Biol Chem.; 284(21):14347-58. doi: 10.1074/jbc.M901568200.
- Chang LH, Chen P, Lien MT, Ho YH, Lin CM, Pan YT, Wei SY, Hsu JC (2011). Differential adhesion and actomyosin cable collaborate to drive Echinoid-mediated cell sorting. Development; 138(17):3803-12. doi: 10.1242/dev.062257.
- Chappell SA, LeQuesne JP, Paulin FE, deSchoolmeester ML, Stoneley M, Soutar RL, Ralston SH, Helfrich MH, Willis AE (2000). A mutation in the c-myc-IRES leads to enhanced internal ribosome entry in multiple myeloma: a novel mechanism of oncogene de-regulation. Oncogene; 19(38):4437-40.

- Chell JM, Brand AH (2010). Nutrition-responsive glia control exit of neural stem cells from quiescence. Cell; 143(7):1161-73. doi: 10.1016/j.cell.2010.12.007.
- Chen CL, Gajewski KM, Hamaratoglu F, Bossuyt W, Sansores-Garcia L, Tao C, Halder G (2010). The apical-basal cell polarity determinant Crumbs regulates Hippo signaling in Drosophila. Proc Natl Acad Sci U S A; 107(36):15810-5. doi: 10.1073/pnas.1004060107.
- Chen L, Chan SW, Zhang X, Walsh M, Lim CJ, Hong W, Song H (2010). Structural basis of YAP recognition by TEAD4 in the hippo pathway. Genes Dev.; 24(3):290-300. doi: 10.1101/gad.1865310.
- Chen L, Chan SW, Zhang X, Walsh M, Lim CJ, Hong W, Song H (2010). Structural basis of YAP recognition by TEAD4 in the hippo pathway. Genes Dev.; 24(3):290-300. doi: 10.1101/gad.1865310.
- Cheung TH, Rando TA (2013). Molecular regulation of stem cell quiescence. Nat Rev Mol Cell Biol;14(6):329-40. doi: 10.1038/nrm3591.
- Chia W, Somers WG, Wang H (2008). *Drosophila* neuroblast asymmetric divisions: cell cycle regulators, asymmetric protein localization, and tumorigenesis. J Cell Biol.; 180(2): 267–272. doi: 10.1083/jcb.200708159
- Cho E, Feng Y, Rauskolb C, Maitra S, Fehon R, Irvine KD (2006). Delineation of a Fat tumor suppressor pathway. Nat Genet; 38(10):1142-50.
- Cho E, Irvine KD (2004). Action of fat, four-jointed, dachsous and dachs in distal-to-proximal wing signaling. Development; 131(18):4489-500.
- Cleary MD, Doe CQ (2006). Regulation of neuroblast competence: multiple temporal identity factors specify distinct neuronal fates within a single early competence window. Genes Dev.; 20(4):429-34.
- Coller HA, Sang L, Roberts JM (2006). A New Description of Cellular Quiescence. PLoS Biol; 4(3): e83. doi: 10.1371/journal.pbio.0040083
- Colombani J, Raisin S, Pantalacci S, Radimerski T, Montagne J, Léopold P (2003). A nutrient sensor mechanism controls Drosophila growth. Cell; 114(6):739-49.
- Cordenonsi M, Zanconato F, Azzolin L, Forcato M, Rosato A, Frasson C, Inui M, Montagner M, Parenti AR, Poletti A, Daidone MG, Dupont S, Basso G, Bicciato S, Piccolo S (2011). The Hippo transducer TAZ confers cancer stem cell-related traits on breast cancer cells. Cell; 147(4):759-72. doi: 10.1016/j.cell.2011.09.048.

- Costa MR, Ortega F, Brill MS, Beckervordersandforth R, Petrone C, Schroeder T, Götz M, Berninger B (2011). Continuous live imaging of adult neural stem cell division and lineage progression in vitro. Development; 138(6):1057-68. doi: 10.1242/dev.061663.
- Crosio C, Fimia GM, Loury R, Kimura M, Okano Y, Zhou H, Sen S, Allis CD, Sassone-Corsi P (2002). Mitotic phosphorylation of histone H3: spatio-temporal regulation by mammalian Aurora kinases. Mol Cell Biol; 22(3):874-85.
- Cubas P, de Celis JF, Campuzano S, Modolell J (1991). Proneural clusters of achaete-scute expression and the generation of sensory organs in the Drosophila imaginal wing disc. Genes Dev.; 5(6):996-1008.
- de la Cova C, Abril M, Bellosta P, Gallant P, Johnston LA (2004). Drosophila myc regulates organ size by inducing cell competition. Cell; 117(1):107-16.
- DeRan M, Yang J, Shen CH, Peters EC, Fitamant J, Chan P, Hsieh M, Zhu S, Asara JM, Zheng B, Bardeesy N, Liu J, Wu X (2014). Energy stress regulates hippo-YAP signaling involving AMPK-mediated regulation of angiomotin-like 1 protein. Cell Rep; 9(2):495-503. doi: 10.1016/j.celrep.2014.09.036.
- Dong J, Feldmann G, Huang J, Wu S, Zhang N, Comerford SA, Gayyed MF, Anders RA, Maitra A, Pan D (2007). Elucidation of a universal size-control mechanism in Drosophila and mammals. Cell; 130(6):1120-33.
- Dumstrei K, Wang F, Hartenstein V (2003). Role of DE-cadherin in neuroblast proliferation, neural morphogenesis, and axon tract formation in Drosophila larval brain development. J Neurosci; 23(8):3325-35.
- Ebens AJ, Garren H, Cheyette BN, Zipursky SL (1993). The Drosophila anachronism locus: a glycoprotein secreted by glia inhibits neuroblast proliferation. Cell; 74(1):15-27.
- Ekholm SV, Reed SI (2000). Regulation of G(1) cyclin-dependent kinases in the mammalian cell cycle. Curr Opin Cell Biol; 12(6):676-84.
- Feng Y, Irvine KD (2007). Fat and expanded act in parallel to regulate growth through warts. Proc Natl Acad Sci U S A; 104(51):20362-7.
- Finch-Edmondson ML, Strauss RP, Clayton JS, Yeoh GC, Callus BA (2016). Splice variant insertions in the C-terminus impairs YAP's transactivation domain. Biochem Biophys Rep.; 6:24-31. doi: 10.1016/j.bbrep.2016.02.015. eCollection 2016.

- Forsberg EC, Passegué E, Prohaska SS, Wagers AJ, Koeva M, Stuart JM, Weissman IL (2010). Molecular signatures of quiescent, mobilized and leukemia-initiating hematopoietic stem cells. PLoS One; 5(1):e8785. doi: 10.1371/journal.pone.0008785.
- Fukada S, Uezumi A, Ikemoto M, Masuda S, Segawa M, Tanimura N, Yamamoto H, Miyagoe-Suzuki Y, Takeda S (2007). Molecular signature of quiescent satellite cells in adult skeletal muscle. Stem Cells; 25(10):2448-59.
- Gaffney CJ, Oka T, Mazack V, Hilman D, Gat U, Muramatsu T, Inazawa J, Golden A, Carey DJ, Farooq A, Tromp G, Sudol M (2012). Identification, basic characterization and evolutionary analysis of differentially spliced mRNA isoforms of human YAP1 gene. Gene.; 509(2):215-22. doi: 10.1016/j.gene.2012.08.025.
- Gailite I, Aerne BL, Tapon N (2015). Differential control of Yorkie activity by LKB1/AMPK and the Hippo/Warts cascade in the central nervous system. Proc Natl Acad Sci U S A; 112(37):E5169-78. doi: 10.1073/pnas.1505512112.
- Genevet A, Wehr MC, Brain R, Thompson BJ, Tapon N (2010). Kibra is a regulator of the Salvador/Warts/Hippo signaling network. Dev Cell; 18(2):300-8. doi: 10.1016/j.devcel.2009.12.011.
- Gerdes J, Lemke H, Baisch H, Wacker HH, Schwab U, Stein H (1984). Cell cycle analysis of a cell proliferation-associated human nuclear antigen defined by the monoclonal antibody Ki-67. J Immunol.; 133(4):1710-5.
- Goulev Y, Fauny JD, Gonzalez-Marti B, Flagiello D, Silber J, Zider A (2008). SCALLOPED interacts with YORKIE, the nuclear effector of the hippo tumor-suppressor pathway in Drosophila. Curr Biol; 18(6):435-41. doi: 10.1016/j.cub.2008.02.034.
- Green P, Hartenstein AY, Hartenstein V (1993). The embryonic development of the Drosophila visual system. Cell Tissue Res; 273(3):583-98.
- Grzeschik NA, Parsons LM, Allott ML, Harvey KF, Richardson HE (2010). Lgl, aPKC, and Crumbs regulate the Salvador/Warts/Hippo pathway through two distinct mechanisms. Curr Biol; 20(7):573-81. doi: 10.1016/j.cub.2010.01.055.
- Halbleib JM, Nelson WJ (2006). Cadherins in development: cell adhesion, sorting, and tissue morphogenesis. Genes Dev; 20(23):3199-214.
- Halder G, Johnson RL (2011). Hippo signaling: growth control and beyond. Development; 138(1):9-22. doi: 10.1242/dev.045500.

- Hamaratoglu F, Willecke M, Kango-Singh M, Nolo R, Hyun E, Tao C, Jafar-Nejad H, Halder G (2006). The tumour-suppressor genes NF2/Merlin and Expanded act through Hippo signalling to regulate cell proliferation and apoptosis. Nat Cell Biol; 8(1):27-36.
- Harvey KF, Pfleger CM, Hariharan IK (2003). The Drosophila Mst ortholog, hippo, restricts growth and cell proliferation and promotes apoptosis. Cell; 114(4):457-67.
- Hiemer SE, Szymaniak AD, Varelas X (2014). The transcriptional regulators TAZ and YAP direct transforming growth factor β-induced tumorigenic phenotypes in breast cancer cells. J Biol Chem.; 289(19):13461-74. doi: 10.1074/jbc.M113.529115.
- Hipfner DR, Weigmann K, Cohen SM (2002). The bantam gene regulates Drosophila growth. Genetics; 161(4):1527-37.
- Hirning U, Schmid P, Schulz WA, Kozak LP, Hameister H (1989). In developing brown adipose tissue c-myc protooncogene expression is restricted to early differentiation stages. Cell Differ Dev; 27(3):243-8.
- Homem CC, Knoblich JA (2012). Drosophila neuroblasts: a model for stem cell biology. Development; 139(23):4297-310. doi: 10.1242/dev.080515.
- Hoyle G (1986). Glial cells of an insect ganglion. J Comp Neurol; 246(1):85-103.
- Huang J, Wu S, Barrera J, Matthews K, Pan D (2005). The Hippo signaling pathway coordinately regulates cell proliferation and apoptosis by inactivating Yorkie, the Drosophila Homolog of YAP. Cell; 122(3):421-34.
- Hüttmann A, Liu SL, Boyd AW, Li CL (2001). Functional heterogeneity within rhodamine123(lo) Hoechst33342(lo/sp) primitive hemopoietic stem cells revealed by pyronin Y. Exp Hematol; 29(9):1109-16.
- Hulf T, Bellosta P, Furrer M, Steiger D, Svensson D, Barbour A, Gallant P (2005). Whole-genome analysis reveals a strong positional bias of conserved dMyc-dependent E-boxes. Mol Cell Biol; 25(9):3401-10.
- Ishikawa HO, Takeuchi H, Haltiwanger RS, Irvine KD (2008). Four-jointed is a Golgi kinase that phosphorylates a subset of cadherin domains. Science; 321(5887):401-4. doi: 10.1126/science.1158159.
- Jia J, Zhang W, Wang B, Trinko R, Jiang J (2003). The Drosophila Ste20 family kinase dMST functions as a tumor suppressor by restricting cell proliferation and promoting apoptosis. Genes Dev; 17(20):2514-9.
- Johnston LA, Prober DA, Edgar BA, Eisenman RN, Gallant P (1999). Drosophila myc regulates cellular growth during development. Cell; 98(6):779-90.

- Kawamori H, Tai M, Sato M, Yasugi T, Tabata T (2011). Fat/Hippo pathway regulates the progress of neural differentiation signaling in the Drosophila optic lobe. Dev Growth Differ; 53(5):653-67. doi: 10.1111/j.1440-169X.2011.01279.x.
- Kawase E, Wong MD, Ding BC, Xie T (2004). Gbb/Bmp signaling is essential for maintaining germline stem cells and for repressing bam transcription in the Drosophila testis. Development; 131(6):1365-75.
- Kiger AA, Jones DL, Schulz C, Rogers MB, Fuller MT (2001). Stem cell self-renewal specified by JAK-STAT activation in response to a support cell cue. Science; 294(5551):2542-5.
- Kim M, Kim T, Johnson RL, Lim DS (2015). Transcriptional co-repressor function of the hippo pathway transducers YAP and TAZ. Cell Rep; 11(2):270-82. doi: 10.1016/j.celrep.2015.03.015.
- Kim S H, Crews S T (1993). Influence of Drosophila ventral epidermal development by the CNS midline cells and spitz class genes. Development; 118(3):893-901.
- Knoblich JA (2010). Asymmetric cell division: recent developments and their implications for tumour biology. Nat Rev Mol Cell Biol; 11(12):849-60. doi: 10.1038/nrm3010.
- Komuro A, Nagai M, Navin NE, Sudol M (2003). WW domain-containing protein YAP associates with ErbB-4 and acts as a co-transcriptional activator for the carboxyl-terminal fragment of ErbB-4 that translocates to the nucleus. J Biol Chem.; 278(35):33334-41.
- Koontz LM, Liu-Chittenden Y, Yin F, Zheng Y, Yu J, Huang B, Chen Q, Wu S, Pan D (2013). The Hippo effector Yorkie controls normal tissue growth by antagonizing scalloped-mediated default repression. Dev Cell; 25(4):388-401. doi: 10.1016/j.devcel.2013.04.021.
- Kreso A, Dick JE (2014). Evolution of the cancer stem cell model. Cell Stem Cell.; 14(3):275-91. doi: 10.1016/j.stem.2014.02.006.
- Lai SL, Doe CQ (2014). Transient nuclear Prospero induces neural progenitor quiescence. Elife; 3. doi: 10.7554/eLife.03363.
- Lechman ER, Gentner B, van Galen P, Giustacchini A, Saini M, Boccalatte FE, Hiramatsu H, Restuccia U, Bachi A, Voisin V, Bader GD, Dick JE, Naldini L (2012). Attenuation of miR-126 activity expands HSC in vivo without exhaustion. Cell Stem Cell; 11(6):799-811. doi: 10.1016/j.stem.2012.09.001.

- Letizia A, Ricardo S, Moussian B, Martín N, Llimargas M (2013). A functional role of the extracellular domain of Crumbs in cell architecture and apicobasal polarity. J Cell Sci; 126(Pt 10):2157-63. doi: 10.1242/jcs.122382.
- Li S, Wang H, Groth C (2014). *Drosophila* neuroblasts as a new model for the study of stem cell self-renewal and tumour formation. Biosci Rep.; 34(4): e00125.
- Li Z, Zhao B, Wang P, Chen F, Dong Z, Yang H, Guan KL, Xu Y (2010). Structural insights into the YAP and TEAD complex. Genes Dev.; 24(3):235-40. doi: 10.1101/gad.1865810.
- Lim DA, Tramontin AD, Trevejo JM, Herrera DG, García-Verdugo JM, Alvarez-Buylla A (2000). Noggin antagonizes BMP signaling to create a niche for adult neurogenesis. Neuron ;28(3):713-26.
- Ling C, Zheng Y, Yin F, Yu J, Huang J, Hong Y, Wu S, Pan D (2010). The apical transmembrane protein Crumbs functions as a tumor suppressor that regulates Hippo signaling by binding to Expanded. Proc Natl Acad Sci U S A; 107(23):10532-7. doi: 10.1073/pnas.1004279107.
- Llorens-Bobadilla E, Martin-Villalba A (2016). Adult NSC diversity and plasticity: the role of the niche. Curr Opin Neurobiol.; 42:68-74. doi: 10.1016/j.conb.2016.11.008.
- Losick VP, Morris LX, Fox DT, Spradling A (2011). Drosophila stem cell niches: a decade of discovery suggests a unified view of stem cell regulation. Dev Cell.; 21(1):159-71. doi: 10.1016/j.devcel.2011.06.018
- Lu L, Li Y, Kim SM, Bossuyt W, Liu P, Qiu Q, Wang Y, Halder G, Finegold MJ, Lee JS, Johnson RL (2010). Hippo signaling is a potent in vivo growth and tumor suppressor pathway in the mammalian liver. Proc Natl Acad Sci U S A; 107(4):1437-42. doi: 10.1073/pnas.0911427107.
- Lüer K, Technau GM (2009). Single cell cultures of Drosophila neuroectodermal and mesectodermal central nervous system progenitors reveal different degrees of developmental autonomy. Neural Dev; 4:30. doi: 10.1186/1749-8104-4-30.
- Ma D, Yang CH, McNeill H, Simon MA, Axelrod JD (2003). Fidelity in planar cell polarity signalling. Nature; 421(6922):543-7.
- Ma J, Ptashne M (1987). The carboxy-terminal 30 amino acids of GAL4 are recognized by GAL80. Cell; 50(1):137-42.
- Martynoga B, Mateo JL, Zhou B, Andersen J, Achimastou A, Urbán N, van den Berg D, Georgopoulou D, Hadjur S, Wittbrodt J, Ettwiller L, Piper M, Gronostajski RM,

Guillemot F (2013). Epigenomic enhancer annotation reveals a key role for NFIX in neural stem cell quiescence. Genes Dev; 27(16):1769-86. doi: 10.1101/gad.216804.113.

- Matakatsu H, Blair SS (2004). Interactions between Fat and Dachsous and the regulation of planar cell polarity in the Drosophila wing. Development; 131(15):3785-94.
- Mateyak MK, Obaya AJ, Adachi S, Sedivy JM (1997). Phenotypes of c-Myc-deficient rat fibroblasts isolated by targeted homologous recombination. Cell Growth Differ; 8(10):1039-48.
- McCartney BM, Kulikauskas RM, LaJeunesse DR, Fehon RG (2000). The neurofibromatosis-2 homologue, Merlin, and the tumor suppressor expanded function together in Drosophila to regulate cell proliferation and differentiation. Development; 127(6):1315-24.
- McGuire SE, Mao Z, Davis RL (2004). Spatiotemporal gene expression targeting with the TARGET and gene-switch systems in Drosophila. Sci STKE; 2004(220):pl6.
- Meng W, Takeichi M (2009). Adherens junction: molecular architecture and regulation. Cold Spring Harb Perspect Biol; 1(6):a002899. doi: 10.1101/cshperspect.a002899.
- Mira H, Andreu Z, Suh H, Lie DC, Jessberger S, Consiglio A, San Emeterio J, Hortigüela R, Marqués-Torrejón MA, Nakashima K, Colak D, Götz M, Fariñas I, Gage FH (2010). Signaling through BMPR-IA regulates quiescence and long-term activity of neural stem cells in the adult hippocampus. Cell Stem Cell; 7(1):78-89. doi: 10.1016/j.stem.2010.04.016.
- Mohseni M, Sun J, Lau A, Curtis S, Goldsmith J, Fox VL, Wei C, Frazier M, Samson O, Wong KK, Kim C, Camargo FD (2014). A genetic screen identifies an LKB1-MARK signalling axis controlling the Hippo-YAP pathway. Nat Cell Biol; 16(1):108-17. doi: 10.1038/ncb2884.
- Moreno E, Basler K (2004). dMyc transforms cells into super-competitors. Cell; 117(1):117-29.
- Mourikis P, Gopalakrishnan S, Sambasivan R, Tajbakhsh S (2012). Cell-autonomous Notch activity maintains the temporal specification potential of skeletal muscle stem cells. Development; 139(24):4536-48. doi: 10.1242/dev.084756.

- Murakami M, Nakagawa M, Olson EN, Nakagawa O (2005). A WW domain protein TAZ is a critical coactivator for TBX5, a transcription factor implicated in Holt-Oram syndrome. Proc Natl Acad Sci U S A.; 102(50):18034-9.
- Muskavitch MA (1994). Delta-notch signaling and Drosophila cell fate choice. Dev Biol.; 166(2):415-30.
- Nguyen HB, Babcock JT, Wells CD, Quilliam LA (2013). LKB1 tumor suppressor regulates AMP kinase/mTOR-independent cell growth and proliferation via the phosphorylation of Yap. Oncogene; 32(35):4100-9. doi: 10.1038/onc.2012.431.
- Nolo R, Morrison CM, Tao C, Zhang X, Halder G (2006). The bantam microRNA is a target of the hippo tumor-suppressor pathway. Curr Biol; 16(19):1895-904.
- Obaya AJ, Mateyak MK, Sedivy JM (1999). Mysterious liaisons: the relationship between c-Myc and the cell cycle. Oncogene; 18(19):2934-41.
- Oh H, Irvine KD (2008). In vivo regulation of Yorkie phosphorylation and localization. Development; 135(6):1081-8. doi: 10.1242/dev.015255.
- Oka T, Mazack V, Sudol M (2008). Mst2 and Lats kinases regulate apoptotic function of Yes kinase-associated protein (YAP). J Biol Chem.; 283(41):27534-46. doi: 10.1074/jbc.M804380200.
- Oka T, Schmitt AP, Sudol M (2012). Opposing roles of angiomotin-like-1 and zona occludens-2 on pro-apoptotic function of YAP. Oncogene.; 31(1):128-34. doi: 10.1038/onc.2011.216.
- Orian A, van Steensel B, Delrow J, Bussemaker HJ, Ling Li, Sawado T, Williams E, Loo LWM, Cowley SM, Yost C, Pierce S, Edgar BA, Parkhurst SM, Eisenman RN (2003). Genomic binding by the *Drosophila* Myc, Max, Mad/Mnt transcription factor network. Genes Dev; 17(9): 1101–1114. doi: 10.1101/gad.1066903
- Ortega F, Costa MR, Simon-Ebert T, Schroeder T, Götz M, Berninger B (2011). Using an adherent cell culture of the mouse subependymal zone to study the behavior of adult neural stem cells on a single-cell level. Nat Protoc; 6(12):1847-59. doi: 10.1038/nprot.2011.404.
- Pan D (2007). Hippo signaling in organ size control. Genes Dev; 21(8):886-97.
- Panciera T, Azzolin L, Fujimura A, Di Biagio D, Frasson C, Bresolin S, Soligo S, Basso G, Bicciato S, Rosato A, Cordenonsi M, Piccolo S (2016). Induction of Expandable Tissue-Specific Stem/Progenitor Cells through Transient Expression of YAP/TAZ. Cell Stem Cell.; 19(6):725-737. doi: 10.1016/j.stem.2016.08.009.

- Pantalacci S, Tapon N, Léopold P (2003). The Salvador partner Hippo promotes apoptosis and cell-cycle exit in Drosophila. Nat Cell Biol; 5(10):921-7.
- Park Y, Rangel C, Reynolds MM, Caldwell MC, Johns M, Nayak M, Welsh CJ, McDermott S, Datta S (2003). Drosophila perlecan modulates FGF and hedgehog signals to activate neural stem cell division. Dev Biol.; 253(2):247-57.
- Peng HW, Slattery M, Mann RS (2009). Transcription factor choice in the Hippo signaling pathway: homothorax and yorkie regulation of the microRNA bantam in the progenitor domain of the Drosophila eye imaginal disc. Genes Dev; 23(19):2307-19. doi: 10.1101/gad.1820009.
- Pierce SB, Yost C, Britton JS, Loo LW, Flynn EM, Edgar BA, Eisenman RN (2004). dMyc is required for larval growth and endoreplication in Drosophila. Development; 131(10):2317-27.
- Pleasure SJ, Collins AE, Lowenstein DH (2000). Unique expression patterns of cell fate molecules delineate sequential stages of dentate gyrus development. J Neurosci.; 20(16):6095-105.
- Poon CL, Lin JI, Zhang X, Harvey KF (2011). The sterile 20-like kinase Tao-1 controls tissue growth by regulating the Salvador-Warts-Hippo pathway. Dev Cell; 21(5):896-906. doi: 10.1016/j.devcel.2011.09.012.
- Prendergast GC (1999). Mechanisms of apoptosis by c-Myc. Oncogene; 18(19):2967-87.
- Prokop A, Technau GM (1991). The origin of postembryonic neuroblasts in the ventral nerve cord of Drosophila melanogaster. Development; 111(1):79-88.
- Qing Y, Yin F, Wang W, Zheng Y, Guo P, Schozer F, Deng H, Pan D (2014). The Hippo effector Yorkie activates transcription by interacting with a histone methyltransferase complex through Ncoa6. Elife; 3. doi: 10.7554/eLife.02564.
- Raisin S, Pantalacci S, Breittmayer JP, Léopold P (2003). A new genetic locus controlling growth and proliferation in Drosophila melanogaster. Genetics; 164(3):1015-25.
- Rauskolb C, Pan G, Reddy BV, Oh H, Irvine KD (2011). Zyxin links fat signaling to the hippo pathway. PLoS Biol; 9(6):e1000624. doi: 10.1371/ journal.pbio.1000624.
- Rawls AS, Guinto JB, Wolff T (2002). The cadherins fat and dachsous regulate dorsal/ventral signaling in the Drosophila eye. Curr Biol; 12(12):1021-6.

- Reddy BV, Irvine KD (2008). The Fat and Warts signaling pathways: new insights into their regulation, mechanism and conservation. Development; 135(17):2827-38. doi: 10.1242/dev.020974.
- Reddy BV, Rauskolb C, Irvine KD (2010). Influence of fat-hippo and notch signaling on the proliferation and differentiation of Drosophila optic neuroepithelia. Development; 137(14):2397-408. doi: 10.1242/dev.050013.
- Ren F, Zhang L, Jiang J (2010). Hippo signaling regulates Yorkie nuclear localization and activity through 14-3-3 dependent and independent mechanisms. Dev Biol; 337(2):303-12. doi: 10.1016/j.ydbio.2009.10.046.
- Richardson H, O'Keefe LV, Marty T, Saint R (1995). Ectopic cyclin E expression induces premature entry into S phase and disrupts pattern formation in the Drosophila eye imaginal disc. Development; 121(10):3371-9.
- Robinson BS, Huang J, Hong Y, Moberg KH (2010). Crumbs regulates Salvador/Warts/Hippo signaling in Drosophila via the FERM-domain protein Expanded. Curr Biol; 20(7):582-90. doi: 10.1016/j.cub.2010.03.019.
- Rogulja D, Rauskolb C, Irvine KD (2008). Morphogen control of wing growth through the Fat signaling pathway. Dev Cell; 15(2):309-21. doi: 10.1016/j.devcel.2008.06.003.
- Rooke JE, Xu T (1998). Positive and negative signals between interacting cells for establishing neural fate. Bioessays; 20(3):209-14.
- Scadden DT (2006). The stem-cell niche as an entity of action. Nature; 441(7097):1075-9.
- Schlegelmilch K, Mohseni M, Kirak O, Pruszak J, Rodriguez JR, Zhou D, Kreger BT, Vasioukhin V, Avruch J, Brummelkamp TR, Camargo FD (2011). Yap1 acts downstream of α-catenin to control epidermal proliferation. Cell; 144(5):782-95. doi: 10.1016/j.cell.2011.02.031.
- Schmidt EV (1999). The role of c-myc in cellular growth control. Oncogene; 18(19):2988-96.
- Schweitzer R, Shilo B Z (1997). A thousand and one roles for the Drosophila EGF receptor. Trends Genet; 13(5):191-6.
- Semsei I, Ma SY, Cutler RG (1989). Tissue and age specific expression of the myc proto-oncogene family throughout the life span of the C57BL/6J mouse strain. Oncogene; 4(4):465-71.

- Shaw RJ, Kosmatka M, Bardeesy N, Hurley RL, Witters LA, DePinho RA, Cantley LC (2004). The tumor suppressor LKB1 kinase directly activates AMP-activated kinase and regulates apoptosis in response to energy stress. Proc Natl Acad Sci U S A; 101(10):3329-35.
- Shin J, Berg DA, Zhu Y, Shin JY, Song J, Bonaguidi MA, Enikolopov G, Nauen DW, Christian KM, Ming GL, SongH (2015). Single-Cell RNA-Seq with Waterfall Reveals Molecular Cascades underlying Adult Neurogenesis. Cell Stem Cell; 17(3):360-72. doi: 10.1016/j.stem.2015.07.013
- Siegrist SE, Doe CQ (2006). Extrinsic cues orient the cell division axis in Drosophila embryonic neuroblasts. Development; 133(3):529-36.
- Silva E, Tsatskis Y, Gardano L, Tapon N, McNeill H (2006). The tumor-suppressor gene fat controls tissue growth upstream of expanded in the hippo signaling pathway. Curr Biol; 16(21):2081-9.
- Simon MA, Xu A, Ishikawa HO, Irvine KD (2010). Modulation of fat:dachsous binding by the cadherin domain kinase four-jointed. Curr Biol; 20(9):811-7. doi: 10.1016/j.cub.2010.04.016.
- Simons M, Mlodzik M (2008). Planar cell polarity signaling: from fly development to human disease. Annu Rev Genet; 42:517-40. doi: 10.1146/annurev.genet. 42.110807.091432
- Simpson P, Carteret C (1990). Proneural clusters: equivalence groups in the epithelium of Drosophila. Development; 110(3):927-32.
- Song H, Mak KK, Topol L, Yun K, Hu J, Garrett L, Chen Y, Park O, Chang J, Simpson RM, Wang CY, Gao B, Jiang J, Yang Y (2010). Mammalian Mst1 and Mst2 kinases play essential roles in organ size control and tumor suppression. Proc Natl Acad Sci U S A; 107(4):1431-6. doi: 10.1073/pnas.0911409107.
- Song J, Zhong C, Bonaguidi MA, Sun GJ, Hsu D, Gu Y, Meletis K, Huang ZJ, Ge S, Enikolopov G, Deisseroth K, Luscher B, Christian KM, Ming GL, Song H (2012). Neuronal circuitry mechanism regulating adult quiescent neural stem-cell fate decision. Nature ;489(7414):150-4. doi: 10.1038/nature11306.
- Song S, Ajani JA, Honjo S, Maru DM, Chen Q, Scott AW, Heallen TR, Xiao L, Hofstetter WL, Weston B, Lee JH, Wadhwa R, Sudo K, Stroehlein JR, Martin JF, Hung MC, Johnson RL (2014). Hippo coactivator YAP1 upregulates SOX9 and endows esophageal cancer cells with stem-like properties. Cancer Res.; 74(15):4170-82. doi: 10.1158/0008-5472.CAN-13-3569.

- Sousa-Nunes R, Yee LL, Gould AP (2011). Fat cells reactivate quiescent neuroblasts via TOR and glial insulin relays in Drosophila. Nature; 471(7339):508-12. doi: 10.1038/nature09867.
- Spéder P, Brand AH (2014). Gap junction proteins in the blood-brain barrier control nutrient-dependent reactivation of Drosophila neural stem cells. Dev Cell; 30(3):309-21. doi: 10.1016/j.devcel.2014.05.021.
- Stein C, Bardet AF, Roma G, Bergling S, Clay I, Ruchti A, Agarinis C, Schmelzle T, Bouwmeester T, Schübeler D, Bauer A (2015). YAP1 Exerts Its Transcriptional Control via TEAD-Mediated Activation of Enhancers. PLoS Genet.; 11(8):e1005465. doi: 10.1371/journal.pgen.1005465.
- Strano S, Munarriz E, Rossi M, Castagnoli L, Shaul Y, Sacchi A, Oren M, Sudol M, Cesareni G, Blandino G (2001). Physical interaction with Yes-associated protein enhances p73 transcriptional activity. J Biol Chem.; 276(18):15164-73.
- Straßburger K, Tiebe M, Pinna F, Breuhahn K, Teleman AA (2012). Insulin/IGF signaling drives cell proliferation in part via Yorkie/YAP. Dev Biol; 367(2):187-96. doi: 10.1016/j.ydbio.2012.05.008.
- Strutt H, Strutt D (2002). Nonautonomous planar polarity patterning in Drosophila: dishevelled-independent functions of frizzled. Dev Cell; 3(6):851-63.
- Tapon N, Harvey KF, Bell DW, Wahrer DC, Schiripo TA, Haber D, Hariharan IK (2002). salvador Promotes both cell cycle exit and apoptosis in Drosophila and is mutated in human cancer cell lines. Cell; 110(4):467-78.
- Tepass U, Theres C, Knust E (1990). crumbs encodes an EGF-like protein expressed on apical membranes of Drosophila epithelial cells and required for organization of epithelia. Cell; 61(5):787-99.
- Thompson BJ, Cohen SM (2006). The Hippo pathway regulates the bantam microRNA to control cell proliferation and apoptosis in Drosophila. Cell; 126(4):767-74.
- Tothova Z, Kollipara R, Huntly BJ, Lee BH, Castrillon DH, Cullen DE, McDowell EP, Lazo-Kallanian S, Williams IR, Sears C, Armstrong SA, Passegué E, DePinho RA, Gilliland DG (2007). FoxOs are critical mediators of hematopoietic stem cell resistance to physiologic oxidative stress. Cell; 128(2):325-39.
- Truman J W, Schuppe H, Shepherd D, Williams D W (2004). Developmental architecture of adult-specific lineages in the ventral CNS of Drosophila. Development; 131, 5167–5184.

- Truman JW, Bate M (1988). Spatial and temporal patterns of neurogenesis in the central nervous system of Drosophila melanogaster. Dev Biol; 125(1):145-57.
- Tsuji T, Hasegawa E, Isshiki T (2008). Neuroblast entry into quiescence is regulated intrinsically by the combined action of spatial Hox proteins and temporal identity factors. Development; 135(23):3859-69. doi: 10.1242/dev.025189.
- Tyler DM, Baker NE (2007). Expanded and fat regulate growth and differentiation in the Drosophila eye through multiple signaling pathways. Dev Biol; 305(1):187-201.
- Udan RS, Kango-Singh M, Nolo R, Tao C, Halder G (2003). Hippo promotes proliferation arrest and apoptosis in the Salvador/Warts pathway. Nat Cell Biol; 5(10):914-20.
- Urbach R, Technau GM (2003). Molecular markers for identified neuroblasts in the developing brain of Drosophila. Development; 130(16):3621-37.
- van Riggelen J, Yetil A, Felsher DW (2010). MYC as a regulator of ribosome biogenesis and protein synthesis. Nat Rev Cancer; 10(4):301-9. doi: 10.1038/nrc2819.
- Varlakhanova NV, Cotterman RF, deVries WN, Morgan J, Donahue LR, Murray S, Knowles BB, Knoepfler PS (2010). myc maintains embryonic stem cell pluripotency and self-renewal. Differentiation; 80(1):9-19. doi:10.1016/j.diff.2010.05.001.
- Verghese S, Waghmare I, Kwon H, Hanes K, Kango-Singh M (2012). Scribble acts in the Drosophila fat-hippo pathway to regulate warts activity. PLoS One; 7(11):e47173. doi: 10.1371/journal.pone.0047173.
- Visvader JE, Lindeman GJ (2008). Cancer stem cells in solid tumours: accumulating evidence and unresolved questions. Nat Rev Cancer.; 8(10):755-68. doi: 10.1038/nrc2499.
- Voog J and Jones DL (2010). Stem Cells and the Niche: A Dynamic Duo. Cell Stem Cell. 2010 Feb 5; 6(2): 103–115. doi: 10.1016/j.stem.2010.01.011
- Vucic D, Kaiser WJ, Harvey AJ, Miller LK (1997). Inhibition of reaper-induced apoptosis by interaction with inhibitor of apoptosis proteins (IAPs). Proc Natl Acad Sci U S A; 94(19):10183-8.
- Vucic D, Kaiser WJ, Miller LK (1998). A mutational analysis of the baculovirus inhibitor of apoptosis Op-IAP. J Biol Chem; 273(51):33915-21.
- Wei SY, Escudero LM, Yu F, Chang LH, Chen LY, Ho YH, Lin CM, Chou CS, Chia W, Modolell J, Hsu JC (2005). Echinoid is a component of adherens junctions that cooperates with DE-Cadherin to mediate cell adhesion. Dev Cell; 8(4):493-504.

- Weissman IL (2000). Stem cells: units of development, units of regeneration, and units in evolution. Cell; 100(1):157-68.
- White K, Grether ME, Abrams JM, Young L, Farrell K, Steller H (1994). Genetic control of programmed cell death in Drosophila. Science; 264(5159):677-83.
- Willecke M, Hamaratoglu F, Sansores-Garcia L, Tao C, Halder G (2008). Boundaries of Dachsous Cadherin activity modulate the Hippo signaling pathway to induce cell proliferation. Proc Natl Acad Sci U S A; 105(39):14897-902. doi: 10.1073/pnas.0805201105.
- Woods A, Vertommen D, Neumann D, Turk R, Bayliss J, Schlattner U, Wallimann T, Carling D, Rider MH (2003). Identification of phosphorylation sites in AMP-activated protein kinase (AMPK) for upstream AMPK kinases and study of their roles by site-directed mutagenesis. J Biol Chem; 278(31):28434-42.
- Wu S, Huang J, Dong J, Pan D (2003). hippo encodes a Ste-20 family protein kinase that restricts cell proliferation and promotes apoptosis in conjunction with salvador and warts. Cell; 114(4):445-56.
- Wu S, Liu Y, Zheng Y, Dong J, Pan D (2008). The TEAD/TEF family protein Scalloped mediates transcriptional output of the Hippo growth-regulatory pathway. Dev Cell; 14(3):388-98. doi: 10.1016/j.devcel.2008.01.007.
- Yang CH, Axelrod JD, Simon MA (2002). Regulation of Frizzled by fat-like cadherins during planar polarity signaling in the Drosophila compound eye. Cell; 108(5):675-88.
- Yimlamai D, Fowl BH, Camargo FD (2015). Emerging evidence on the role of the Hippo/YAP pathway in liver physiology and cancer. J Hepatol.; 63(6):1491-501. doi: 10.1016/j.jhep.2015.07.008. Epub 2015 Jul 28.
- Yu FX, Guan KL (2013). The Hippo pathway: regulators and regulations. Genes Dev; 27(4):355-71. doi: 10.1101/gad.210773.112.
- Yu J, Zheng Y, Dong J, Klusza S, Deng WM, Pan D (2010). Kibra functions as a tumor suppressor protein that regulates Hippo signaling in conjunction with Merlin and Expanded. Dev Cell; 18(2):288-99. doi: 10.1016/j.devcel.2009.12.012.
- Yue T, Tian A, Jiang J (2012). The cell adhesion molecule echinoid functions as a tumor suppressor and upstream regulator of the Hippo signaling pathway. Dev Cell; 22(2):255-67. doi: 10.1016/j.devcel.2011.12.011.
- Zanconato F, Forcato M, Battilana G, Azzolin L, Quaranta E, Bodega B, Rosato A, Bicciato S, Cordenonsi M, Piccolo S (2015). Genome-wide association between

YAP/TAZ/TEAD and AP-1 at enhancers drives oncogenic growth. Nat Cell Biol.; 17(9):1218-27. doi: 10.1038/ncb3216.

- Zhang H, Liu CY, Zha ZY, Zhao B, Yao J, Zhao S, Xiong Y, Lei QY, Guan KL (2009). TEAD transcription factors mediate the function of TAZ in cell growth and epithelial-mesenchymal transition. J Biol Chem.; 284(20):13355-62. doi: 10.1074/jbc.M900843200.
- Zhang H, Pasolli HA, Fuchs E (2011). Yes-associated protein (YAP) transcriptional coactivator functions in balancing growth and differentiation in skin. Proc Natl Acad Sci U S A; 108(6):2270-5. doi: 10.1073/pnas.1019603108.
- Zhang L, Ren F, Zhang Q, Chen Y, Wang B, Jiang J (2008). The TEAD/TEF family of transcription factor Scalloped mediates Hippo signaling in organ size control. Dev Cell; 14(3):377-87. doi: 10.1016/j.devcel.2008.01.006.
- Zhang Y, Sivasankar S, Nelson WJ, Chu S (2009). Resolving cadherin interactions and binding cooperativity at the single-molecule level. Proc Natl Acad Sci U S A; 106(1):109-14. doi: 10.1073/pnas.0811350106.
- Zhao B, Li L, Guan KL (2010). Hippo signaling at a glance. J Cell Sci; 123(Pt 23):4001-6. doi: 10.1242/jcs.069070.
- Zhao B, Li L, Lei Q, Guan KL (2010). The Hippo-YAP pathway in organ size control and tumorigenesis: an updated version. Genes Dev; 24(9):862-74. doi: 10.1101/gad.1909210.
- Zhao B, Ye X, Yu J, Li L, Li W, Li S, Yu J, Lin JD, Wang CY, Chinnaiyan AM, Lai ZC, Guan KL (2008). TEAD mediates YAP-dependent gene induction and growth control. Genes Dev; 22(14):1962-71. doi: 10.1101/gad.1664408.
- Zhou D, Conrad C, Xia F, Park JS, Payer B, Yin Y, Lauwers GY, Thasler W, Lee JT, Avruch J, Bardeesy N (2009). Mst1 and Mst2 maintain hepatocyte quiescence and suppress hepatocellular carcinoma development through inactivation of the Yap1 oncogene. Cancer Cell; 16(5):425-38. doi: 10.1016/j.ccr.2009.09.026.
- Zhou D, Zhang Y, Wu H, Barry E, Yin Y, Lawrence E, Dawson D, Willis JE, Markowitz SD, Camargo FD, Avruch J (2011). Mst1 and Mst2 protein kinases restrain intestinal stem cell proliferation and colonic tumorigenesis by inhibition of Yes-associated protein (Yap) overabundance. Proc Natl Acad Sci U S A; 108(49):E1312-20. doi: 10.1073/pnas.1110428108.

8. Supplement

8.1 Restriction maps of the used vectors

8.1.1 pEGFP-c3

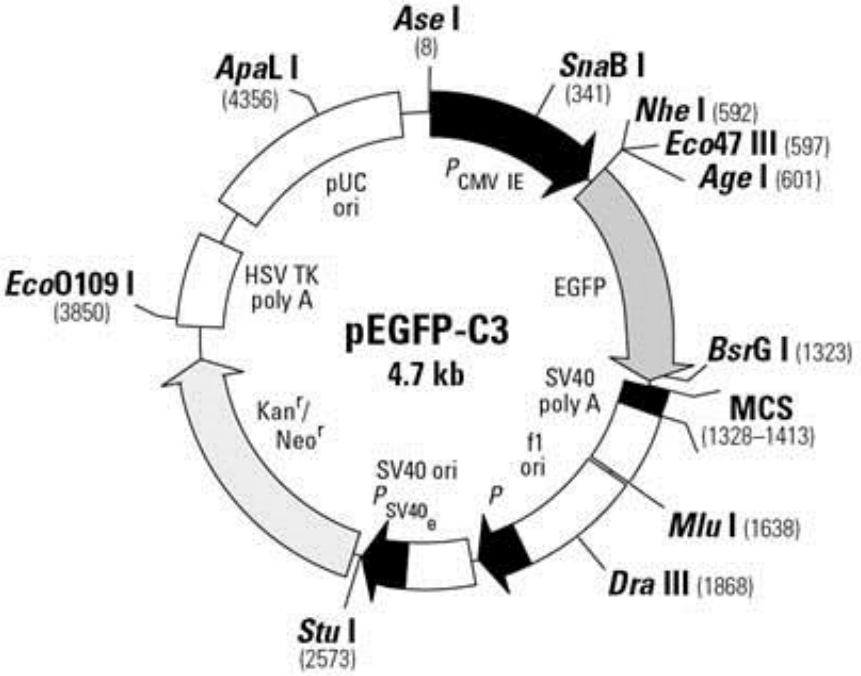

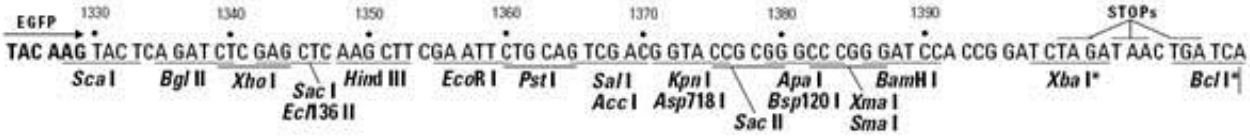

8.1.2 pEZX-MR04

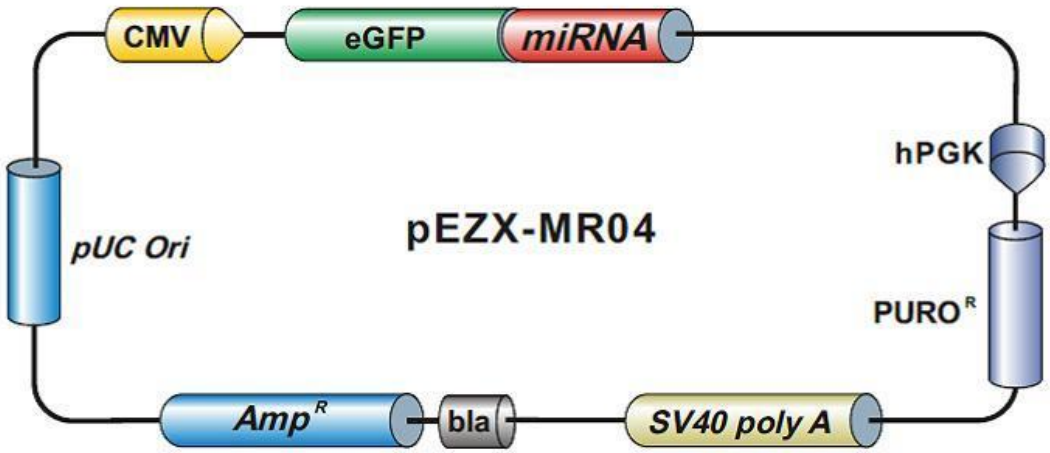

8.1.3 pmirGLO

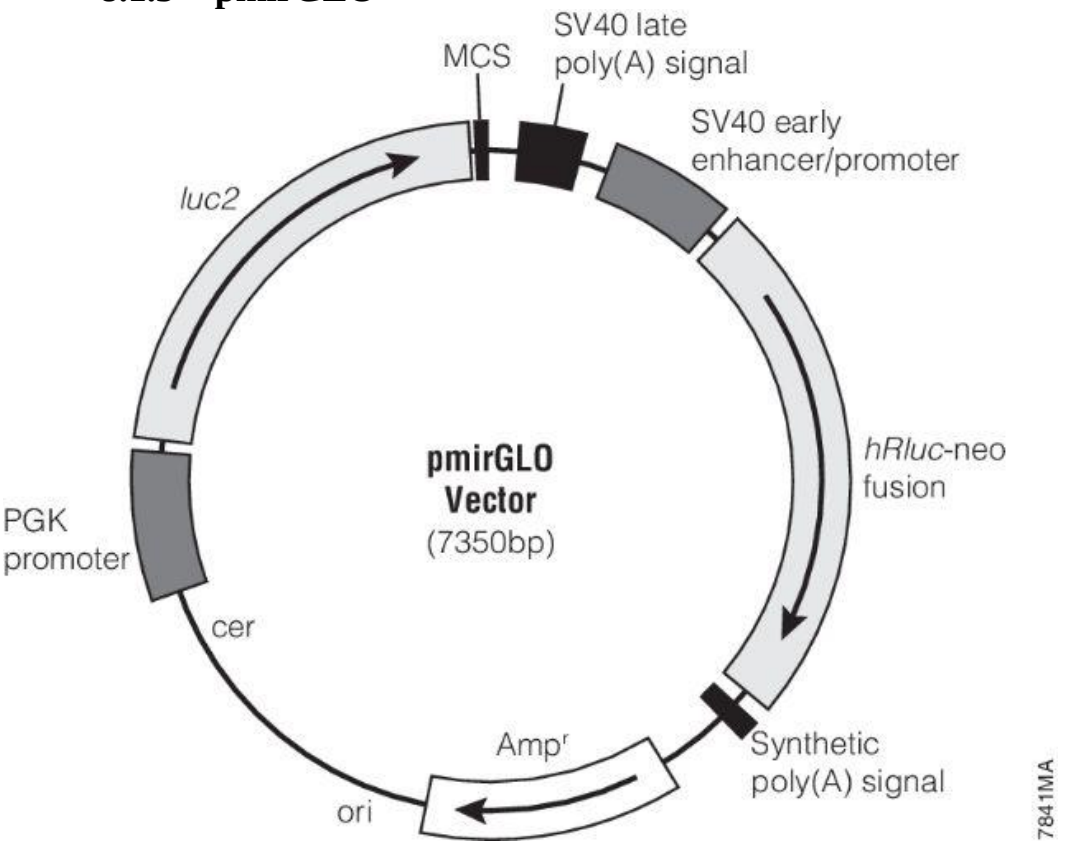

8.1.4 Scramble vector

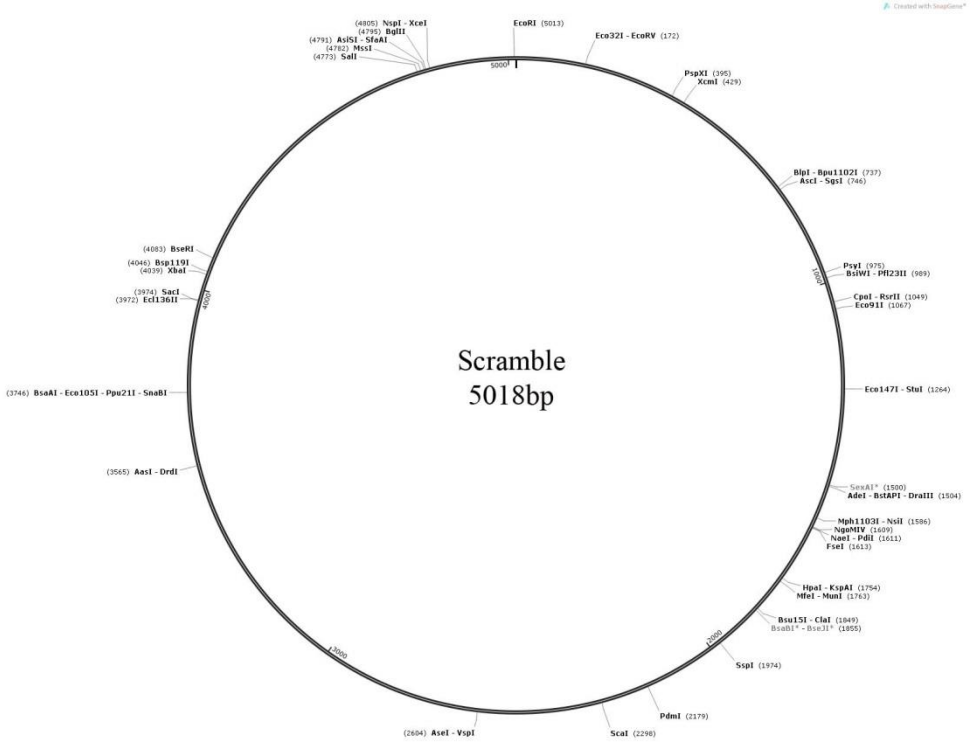

8.1.5 pCR®2.1-TOPO

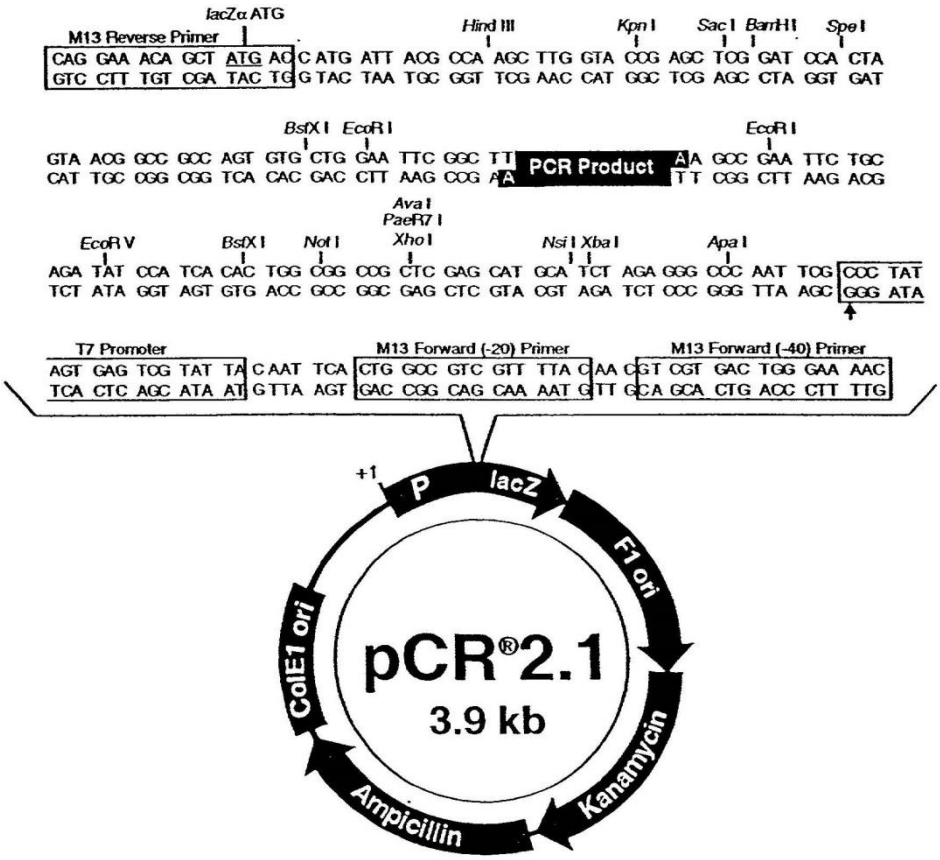

8.2 Raw data

8.2.1 *babo*-RNAi

Loss of *babo* causes no reactivation phenotypes in *Drosophila* NSCs.
Quantification of NSC diameters after loss of *babo* (4h ALH) and wt (4h ALH)

WT	*babo*-RNAi	WT	*babo*-RNAi	WT	*babo*-RNAi
4,3954	4,3954	4,6974	4,6974	4,2758	4,2758
4,2092	4,2092	3,9786	3,9786	4,4637	4,4637
4,5346	4,5346	5,3572	5,3572	4,1918	4,1918
3,9033	3,9033	3,4241	3,4241	3,9848	3,9848
4,6830	4,2342	4,2223	4,2223	4,1849	4,1849
4,8371	4,8371	4,6250	4,6250	3,7800	3,7800
4,7117	5,2342	3,8761	3,8761	4,5154	4,5154
4,1644	4,1644	4,4013	4,4013	4,3863	4,3863
4,2708	4,2708	4,5189	4,5189	3,0161	3,0161
4,6974	4,2342	3,7623	3,7623	4,1163	4,1163
4,5699	4,5699	5,2262	5,2262	4,0230	4,0230
3,6577	3,6577	4,0701	4,0701	3,9874	3,9874
3,9497	3,9497	4,0855	4,0855	3,3943	3,3943
3,9305	4,2342	3,9377	3,9377	4,5289	4,5289
4,6724	4,6724	4,1681	4,1681	3,2566	3,2566
4,1413	4,1413	4,0866	4,0866	3,5477	3,5477
3,7954	3,7954	4,1274	4,1274	3,8053	3,8053
4,4283	3,4352	5,8613	5,8613	4,0450	4,0450
4,0601	4,2349	4,2668	4,2668	4,3212	4,3212
3,8995	3,8995	4,2668	4,2668	4,0881	4,2134
4,7675	4,7675	6,9891	6,9891	4,4739	4,4739
6,0847	6,0847	5,1455	5,1455	3,8610	3,8610
7,1788	7,1788	4,6674	4,6674	5,2945	5,2945
5,1665	5,2385	5,1847	5,1847	4,5697	4,2135
4,8483	6,2425	4,6974	4,6974	4,0853	4,0853
5,1455	5,1455	6,7680	6,2346	3,5607	4,2138
4,0656	4,4542	3,9944	3,9944		5,2346
4,7367	4,7367	4,4352	4,4352		4,2148
4,9813	4,9813	4,7432	4,7432		6,4357
5,9194	5,9194	4,5129	4,5129		5,2135
6,4456	7,3425	4,9602	4,9602		4,2135
5,1728	5,1728	4,4360	4,4360		4,2135
3,7263	3,7263	3,9477	3,9477		
5,6928	5,6928	4,4602	4,4602		
6,2041	6,2041	4,1293	4,1293		
5,3235	5,3235	4,4909	4,4909		
5,8033	5,8033	5,2314	5,2314		
5,7479	5,8979	5,9146	5,9146		
4,7630	5,2135	4,7748	4,7748		
4,2244	4,2244	4,0904	4,0904		
4,6038	4,6038	4,6541	4,6541		
4,4937	4,2345	4,1358	4,1358		
5,4480	5,4480	4,0081	4,0081		
4,4602	6,4235	4,0856	4,0856		
6,6146	6,6146	3,5354	3,5354		
5,1569	5,1569	2,8889	2,8889		
4,3172	4,3172	4,4584	4,2346		
4,6483	4,6483	3,5884	3,5884		
5,1016	5,1016	4,2596	4,2596		
8,2224	6,4236	4,0119	4,0119		
4,2813	4,2813	3,9508	4,2349		
4,3305	5,4235	3,1893	3,1893		
4,2143	4,2354	3,8971	3,8971		
3,8105	3,8105	3,6361	3,6361		
4,6981	4,6981	3,9159	3,9159		
3,8025	3,8025	3,9138	3,9138		
4,0102	5,2435	3,6341	3,2146		
4,8042	4,8042	3,8842	3,8842		
4,4067	4,4067	4,1952	4,1952		
4,4555	4,4555	3,5430	3,5430		
4,1121	4,1121	3,8449	3,8449		
4,4602	4,4602	4,7059	4,7059		

8.2.2 *stat92e*-RNAi

Loss of *stat92e* causes no reactivation phenotypes in *Drosophila* NSCs.

Quantification of NSC diameters after loss of *stat92e* (24h ALH) and wt (24h ALH)

WT	*stat92e*-RNAi
8,9700	8,9900
9,4600	9,5400
7,7900	7,4900
10,1100	10,2142
10,2200	10,25
8,8700	9,1231
10,1000	10,14
8,3000	9,2342
8,5900	8,4
10,6600	10,654
10,3400	9,9437
8,9400	8,974
11,8500	10,2352
10,9200	10,1023
10,8700	10,854
10,1300	10,2342
9,4600	9,534
10,7700	10,234
8,2500	8,2234
9,1700	8,2352
8,9600	8,932
8,2800	8,2332
9,3600	10,2343
11,3800	11,334
8,0600	8,0980
10,6500	10,434
8,9900	8,4342
10,7900	10,8623
10,2900	11,2352
10,0300	10,2423
11,2300	11,223
8,6600	9,2342
10,5500	10,5342
7,9500	8,2342
9,3300	9,3323
9,9100	9,423
11,2900	11,4234
12,6300	12,3242
10,1600	9,2342
6,4700	7,4356
7,5900	7,4232
10,3400	10,6543
11,6200	10,2314
10,6200	10,5435
10,6400	10,5435
13,2700	12,2134
11,1900	11,435
11,5000	11,433
11,2300	11,4353
12,5400	11,2134
11,2400	12,5343

WT	*stat92e*-RNAi
10,4800	11,2342
13,7500	13,2342
11,0600	11,332
9,8600	9,823
12,3100	12,2323
10,5700	9,2352
8,3003	8,2342
10,0354	9,4364
8,0488	8,3422
10,9906	10,232
8,2503	9,464
10,7074	10,7432
10,8919	9,2352
10,7620	12,213
9,8790	9,8234
11,0193	11,0342
12,4351	12,3223
12,6148	12,6234
9,3061	9,3323
12,0516	12,342
10,2504	10,232
14,1386	14,324
10,3213	11,2342
9,8663	9,2342
9,2480	8,3464
12,4030	11,21342
11,7713	11,4543
12,8585	11,2342
10,7673	10,42323
11,2889	11,43234
11,9013	10,234
11,9579	10,84353
11,4728	10,2342
11,5404	11,45423
10,1080	10,14354
12,8512	11,2342
12,9388	12,4334
11,7221	11,454
10,5184	10,4434
10,4456	10,43434
14,6247	14,4343
10,7228	10,4355
7,1607	7,433
13,4523	13,43533
13,9427	14,2342
11,1732	11,4235
12,2900	11,3423
11,3803	11,3435345
12,5081	12,434
11,9624	11,6454
8,4032	9,3454

WT	*stat92e*-RNAi
9,0369	9,0453
8,2520	9,5353
8,8360	9,6457
7,9064	7,4353
10,6548	10,4334
9,2801	10,2342
11,3332	10,2342

8.2.3 *hpo*-RNAi

SWH maintains quiescence in larval NSCs.

Quantification of the NSC diameters for hpo RNAi at 4h ALH

WT	*hpo*-RNAi	WT	*hpo*-RNAi	WT	*hpo*-RNAi	WT	*hpo*-RNAi	WT	*hpo*-RNAi
3,8000	3,9800	5,2600	5,4400	4,7700	5,9600	3,4100	6,3000	3,6900	6,5800
3,8900	4,2800	5,2600	5,4500	4,8200	5,9600	4,3400	6,3000	2,8100	6,5900
3,9000	4,3500	5,2700	5,4600	4,8500	5,9600	3,5100	6,3000	3,4300	6,5900
4,0500	4,5200	5,2900	5,4600	4,8600	5,9700	3,2100	6,3000	3,2200	6,5900
4,2000	4,5300	5,2900	5,4600	4,9200	5,9700	4,2000	6,3100	2,8900	6,6000
4,2400	4,6400	5,3900	5,4800	4,9400	6,0200	3,6900	6,3100	3,4800	6,6100
4,2500	4,6600	5,4500	5,4800	4,9500	6,0300	4,3300	6,3100	3,7900	6,6100
4,3000	4,6700	5,4600	5,5100	5,0900	6,0300	5,0000	6,3200	4,7900	6,6200
4,3000	4,7200	5,5100	5,5100	5,0900	6,0300	4,6600	6,3300	4,8000	6,6200
4,3500	4,7200	5,5800	5,5200	5,1100	6,0400	5,2600	6,3500	3,1600	6,6200
4,3700	4,7800	5,5800	5,5300	5,1100	6,0500	3,9400	6,3500	3,2600	6,6200
4,3800	4,7800	5,5800	5,5300	5,1400	6,0700	4,1300	6,3600	4,4000	6,6500
4,4000	4,7900	5,6400	5,5500	5,2000	6,0800	4,4000	6,3600	3,9700	6,6700
4,4100	4,8000	5,6800	5,5600	5,2400	6,0800	3,6200	6,3800	4,2900	6,6800
4,4300	4,8400	5,7000	5,6100	5,2500	6,0800	3,6200	6,3800	3,2800	6,7000
4,4500	4,8900	5,7900	5,6200	5,2800	6,0800	3,5200	6,3900	3,7800	6,7100
4,4500	4,9000	6,0600	5,6200	5,3200	6,1000	5,0200	6,4000	4,7000	6,7300
4,4700	4,9200	6,1100	5,6300	5,4200	6,1000	3,0800	6,4000	4,7400	6,7400
4,4900	4,9900	6,2400	5,6400	5,4500	6,1100	3,6500	6,4000	4,1800	6,7500
4,5000	5,0000	6,4800	5,6500	5,4800	6,1100	3,9000	6,4000	4,3100	6,7500
4,5100	5,0200	3,2100	5,6500	5,4800	6,1200	3,2200	6,4000	4,3300	6,7600
4,5100	5,0400	3,5600	5,6500	5,6900	6,1200	3,9100	6,4000	3,1300	6,7600
4,5900	5,0400	3,5600	5,6600	5,7000	6,1200	4,5300	6,4000	3,7600	6,7600
4,6200	5,0600	3,6200	5,7200	5,7200	6,1400	4,0000	6,4100	2,7600	6,7600
4,6300	5,0700	3,6300	5,7300	5,8600	6,1600	4,0900	6,4200	3,3300	6,7700
4,6600	5,0900	3,8300	5,7300	6,0200	6,1600	3,5400	6,4200	4,2100	6,7800
4,6700	5,1100	3,8500	5,7600	6,2500	6,1600	3,7800	6,4400	2,9300	6,7900
4,7000	5,1300	3,9100	5,7800	5,4100	6,1700	4,0500	6,4400	3,3300	6,7900
4,7000	5,1400	3,9500	5,8100	4,2800	6,1700	3,9600	6,4500	3,1400	6,8000
4,7500	5,1500	3,9600	5,8100	3,7700	6,1700	4,6000	6,4700	3,1500	6,8000
4,7700	5,1500	4,0000	5,8100	3,3500	6,1700	4,6100	6,4700	3,3300	6,8000
4,8200	5,1600	4,0100	5,8100	4,9700	6,1900	4,3100	6,4700	3,2000	6,8000
4,8300	5,1700	4,0100	5,8100	3,0200	6,1900	4,1800	6,4800	4,2700	6,8000
4,8600	5,1900	4,0900	5,8200	3,9600	6,1900	4,6600	6,4800	3,4500	6,8100
4,8900	5,2000	4,2000	5,8200	2,9500	6,1900	4,3600	6,4900	3,5000	6,8100
4,8900	5,2000	4,2300	5,8400	4,2400	6,1900	4,6200	6,5000	3,8300	6,8200
4,9000	5,2000	4,3000	5,8500	3,2100	6,2000	4,5500	6,5000	3,9200	6,8200
4,9300	5,2400	4,3600	5,8600	3,7400	6,2000	4,6000	6,5100	3,4500	6,8200
4,9400	5,2700	4,3900	5,8700	4,3300	6,2100	4,0500	6,5200	2,9100	6,8200
4,9400	5,2900	4,4600	5,8700	4,1800	6,2100	3,9600	6,5300	4,4300	6,8300
4,9600	5,2900	4,4800	5,8800	3,5700	6,2300	4,3700	6,5300	3,2800	6,8400
5,0200	5,2900	4,5300	5,8800	4,6300	6,2300	4,0700	6,5300	3,8300	6,8500
5,0900	5,3200	4,5900	5,8800	4,0800	6,2300	4,1400	6,5300	3,8100	6,8800
5,1100	5,3200	4,6000	5,8900	4,5400	6,2300	3,0300	6,5400	3,8300	6,8800
5,1100	5,3300	4,6000	5,8900	4,1500	6,2400	3,9400	6,5600	2,9700	6,9000
5,1500	5,3400	4,6100	5,9000	4,6600	6,2400	3,5800	6,5600	3,8800	6,9000
5,1600	5,3600	4,6100	5,9200	3,9500	6,2600	4,4400	6,5600	4,0100	6,9100
5,1800	5,3700	4,6900	5,9200	2,4800	6,2700	2,9400	6,5600	4,4500	6,9300
5,1800	5,3900	4,6900	5,9500	3,7700	6,2900	3,4600	6,5700	3,2200	6,9300
5,2000	5,3900	4,7100	5,9500	3,9200	6,2900	3,7400	6,5700	3,9600	6,9300
5,2100	5,4400	4,7700	5,9500	5,0400	6,2900	2,9300	6,5700	3,9100	6,9400

WT	*hpo*-RNAi	WT	*hpo*-RNAi	*hpo*-RNAi	*hpo*-RNAi	*hpo*-RNAi
5,1800	6,9400	4,6500	7,2900	7,6700	8,0800	8,7000
3,2900	6,9700	4,1000	7,2900	7,6700	8,0800	8,7200
3,8500	6,9700	4,5400	7,3000	7,6800	8,0900	8,7400
4,0800	6,9700	4,4800	7,3200	7,6900	8,1100	8,7500
3,9800	6,9700	3,9700	7,3200	7,6900	8,1200	8,7600
3,5600	6,9700	4,6900	7,3200	7,6900	8,1500	8,7600
3,5800	6,9800	4,4300	7,3300	7,6900	8,1900	8,7700
3,6800	6,9800	4,6400	7,3400	7,7000	8,2100	8,7700
4,3400	6,9900	3,8100	7,3400	7,7000	8,2100	8,8000
4,8000	6,9900	3,7600	7,3400	7,7100	8,2100	8,8100
3,0900	6,9900	4,7400	7,3600	7,7300	8,2300	8,8200
4,7400	7,0000	4,0600	7,3700	7,7400	8,2400	8,8300
4,1400	7,0100	4,2300	7,3800	7,7400	8,2500	8,8400
3,4700	7,0100	5,1000	7,3800	7,7500	8,2500	8,8400
3,6900	7,0100	4,1000	7,4100	7,7500	8,2500	8,8600
3,4300	7,0200	4,1000	7,4100	7,7500	8,2500	8,8600
4,3200	7,0300	5,2300	7,4200	7,7600	8,2600	8,8700
4,7100	7,0300	4,2300	7,4300	7,7700	8,2700	8,8900
3,8600	7,0400	4,3500	7,4300	7,7800	8,2800	8,9000
4,5800	7,0500	4,8600	7,4400	7,7900	8,3000	8,9300
3,6800	7,0700	3,2700	7,4500	7,8000	8,3100	8,9300
3,6700	7,0700	5,4900	7,4500	7,8100	8,3200	8,9500
3,5400	7,0800	3,5800	7,4600	7,8100	8,3200	8,9500
4,0200	7,0900	4,5100	7,4600	7,8200	8,3300	8,9600
3,6200	7,1000	4,9300	7,4700	7,8500	8,3400	9,0000
4,0800	7,1000	5,0400	7,4700	7,8600	8,3600	9,0200
3,5100	7,1000	4,1500	7,4700	7,8700	8,3800	9,0200
5,1000	7,1100	3,4700	7,5100	7,8800	8,3800	9,0200
3,4900	7,1200	3,1500	7,5200	7,8800	8,4000	9,0200
4,7100	7,1200	4,7800	7,5200	7,9000	8,4000	9,0600
3,4300	7,1200	3,9100	7,5300	7,9000	8,4100	9,0800
3,9100	7,1300	4,8200	7,5300	7,9100	8,4200	9,0900
4,1800	7,1500	3,4800	7,5300	7,9200	8,4300	9,1000
3,9900	7,1600	3,8100	7,5400	7,9200	8,4500	9,1200
3,8700	7,1700	4,4900	7,5400	7,9200	8,4800	9,1300
3,8900	7,1700	4,3500	7,5400	7,9200	8,4800	9,1700
4,1300	7,1800	5,1900	7,5500	7,9400	8,4900	9,2000
3,7700	7,1800	4,4600	7,5500	7,9400	8,5100	9,2000
3,2300	7,2000	4,7900	7,5500	7,9500	8,5100	9,2500
5,2100	7,2100	4,4300	7,5600	7,9600	8,5100	9,2500
5,7800	7,2200	3,7900	7,5800	7,9800	8,5200	9,3000
3,4600	7,2300	4,2700	7,5900	7,9800	8,5400	9,3000
4,0100	7,2300	4,0500	7,5900	7,9800	8,5600	9,3400
3,7700	7,2400	3,5900	7,6000	7,9900	8,5700	9,3700
4,0500	7,2500	3,4900	7,6000	8,0200	8,5900	9,3800
5,3100	7,2500	3,8100	7,6100	8,0200	8,6200	9,4200
4,3200	7,2600	5,0900	7,6400	8,0300	8,6200	9,4400
4,3500	7,2600	4,1300	7,6400	8,0300	8,6600	9,4600
4,8800	7,2700	4,0000	7,6600	8,0400	8,6600	9,4900
4,2700	7,2800		7,6700	8,0400	8,7000	9,5300
4,1300	7,2800		7,6700	8,0400	8,7000	9,5700

	hpo-RNAi		*hpo*-RNAi
	9,6300		10,9700
	9,6500		11,0100
	9,6600		11,1500
	9,6800		11,1500
	9,6900		11,2500
	9,7100		11,6200
	9,7300		11,6800
	9,7800		11,6900
	9,7900		11,7500
	9,8000		11,7800
	9,8300		11,7900
	9,8300		12,0200
	9,8300		12,6300
	9,8500		12,6900
	9,9000		
	9,9200		
	9,9500		
	9,9600		
	10,0000		
	10,0200		
	10,0300		
	10,0600		
	10,1200		
	10,1400		
	10,1700		
	10,2300		
	10,2700		
	10,2700		
	10,2700		
	10,2900		
	10,2900		
	10,3000		
	10,3000		
	10,3200		
	10,3500		
	10,3800		
	10,4200		
	10,4500		
	10,5600		
	10,5800		
	10,6600		
	10,7000		
	10,7300		
	10,7400		
	10,7600		
	10,7800		
	10,7800		
	10,8000		
	10,8900		
	10,9000		
	10,9500		

8.2.4 *wts*-RNAi

SWH maintains quiescence in larval NSCs.

Quantification of the NSC diameters for wts RNAi 4h ALH

WT	*wts*-RNAi	WT	*wts*-RNAi	WT	*wts*-RNAi	WT	*wts*-RNAi	WT		WT	
3,8000	4,8900	5,5800	9,5600	5,7000	7,4100	4,6600	6,1700	2,9700		3,9700	
3,8900	4,9600	5,6400	9,6900	5,7200	7,4100	4,3600	6,2100	3,8800		4,6900	
3,9000	4,9600	5,6800	9,7100	5,8600	7,4800	4,6200	6,2600	4,0100		4,4300	
4,0500	4,9700	5,7000	9,8700	6,0200	7,6300	4,5500	6,2700	4,4500		4,6400	
4,2000	5,0200	5,7900	9,9700	6,2500	7,9400	4,6000	6,3000	3,2200		3,8100	
4,2400	5,1600	6,0600	9,9900	5,4100	7,9500	4,0500	6,3100	3,9600		3,7600	
4,2500	5,3200	6,1100	10,0800	4,2800	8,0000	3,9600	6,3100	3,9100		4,7400	
4,3000	5,4000	6,2400	10,4300	3,7700	8,0800	4,3700	6,3800	5,1800		4,0600	
4,3000	5,5500	6,4800	10,4600	3,3500	8,1900	4,0700	6,4100	3,2900		4,2300	
4,3500	5,5900	3,2100	10,8800	4,9700	8,2000	4,1400	6,4800	3,8500		5,1000	
4,3700	5,6800	3,5600	11,2400	3,0200	8,2700	3,0300	6,5400	4,0800		4,1000	
4,3800	5,7300	3,5600	11,3400	3,9600	8,3300	3,9400	6,6300	3,9800		4,1000	
4,4000	5,9300	3,6200	11,9800	2,9500	8,3900	3,5800	6,6800	3,5600		5,2300	
4,4100	5,9600	3,6300	12,0400	4,2400	8,4900	4,4400	6,6800	3,5800		4,2300	
4,4300	6,0000	3,8300	12,3100	3,2100	8,6600	2,9400	6,7000	3,6800		4,3500	
4,4500	6,0000	3,8500	13,3500	3,7400	8,7600	3,4600	6,7500	4,3400		4,8600	
4,4500	6,1300	3,9100	4,2600	4,3300	8,9500	3,7400	6,7600	4,8000		3,2700	
4,4700	6,2500	3,9500	4,4500	4,1800	8,9900	2,9300	6,7700	3,0900		5,4900	
4,4900	6,3400	3,9600	4,7900	3,5700	9,0400	3,6900	6,8200	4,7400		3,5800	
4,5000	6,5300	4,0000	4,8200	4,6300	9,1300	2,8100	6,8200	4,1400		4,5100	
4,5100	6,6800	4,0100	4,8400	4,0800	9,3900	3,4300	6,8800	3,4700		4,9300	
4,5100	6,7100	4,0100	4,9400	4,5400	9,5500	3,2200	6,9000	3,6900		5,0400	
4,5900	6,7600	4,0900	4,9700	4,1500	9,5500	2,8900	6,9100	3,4300		4,1500	
4,6200	6,7800	4,2000	5,1000	4,6600	9,7100	3,4800	6,9400	4,3200		3,4700	
4,6300	6,7900	4,2300	5,1100	3,9500	9,8600	3,7900	6,9900	4,7100		3,1500	
4,6600	6,8100	4,3000	5,1300	2,4800	9,9900	4,7900	7,0400	3,8600		4,7800	
4,6700	6,9200	4,3600	5,2600	3,7700	10,4700	4,8000	7,0900	4,5800		3,9100	
4,7000	6,9800	4,3900	5,4300	3,9200	10,5500	3,1600	7,1900	3,6800		4,8200	
4,7000	7,0000	4,4600	5,5700	5,0400	10,5900	3,2600	7,2400	3,6700		3,4800	
4,7500	7,0500	4,4800	5,6100	3,4100	10,7000	4,4000	7,2800	3,5400		3,8100	
4,7700	7,0600	4,5300	5,7300	4,3400	10,7500	3,9700	7,3500	4,0200		4,4900	
4,8200	7,1200	4,5900	5,7400	3,5100	11,2300	4,2900	7,4700	3,6200		4,3500	
4,8300	7,2000	4,6000	5,7700	3,2100	11,2700	3,2800	8,1100	4,0800		5,1900	
4,8600	7,2800	4,6000	5,8000	4,2000	12,3900	3,7800	8,1100	3,5100		4,4600	
4,8900	7,2800	4,6100	5,8500	3,6900	4,4000	4,7000	8,2300	5,1000		4,7900	
4,8900	7,3100	4,6100	5,8500	4,3300	4,9500	4,7400	8,2600	3,4900		4,4300	
4,9000	7,3400	4,6900	6,0900	5,0000	4,9900	4,1800	8,4100	4,7100		3,7900	
4,9300	7,4300	4,6900	6,1300	4,6600	4,9900	4,3100	8,4600	3,4300		4,2700	
4,9400	7,4400	4,7100	6,1400	5,2600	5,0700	4,3300	8,6000	3,9100		4,0500	
4,9400	7,5000	4,7700	6,2200	3,9400	5,1200	3,1300	9,0900	4,1800		3,5900	
4,9600	7,6600	4,7700	6,2900	4,1300	5,1200	3,7600	9,1200	3,9900		3,4900	
5,0200	7,6800	4,8200	6,3000	4,4000	5,2300	2,7600	9,4500	3,8700		3,8100	
5,0900	7,7400	4,8500	6,3100	3,6200	5,2400	3,3300	9,5800	3,8900		5,0900	
5,1100	7,7500	4,8600	6,3200	3,6200	5,2600	4,2100	9,7400	4,1300		4,1300	
5,1100	7,8300	4,9200	6,3600	3,5200	5,4700	2,9300	9,8200	3,7700		4,0000	
5,1500	7,8400	4,9400	6,4100	5,0200	5,5600	3,3300	10,2100	3,2300			
5,1600	7,8900	4,9500	6,4100	3,0800	5,6200	3,1400	11,3600	5,2100			
5,1800	8,0200	5,0900	6,4700	3,6500	5,6200	3,1500	11,9400	5,7800			
5,1800	8,0300	5,0900	6,6900	3,9000	5,6400	3,3300	12,0800	3,4600			
5,2000	8,0700	5,1100	6,7300	3,2200	5,6700	3,2000	13,6200	4,0100			
5,2100	8,2600	5,1100	6,7400	3,9100	5,6900	4,2700		3,7700			
5,2600	8,3100	5,1400	6,8500	4,5300	5,7900	3,4500		4,0500			
5,2600	8,3200	5,2000	6,8900	4,0000	5,8100	3,5000		5,3100			
5,2700	8,6500	5,2400	6,9100	4,0900	5,8200	3,8300		4,3200			
5,2900	8,9200	5,2500	6,9500	3,5400	5,8300	3,9200		4,3500			
5,2900	8,9600	5,2800	7,0100	3,7800	5,8600	3,4500		4,8800			
5,3900	9,1100	5,3200	7,1200	4,0500	5,9700	2,9100		4,2700			
5,4500	9,1500	5,4200	7,1400	3,9600	5,9800	4,4300		4,1300			
5,4600	9,2500	5,4500	7,1500	4,6000	5,9900	3,2800		4,6500			
5,5100	9,2800	5,4800	7,1600	4,6100	5,9900	3,8300		4,1000			
5,5800	9,3200	5,4800	7,2200	4,3100	6,0200	3,8100		4,5400			
5,5800	9,3500	5,6900	7,3400	4,1800	6,1600	3,8300		4,4800			

8.2.5 *hpo*-mutant (0-2h ALH)

Quantification of NSC diameters in hpo*JM1/hpoKC202* trans-heterozygous mutants at 0-2h ALH

WT	hpo*JM1/hpoKC202*	WT	hpo*JM1/hpoKC202*	WT	
4,3954	4,64	4,3305	4,84	4,6541	
4,2092	4,19	4,2143	4,82	4,1358	
4,5346	4,36	3,8105	4,69	4,0081	
3,9033	4,37	4,6981	4,64	4,0856	
4,6830	3,99	3,8025	4,6	3,5354	
4,8371	4,84	4,0102	4,52	2,8889	
4,7117	3,78	4,8042	4,25	4,4584	
4,1644	4,82	4,4067	4,62	3,5884	
4,2708	4,82	4,4555	4,37	4,2596	
4,6974	4,27	4,1121	4,75	4,0119	
4,5699	4,36	4,4602	4,65	3,9508	
3,6577	4,71	4,6974	4,95	3,1893	
3,9497	4,39	3,9786	4,96	3,8971	
3,9305	4,78	5,3572	3,72	3,6361	
4,6724	4,71	3,4241		3,9159	
4,1413	3,25	4,2223		3,9138	
3,7954	3,47	4,6250		3,6341	
4,4283	4,61	3,8761		3,8842	
4,0601	5,27	4,4013		4,1952	
3,8995	5,29	4,5189		3,5430	
4,7675	4,3	3,7623		3,8449	
6,0847	4,19	5,2262		4,7059	
7,1788	4,68	4,0701		4,2758	
5,1665	4,5	4,0855		4,4637	
4,8483	4,43	3,9377		4,1918	
5,1455	4,55	4,1681		3,9848	
4,0656	4,64	4,0866		4,1849	
4,7367	5,13	4,1274		3,7800	
4,9813	4,27	5,8613		4,5154	
5,9194	4,75	4,2668		4,3863	
6,4456	5,19	4,2668		3,0161	
5,1728	5,41	6,9891		4,1163	
3,7263	5,83	5,1455		4,0230	
5,6928	4,52	4,6674		3,9874	
6,2041	4,14	5,1847		3,3943	
5,3235	4,7	4,6974		4,5289	
5,8033	4,31	6,7680		3,2566	
5,7479	4,84	3,9944		3,5477	
4,7630	4,37	4,4352		3,8053	
4,2244	4,9	4,7432		4,0450	
4,6038	3,86	4,5129		4,3212	
4,4937	4,45	4,9602		4,0881	
5,4480	4,06	4,4360		4,4739	
4,4602	4,99	3,9477		3,8610	
6,6146	3,56	4,4602		5,2945	
5,1569	3,59	4,1293		4,5697	
4,3172	4,58	4,4909		4,0853	
4,6483	4,3	5,2314		3,5607	
5,1016	4,53	5,9146			
8,2224	5,07	4,7748			
4,2813	4,19	4,0904			

8.2.6 *hpo*-mutant (4h ALH)

Quantification of NSC diameters in hpo*JM1/hpoKC202* trans-heterozygous mutants at 4h ALH

WT	hpo*JM1/hpoKC202*	WT	hpo*JM1/hpoKC202*	WT	
3,8000	5,9752	5,5800	6,2637	5,7000	
3,8900	7,8894	5,6400	8,5416	5,7200	
3,9000	6,7005	5,6800	8,0895	5,8600	
4,0500	8,1163	5,7000	5,5770	6,0200	
4,2000	5,7547	5,7900	6,2492	6,2500	
4,2400	6,6046	6,0600	6,4638	5,4100	
4,2500	6,9704	6,1100	5,7572	4,2800	
4,3000	5,5253	6,2400	7,7979	3,7700	
4,3000	6,2080	6,4800	6,8973	3,3500	
4,3500	5,8628	3,2100	6,1269	4,9700	
4,3700	4,7267	3,5600	6,0480	3,0200	
4,3800	6,6530	3,5600	6,5820	3,9600	
4,4000	6,4052	3,6200	5,9901	2,9500	
4,4100	7,2233	3,6300	6,3646	4,2400	
4,4300	6,3675	3,8300	6,5900	3,2100	
4,4500	5,8746	3,8500	6,2502	3,7400	
4,4500	5,8292	3,9100	6,9792	4,3300	
4,4700	6,5872	3,9500	5,5659	4,1800	
4,4900	5,2262	3,9600	7,7982	3,5700	
4,5000	8,8470	4,0000	7,5699	4,6300	
4,5100	8,8778	4,0100	6,8943	4,0800	
4,5100	7,0068	4,0100	7,0538	4,5400	
4,5900	6,1838	4,0900	5,6203	4,1500	
4,6200	7,0965	4,2000	5,2092	4,6600	
4,6300	6,4427	4,2300	5,3262	3,9500	
4,6600	6,4863	4,3000	6,8639	2,4800	
4,6700	6,4854	4,3600	6,4153		
4,7000	6,1696	4,3900	9,1978		
4,7000	6,2621	4,4600	8,2786		
4,7500	6,6078	4,4800	6,0278		
4,7700	5,7049	4,5300	6,9674		
4,8200	5,9304	4,5900	4,4563		
4,8300	6,6568	4,6000	4,6321		
4,8600	6,0236	4,6000	4,9667		
4,8900	5,4162	4,6100	4,9493		
4,8900	6,1618	4,6100	5,6700		
4,9000	5,9023	4,6900	6,8950		
4,9300	5,7982	4,6900	4,7979		
4,9400	5,3898	4,7100	5,0219		
4,9400	7,1248	4,7700	5,3937		
4,9600	6,3891	4,7700	5,5544		
5,0200	6,8026	4,8200	6,1913		
5,0900	5,7008	4,8500	5,8108		
5,1100	8,1644	4,8600	4,5907		
5,1100	7,5460	4,9200	4,8405		
5,1500	6,8505	4,9400	5,9554		
5,1600	7,1683	4,9500	4,1900		
5,1800	7,2014	5,0900	5,3192		
5,1800	5,8379	5,0900	5,0682		
5,2000	7,5569	5,1100	4,7414		
5,2100	6,3507	5,1100	4,7738		
5,2600	6,0698	5,1400	5,0735		
5,2600	5,5258	5,2000	5,4200		
5,2700	6,3543	5,2400	4,5277		
5,2900	6,6499	5,2500	5,3440		
5,2900	7,1771	5,2800	5,1561		
5,3900	6,4797	5,3200	5,3869		
5,4500	6,8934	5,4200	4,4171		
5,4600	6,6683	5,4500	4,8321		
5,5100	6,6769	5,4800			
5,5800	5,2560	5,4800			
5,5800	5,5196	5,6900			

8.2.7 *hpo*- and *wts* RNAi (gal80ts)

Premature reactivation of NSCs after loss of SWH signalling is not due to impaired entry of quiescence.
Quantification of NSC diameters of larval-restricted RNAi using the GAL80ts system of hpo and wts.

WT	*hpo*-RNAi	*wts*-RNAi	WT	*hpo*-RNAi	*wts*-RNAi	WT	*hpo*-RNAi	*wts*-RNAi		*hpo*-RNAi	
4,3954	7,2300	8,0900	4,3305	8,0056	8,5900	4,6541	7,1539	6,0700		7,0957	
4,2092	9,5600	6,8400	4,2143	7,4260	6,9800	4,1358	7,4103	7,1400		8,1252	
4,5346	6,2900	8,4900	3,8105	6,3406	7,9600	4,0081	7,2594	9,1300		7,3595	
3,9033	5,1200	7,0900	4,6981	5,1851	7,9600	4,0856	7,1050	6,6600		5,8841	
4,6830	7,3400	8,2000	3,8025	9,9002	5,1300	3,5354	7,1689	7,3500		10,0843	
4,8371	6,5200	9,1800	4,0102	10,5744	6,0300	2,8889	5,1406	6,8700		10,3274	
4,7117	6,0800	7,4200	4,8042	6,0757	6,5900	4,4584	6,4301	7,1000		7,2369	
4,1644	7,1900	7,4200	4,4067	6,7948	8,7800	3,5884	11,0860	6,4700		7,1349	
4,2708	7,5300	6,4800	4,4555	6,5720	6,8500	4,2596	8,4875	5,5600		7,0026	
4,6974	6,6600	6,8900	4,1121	6,7108	7,7700	4,0119	9,2540	6,6900		7,4670	
4,5699	5,3800	4,8900	4,4602	5,9512	7,5600	3,9508	8,1399	8,7300		6,8511	
3,6577	5,5200	9,1500	4,6974	7,7282	7,6900	3,1893	9,3455	8,3500		8,1113	
3,9497	7,4400	7,2200	3,9786	6,6967	7,5900	3,8971	9,5458	6,5300		7,0358	
3,9305	5,9700	6,4900	5,3572	7,4082	6,6900	3,6361	5,6578	7,1200		8,6626	
4,6724	7,9100	6,5200	3,4241	8,0879	4,7200	3,9159	5,8928	5,7400		5,8011	
4,1413	9,1300	5,7100	4,2223	6,4255	5,2800	3,9138	6,7528	5,4000		6,2545	
3,7954	6,4800	9,0600	4,6250	7,0466	8,0200	3,6341	7,7210	5,5400		7,5050	
4,4283	6,5400	6,9000	3,8761	7,9975	4,7100	3,8842	7,4674	6,5800		5,9229	
4,0601	7,1600	7,2200	4,4013	5,9619	7,1300	4,1952	7,1814			5,6619	
3,8995	6,5100	8,1400	4,5189	6,9719	6,0300	3,5430	7,4470				
4,7675	6,2800	6,4000	3,7623	6,0999	5,4700	3,8449	7,2032				
6,0847	6,5600	7,7800	5,2262	7,4650	8,6300	4,7059	6,2730				
7,1788	6,8400	6,8800	4,0701	9,1319	7,2500	4,2758	6,8129				
5,1665	7,5200	7,2500	4,0855	8,4737	6,0700	4,4637	4,5816				
4,8483	9,2400	6,2800	3,9377	8,9839	7,1400	4,1918	7,7561				
5,1455	6,7900	6,5500	4,1681	6,9758	9,1300	3,9848	7,3594				
4,0656	5,8500	7,8400	4,0866	5,4797	6,6600	4,1849	7,4033				
4,7367	7,0400	7,8800	4,1274	8,1186	7,3500	3,7800	7,2752				
4,9813	6,8800	7,3900	5,8613	7,9196	6,8700	4,5154	7,2032				
5,9194	7,3200	7,2700	4,2668	7,9057	7,1000	4,3863	8,0375				
6,4456	6,2600	8,1400	4,2668	5,1298	6,4700	3,0161	7,6143				
5,1728	5,5600	6,6400	6,9891	7,3198	5,5600	4,1163	7,1913				
3,7263	6,0000	5,6000	5,1455	7,2540	6,6900	4,0230	6,2594				
5,6928	6,6000	7,9600	4,6674	10,1314	8,7300	3,9874	5,9164				
6,2041	6,2600	7,4400	5,1847	8,5554	8,3500	3,3943	7,7011				
5,3235	5,3900	5,5300	4,6974	7,8306	6,5300	4,5289	7,0533				
5,8033	6,9139	6,5700	6,7680	7,3230	7,1200	3,2566	7,1428				
5,7479	8,4894	6,6000	3,9944	6,5447	5,7400	3,5477	7,2405				
4,7630	9,4142	6,3300	4,4352	6,2886	5,4000	3,8053	6,1806				
4,2244	7,0061	6,4200	4,7432	7,5108	5,5400	4,0450	8,4348				
4,6038	6,0937	6,6100	4,5129	6,7218	6,5800	4,3212	5,8989				
4,4937	7,9818	9,5400	4,9602	7,2703	6,6900	4,0881	5,5850				
5,4480	9,6866	8,3600	4,4360	6,1484	4,7200	4,4739	6,8186				
4,4602	7,2744	10,8400	3,9477	6,8334	5,2800	3,8610	8,4147				
6,6146	6,8733	7,4300	4,4602	7,6834	8,0200	5,2945	7,0142				
5,1569	9,3534	6,8600	4,1293	7,3904	4,7100	4,5697	7,8066				
4,3172	5,6730	5,5900	4,4909	5,3634	7,1300	4,0853	10,2194				
4,6483	8,4717	9,6600	5,2314	7,9400	6,0300	3,5607	7,2809				
5,1016	8,7165	5,1500	5,9146	7,2486	5,4700		6,6070				
8,2224	5,8709	6,7900	4,7748	7,3546	8,6300		6,7821				
4,2813	6,2775	5,3900	4,0904	6,2601	7,2500		6,4579				

8.2.8 UAS-*wts*

Ectopic expression of Wts causes decreased NSC diameters
Quantification of NSC diameters after Wts overexpression.

WT	UAS-wts	WT	UAS-wts		UAS-wts		UAS-wts
12,5778	9,8119	12,1705	6,5130		8,0046		8,8416
11,6576	9,3731	13,5018	6,2953		10,1332		8,4886
11,8467	9,3168	9,7051	10,7436		8,6155		6,3341
11,4903	10,2604	10,2279	10,0835		8,4864		10,1191
11,3113	10,4328	13,8305	6,5860		8,5210		8,5029
8,3238	10,9517	9,6888	8,6547		7,9471		6,2096
10,4214	10,7699	8,3111	9,3278		9,5172		8,5978
10,3991	11,3202	10,6954	10,0692		9,1104		7,9380
8,1649	7,4383	8,1558	9,0339		10,0625		7,7885
10,0778	9,3918	12,2516	6,5909		11,4087		8,9625
12,3669	13,6654	12,4133	9,4923		10,7910		8,2385
9,3816	10,7952	9,7051	9,1701		11,0044		8,5980
8,2432	6,8297	10,2302	9,7275		9,6450		6,8103
9,0260	6,8162	11,3024	10,1735		9,1240		10,6502
9,3068	5,7395	9,1740	6,4326		8,5895		10,1132
8,2488	7,9745	7,4521	6,2268		8,0878		9,2303
11,4505	8,8869	6,3243	7,3100		8,7513		9,4588
8,7124	10,2914	10,3163	9,5567		8,7504		12,7406
12,0980	8,3651	10,9324	11,5418		8,0850		9,7194
12,2478	9,4398	12,3789	8,2278		9,4398		7,2375
11,9810	9,0158	9,2041	8,2102		9,5520		7,5268
7,6175	8,9906	9,3719	8,2589		8,4014		9,2269
8,6371	6,8710	10,8406	9,1701		6,8888		7,2733
9,0030	10,2144	11,3789	10,1205		9,8180		9,2089
9,5821	9,2380	10,9583	8,2693		7,4812		8,2185
9,5170	8,2098	11,3435	9,7661		8,8066		8,4394
11,9529	8,4749	9,9743	11,6502		8,9510		8,1062
6,0870	8,0118	10,9439	9,6212		11,8092		7,9428
10,2511	6,5813	10,2568	8,8072		6,5994		9,2497
9,2218	8,1360	8,8855	8,7824		6,7093		7,6970
10,3441	8,3138	7,7553	10,0472		7,2744		9,5525
9,1059	7,7912	11,2298	10,0606		9,6261		9,3970
10,2045	7,6743	12,4539	6,4189		11,0540		9,0220
8,7551	9,6126	13,3923	7,9245		8,1582		9,4569
9,3705	7,2540	8,9439	7,8090		6,9680		9,9718
10,8423	9,5134	11,2003	7,8872		8,6055		9,6749
9,8974	9,6165	11,9466	6,3578		9,6115		6,8425
11,0561	8,6915	10,3964	6,3425		7,0945		6,6325
8,5352	10,5992	9,9968	6,4056		7,4567		6,4047
10,7829	8,4884	8,6769	9,8075		9,6624		6,7049
9,2834	9,4653	10,1286	9,6167		8,5955		7,0269
9,9683	5,6534	9,1455	10,5396		9,4971		8,6299
10,2511	10,9172	11,6589	8,1918		8,1231		9,7724
7,8446	9,6962	11,7507	7,6155		9,1824		8,5863
9,1440	7,6345	10,8406	5,5653		7,0920		8,7826
8,5709	9,3168	9,2178	7,4310		9,9013		8,8432
10,6670	7,0637	7,9697	7,2042		9,0753		9,7132
10,5149	8,6315	9,8741	6,3138		10,0654		9,2894
8,5788	8,4983	11,9423	6,4078		8,2883		10,8275
8,0718	7,6909		9,6639		10,4597		9,0319
12,2790	6,0492		9,2810		6,6134		8,8665

Ectopic expression of Wts causes decreased NSC diameters
Quantification of NSC diameters after Wts overexpression.

	UAS-wts		UAS-wts
	6,3264		7,5145
	6,2938		9,8707
	6,3434		9,2776
	5,8211		9,1549
	9,9293		9,2184
	9,3875		6,4131
	9,2415		13,2465
	10,3085		12,2516
	8,8305		11,4880
	4,8637		8,6369
	4,7547		12,5965
	8,6698		7,0051
	8,2114		7,0005
	10,0125		9,1646
	9,8630		8,2012
	8,3310		10,7239
	7,0598		6,7522
	8,7255		7,0059
	8,6102		9,8490
	7,8507		6,8676
	7,2749		8,0473
	6,7640		9,7119
	7,4236		8,7588
	7,7675		8,1299
	6,5036		9,7297
	5,4688		8,4480
	8,6568		9,9109
	7,5777		9,5643
	8,7012		9,9743
	8,2630		9,7496
	7,0120		7,6618
	8,0733		7,6467
	7,6406		
	8,6752		
	7,6744		
	8,9104		
	8,1837		
	9,3593		
	8,2508		
	9,5022		
	9,5440		
	10,6905		
	8,7441		
	9,2039		
	9,2219		
	7,8827		
	8,2056		
	6,8905		
	11,1695		
	9,3824		
	7,7451		

8.2.9 UAS-*hpo*

Ectopic expression of Hpo causes decreased NSC diameters
Quantification of NSC diameters after hpo overexpression.

WT	UAS-hpo	WT	UAS-hpo		UAS-hpo		UAS-hpo		UAS-hpo
8,9700	6,1100	10,7074	9,2800		6,6200		7,2900		8,4000
9,4600	6,1400	10,8919	10,7200		7,4000		6,9900		7,3600
7,7900	6,6200	10,7620	6,8900		10,5400		6,7100		9,0000
10,1100	6,1100	9,8790	8,5700		9,6600		8,8400		9,0800
10,2200	7,4400	11,0193	7,9700		8,5900		10,8700		7,8200
8,8700	6,7700	12,4351	9,0200		5,5700		8,9400		7,7000
10,1000	5,1200	12,6148	9,1300		7,2500		6,2800		8,6900
8,3000	4,2700	9,3061	9,0100		7,2200		6,7100		7,7000
8,5900	8,3500	12,0516	6,6700		8,6500		8,0600		8,1900
10,6600	10,9400	10,2504	7,2800		8,0000		7,4800		9,9500
10,3400	9,1400	14,1386	6,1500		7,7100		9,7300		7,3800
8,9400	9,5700	10,3213	7,3400		7,3000		7,9700		9,2500
11,8500	6,5000	9,8663	8,3400		9,3100		7,5700		8,2900
10,9200	7,9600	9,2480	8,5400		6,8200		6,7600		8,4300
10,8700	8,7000	12,4030	8,2700		9,3200		7,4600		7,6800
10,1300	10,2200	11,7713	9,8500		10,5400		8,5100		9,0300
9,4600	8,2400	12,8585	8,3600		7,9600		8,7900		10,4000
10,7700	8,9600	10,7673	6,1900		7,1400		7,2300		9,0300
8,2500	8,1200	11,2889	6,9300		5,8900		10,6000		8,9000
9,1700	8,7900	11,9013	9,5100		7,9200		8,2300		8,9900
8,9600	6,5300	11,9579	8,4900		7,5200		9,8300		7,9200
8,2800	7,2400	11,4728	9,0800		7,5500		9,2500		9,8800
9,3600	8,6800	11,5404	7,8700		8,4800		7,1500		7,4400
11,3800	10,1400	10,1080	10,0500		8,6700		7,7500		8,5100
8,0600	7,2700	12,8512	7,9700		7,7800		6,3100		6,9400
10,6500	6,7600	12,9388	10,6400		7,9500		6,1700		7,5900
8,9900	8,8200	11,7221	8,2900		6,6200		7,7900		8,9800
10,7900	6,2600	10,5184	8,9400		9,6800		8,7100		7,7900
10,2900	7,1400	10,4456	7,9400		7,4100		9,8200		8,4300
10,0300	6,6300	14,6247	10,6000		12,7700		8,3100		9,6300
11,2300	7,4800	10,7228	8,3600		9,9100		6,8900		4,8600
8,6600	9,8100	7,1607	9,1400		7,5500		7,0900		6,2700
10,5500	7,7600	13,4523	7,6900		8,8000		7,9900		8,4100
7,9500	7,2200	13,9427	9,5800		7,9900		9,7300		5,6500
9,3300	9,7300	11,1732	8,4400		7,3500		10,2500		6,6700
9,9100	6,6200	12,2900	7,4900		8,0600		9,8700		9,0900
11,2900	8,2200	11,3803	9,6200		7,7000		8,3100		8,3300
12,6300	7,6600	12,5081	7,6500		8,0300		5,3900		7,9100
10,1600	8,0000	11,9624	8,9800		7,1000		6,7300		8,2400
6,4700	10,0600	8,4032	8,1400		6,7200		5,7600		7,5000
7,5900	9,1600	9,0369	7,5300		8,8900		5,9100		9,8400
10,3400	7,4200	8,2520	7,7100		9,1200		7,0200		9,4600
11,6200	6,9900	8,8360	8,5900		7,9800		7,6500		7,6900
10,6200	9,1300	7,9064	9,5700		7,7000		8,2100		8,1200
10,6400	7,0600	10,6548	10,5200		8,9200		9,2500		6,7000
13,2700	7,5700	9,2801	9,4700		7,6300		9,2700		9,3800
11,1900	8,8500	11,3332	12,1500		9,1800		6,1500		8,4600
11,5000	8,2500		11,7300		6,7700		7,0400		9,2600
11,2300	8,7700		9,3600		8,5900		9,0300		7,0000
12,5400	9,4800		8,0000		5,8900		6,3700		6,1400
11,2400	7,1200		8,5700		7,9500		5,9800		5,8200
10,4800	6,2900		8,2800		8,7700		8,7300		5,6800
13,7500	8,4200		9,2800		7,3500		10,0900		7,1400
11,0600	7,0500		8,7700		8,6600		5,9800		8,2200
9,8600	10,0100		9,6600		6,6600		8,6100		5,7700
12,3100	8,8300		6,6500		8,2300		6,9000		9,4900
10,5700	7,4200		8,2300		7,4600		7,4200		8,1700
8,3003	9,7900		9,1000		8,4100		6,5500		7,9900
10,0354	8,0200		10,2100		9,5800		7,3700		8,9900
8,0488	8,5000		8,8600		5,9300		7,5900		6,4800
10,9906	9,4600		8,4400		4,5900		6,3700		6,9100
8,2503	7,8400		7,3700		6,4600		9,1000		8,6900
									9,0700

8.2.10 *14-3-3zeta*-RNAi

NSC-specific RNAi of 14-3-3zeta leads to premature growth of NSCs at 4h ALH.
Quantification of NSC diameters in wild type and 14-3-3zeta RNAi at 4h ALH

WT	UAS-14-3-3	WT	UAS-14-3-3	WT	UAS-14-3-3	WT	UAS-14-3-3	WT	UAS-14-3-3
3,2800	6,4400	4,1000	5,9300	4,1900	6,1200	4,0100	6,7773	4,1800	6,9545
3,9600	8,7200	4,1400	6,2000	4,2100	5,9600	4,0100	5,8264	4,2500	6,0484
4,0300	6,5600	4,1700	9,1100	4,2200	6,3100	4,0400	6,6803	4,2700	
4,0900	5,8400	4,2000	8,9800	4,2500	6,3400	4,0500	5,4170	4,2800	
4,1500	5,8800	4,2100	7,1100	4,2800	6,1600	4,0600	6,6172	4,2900	
4,2400	5,5100	4,2200	6,2900	4,3000	5,5400	4,0800	6,3952	4,3100	
4,2400	5,4100	4,2500	5,2000	4,3300	6,1400	4,1400	4,7679	4,3200	
4,2800	5,9000	4,2800	6,1300	4,3300	5,7800	4,2700	5,9536	4,3300	
4,2900	6,6600	4,3700	5,2700	4,3500	7,3500	4,2900	5,4004	4,3500	
4,2900	6,2200	4,4900	4,9600	4,3500	5,7500	4,2900	4,2401	4,3500	
4,3100	5,9900	4,5000	5,8900	4,3500	5,7800	4,3000	5,6890	4,3500	
4,3200	6,2400	4,5200	6,9900	4,3800	5,3000	4,3500	4,6910	4,3600	
4,3700	6,6500	4,5500	6,4600	4,3800	5,6700	4,3500	4,4407	4,3800	
4,4700	9,6200	4,5700	6,0300	4,3900	6,0800	4,3800	5,7044	4,3900	
4,5400	6,0100	4,6100	7,2800	4,4000	5,9900	4,5000	7,7154	4,4000	
4,5500	5,4800	4,6200	5,0100	4,4100	5,2500	4,5700	7,6504	4,4400	
4,6100	6,5900	4,6500	5,8600	4,4400	5,7700	4,5800	7,9110	4,4700	
4,6200	5,5500	4,7600	7,2900	4,4600	6,0200	4,6200	6,0220	4,4700	
4,6200	6,6000	4,8000	6,2900	4,4800	4,8000	4,6200	4,5518	4,4700	
4,6400	6,2600	4,8100	5,8500	4,4900	6,0100	4,6700	6,3989	4,5100	
4,6500	5,2300	4,8100	6,1900	4,5100	5,1400	4,6800	8,8592	4,5100	
4,6600	9,1300	4,8400	8,1100	4,6000	5,3900	4,7000	6,8208	4,6000	
4,6600	6,9600	4,9300	9,1000	4,6000	5,1300	4,7600	6,5180	4,6300	
4,6700	7,2200	4,9300	7,0300	4,7400	6,0900	4,8000	8,3589	4,6300	
4,7400	6,1000	4,9500	6,2800	4,8100	5,8000	4,8400	7,2333	4,6400	
4,7600	7,9900	4,9900	7,1300	4,8400	5,6700	4,8500	6,1207	4,6600	
4,8100	5,9700	5,0100	7,0500	4,8500	7,5664	4,8900	5,8377	4,8500	
4,8300	5,6400	5,0500	5,9500	4,9100	7,9435	4,9400	6,7941	4,8800	
4,8400	8,0300	5,0800	6,4000	4,9200	7,9824	4,9900	6,1269	4,9100	
4,9300	7,0500	5,1200	6,8000	4,9500	7,7271	4,9900	6,1207	4,9400	
4,9800	6,6500	5,1300	7,0800	4,9600	7,1533	5,0200	5,8103	5,0200	
5,0800	8,7900	5,3300	8,1700	4,9600	6,7359	5,1200	5,3503	5,0500	
5,1200	6,8000	5,3500	7,2400	4,9700	6,7178	5,2400	8,1887	5,2300	
5,1700	6,0400	5,3700	5,1800	5,0700	7,7611	5,2900	7,3116	5,2500	
5,1900	5,5900	5,6500	5,4900	5,1600	5,6269	5,3000	5,2466	5,2700	
5,2100	6,7400	5,8100	5,1500	5,1600	6,7900	5,3100	5,5117	5,3200	
5,2300	6,5000	5,8500	5,2000	5,2000	4,8224	5,3300	7,5471	5,4000	
5,2600	5,4200	5,8700	5,3600	5,3100	7,0795	5,3400	8,6769	5,5600	
5,2600	6,7800	6,1600	7,4200	5,3600	7,1480	5,3600	6,4459	5,5900	
5,2700	5,3500	6,2800	6,4000	5,6500	5,8796	5,4100	5,5052	5,6600	
5,4900	4,9900	6,3400	5,6900	5,6800	5,1451	5,4200	5,8264	5,8700	
5,5300	6,7000	6,4600	5,0300	5,7400	4,8075	5,4300	6,0679	6,2700	
5,6500	6,8500	7,2100	7,0400	6,1100	5,6693	5,4600	9,3438	6,4900	
5,7600	5,9500	7,2300	7,3800	6,3500	8,5608	5,5700	6,7915	3,6400	
6,0100	5,6800	3,3900	7,2600	6,8600	6,8500	5,9800	6,0554	3,7200	
6,2500	6,5500	3,4100	6,1000	6,8700	5,7393	6,0600	6,4039	3,7300	
6,8900	5,1700	3,4200	7,3400	3,3500	5,7550	6,0900	7,6679	3,7600	
7,1500	6,7100	3,6600	6,9500	3,3900	7,3157	6,2900	9,9789	3,7700	
7,4200	5,6400	3,6600	5,8800	3,4600	8,6400	6,3200	6,5397	3,8500	
7,9300	6,4300	3,7300	7,0100	3,5000	6,8454	6,5100	7,1379	3,8900	
3,1100	9,7900	3,7500	5,3400	3,5500	5,9428	3,3700	5,5428	3,9000	
3,5200	7,0800	3,8300	6,2300	3,6900	5,9297	3,5400	6,6608	3,9300	
3,5700	6,5100	3,8500	5,2500	3,7200	5,6109	3,7200	7,0183	3,9900	
3,8100	5,2200	3,8700	5,5500	3,8000	5,1540	3,7300	6,6042	4,0000	
3,9300	5,3100	3,9600	6,4200	3,8500	6,3617	3,8300	5,2443	4,1200	
3,9300	6,5000	3,9800	8,7400	3,8600	6,1115	3,9500	5,5698	4,1500	
3,9400	5,5800	4,0200	6,4800	3,8700	6,9840	3,9800	5,7390	4,1500	
3,9600	5,0500	4,0500	6,4900	3,9000	6,1946	4,0200	6,1574	4,2100	
3,9800	6,2000	4,1000	6,3000	3,9100	5,9499	4,0500	5,4874	4,2400	
4,0300	4,8700	4,1300	5,6800	3,9300	5,2584	4,1000	6,3362	4,2400	
4,0400	5,7300	4,1800	5,7200	3,9600	5,1645	4,1100	6,6563	4,2800	
4,0600	5,5800	4,1900	7,0900	3,9600	5,4724	4,1200	5,3428	4,2900	

NSC-specific RNAi of 14-3-3zeta leads to premature growth of NSCs at 4h ALH.
Quantification of NSC diameters in wild type and 14-3-3zeta RNAi at 4h ALH

WT	
4,2900	
4,3200	
4,3400	
4,3800	
4,4900	
4,5000	
4,5000	
4,5600	
4,6300	
4,6400	
4,6400	
4,7100	
4,7200	
4,7400	
4,8200	
4,8300	
4,8500	
4,8500	
4,8900	
4,9100	
4,9600	
4,9700	
5,0000	
5,1500	
5,1600	
5,2000	
5,2500	
5,3500	
5,4100	
5,6200	
5,8700	
5,8900	
6,1500	
6,3200	
7,1200	
7,5000	
7,8100	

8.2.11 ykiB5 (mutant)

Yki is necessary for reactivation.

Quantification of NSC diameters in ykiB5 deletion mutants at 48h ALH

WT	ykiB5	WT	ykiB5	WT	ykiB5	WT	ykiB5		ykiB5
10,9500	5,3900	10,4400	4,3500	8,7800	4,4400	9,6900	5,6700		6,0100
10,7100	5,3000	11,6500	4,1500	9,8900	4,4800	10,6100	4,8400		4,5000
11,4100	4,5800	10,4200	5,1000	9,5700	7,0700	9,8200	5,6500		4,8600
12,0800	3,7700	9,8000	4,3100	8,8500	6,0700	11,3500	5,2700		4,4200
9,1200	5,5500	9,6700	3,8100	9,0600	5,6300	10,6300	4,5100		4,9600
10,6700	5,7700	10,0600	3,5600	9,5000	5,9100	12,0500	4,5700		4,5100
8,1800	6,8600	11,1500	4,3500	13,3000	7,1500	10,3600	5,0300		4,9500
9,3400	5,4800	10,5400	4,7700	11,6900	5,3800	11,1400	5,4400		5,2900
11,0800	4,9700	10,4600	4,7500	12,9400	5,6000	12,5100	4,4500		3,8500
10,2700	5,9300	10,2200	4,9600	8,8700	4,8500	12,7400	3,9700		4,1500
9,0600	5,2400	10,1700	4,3800	13,5000	6,2400	11,1300	4,2700		4,3600
8,8700	5,1200	12,0600	4,7800	6,7000	5,2800	7,8600	4,1600		4,0500
9,1000	4,9900	11,1300	4,5900	9,4200	5,6300	8,4900	5,2100		3,9900
8,9500	6,1000	11,1200	3,5200	10,0300	4,7900	10,2200	5,2500		5,8300
8,6900	4,7200	8,5400	3,7900	13,4600	6,1000	7,5300	4,7400		4,3000
9,9900	4,4400	13,5800	3,6000	15,2200	5,4700	9,4200	5,4300		4,4700
8,8000	5,7100	7,3200	4,6500	10,1400	5,9000	10,1100	4,6300		4,4100
12,3900	7,3000	10,8200	4,8400	9,5500	6,2300	10,7500	5,1400		4,6700
11,0800	5,2300	10,0900	5,2800	9,5400	5,7800	11,3400	6,0300		4,1300
11,6900	6,0000	11,5400	4,6900	8,4900	5,1500	11,3100	5,2400		5,8700
10,8100	5,2200	11,4300	4,7900	9,8900	5,3200	7,6600	4,8000		5,6700
10,4100	6,4100	11,9600	5,5600	14,2500	4,9600	11,5300	5,1200		5,5600
11,9000	4,0200	12,7700	4,1100	12,6900	4,6500	9,4800	5,6500		5,8800
9,4500	6,1700	10,6100	7,7300	11,7600	4,5400	10,5000	4,0600		5,5000
13,0700	6,0800	10,4700	5,9500	11,9200	5,4100	8,6500	5,8500		5,0200
10,5300	5,1300	10,2400	4,7400	12,5400	5,1400	9,4500	4,8100		4,4700
9,9400	5,7500	9,9000	5,0300	10,9400	4,9800	12,8800	5,9100		5,7000
11,3300	5,2400	11,3700	5,3200	12,6900	4,4200	9,1700	4,8500		5,1800
12,4100	5,1400	10,1300	5,9000	11,6100	6,0100	11,0400	5,5800		4,1700
13,1300	6,0100	12,2200	3,9100	10,2400	4,9600	9,7800	4,3900		5,6600
9,3700	4,6400	12,6000	4,7000	11,6300	5,5000	9,9400	4,9700		5,3400
10,8500	6,4200	11,2300	6,3000	11,1800	4,8100	9,2800	3,4600		3,7800
9,0200	5,3600	10,5300	4,6900	10,0900	4,9500	11,8000	3,8500		4,4900
10,8100	5,7900	10,0400	5,3800	10,0700	5,0500	7,7800	4,1700		4,0100
11,2000	6,0700	11,9900	5,2100	9,1900	5,8300	11,5800	5,8600		4,4600
10,7100	6,1000	10,6300	4,3800	13,9100	6,0100	9,6500	5,0200		4,6200
12,8700	4,5900	12,1000	5,7900	13,0300	7,0200	11,9400	4,9400		4,1700
10,4200	5,7500	10,6900	5,5000	11,8900	7,5600	9,7900	4,9700		4,3400
11,1200	5,3600	11,5800	3,8000	12,8100	4,5500	10,9200	4,8100		3,8000
12,7000	5,0200	11,3600	4,7300	11,0200	4,3200	10,5500	4,6600		4,1000
10,1400	4,1200	11,0100	5,4800	10,6200	4,7900	6,3700	5,6900		4,4100
11,5100	5,1000	13,1100	5,7400	10,5900	4,4200	7,8100	5,2200		5,1600
9,2800	5,2100	9,6800	4,9200	9,8400	5,6000	7,4200	6,0800		4,2700
11,1900	4,9000	8,8800	4,9900	9,7700	4,3300	12,0300	5,1100		4,3300
10,6100	5,2000	10,0400	3,6500	9,3700	3,7600	9,6600	5,1600		4,8000
8,0300	4,7900	10,5900	3,1700	11,0400	4,8900	10,6700	5,4000		4,8000
9,7600	4,5400	10,9400	3,5700	11,1300	4,9400	13,0400	6,3700		4,5400
11,2100	4,1600	9,5300	4,5200	9,7000	5,5600	8,4000	6,0700		3,5800
10,4400	4,7900	8,1200	4,7100	9,0200	5,5900	12,7800	6,3900		4,3200
10,8300	4,0700	9,8700	4,0500	9,8500	4,4700	7,9500	6,7800		5,2300
10,7100	5,5600	9,9900	4,9900	11,7700	6,2500	8,4000	5,6000		4,6600
10,1800	5,6600	9,0400	5,1000	11,4800	4,6400	7,8600	5,9700		3,5100
9,7200	5,9400	10,5700	4,7000	11,5600	4,9200	7,0500	5,5200		4,3600
8,7000	4,9000	13,3500	4,2600	9,3300	5,5900	10,9900	6,8300		4,6100
9,8100	4,9900	11,4800	4,5700	10,5300	4,7200		4,6900		3,7900
10,6500	4,7100	14,9100	4,6000	9,5300	4,7400		4,2700		4,0000
10,0300	4,7100	10,3200	4,3100	9,7800	4,0700		4,1400		4,9300
12,4300	5,6000	11,0800	3,8300	9,7300	5,6400		4,8000		4,3500
9,4400	5,8200	11,1200	4,3800	8,6900	5,0500		5,5500		4,6900
11,9100	4,6600	8,8500	4,4700	11,0500	5,2900		4,2400		5,7500
12,8300	5,8300	9,7900	6,1100	10,6100	6,2600		5,3800		5,7800
10,4400	4,8100	13,0100	4,7300	12,1000	5,5100		5,9400		4,3000

Yki is necessary for reactivation.

Quantification of NSC diameters in ykiB5 deletion mutants at 48h ALH

ykiB5	ykiB5	ykiB5
5,3800	5,7900	7,5700
6,7500	4,4900	5,8200
4,7300	5,4300	5,8000
3,8300	5,1500	4,7000
4,5000	5,3300	5,3100
5,3700	5,6400	4,9400
4,7600	5,9300	4,6400
3,9600	5,2900	5,2400
5,8000	5,7500	4,7900
5,5500	5,6800	4,9700
3,6500	4,9800	4,7200
4,2000	4,7300	4,6300
5,6700	5,7700	4,7900
5,5300	5,7500	3,8800
4,9200	5,3900	5,5800
7,5200	4,7600	5,7500
4,2700	5,7800	4,5700
4,0600	4,5600	4,8200
4,0900	5,0400	6,4100
4,4300	4,9000	4,6000
4,9700	5,3400	4,9100
3,9400	5,3100	5,6800
4,5500	4,4100	4,4800
4,3600	5,5400	
4,1000	4,4800	
3,5800	5,9700	
5,1700	4,7700	
4,6200	5,5500	
5,5000	4,7900	
6,3300	4,0000	
3,3000	5,4600	
5,6900	4,1300	
5,0100	4,6200	
5,5100	4,5000	
4,7100	4,5300	
4,2500	6,4300	
5,2200	3,7100	
4,7200	5,4600	
4,3800	6,1500	
4,4600	3,7500	
5,8100	5,9600	
5,4400	6,1700	
6,0400	5,3900	
5,0800	5,9700	
5,4600	5,8800	
6,1000	5,3900	
6,9300	4,0200	
6,0200	5,6300	
4,6800	5,2000	
3,8000	6,4600	
4,6900	5,0200	
4,1100	4,5700	
5,3200	4,4900	
6,3500	4,6300	
5,7200	5,1300	
4,9200	4,4600	
4,4300	5,6300	
5,5500	4,1600	
4,4200	4,7400	
5,3300	7,1300	
5,5900	5,7700	

8.2.12 MBNB

Quantification of the cell diameter of NSCs of the mushroom bodies (MBNBs) at 4h ALH and 48h ALH.

4h	48h
8,4830	13,5544
9,3795	12,9313
8,5681	13,9693
8,5118	13,4658
8,3975	13,2269
10,2357	14,4944
8,5840	12,0706
8,6851	13,3738
8,2928	14,5392
8,6461	13,2528
8,6454	14,8110
9,7121	13,8279
8,2845	13,4572
9,1624	13,2021
7,7263	13,4191
9,1561	14,2697
8,9620	12,3837
10,1229	13,1082
8,9161	13,9901
8,7070	12,5710
8,0739	
8,4957	
8,4968	
9,2447	
8,0581	
8,4942	
8,4073	
8,0889	

8.2.13 UAS-*ykiS168A*

Yki is sufficient for NSC reactivation.
Quantification of NSC diameters in ectopic expression of inscG4>UAS-ykiS168A at 4h ALH.

WT	UAS-yki	UAS-yki gal80	WT	UAS-yki		WT	UAS-yki			UAS-yki	
4,3954	8,8891	6,7910	4,6974	9,2594		4,2758	8,0493			6,5631	
4,2092	8,3792	5,5171	3,9786	8,1763		4,4637	8,0990			5,8045	
4,5346	10,0974	8,0879	5,3572	7,5077		4,1918	6,4125			7,4287	
3,9033	8,1599	5,6217	3,4241	8,1769		3,9848	7,9732			7,9311	
4,6830	10,2822	6,5008	4,2223	8,6138		4,1849	11,0470			7,6355	
4,8371	9,7184	8,1570	4,6250	9,9491		3,7800	7,1812			7,9632	
4,7117	7,9415	8,5964	3,8761	11,0675		4,5154	7,9078			8,3099	
4,1644	6,4481	6,7297	4,4013	8,7530		4,3863	11,2324			8,4515	
4,2708	7,9125	8,5460	4,5189	9,8720		3,0161	9,1120			7,5552	
4,6974	9,3101	8,1294	3,7623	8,8393		4,1163	8,3526			8,4040	
4,5699	10,3532	7,7895	5,2262	6,9220		4,0230	7,3591			6,6143	
3,6577	10,2916	7,3541	4,0701	6,8388		3,9874	10,1234			6,8912	
3,9497	8,5687	5,9226	4,0855	7,9836		3,3943	7,4348			8,6209	
3,9305	7,0166	6,6014	3,9377	7,4685		4,5289	5,8595			5,8502	
4,6724	9,1098	7,5267	4,1681	9,0084		3,2566	6,8328				
4,1413	7,9898	6,8897	4,0866	7,9616		3,5477	7,2062				
3,7954	8,5277	8,4077	4,1274	8,4358		3,8053	7,8558				
4,4283	9,9992	7,0330	5,8613	7,6707		4,0450	7,8488				
4,0601	8,1020	6,6265	4,2668	8,7647		4,3212	7,6095				
3,8995	10,6632	7,1607	4,2668	5,9024		4,0881	6,8852				
4,7675	10,2107	6,5797	6,9891	8,1214		4,4739	5,4411				
6,0847	7,9194	7,8073	5,1455	8,2888		3,8610	6,9837				
7,1788	8,2060	7,9504	4,6674	9,3918		5,2945	6,8244				
5,1665	7,4829	6,7123	5,1847	7,2949		4,5697	6,4962				
4,8483	6,6691	8,8681	4,6974	8,1484		4,0853	6,0443				
5,1455	7,9793	8,2454	6,7680	6,6691		3,5607	6,4965				
4,0656	7,6297	8,0630	3,9944	6,7288			10,1047				
4,7367	7,5119	7,6616	4,4352	6,3722			8,0358				
4,9813	7,4478	8,3249	4,7432	9,7214			9,7194				
5,9194	6,7277	8,9184	4,5129	10,1160			8,7905				
6,4456	7,8337	7,8063	4,9602	9,9617			10,3953				
5,1728	5,5417	7,1486	4,4360	7,3663			6,5520				
3,7263	7,9915	6,4682	3,9477	6,8723			12,2057				
5,6928	7,7373	7,6170	4,4602	7,3914			10,4643				
6,2041	7,3074	6,9977	4,1293	7,6803			5,8436				
5,3235	7,1639	9,7861	4,4909	6,2461			8,6985				
5,8033	6,9099	6,9806	5,2314	6,9597			6,7574				
5,7479	7,2467	6,0985	5,9146	6,6124			6,1770				
4,7630	8,6879	8,0936	4,7748	9,1569			8,6925				
4,2244	7,2282	9,8643	4,0904	10,3637			6,9579				
4,6038	5,2687	10,2170	4,6541	10,7723			10,3049				
4,4937	5,7288	6,9123	4,1358	11,5793			6,2780				
5,4480	6,6601	6,8924	4,0081	10,8959			6,1203				
4,4602	6,5123	8,7453	4,0856	11,1029			7,8290				
6,6146	5,2766	7,3094	3,5354	7,5455			9,0408				
5,1569	7,4116	5,8086	2,8889	8,5395			6,9396				
4,3172	7,0468	7,0716	4,4584	8,5480			9,8138				
4,6483	5,7187	6,4834	3,5884	8,1136			8,0383				
5,1016	6,7490	7,6432	4,2596	7,3795			10,4478				
8,2224	9,0516	9,2557	4,0119	9,2033			5,7239				
4,2813	8,4125	7,0964	3,9508	9,9749			9,6783				
4,3305	8,3988	6,7738	3,1893	7,7333			10,1656				
4,2143	9,6120	5,4044	3,8971	8,8884			9,4978				
3,8105	8,8075	6,2177	3,6361	7,0812			8,5900				
4,6981	9,8402	6,2577	3,9159	9,7018			8,3480				
3,8025	10,7148	5,9658	3,9138	7,2594			5,9406				
4,0102	9,3168	8,1582	3,6341	9,1751			6,6418				
4,8042	7,3655	5,9490	3,8842	7,4192			8,1060				
4,4067	7,8617	7,3669	4,1952	8,3861			9,1240				
4,4555	8,2276	8,3266	3,5430	6,3087			5,9716				
4,1121	11,3146	5,9803	3,8449	6,8806			8,8537				
4,4602	9,4603	6,7771	4,7059	8,9608			7,3399				

8.2.14 *ban*(delta1) mutant

The bantam miRNA is necessary for the reactivation of larval NSCs.
Quantification of NSC diameters in ban*delta*1 mutants and wild type brains at 24h ALH.

WT Brain	*ban* Brain	WT VNC	*ban* VNC	WT Brain	*ban* Brain	WT VNC	*ban* VNC		*ban* Brain	WT VNC	
8,8600	10,4700	6,0600	8,7627	9,8000	9,2800	5,7100	7,2529		8,0200	5,9500	
8,0600	8,6200	5,5400	8,3670	10,2500	7,3300	4,8800	8,2522		7,2000	5,2400	
8,2100	7,5200	4,5000	7,7152	8,5200	8,0500	4,7000	7,7836		9,2500	5,5100	
9,3800	7,7100	5,5700	7,4948	8,3500	7,3200	4,4500	7,3044		5,3400	6,0900	
8,5700	10,6900	6,5200	7,3423	8,8700	5,1500	5,5700	6,7615		6,8900	5,1200	
9,2800	7,1800	6,2300	9,2424	9,1600	5,7600	4,6900	8,2660		9,7200	5,2700	
10,1400	9,3400	5,2700	8,8079	7,7200	6,5500	4,5300	6,7215		8,6200	5,0800	
10,3900	5,6100	5,8800	8,3699	11,7400	7,7400	5,3600	8,3682		9,1700	5,3700	
9,0700	7,4000	6,4900	9,4619	9,7900	7,0300	3,9600	7,3427		8,3500	6,3000	
8,8100	7,3300	4,5700	8,3731	11,5200	7,2500	5,8400	7,4848		5,7500	6,1500	
9,3600	8,4400	5,0900	6,9957	9,6000	7,8400	4,7900	8,3346		4,5800	5,6200	
8,5600	6,0700	6,4100	8,0430	11,5200	6,4000	4,9900	6,1579		5,1300	6,6600	
9,0300	7,4000	4,8900	9,1857	10,0600	5,6300	6,0600	8,0838		7,2300	5,5400	
7,1000	9,4000	5,9200	8,6275	10,1800	5,7900	4,4900	6,3701		8,5300	4,3600	
8,0000	5,8300	6,4300	7,1054	10,9000	6,3700	4,8900	7,2797		4,8900	6,1800	
9,0500	7,0000	6,2900	7,1341	7,3100	6,1900	4,8700	9,0795		8,8300	5,6800	
5,8200	7,2000	6,1800	10,5177	9,7900	5,1700	5,7400	7,5868		6,7700	4,7100	
7,5000	4,9200	4,8400	8,3289	8,6900	8,6400	4,4600	7,4547		6,1600	4,4600	
11,6800	8,4000	5,7900	7,9148	11,2500	10,2900	5,3300	6,4280		7,4100	4,8400	
9,5700	7,1600	5,8700	8,9001	8,2100	6,6300	5,6000	8,7023		9,2100	4,4600	
10,1100	10,3400	5,4600	7,3034	9,4600	8,5000	4,6400	8,0502		5,0500	5,7900	
8,9900	8,7500	5,7900	9,1403	8,5500	5,8500	6,2100	9,2906		5,7700	6,5300	
7,6800	9,5300	5,6400	9,8600	7,2800	5,2300	6,7900	9,3075		5,0900	5,1200	
7,0500	7,0600	4,7900	9,4199	10,0100	5,0700	4,7800	6,0147		7,1600	5,3400	
6,9600	7,3500	5,4600	12,2415	9,2600	5,3600	8,0900	8,2226		6,3000	4,4500	
10,0300	8,8900	6,0500	8,3032	8,7100	5,7400	6,7400	8,4733		6,5700	4,7500	
11,8500	10,8100	5,7700	9,2796	7,4400	5,4600	5,2900	7,8274		6,4400	4,7300	
9,6100	8,5900	6,1200	9,2289	11,2400	6,7300	5,4600	8,8145		6,2300	5,2300	
8,0900	8,2200	5,0800	9,1328	9,1800	6,1000	4,4900	7,2519		5,8900	4,4000	
8,9800	6,6000	4,7500	6,5229	9,6200	6,0200	5,9200	7,9892		5,6900	4,3700	
9,3400	6,7900	6,2200	9,4199	10,3300	5,6500	5,1700	8,6727		6,1900	4,6300	
10,4000	5,9600	4,7000	7,8491	8,8100	6,4400	4,7000	7,4658		7,5400	4,6200	
12,5700	5,6300	4,9400	7,6283	7,5900	6,8900	5,0100	8,3884		4,7000	5,7400	
14,4700	5,7300	5,1200	7,6803	8,2200	7,3500	6,3600	8,3852		5,0200	5,4400	
11,2800	7,6900	5,2000	8,8053	8,9900	6,5000	5,0800	8,4161		7,1400	5,5300	
10,2100	6,1900	5,3700	9,4425	7,4800	7,0100	5,3000	8,5442		9,0800	4,8800	
9,0900	7,2400	5,4800	8,6186	10,8000	6,2500	4,9400	8,3287		6,4700	4,6000	
12,0700	8,5700	5,9600	8,4642	11,5500	7,0700	4,4700	7,8126		5,3600	4,7500	
10,8600	9,8400	5,9900	10,0523	11,0700	9,1900	5,3000	7,7752		6,2400	7,3900	
11,4700	9,5300	5,5300	9,3066	8,9600	5,2800	6,1800	8,1049		10,5900	4,7900	
11,9000	6,1800	5,5600	6,7823	5,7700	8,7400	4,4200	7,5119		8,5300	5,0300	
10,9100	6,6300	6,3500	7,7810	6,1300	5,6000	6,3200	8,2397		9,0500	4,7000	
10,1900	8,3400	5,0200	8,1039	5,8900	6,1000	5,2800	8,7278		8,0400	5,4800	
5,9400	8,5400	6,1900	9,2289	7,8900	5,5100	4,5900	8,4103		7,3200	5,6500	
10,6600	6,2500	4,7500	8,7633	9,1700	4,7600	5,8000	6,7685		7,8100	3,8800	
8,3300	6,5500	6,4500	8,6856	8,0400	5,6100	6,0800	6,1557		6,0300	4,0200	
13,1300	6,1200	5,9600	6,6795	6,9900	5,1400	5,7600	9,0690		8,5000	5,6000	
8,9400	6,7200	4,6800	10,5897		7,1900	6,0300			7,2300	5,6600	
9,1400	7,6000	5,4000	8,9144		7,4800	6,0800			7,8300	4,4600	
9,6000	9,2100	7,2600	8,1226		5,7300	5,3200			6,1300	4,9900	
8,0200	7,1100	5,4000	9,2667		7,9500	5,3300			5,6200	6,1700	
9,1300	6,2900	4,4900	9,4547		7,2700	5,6400			6,4000	5,1100	
10,0400	9,4700	7,9000	8,8533		6,1700	4,8600			7,4700	5,1200	
9,9800	8,4800	6,7200	9,8037		7,0700	5,4700			6,8900	5,1500	
11,5400	7,7800	6,0100	10,3740		6,3700	5,4500			7,1500	5,5600	
6,5800	7,8300	5,9900	7,3220		7,2500	6,0200			7,7600	4,8000	
9,7800	5,0800	5,2600	8,1902		7,6300	5,2100			5,5200	5,0800	
8,5900	7,0400	5,7500	8,2471		6,4000	5,2100			7,1200	3,7600	
8,9000	5,4900	6,9500	9,3203		6,0400	6,3800			5,8100	4,8500	
11,8000	8,0200	6,4000	8,0073		5,6300	5,8000			5,4000	5,2800	
14,2800	9,0600	4,5500	7,3930		7,2800	5,7000			4,8800	5,5700	
10,2900	7,9900	5,5600	7,4226		8,3200	5,1300			6,0100	5,6400	

The bantam miRNA is necessary for the reactivation of larval NSCs.
Quantification of NSC diameters in ban*delta*1 mutants and wild type brains at 24h ALH.

	ban Brain	WT VNC			*ban* Brain	WT VNC			*ban* Brain		
	9,1800	5,9600			6,7500	6,1300			6,3500		
	7,1800	5,2300			5,7700	4,5700			5,3300		
	9,1200	4,3500			6,0500	4,7400			5,3900		
	7,3100	5,9400			8,0200	6,7500			6,2400		
	5,5100	5,7700			5,7500	5,9300			4,9400		
	4,9000	4,5900			6,3900				8,0300		
	9,5700	6,3000			5,5400				7,2700		
	5,0400	5,7500			6,6600				5,8200		
	7,0000	5,8800			7,3300				6,3000		
	6,7200	4,4100			4,8100						
	6,5700	5,6100			5,0800						
	4,6600	5,1100			5,8400						
	7,1700	5,4000			7,6300						
	6,4000	4,3600			7,3000						
	4,8000	4,9000			9,3800						
	8,8300	5,2800			8,9100						
	5,9800	5,8300			7,2800						
	6,9100	5,9800			7,0400						
	6,2300	5,7000			4,9800						
	6,2300	5,1800			7,0200						
	6,2800	6,1100			6,3500						
	7,1000	6,9900			7,0000						
	7,9100	6,3200			7,5100						
	6,4900	5,9500			6,2600						
	5,7200	5,0700			6,5200						
	5,2600	6,0700			6,7600						
	6,5400	6,6900			5,6300						
	5,9300	7,0000			5,9600						
	7,3100	6,6000			5,4000						
	7,9500	5,5600			6,0300						
	6,0700	6,0700			7,2000						
	8,3600	6,2800			7,2000						
	8,9600	6,7000			6,1000						
	6,7700	5,1200			6,1200						
	7,1900	5,5700			7,2700						
	5,5300	5,9000			8,5900						
	5,1400	5,0700			5,4000						
	6,8300	5,7300			7,7300						
	6,5400	5,1800			5,5300						
	6,0000	5,4800			6,1900						
	7,2500	6,0200			7,1700						
	6,9100	4,6800			6,6100						
	5,8000	6,5800			7,0000						
	8,0400	5,7300			7,0500						
	7,1700	7,4100			6,5900						
	6,7200	5,0900			5,6200						
	7,4600	6,1900			5,3800						
	6,6300	5,0600			7,0700						
	6,3500	5,5000			5,0000						
	9,5200	6,9000			9,2200						
	8,9600	4,6500			6,8800						
	9,6200	5,4900			5,9300						
	8,3400	5,3900			5,3800						
	6,9400	5,7000			7,1100						
	6,2000	6,6300			8,2200						
	6,6300	5,7700			5,6900						
	5,1400	5,7600			6,0600						
	6,7200	5,4700			5,3200						
	6,5600	6,9300			5,3900						
	6,6900	5,8600			5,9100						
	6,8200	4,9900			5,5300						
	7,8000	6,6800			6,1000						

8.2.15 UAS-*ban*

Overexpression of ban prematurely reactivates NSCs.

Quantification of NSC diameters in ectopic expression of inscG4>UAS-UAS-*ban* at 4h ALH.

WT	UAS-*ban*	WT	UAS-*ban*	WT	UAS-*ban*		UAS-*ban*		UAS-*ban*
4,3954	5,3300	4,6974	5,2700	4,2758	7,0500		6,7500		6,3530
4,2092	5,1400	3,9786	6,9800	4,4637	4,8700		7,3100		4,4500
4,5346	5,2375	5,3572	8,3453	4,1918	5,5900		5,6400		
3,9033	5,3900	3,4241	5,4400	3,9848	5,1000		6,1400		
4,6830	6,3500	4,2223	6,3500	4,1849	8,8100		5,7000		
4,8371	7,2400	4,6250	6,0200	3,7800	9,6500		5,5100		
4,7117	6,2395	3,8761	6,8600	4,5154	11,2300		6,9400		
4,1644	4,9300	4,4013	6,8800	4,3863	7,2200		5,8790		
4,2708	4,7300	4,5189	6,8200	3,0161	6,7700		7,3000		
4,6974	5,7700	3,7623	5,9400	4,1163	5,8760		6,1100		
4,5699	5,2895	5,2262	5,9400	4,0230	5,1900		5,9100		
3,6577	5,5800	4,0701	8,1200	3,9874	6,6800		5,6100		
3,9497	6,2389	4,0855	5,8700	3,3943	7,5000		5,8000		
3,9305	6,9500	3,9377	5,4300	4,5289	6,6800		5,7600		
4,6724	7,6100	4,1681	6,7600	3,2566	6,9000		5,4400		
4,1413	8,9100	4,0866	7,2400	3,5477	7,5400		5,6700		
3,7954	8,9200	4,1274	6,2600	3,8053	8,8800		4,8400		
4,4283	5,9800	5,8613	7,8700	4,0450	6,9800		4,4600		
4,0601	6,1600	4,2668	6,5100	4,3212	5,3400		8,7200		
3,8995	6,6400	4,2668	10,6600	4,0881	6,4300		7,0200		
4,7675	5,9800	6,9891	9,2100	4,4739	6,5800		5,3400		
6,0847	5,7900	5,1455	6,7700	3,8610	5,8500		5,2800		
7,1788	4,8800	4,6674	6,6500	5,2945	6,8000		6,3700		
5,1665	7,0400	5,1847	7,5400	4,5697	5,4300		6,5400		
4,8483	5,2386	4,6974	7,4600	4,0853	5,6500		6,6400		
5,1455	4,7800	6,7680	5,3600	3,5607	6,1000		4,6900		
4,0656	6,1100	3,9944	6,5400		5,6300		5,4360		
4,7367	5,1200	4,4352	5,6300		5,9000		8,2400		
4,9813	6,8300	4,7432	6,1200		7,0100		5,7400		
5,9194	5,8900	4,5129	8,0100		7,0300		4,7600		
6,4456	6,4600	4,9602	8,3400		7,4100		5,0800		
5,1728	5,8800	4,4360	6,5200		7,3800		5,1000		
3,7263	5,7600	3,9477	6,6400		6,3000		5,7600		
5,6928	6,0200	4,4602	5,9800		8,4200		5,5300		
6,2041	5,1700	4,1293	5,8100		7,0900		6,2800		
5,3235	5,8300	4,4909	5,0600		5,1600		8,7900		
5,8033	11,4354	5,2314	6,3500		4,0200		7,2350		
5,7479	5,1800	5,9146	4,8500		6,4320		7,4300		
4,7630	5,2387	4,7748	5,3400		6,3800		7,5435		
4,2244	6,4100	4,0904	5,8000		6,6900		9,2000		
4,6038	7,2300	4,6541	5,4330		6,7100		7,0200		
4,4937	7,9800	4,1358	5,1200		10,5400		6,6000		
5,4480	5,2300	4,0081	5,3900		9,1700		5,9400		
4,4602	6,3400	4,0856	6,2200		7,6000		6,3300		
6,6146	6,8700	3,5354	8,3800		8,3600		5,7800		
5,1569	6,5900	2,8889	6,2350		7,2300		4,8500		
4,3172	4,5700	4,4584	7,5500		7,5400		5,9860		
4,6483	4,0800	3,5884	6,7900		5,7200		4,7300		
5,1016	5,2134	4,2596	7,7100		7,0500		5,3900		
8,2224	5,0600	4,0119	8,1400		5,2700		5,0900		
4,2813	5,4500	3,9508	5,9000		8,6540		5,7200		
4,3305	4,5100	3,1893	7,3400		6,4300		5,4353		
4,2143	6,6900	3,8971	5,2340		8,9400		6,7700		
3,8105	5,3240	3,6361	7,2800		5,9200		6,2200		
4,6981	6,0500	3,9159	9,1200		6,8000		5,6100		
3,8025	5,9300	3,9138	6,1800		6,7000		6,7600		
4,0102	4,6900	3,6341	7,5800		6,6400		6,5100		
4,8042	4,2100	3,8842	9,2600		6,0200		4,5500		
4,4067	8,2400	4,1952	6,2800		7,7000		5,5670		
4,4555	7,1400	3,5430	6,3400		6,8400		6,1500		
4,1121	7,4350	3,8449	6,5200		6,3400		4,5400		
4,4602	6,3400	4,7059	5,7500		6,3900		4,4640		

8.2.16 *wts*-RNAi (well-fed and nutrition deprived)

Premature reactivation of NSCs via SWH signalling depends on the nutritional status.
Quantification of NSC diameters upon wts-RNAi in well-fed (wf) or nutrition-deprived (nd) larvae at 4h ALH.

WT	*wts*-RNAi wf	*wts*-RNAi nd	WT	*wts*-RNAi wf	*wts*-RNAi nd	WT	*wts*-RNAi wf	*wts*-RNAi nd	WT	*wts*-RNAi wf	*wts*-RNAi nd
3,8000	5,7116	4,0511	5,5800	6,2183	4,5975	5,7000	6,1467	5,2258	4,6600	7,4990	4,7204
3,8900	7,6934	4,4736	5,6400	5,5087	4,8489	5,7200	6,9025	4,6552	4,3600	7,8327	4,0470
3,9000	7,9899	5,6352	5,6800	6,3912	3,9724	5,8600	7,4178	5,5214	4,6200	6,5522	4,4849
4,0500	6,7437	5,7291	5,7000	6,7098	4,2479	6,0200	6,3826	3,9295	4,5500	5,4687	4,4512
4,2000	5,8635	6,0966	5,7900	5,4472	4,6472	6,2500	6,8532	4,4736	4,6000	6,9616	5,1259
4,2400	5,5562	6,4194	6,0600	9,8585	6,0689	5,4100	5,9503	4,4937	4,0500	6,4650	5,9179
4,2500	6,6408	4,9958	6,1100	8,8463	4,1808	4,2800	6,5716	4,7991	3,9600	6,2311	6,0720
4,3000	5,6720	5,3009	6,2400	6,3082	4,4459	3,7700	6,2084	4,2703	4,3700	5,7975	6,7205
4,3000	8,8019	5,5464	6,4800	6,8119	4,4753	3,3500	8,0505	5,7897	4,0700	5,5050	5,1975
4,3500	8,4726	4,5442	3,2100	7,0849	4,0765	4,9700	6,4172	5,7523	4,1400	6,2731	5,2625
4,3700	8,0918	5,4569	3,5600	6,1847	4,7191	3,0200	5,9450	4,9003	3,0300	5,5362	5,0679
4,3800	6,8603	5,0997	3,5600	6,0840	3,6357	3,9600	6,8222	7,1498	3,9400	5,3211	5,9949
4,4000	8,0191	5,1518	3,6200	6,2608	5,8727	2,9500	6,8012	5,8538	3,5800	5,5256	5,3738
4,4100	6,0552	4,4652	3,6300	8,6471	4,5613	4,2400	6,6141	5,0601	4,4400	5,8196	4,6820
4,4300	6,3065	5,7077	3,8300	6,5605	5,7995	3,2100	6,5488	4,7339	2,9400	6,9871	4,8451
4,4500	6,4364	3,8866	3,8500	6,3553	4,9821	3,7400	5,5814	4,9641	3,4600	6,7847	5,1633
4,4500	5,3423	4,9687	3,9100	6,8379	4,4646	4,3300	5,5220	4,7547	3,7400	8,9967	5,0445
4,4700	6,2548	4,6164	3,9500	6,3262	5,8195	4,1800	6,1696	4,6496	2,9300	7,7240	4,5643
4,4900	4,8383	4,6259	3,9600	5,8317	5,5493	3,5700	5,2064	5,3334	3,6900	6,3047	4,4882
4,5000	5,0704	4,9385	4,0000	7,2055	5,8405	4,6300	5,9331	4,2499	2,8100	6,6518	6,2679
4,5100	5,8902	5,2695	4,0100	6,8634	4,6983	4,0800	5,7076	4,8799	3,4300	7,4474	4,4673
4,5100	6,5678	4,4110	4,0100	8,0696	5,2412	4,5400	6,4117	3,9829	3,2200	6,8967	4,5224
4,5900	5,9308	4,0746	4,0900	6,7480	4,5475	4,1500	5,0966	5,5804	2,8900	6,3370	4,1715
4,6200	6,6740	4,4292	4,2000	6,1591	5,2966	4,6600	5,3558	4,8124	3,4800	6,1150	5,3994
4,6300	9,3656	4,4828	4,2300	5,3286	4,3453	3,9500	5,5680	3,8925	3,7900	5,4579	6,1921
4,6600	9,0760	4,5028	4,3000	7,5922	4,8224	2,4800	6,4133	5,1985	4,7900	6,2236	4,4201
4,6700	7,4997	5,9448	4,3600	7,4373	4,1069	3,7700	5,7492	5,0981	4,8000	7,8593	5,2060
4,7000	6,9410	6,2178	4,3900	5,7477	5,1690	3,9200	5,7759	4,1108	3,1600	7,0792	4,5772
4,7000	6,2256	4,9755	4,4600	5,5981	4,7506	5,0400	5,8973	5,2347	3,2600	6,8716	4,8587
4,7500	5,8167	4,5609	4,4800	6,3087	5,2828	3,4100	7,3849	5,2586	4,4000	6,5592	5,5649
4,7700	6,3200	4,6552	4,5300	5,7594	4,1772	4,3400	5,8583	4,3952	3,9700	6,2353	5,0509
4,8200	6,6370	4,1882	4,5900	6,5628	4,9670	3,5100	6,7208	5,7770	4,2900	7,0848	4,9264
4,8300	6,8707	4,6095	4,6000	5,9677	4,2016	3,2100	5,5809	5,5995	3,2800	7,4277	5,1259
4,8600	6,4942	5,1979	4,6000	6,2491	4,9800	4,2000	5,9537	5,8037	3,7800	9,4920	4,6397
4,8900	6,4332	4,5203	4,6100	6,2303	4,5834	3,6900	5,5079	4,6702	4,7000	6,7796	5,3820
4,8900	6,2071	4,0065	4,6100	5,7278	4,8164	4,3300	5,6490	4,3137	4,7400	5,9860	6,0372
4,9000	6,7715	4,7182	4,6900	7,0099	4,8905	5,0000	6,0704	5,9239	4,1800	8,1934	5,7838
4,9300	6,6829	4,5985	4,6900	5,2311	5,1661	4,6600	5,7343	4,3073	4,3100	6,5002	5,2844
4,9400	6,4312	4,2373	4,7100	9,0706	4,5490	5,2600	6,0649	4,0026	4,3300	8,7998	5,5063
4,9400	5,9495	4,8041	4,7700	6,1650	7,8421	3,9400	6,4910	4,6912	3,1300	6,5998	6,2769
4,9600	6,1454	4,3376	4,7700	7,5420	4,3891	4,1300	7,9747	4,3655	3,7600	6,4932	4,8918
5,0200	7,2462	4,8212	4,8200	8,5607	4,8820	4,4000	5,2200	5,3948	2,7600	6,2634	4,9264
5,0900	7,0277	4,9355	4,8500	8,0805	5,6428	3,6200	6,8947	4,7615	3,3300	7,8189	5,5336
5,1100	6,2484	4,8172	4,8600	7,8957	4,8705	3,6200	6,5220	5,1916	4,2100	6,8716	4,7078
5,1100	5,7745	4,6461	4,9200	7,5237	4,2060	3,5200	6,0704	5,5409	2,9300	7,7635	4,5720
5,1500	5,8640	4,2123	4,9400	6,6679	4,9823	5,0200	7,4674	4,6158	3,3300	6,5177	4,6354
5,1600	6,1550	5,3655	4,9500	5,5509	4,4087	3,0800	6,3507	4,2924	3,1400	5,7270	4,7183
5,1800	5,8905	4,6510	5,0900	6,9766	4,9288	3,6500	8,1040	5,2766	3,1500	7,1613	4,6286
5,1800	6,5007	5,2412	5,0900	7,0643	4,7656	3,9000	9,3694	4,5567	3,3300	6,0745	
5,2000	6,9321	5,2431	5,1100	6,8082	4,4072	3,2200	6,3924	5,3205	3,2000	8,2119	
5,2100	8,4066	5,3387	5,1100	6,7319	3,8598	3,9100	5,3065	5,6896	4,2700	6,9989	
5,2600	7,1249	4,1315	5,1400	6,5242	4,4343	4,5300	6,9655	5,3355	3,4500	6,7636	
5,2600	7,2538	4,7372	5,2000	6,1136	4,3246	4,0000	6,1594	4,9959	3,5000	6,3690	
5,2700	5,7252	4,7885	5,2400	5,1102	4,1880	4,0900	5,8183	4,3476	3,8300	7,0023	
5,2900	7,8389	4,9227	5,2500	8,6714	4,5771	3,5400	7,7696	4,7516	3,9200	7,3003	
5,2900	6,5499	4,2633	5,2800	7,4738	5,3599	3,7800	7,7939	4,5302	3,4500	7,1219	
5,3900	5,8569	4,9185	5,3200	8,7570	4,1172	4,0500	7,7032	4,2880	2,9100	6,5937	
5,4500	6,7709	4,0270	5,4200	6,6593	4,8749	3,9600	6,4272	4,7497	4,4300	6,0626	
5,4600	6,2924	5,3485	5,4500	7,8296	3,7355	4,6000	6,2871	3,8005	3,2800	7,4521	
5,5100	6,9466	4,6845	5,4800	6,3019	4,6671	4,6100	6,0370	4,6395	3,8300	8,3788	
5,5800	7,2084	4,1532	5,4800	6,2556	5,7352	4,3100	6,5781	5,0121	3,8100	6,2977	
5,5800	5,8610	4,1637	5,6900	7,4058	5,1449	4,1800	6,3582	5,1320	3,8300	7,4665	

Premature reactivation of NSCs via SWH signalling depends on the nutritional status.
Quantification of NSC diameters upon wts-RNAi in well-fed (wf) or nutrition-deprived (nd) larvae at 4h ALH.

WT	*wts*-RNAi wf		WT		
2,9700	7,2491		3,9700		
3,8800	8,4535		4,6900		
4,0100	8,0298		4,4300		
4,4500	8,4591		4,6400		
3,2200	7,4746		3,8100		
3,9600	6,1045		3,7600		
3,9100	7,4268		4,7400		
5,1800	6,4274		4,0600		
3,2900	6,8186		4,2300		
3,8500	7,2312		5,1000		
4,0800	7,6527		4,1000		
3,9800	6,4215		4,1000		
3,5600	9,1760		5,2300		
3,5800	8,6048		4,2300		
3,6800	10,7097		4,3500		
4,3400	5,8627		4,8600		
4,8000	7,3924		3,2700		
3,0900	5,2265		5,4900		
4,7400	7,7289		3,5800		
4,1400	6,9240		4,5100		
3,4700	6,7831		4,9300		
3,6900	6,1003		5,0400		
3,4300	7,8349		4,1500		
4,3200	6,9704		3,4700		
4,7100	7,8449		3,1500		
3,8600	7,5480		4,7800		
4,5800	7,0392		3,9100		
3,6800	6,7178		4,8200		
3,6700	6,4799		3,4800		
3,5400	6,8407		3,8100		
4,0200	6,5814		4,4900		
3,6200	6,3925		4,3500		
4,0800	7,1931		5,1900		
3,5100	8,6318		4,4600		
5,1000	6,2742		4,7900		
3,4900	4,8168		4,4300		
4,7100	5,7193		3,7900		
3,4300	6,1148		4,2700		
3,9100	6,1801		4,0500		
4,1800	7,2053		3,5900		
3,9900	5,8129		3,4900		
3,8700	6,4644		3,8100		
3,8900			5,0900		
4,1300			4,1300		
3,7700			4,0000		
3,2300					
5,2100					
5,7800					
3,4600					
4,0100					
3,7700					
4,0500					
5,3100					
4,3200					
4,3500					
4,8800					
4,2700					
4,1300					
4,6500					
4,1000					
4,5400					
4,4800					

8.2.17 *lkb1*-RNAi

NSC specific loss of the LKB1 kinase leads to premature reactivation.
Quantification of NSC diameters in *lkb1*-RNAi

WT	*lkb1* -RNAi	WT	*lkb1* -RNAi	WT	*lkb1* -RNAi
4,3954	5,4324	4,3305	7,3243	4,6541	7,2344
4,2092	7,4234	4,2143	7,4323	4,1358	8,5432
4,5346	6,3332	3,8105	5,2340	4,0081	8,3202
3,9033	5,8645	4,6981	7,2302	4,0856	7,4323
4,6830	5,4534	3,8025	6,2302	3,5354	7,4233
4,8371	5,6446	4,0102	5,2206	2,8889	6,3423
4,7117	6,5456	4,8042	6,3403	4,4584	5,3423
4,1644	4,2343	4,4067	6,3403	3,5884	5,2343
4,2708	8,5443	4,4555	6,3403	4,2596	7,3244
4,6974	8,4443	4,1121	7,3306	4,0119	6,2323
4,5699	8,4353	4,4602	5,4506	3,9508	5,2342
3,6577	6,4344	4,6974	6,3405	3,1893	7,2342
3,9497	8,7865	3,9786	5,3404	3,8971	5,2342
3,9305	6,2574	5,3572	6,4505	3,6361	5,2342
4,6724	6,3445	3,4241	6,3432	3,9159	8,2343
4,1413	5,4354	4,2223	5,3443	3,9138	7,3223
3,7954	5,6545	4,6250	9,2342	3,6341	8,2332
4,4283	6,8553	3,8761	8,2342	3,8842	6,4244
4,0601	4,5665	4,4013	6,3444	4,1952	7,3243
3,8995	5,5435	4,5189	6,3442	3,5430	5,5665
4,7675	5,5645	3,7623	7,0523	3,8449	6,7686
6,0847	5,4353	5,2262	6,2042	4,7059	7,4343
7,1788	5,3433	4,0701	6,2342	4,2758	6,7756
5,1665	6,6543	4,0855	6,2234	4,4637	6,1550
4,8483	9,5346	3,9377	8,2344	4,1918	7,4354
5,1455	9,5456	4,1681	7,4243	3,9848	6,6435
4,0656	7,4353	4,0866	6,3423	4,1849	5,4523
4,7367	5,4534	4,1274	6,4243	3,7800	5,4543
4,9813	6,4343	5,8613	6,3423	4,5154	6,4353
5,9194	5,6545	4,2668	5,2342	4,3863	6,3343
6,4456	6,7545	4,2668	7,4234	3,0161	7,2342
5,1728	6,7800	6,9891	6,4233	4,1163	6,3344
3,7263	6,7809	5,1455	7,4544	4,0230	5,4354
5,6928	6,4560	4,6674	6,4354	3,9874	6,5465
6,2041	6,4350	5,1847	5,2343	3,3943	6,6756
5,3235	6,0433	4,6974	6,2342	4,5289	6,6656
5,8033	6,4354	6,7680	7,2343	3,2566	6,5464
5,7479	6,4334	3,9944	7,3242	3,5477	5,5464
4,7630	6,2302	4,4352	5,3422	3,8053	4,9054
4,2244	5,4544	4,7432	7,4344	4,0450	6,1544
4,6038	6,2343	4,5129	5,2343	4,3212	5,4534
4,4937	7,4234	4,9602	6,2342	4,0881	5,4334
5,4480	7,3434	4,4360	7,2343	4,4739	5,7453
4,4602	6,6545	3,9477	4,3423	3,8610	
6,6146	5,5654	4,4602	6,4233	5,2945	
5,1569	5,5654	4,1293	6,4553	4,5697	
4,3172	6,4333	4,4909	5,5443	4,0853	
4,6483	5,2302	5,2314	7,0660	3,5607	
5,1016	6,3002	5,9146	5,4243		
8,2224	6,3040	4,7748	9,2342		
4,2813	8,3242	4,0904	6,3242		

8.2.18 *wts*- and *lkb1*-RNAi

NSC specific loss of the LKB1 kinase leads to premature reactivation.
Quantification of NSC diameters in *lkb1*/*wts*-RNAi and *wts*-RNAi.

WT	*wts lkb1*	*wts*	WT	*wts lkb1*	*wts*	WT	*wts lkb1*	*wts*			*wts*
4,3954	7,2603	5,7116	4,6974	7,9985	6,2183	4,2758	9,4918	6,1467			7,4990
4,2092	7,9691	7,6934	3,9786	8,5828	5,5087	4,4637	6,3989	6,9025			7,8327
4,5346	6,9103	7,9899	5,3572	7,8440	6,3912	4,1918	8,3461	7,4178			6,5522
3,9033	5,9240	6,7437	3,4241	6,5619	6,7098	3,9848	5,8788	6,3826			5,4687
4,6830	5,7878	5,8635	4,2223	9,3158	5,4472	4,1849	5,1079	6,8532			6,9616
4,8371	6,4358	5,5562	4,6250	10,2524	9,8585	3,7800	7,3029	5,9503			6,4650
4,7117	7,4209	6,6408	3,8761	6,9086	8,8463	4,5154	6,4368	6,5716			6,2311
4,1644	7,3936	5,6720	4,4013	9,1533	6,3082	4,3863	6,4380	6,2084			5,7975
4,2708	6,4623	8,8019	4,5189	5,5933	6,8119	3,0161	5,5193	8,0505			5,5050
4,6974	5,2976	8,4726	3,7623	7,4172	7,0849	4,1163	5,5458	6,4172			6,2731
4,5699	5,5940	8,0918	5,2262	7,3940	6,1847	4,0230		5,9450			5,5362
3,6577	7,1438	6,8603	4,0701	6,0291	6,0840	3,9874		6,8222			5,3211
3,9497	8,5026	8,0191	4,0855	6,2577	6,2608	3,3943		6,8012			5,5256
3,9305	6,6507	6,0552	3,9377	6,1933	8,6471	4,5289		6,6141			5,8196
4,6724	6,3766	6,3065	4,1681	7,1367	6,5605	3,2566		6,5488			6,9871
4,1413	6,0012	6,4364	4,0866	7,5849	6,3553	3,5477		5,5814			6,7847
3,7954	6,1321	5,3423	4,1274	7,9657	6,8379	3,8053		5,5220			8,9967
4,4283	5,4434	6,2548	5,8613	5,9228	6,3262	4,0450		6,1696			7,7240
4,0601	5,2271	4,8383	4,2668	5,7010	5,8317	4,3212		5,2064			6,3047
3,8995	6,8327	5,0704	4,2668	6,7016	7,2055	4,0881		5,9331			6,6518
4,7675	5,9483	5,8902	6,9891	9,3893	6,8634	4,4739		5,7076			7,4474
6,0847	9,0527	6,5678	5,1455	8,0655	8,0696	3,8610		6,4117			6,8967
7,1788	6,7061	5,9308	4,6674	7,8260	6,7480	5,2945		5,0966			6,3370
5,1665	6,0141	6,6740	5,1847	6,6247	6,1591	4,5697		5,3558			6,1150
4,8483	5,9683	9,3656	4,6974	6,9116	5,3286	4,0853		5,5680			5,4579
5,1455	5,8912	9,0760	6,7680	5,8090	7,5922	3,5607		6,4133			6,2236
4,0656	7,5317	7,4997	3,9944	7,7705	7,4373			5,7492			7,8593
4,7367	7,8050	6,9410	4,4352	8,6707	5,7477			5,7759			7,0792
4,9813	8,2510	6,2256	4,7432	8,7127	5,5981			5,8973			6,8716
5,9194	6,6757	5,8167	4,5129	7,0989	6,3087			7,3849			6,5592
6,4456	8,0441	6,3200	4,9602	6,4989	5,7594			5,8583			6,2353
5,1728	6,5471	6,6370	4,4360	6,2153	6,5628			6,7208			7,0848
3,7263	6,5154	6,8707	3,9477	6,9954	5,9677			5,5809			7,4277
5,6928	6,5016	6,4942	4,4602	7,0359	6,2491			5,9537			9,4920
6,2041	5,8776	6,4332	4,1293	6,1566	6,2303			5,5079			6,7796
5,3235	5,0195	6,2071	4,4909	6,6365	5,7278			5,6490			5,9860
5,8033	5,5803	6,7715	5,2314	5,5957	7,0099			6,0704			8,1934
5,7479	5,8832	6,6829	5,9146	5,9280	5,2311			5,7343			6,5002
4,7630	6,5525	6,4312	4,7748	7,4501	9,0706			6,0649			8,7998
4,2244	7,7427	5,9495	4,0904	7,7791	6,1650			6,4910			6,5998
4,6038	8,8808	6,1454	4,6541	8,2855	7,5420			7,9747			6,4932
4,4937	6,5322	7,2462	4,1358	6,8286	8,5607			5,2200			6,2634
5,4480	7,6988	7,0277	4,0081	7,6430	8,0805			6,8947			7,8189
4,4602	9,1017	6,2484	4,0856	7,0156	7,8957			6,5220			6,8716
6,6146	8,4839	5,7745	3,5354	6,5301	7,5237			6,0704			7,7635
5,1569	8,2061	5,8640	2,8889	6,2206	6,6679			7,4674			6,5177
4,3172	5,9639	6,1550	4,4584	7,5565	5,5509			6,3507			5,7270
4,6483	7,6300	5,8905	3,5884	6,9065	6,9766			8,1040			7,1613
5,1016	5,8684	6,5007	4,2596	9,4080	7,0643			9,3694			6,0745
8,2224	7,2059	6,9321	4,0119	8,2315	6,8082			6,3924			8,2119
4,2813	6,8691	8,4066	3,9508	5,9935	6,7319			5,3065			6,9989
4,3305	7,4086	7,1249	3,1893	6,4724	6,5242			6,9655			6,7636
4,2143	7,5089	7,2538	3,8971	7,6602	6,1136			6,1594			6,3690
3,8105	6,9204	5,7252	3,6361	6,9133	5,1102			5,8183			7,0023
4,6981	8,1207	7,8389	3,9159	5,2360	8,6714			7,7696			7,3003
3,8025	9,6659	6,5499	3,9138	6,1173	7,4738			7,7939			7,1219
4,0102	6,6315	5,8569	3,6341	7,4667	8,7570			7,7032			6,5937
4,8042	6,7789	6,7709	3,8842	6,9796	6,6593			6,4272			6,0626
4,4067	6,4553	6,2924	4,1952	8,2641	7,8296			6,2871			7,4521
4,4555	6,3818	6,9466	3,5430	6,5969	6,3019			6,0370			8,3788
4,1121	7,5765	7,2084	3,8449	6,3457	6,2556			6,5781			6,2977
4,4602	6,4748	5,8610	4,7059	7,5130	7,4058			6,3582			7,4665

NSC specific loss of the LKB1 kinase leads to premature reactivation.
Quantification of NSC diameters in *lkb1*/*wts*-RNAi and *wts*-RNAi.

		wts
		7,2491
		8,4535
		8,0298
		8,4591
		7,4746
		6,1045
		7,4268
		6,4274
		6,8186
		7,2312
		7,6527
		6,4215
		9,1760
		8,6048
		10,7097
		5,8627
		7,3924
		5,2265
		7,7289
		6,9240
		6,7831
		6,1003
		7,8349
		6,9704
		7,8449
		7,5480
		7,0392
		6,7178
		6,4799
		6,8407
		6,5814
		6,3925
		7,1931
		8,6318
		6,2742
		4,8168
		5,7193
		6,1148
		6,1801
		7,2053
		5,8129
		6,4644

8.2.19 ex-, mer-, kib-RNAi

Loss of ex, mer or kib leads to premature reactivation of larval NSCs at 4h ALH.
Quantification of NSC diameters in RNAi mediated knockdown of ex, kib and Mer and wild type brains at 4h ALH.

WT	ex	mer	kib	WT	ex	mer	kib	WT	ex	mer	kib		ex	mer	kib
4,3954	4,5000	4,0900	3,6000	4,6974	5,8200	5,4100	5,5700	4,2758	6,1900	6,2000	4,0300		7,0300	6,1500	5,6700
4,2092	4,8300	4,1900	3,6700	3,9786	5,8800	5,4200	5,5900	4,4637	6,2500	6,2300	4,0500		7,1000	6,1900	5,7600
4,5346	5,1100	4,4800	3,7100	5,3572	6,0000	5,4800	5,6500	4,1918	6,3600	6,2300	4,0900		7,1300	6,2200	5,7800
3,9033	5,1400	4,6900	3,8100	3,4241	6,0800	5,5300	5,7800	3,9848	6,4000	6,3100	4,1600		7,1400	6,2200	5,9300
4,6830	5,1600	4,7100	4,0000	4,2223	6,1400	5,6500	5,8700	4,1849	6,4000	6,4100	4,2100		7,2200	6,2200	6,0500
4,8371	5,2000	4,8000	4,0800	4,6250	6,2000	5,6700	5,8900	3,7800	6,5700	6,4500	4,2100		7,2800	6,2500	6,1100
4,7117	5,2400	4,8700	4,1000	3,8761	6,2300	5,7100	5,9100	4,5154	6,5900	6,4700	4,2300		7,3900	6,3100	6,2000
4,1644	5,3700	4,9400	4,1200	4,4013	6,2400	5,7300	5,9200	4,3863	6,6800	6,5000	4,2400		7,5600	6,4700	6,9400
4,2708	5,3800	4,9500	4,1700	4,5189	6,2500	5,7600	6,0900	3,0161	6,7000	6,5400	4,2500		7,6800	6,5100	7,3600
4,6974	5,4000	4,9500	4,1800	3,7623	6,2600	5,8300	6,1700	4,1163	6,7400	6,5500	4,2600		7,7500	6,6100	7,5100
4,5699	5,4200	5,0800	4,3100	5,2262	6,3400	5,8500	6,2200	4,0230	6,8100	6,5500	4,2900		7,8100	6,7100	7,6600
3,6577	5,5200	5,1300	4,3600	4,0701	6,3600	5,9900	6,3200	3,9874	6,9900	6,5600	4,4000		8,0200	6,8300	7,6800
3,9497	5,5800	5,1700	4,4300	4,0855	6,3800	6,0000	6,5200	3,3943	7,1000	6,5900	4,4700		8,3200	6,8400	7,7200
3,9305	5,5900	5,1800	4,5400	3,9377	6,4300	6,1100	6,6100	4,5289	7,1200	6,6200	4,4900		8,9500	6,8800	7,7500
4,6724	5,6700	5,1800	4,5500	4,1681	6,4700	6,1300	6,6300	3,2566	7,1300	6,6900	4,5100		4,6300	6,9200	3,8200
4,1413	5,7000	5,2600	4,5600	4,0866	6,5800	6,1800	6,9500	3,5477	7,1400	6,7200	4,5500		4,7500	7,0200	3,8400
3,7954	5,7700	5,2800	4,5800	4,1274	6,5900	6,1800	7,2300	3,8053	7,2200	6,7400	4,5900		5,0400	7,3300	3,9500
4,4283	5,8400	5,7100	4,5900	5,8613	6,6000	6,1900	7,5800	4,0450	7,2500	6,7700	4,6300		5,2500	7,3600	4,1500
4,0601	5,8800	5,8700	4,6100	4,2668	6,6800	6,2400	3,7600	4,3212	7,7000	6,7800	4,6400		5,2700	7,4000	4,4000
3,8995	5,8900	5,9100	4,6200	4,2668	6,7200	6,2500	3,8900	4,0881	7,7500	6,7800	4,6500		5,4000	7,4700	4,5700
4,7675	5,9100	5,9800	4,6900	6,9891	6,7500	6,2600	4,1500	4,4739	8,1200	6,8100	4,6500		5,5700	7,5800	4,5800
6,0847	5,9300	6,0200	4,7100	5,1455	6,7500	6,2600	4,3800	3,8610	8,2900	7,0500	4,6600		5,6000	7,7000	4,6100
7,1788	5,9500	6,0600	4,7600	4,6674	6,7700	6,2900	4,4600	5,2945	8,3500	7,0800	4,6600		5,6000	7,7600	4,7000
5,1665	5,9800	6,0700	4,7600	5,1847	6,7800	6,3100	4,5100	4,5697	8,5000	7,1300	4,6600		5,6500	8,1100	4,7600
4,8483	6,0100	6,1400	4,7600	4,6974	6,8200	6,3400	4,5200	4,0853	9,1100	7,1500	4,6700		5,6700	8,3900	4,8000
5,1455	6,0300	6,1400	4,7600	6,7680	6,8800	6,4600	4,5800	3,5607	9,5500	7,2500	4,7000		5,6900	8,4800	4,9300
4,0656	6,3300	6,1800	4,7700	3,9944	6,9800	6,6700	4,6100		5,0700	7,2700	4,7500		5,7000	8,6000	5,0400
4,7367	6,3500	6,2900	4,7900	4,4352	7,0900	6,7200	4,6100		5,2200	7,3500	4,7500		5,7200	8,6300	5,1600
4,9813	6,3700	6,3800	4,8100	4,7432	7,1800	6,8000	4,6800		5,2500	7,5800	4,7600		5,7200	9,2900	5,2100
5,9194	6,4000	6,4000	4,8300	4,5129	7,1900	6,8300	4,7100		5,2600	7,6800	4,7800		5,7600	9,4800	5,3000
6,4456	6,4700	6,4400	4,8500	4,9602	7,2400	6,8400	4,7300		5,2700	7,7000	4,7900		5,7700	4,6900	5,3200
5,1728	6,5000	6,5300	4,8600	4,4360	7,2400	6,8500	4,7800		5,3400	7,7100	4,8200		5,8800	5,3300	5,3500
3,7263	6,5100	6,6400	4,8700	3,9477	7,3500	6,9200	4,8500		5,3400	7,7900	4,8300		5,9600	5,3500	5,3600
5,6928	6,6700	6,6500	4,8700	4,4602	7,4100	7,0900	4,9700		5,4700	8,0400	4,8400		6,0100	5,3700	5,4000
6,2041	6,8400	6,6600	4,8900	4,1293	7,5600	7,1900	4,9700		5,5900	8,0800	4,8600		6,0700	5,4300	5,4400
5,3235	6,8500	6,6700	4,9500	4,4909	7,6100	7,2600	4,9700		5,6100	8,1700	4,9200		6,0900	5,4500	5,5100
5,8033	6,9100	6,6700	4,9800	5,2314	7,6200	7,3200	4,9800		5,6100	8,6500	4,9500		6,1600	5,5500	5,5900
5,7479	6,9300	6,6700	5,0000	5,9146	8,1000	7,7200	4,9900		5,6500	9,2400	4,9800		6,1800	5,5800	5,7700
4,7630	6,9700	6,6900	5,0800	4,7748	8,7100	7,7600	4,9900		5,6500	10,1600	4,9800		6,2700	5,6300	5,8000
4,2244	6,9800	6,7000	5,0800	4,0904	8,8300	7,8500	5,0800		5,6800	10,5700	5,0200		6,2800	5,7200	5,8600
4,6038	7,0200	6,8400	5,1100	4,6541	5,0000	7,9400	5,0900		5,7000	4,6900	5,0400		6,3200	5,8500	5,8800
4,4937	7,0300	6,8700	5,1200	4,1358	5,0600	7,9900	5,1500		5,7000	4,9100	5,0600		6,4800	5,9000	5,8900
5,4480	7,0900	7,0900	5,1300	4,0081	5,2400	8,0000	5,2600		5,8000	5,0200	5,0800		6,5000	5,9300	6,1800
4,4602	7,3000	7,1100	5,1300	4,0856	5,3000	8,3100	5,2600		5,8300	5,1800	5,0800		6,5100	5,9400	6,3200
6,6146	7,3800	7,3900	5,1400	3,5354	5,3000	8,8600	5,2600		5,8500	5,2700	5,1000		6,5600	5,9700	6,3900
5,1569	7,4400	7,4100	5,1700	2,8889	5,3700	9,0700	5,3400		5,8700	5,3600	5,1000		6,6600	5,9800	6,3900
4,3172	7,6100	7,4600	5,2100	4,4584	5,3700	9,2100	5,3600		5,9100	5,4300	5,1000		6,6900	6,0200	6,4300
4,6483	7,7300	7,5400	5,2200	3,5884	5,4800	9,5500	5,4100		5,9100	5,4500	5,1500		6,7500	6,0400	6,7100
5,1016	7,8800	7,5600	5,2200	4,2596	5,4900	4,6800	5,5100		5,9300	5,5100	5,1500		6,7500	6,0800	7,1100
8,2224	7,9400	7,5700	5,2200	4,0119	5,5300	4,9200	5,5600		5,9500	5,5700	5,1900		6,7600	6,0800	7,3400
4,2813	8,4800	7,7300	5,2400	3,9508	5,5800	5,0000	5,5700		6,1300	5,6300	5,1900		6,8000	6,1000	3,5700
4,3305	8,7300	7,9800	5,2500	3,1893	5,6000	5,1000	5,7100		6,1400	5,6800	5,2400		6,8600	6,1400	3,6500
4,2143	5,4000	8,1600	5,4100	3,8971	5,6500	5,2500	5,7800		6,1900	5,6800	5,3100		6,8700	6,1700	4,4200
3,8105	5,4500	8,3300	5,4300	3,6361	5,6700	5,4900	5,8300		6,2200	5,7600	5,3200		6,9200	6,2300	4,4800
4,6981	5,4600	8,3400	5,4300	3,9159	5,7200	5,6800	5,8700		6,2600	5,8800	5,3600		6,9400	6,3300	4,5800
3,8025	5,5200	8,4100	5,4500	3,9138	5,7600	5,8600	5,8900		6,3000	5,9000	5,3700		7,0500	6,3700	4,5900
4,0102	5,5700	8,9000	5,4600	3,6341	5,8700	5,9800	6,3200		6,3500	5,9900	5,3800		7,0900	6,4900	4,6300
4,8042	5,5800	9,4400	5,4600	3,8842	5,9200	5,9900	7,0600		6,3700	5,9900	5,4200		7,1600	6,5300	4,6400
4,4067	5,5800	4,8200	5,4700	4,1952	5,9800	5,9900	7,1900		6,6600	6,0200	5,4400		7,3400	6,5800	4,7500
4,4555	5,6000	4,9800	5,4700	3,5430	6,1400	6,0600	3,6900		6,8000	6,0400	5,4800		7,4900	6,9000	4,8200
4,1121	5,7800	5,0600	5,5100	3,8449	6,1500	6,1100	3,8400		6,9800	6,0700	5,6400		7,5900	6,9000	4,8200
4,4602	5,8100	5,1700	5,5100	4,7059	6,1800	6,1500	3,8700		6,9900	6,0700	5,6700		7,6800	6,9200	4,8300

	ex	mer	kib		ex		kib		ex		kib				
	8,9300	6,9400	4,8400		5,6400		4,8200		5,6600		4,4800				4,3000
	9,5300	6,9700	4,8400		5,6500		4,8500		5,7000		4,5200				4,3000
	4,7000	7,0400	4,8600		5,6600		4,8600		5,7800		4,5700				4,3200
	4,8700	7,1900	4,9100		5,7100		4,9100		5,8600		4,5900				4,3900
	4,8900	7,2100	4,9400		5,7400		4,9200		5,9600		4,6700				4,4200
	4,9000	7,3100	4,9400		5,7900		4,9200		6,0400		4,6700				4,4600
	5,0200	7,3400	4,9600		5,8100		5,0200		6,0800		4,7200				4,4800
	5,1300	7,3700	5,0000		5,8500		5,0600		6,1400		4,7300				4,4900
	5,2700	7,4500	5,0100		5,8500		5,0900		6,1700		4,7700				4,4900
	5,2900	7,5700	5,0100		5,8900		5,0900		6,1700		4,7900				4,5600
	5,3100	7,5900	5,0600		5,9100		5,0900		6,2600		4,8100				4,5800
	5,3300	7,8800	5,0600		5,9700		5,1100		6,5300		4,8200				4,5800
	5,4100	7,9500	5,0800		6,0400		5,1300		6,5300		4,8400				4,5900
	5,5600	8,2200	5,1000		6,0600		5,1300		6,6800		4,8400				4,6000
	5,7600	8,9800	5,1300		6,2900		5,3200		6,8600		4,8400				4,6200
	5,8600	9,3100	5,1800		6,3000		5,3600		6,9200		4,8500				4,6200
	5,8900	9,3300	5,1800		6,3000		5,4000		6,9600		4,8600				4,6300
	5,9100	10,1700	5,1900		6,4100		5,4300		7,0700		4,8800				4,6700
	5,9100		5,2200		6,4400		5,4600		7,1300		4,9100				4,7000
	5,9300		5,2500		6,4400		5,4700		7,1800		4,9700				4,7200
	5,9500		5,2500		6,5000		5,4700		7,2800		5,0100				4,7300
	5,9500		5,3100		6,5700		5,5300		7,3900		5,0100				4,7500
	5,9800		5,3400		6,5900		5,5400		7,7300		5,0200				4,7600
	5,9900		5,3600		6,7600		5,5700		8,0100		5,0500				4,7600
	6,0300		5,3800		6,8200		5,6300		8,0500		5,1400				4,7600
	6,0400		5,3900		6,8900		5,6600		8,2400		5,1400				4,7700
	6,0500		5,4100		7,1600		5,7700		9,0700		5,1700				4,8700
	6,0600		5,4300		7,2100		5,7800		9,7900		5,1800				4,8800
	6,1800		5,4600		7,4000		5,8100				5,2700				4,8800
	6,2100		5,5300		7,5600		5,8400				5,3100				4,9300
	6,2400		5,5600		7,5700		5,9000				5,3300				4,9900
	6,2600		5,5800		7,6000		6,0600				5,3400				5,0300
	6,3700		5,6100		7,6200		6,1300				5,3400				5,0500
	6,4300		5,6600		7,8300		6,1500				5,4200				5,0900
	6,5400		5,7800		7,8600		6,2000				5,4300				5,1000
	6,5800		5,8500		7,9400		6,3300				5,4600				5,1100
	6,6900		5,8800		8,0500		6,4600				5,4600				5,1100
	6,7900		5,9000		8,7000		6,6600				5,4800				5,1900
	6,8900		6,0300		8,7800		6,7800				5,5100				5,2300
	7,0100		6,0400		9,3200		6,8800				5,5500				5,2400
	7,1100		6,0600		4,7800		6,8800				5,5600				5,2400
	7,1400		6,1600		4,8900		6,9400				5,5800				5,2400
	7,1700		6,2200		4,9800		6,9400				5,6200				5,2500
	7,3200		6,2200		5,0000		7,5400				5,6300				5,2500
	7,4000		6,2800		5,0800		7,5700				5,8100				5,3000
	7,4400		6,7200		5,1300		8,5700				5,9900				5,3300
	7,6400		6,7600		5,2100		3,8600				6,0200				5,3800
	7,7300		6,7800		5,2400		3,9100				6,0500				5,3900
	7,8500		7,1700		5,2500		4,0100				6,1400				5,3900
	8,0000		7,4500		5,2800		4,0200				6,2500				5,4800
	8,0500		7,5900		5,3100		4,1200				6,6000				5,4800
	8,4500		4,1100		5,3200		4,1800				6,7700				5,4900
	4,6000		4,2800		5,3500		4,2200				7,1900				5,5400
	5,0400		4,3200		5,3700		4,2400				7,3300				5,5700
	5,0800		4,4700		5,4700		4,2400				7,8300				5,5800
	5,2700		4,4700		5,4900		4,3300				3,7700				5,5900
	5,2700		4,5100		5,5100		4,3600				3,8500				5,6000
	5,3000		4,7000		5,5700		4,3800				4,0000				5,6100
	5,4500		4,7100		5,6000		4,3800				4,0800				5,6200
	5,4600		4,7200		5,6100		4,4000				4,2300				5,6300
	5,5100		4,7400		5,6300		4,4200				4,2300				5,6800
	5,5200		4,8100		5,6500		4,4500				4,2400				5,7400
															5,9300
															6,0000
															6,0600
															6,0800
															6,1900
															6,2900
															6,4400
															6,4700
															6,7300
															6,7700

8.2.20 *fat*-RNAi

Loss of fat leads to premature reactivation of larval NSCs.
Quantification of NSC diameters in RNAi fat-RNAi. Wild type brains 4h ALH

WT	*fat*-RNAi	WT	*fat*-RNAi	WT	*fat*-RNAi		*fat*-RNAi		*fat*-RNAi
4,3954	4,1800	4,6974	6,4100	4,2758	6,1900		5,9300		5,7800
4,2092	4,2800	3,9786	6,5600	4,4637	6,2800		5,9300		5,8600
4,5346	4,2900	5,3572	6,6300	4,1918	6,3200		5,9500		5,8800
3,9033	4,3400	3,4241	6,6600	3,9848	6,3200		5,9500		5,9100
4,6830	4,3400	4,2223	6,7400	4,1849	6,4900		6,1700		5,9200
4,8371	4,4100	4,6250	6,9500	3,7800	6,4900		6,1800		5,9300
4,7117	4,4900	3,8761	7,0700	4,5154	6,5600		6,2000		5,9600
4,1644	4,6100	4,4013	7,1300	4,3863	6,5700		6,2800		5,9800
4,2708	4,6400	4,5189	7,2100	3,0161	6,6200		6,2900		6,0200
4,6974	4,6400	3,7623	7,5000	4,1163	6,6400		6,3300		6,0400
4,5699	4,6500	5,2262	7,6100	4,0230	6,8500		6,3800		6,0400
3,6577	4,6500	4,0701	8,4500	3,9874	7,2600		6,4800		6,0900
3,9497	4,7200	4,0855	8,5900	3,3943	7,5400		6,5500		6,2200
3,9305	4,7900	3,9377	4,0200	4,5289	8,7300		6,6000		6,3600
4,6724	4,8500	4,1681	4,1400	3,2566	8,7900		6,6600		6,4700
4,1413	4,9000	4,0866	4,2800	3,5477	4,0800		6,7100		6,5000
3,7954	4,9300	4,1274	4,3500	3,8053	4,3100		6,7100		6,5200
4,4283	4,9600	5,8613	4,3800	4,0450	4,3200		6,8600		6,5600
4,0601	4,9600	4,2668	4,5500	4,3212	4,4000		6,9500		6,5800
3,8995	5,0100	4,2668	4,5600	4,0881	4,4700		6,9600		6,7500
4,7675	5,0100	6,9891	4,6500	4,4739	4,5300		6,9700		6,7700
6,0847	5,0100	5,1455	4,7100	3,8610	4,5700		7,0400		6,7700
7,1788	5,0900	4,6674	4,7200	5,2945	4,6400		7,1600		6,8100
5,1665	5,1100	5,1847	4,8400	4,5697	4,7200		7,6900		6,8300
4,8483	5,2100	4,6974	4,8500	4,0853	4,7200		7,8400		6,8800
5,1455	5,3000	6,7680	4,8800	3,5607	4,8500		8,2800		6,9600
4,0656	5,3400	3,9944	4,8800		4,8800		8,2800		6,9600
4,7367	5,3600	4,4352	4,9400		4,8900		8,5100		7,0600
4,9813	5,3600	4,7432	5,0300		4,9000		8,8700		7,1300
5,9194	5,3800	4,5129	5,0600		4,9100		4,1900		7,4400
6,4456	5,4100	4,9602	5,0600		4,9600		4,2300		7,6800
5,1728	5,4200	4,4360	5,0600		4,9900		4,3900		7,9800
3,7263	5,4500	3,9477	5,0700		5,0000		4,5700		8,8300
5,6928	5,4600	4,4602	5,1000		5,0400		4,6600		9,3400
6,2041	5,4600	4,1293	5,1200		5,1800		4,6800		9,5600
5,3235	5,4800	4,4909	5,1500		5,2200		4,6900		
5,8033	5,5000	5,2314	5,1500		5,2700		4,7400		
5,7479	5,5200	5,9146	5,1600		5,2700		4,7600		
4,7630	5,5600	4,7748	5,1900		5,3000		4,8100		
4,2244	5,5700	4,0904	5,2200		5,3000		4,8300		
4,6038	5,5800	4,6541	5,2400		5,3200		4,8400		
4,4937	5,5900	4,1358	5,2500		5,3200		4,8700		
5,4480	5,6500	4,0081	5,2500		5,3300		4,9000		
4,4602	5,6700	4,0856	5,3000		5,3300		4,9100		
6,6146	5,6800	3,5354	5,4200		5,3700		4,9300		
5,1569	5,6800	2,8889	5,4400		5,3800		5,0200		
4,3172	5,7000	4,4584	5,4500		5,4200		5,1500		
4,6483	5,7100	3,5884	5,4900		5,4400		5,1700		
5,1016	5,7500	4,2596	5,4900		5,4600		5,1900		
8,2224	5,8600	4,0119	5,5000		5,4800		5,2300		
4,2813	5,8700	3,9508	5,5300		5,5000		5,2400		
4,3305	5,9200	3,1893	5,5600		5,5100		5,2600		
4,2143	6,0000	3,8971	5,6200		5,5600		5,3000		
3,8105	6,0700	3,6361	5,6500		5,5800		5,4200		
4,6981	6,1300	3,9159	5,7800		5,5800		5,5300		
3,8025	6,2200	3,9138	5,8500		5,6300		5,5300		
4,0102	6,2700	3,6341	5,8500		5,6400		5,5700		
4,8042	6,3100	3,8842	5,8700		5,7200		5,5800		
4,4067	6,3100	4,1952	5,8800		5,8100		5,6100		
4,4555	6,3500	3,5430	5,8900		5,8300		5,6200		
4,1121	6,3900	3,8449	5,8900		5,8800		5,6600		
4,4602	6,4000	4,7059	5,8900		5,9100		5,7400		

8.2.21 *crb*-, *ed*-RNAi (*insc* and *repo* driverline)

Crumbs and Echinoid are required in NSCs and glial cells in cis and in trans to activate SWH signalling during quiescence.
Quantification of NSC diameters with the insc and repo driver line at 4h ALH.

WT	*crb* insc	*crb* repo	*ed* insc	*ed* repo	*crb/ed* insc	*crb/ed* repo
3,8000	4,3800	4,9468	7,6170	4,9800	5,5031	6,0965
3,8900	4,4700	4,1633	6,3256	5,6200	6,3794	6,4179
3,9000	4,5700	4,0639	5,5106	6,3500	5,7665	6,4882
4,0500	4,7200	4,2382	7,4329	6,2700	7,5661	6,2428
4,2000	4,8400	2,9118	9,1792	4,9800	6,8205	6,3408
4,2400	4,8600	3,8975	5,4410	6,2700	5,6972	8,0237
4,2500	4,8800	4,5436	5,5248	6,1100	7,9076	6,5229
4,3000	5,0200	3,6618	5,7782	5,4100	6,1339	5,6651
4,3000	5,0500	4,3674	5,7721	5,1300	5,5786	6,8799
4,3500	5,0700	4,3646	6,1921	5,6400	5,8756	6,6653
4,3700	5,0900	4,1248	5,5696	4,9600	5,8183	6,9780
4,3800	5,1600	3,7467	6,0655	5,0700	5,5786	6,4715
4,4000	5,1600	4,1682	5,9445	5,4400	6,5797	7,7314
4,4100	5,2100	4,6608	6,2110	5,8200	6,1235	5,9264
4,4300	5,2400	4,2507	6,1015	4,7600	6,6912	6,8044
4,4500	5,2500	4,3336	6,9017	4,6300	6,1162	6,6937
4,4500	5,2800	5,2389	7,1106	6,4000	5,6673	9,3827
4,4700	5,2900	4,9393	6,8530	5,7600	6,6495	6,6622
4,4900	5,3500	4,2523	7,2456	5,7700	7,5408	7,3433
4,5000	5,3500	4,7903	7,8348	6,0800	5,9280	6,3957
4,5100	5,3600	4,7848	6,6126	4,8900	6,2507	6,8605
4,5100	5,3700	5,0827	8,4050	5,1300	6,4824	6,1113
4,5900	5,5000	5,6157	9,1791	7,0600	6,0372	6,5657
4,6200	5,5100	4,6127	7,2422	4,8600	7,1624	6,0612
4,6300	5,5900	4,7601	5,4508	5,3700	6,1074	6,9257
4,6600	5,6100	5,3083	6,5794	5,1200	7,5665	6,6337
4,6700	5,6100	4,4941	6,0979	4,5500	5,9158	6,6174
4,7000	5,6100	5,4548	5,9710	4,9500	6,3962	5,0838
4,7000	5,6300	5,7653	5,7618	5,0900	5,4588	5,1845
4,7500	5,6600	4,7985	6,6722	5,1500	7,0539	5,4419
4,7700	5,6800	6,4248	8,5924	5,2300	6,5753	6,3261
4,8200	5,6800	6,2224	7,9488	6,3900	7,0156	6,1891
4,8300	5,6800	4,2082	7,9396	4,5900	5,8258	5,6635
4,8600	5,7300	4,5497	7,6134	4,8800	5,9939	6,3957
4,8900	5,8500	4,8004	9,6356	4,9900	6,1245	5,3625
4,8900	5,9300	4,4686	6,9265	6,4900	5,7318	5,6778
4,9000	5,9300	4,2597	7,2799	5,2300	6,3265	5,5283
4,9300	5,9800	4,3342	8,6864	4,6000	7,9411	5,9560
4,9400	6,0000	4,8026	8,1715	5,8800	6,6879	6,2283
4,9400	6,0100	4,4662	8,2343	6,7700	6,8814	6,8480
4,9600	6,0800	4,9392	7,2344	5,4500	7,2683	6,0485
5,0200	6,1000	4,4043	4,8844	5,6200	7,2288	5,0392
5,0900	6,1100	4,5101	5,8082	6,3500	4,2535	5,3028
5,1100	6,1400	4,8026	6,4608	6,7900	4,8195	4,1396
5,1100	6,1400	4,2082	5,8767	4,5100	7,9501	5,4456
5,1500	6,1900	5,2907	6,2024	6,0700	6,1136	5,4228
5,1600	6,4500	4,5959	4,7232	5,6600	4,9795	6,4516
5,1800	6,6700	4,3755	6,1658	5,6000	6,6301	4,6092
5,1800	6,7200	3,6924	4,5323	7,0600	8,4268	4,7936
5,2000	6,7800	4,3915	4,9590	4,9200	8,7167	6,0724
5,2100	6,8100	3,7566	8,3446	5,6700	7,1591	7,4018
5,2600	6,8500	5,2536	7,0842	5,3100	5,0068	6,7484
5,2600	7,0400	5,3433	7,9309	5,8600	6,7461	6,4182
5,2700	7,4600	4,8376	7,0585	5,3600	5,3076	5,9317
5,2900	7,7100	4,7143	6,1304	9,5300	5,6748	6,7404
5,2900	8,6000	4,7121	5,8598	5,8100	5,5291	8,1576
5,3900	4,2300	4,7173	7,3492	5,9900	6,8113	6,4379
5,4500	4,4100	4,6821	6,5491	5,6000	6,6418	5,7367
5,4600	4,5600	4,7608	7,3113	7,5200	7,5012	8,8450
5,5100	4,6300	5,7628	7,1834	5,8000	5,1502	8,9251
5,5800	4,6800	4,8233	7,3380	5,8200	6,0071	5,6694
5,5800	5,0000	5,1115	7,7077	4,2000	5,1814	6,0887

WT	*crb* insc	*crb* repo	*ed* insc	*ed* repo	*crb/ed* insc	*crb/ed* repo
5,5800	5,0100	4,4869	7,8349	6,5600	4,5434	5,7524
5,6400	5,1400	4,5137	5,6080	5,7600	5,6692	5,3672
5,6800	5,1400	3,8887	7,4317	6,6500	6,6906	6,6027
5,7000	5,1500	4,9233	7,2758	6,2500	5,7581	5,3549
5,7900	5,1600	4,8595	10,0876	5,4600	7,0215	7,3396
6,0600	5,2500	4,6422	7,3294	5,3000	5,5863	5,8828
6,1100	5,2600	4,9586	6,9444	5,2500	4,9891	5,3756
6,2400	5,3400	5,4769	7,8690	5,6900	7,9093	6,9312
6,4800	5,3700	4,8838	9,6694	4,9800	6,5643	5,8343
3,2100	5,3700	4,3612	7,9927	6,6900	4,5373	6,0564
3,5600	5,4100	4,8943	6,4908	4,4000	5,2590	6,4172
3,5600	5,4700	4,5779	7,1899	7,1400	5,9201	6,9906
3,6200	5,4900	4,2779	5,4989	5,2300	7,3052	4,8544
3,6300	5,5400	4,1110	6,0170	6,6200	5,5707	6,6164
3,8300	5,5700	4,5632	7,6260	4,6200	5,0782	6,9417
3,8500	5,5800	4,6931	6,4567	4,7800	5,2422	5,4461
3,9100	5,6400	5,0377	5,4174	6,3600	4,8543	5,5099
3,9500	5,6500	5,9123	7,4268	5,2300	6,3842	5,5880
3,9600	5,7200	5,2896	6,2009	6,2900	5,6284	5,5771
4,0000	5,8000	6,5621	6,8153	5,8300	5,2715	5,1530
4,0100	5,8600	4,8546	8,5784	8,2600	5,9907	6,5340
4,0100	5,9500	4,8521	8,7255	5,1900	5,3172	6,6514
4,0900	6,0500	4,6669	7,2746	5,2500	6,3576	
4,2000	6,0800	4,9713	9,3856	4,6500	4,8418	
4,2300	6,0800	4,1455	6,1725	7,3200	4,5607	
4,3000	6,1100	4,6880	8,6327	6,3400	5,8376	
4,3600	6,2000	5,6552	6,6040	6,0800	5,7640	
4,3900	6,2300	5,3927	6,9499	6,3500	5,8122	
4,4600	6,3000	5,0923	5,6190	5,4400	5,0311	
4,4800	6,3000	5,7908	7,2702	4,9500	4,6690	
4,5300	6,3500	5,1084	6,4838	6,7500	4,5174	
4,5900	6,4400	5,1695	5,2820	5,3300	4,7003	
4,6000	6,5100	5,1078	5,3320	4,7500	6,5028	
4,6000	6,5500	4,5635	7,9783	3,5900	5,1814	
4,6100	6,6000	4,4685	7,7827	6,2200	5,0555	
4,6100	6,6700	4,5978	5,3218	5,4900	4,5785	
4,6900	6,9300	4,7180	5,8744	6,4800	4,6576	
4,6900	6,9700	4,2199	4,8638	6,8600	4,6920	
4,7100	7,0000	4,2238	7,4320	4,6700	6,0286	
4,7700	7,0500	4,6593	6,1491	4,7500	5,3543	
4,7700	7,1000	5,1238	7,9138	5,3500	5,1790	
4,8200	7,2900	4,4641	6,0608	5,1300	5,9722	
4,8500	7,4200	5,4398	6,6188	5,0100	5,2952	
4,8600	7,5800	6,9660	7,6055	5,0000	6,8313	
4,9200	9,2200	4,6006	6,4571	5,6200	6,0554	
4,9400	3,8100	5,1809	7,6738	5,9700	5,3467	
4,9500	4,1800	5,6064	6,1795	7,0800	5,3014	
5,0900	4,3800	4,0172	9,8094	5,7300	5,5804	
5,0900	4,4500	4,4875	7,1893	6,5500	5,3197	
5,1100	4,4600	4,1300	6,6242	5,1300	4,8418	
5,1100	4,6300	4,7100	7,1064	4,9900	6,2829	
5,1400	4,7100	4,3600	6,2817	7,7700	6,0698	
5,2000	4,7400	4,1300	6,0478	6,4900	4,9836	
5,2400	4,7800	3,6200	10,6898	6,2300	6,3895	
5,2500	4,7900	3,0400	6,2224	7,1000	5,8228	
5,2800	4,8000	4,1100	5,9237	5,3700	6,0906	
5,3200	4,8200	5,3300	8,5564	4,5900	5,8775	
5,4200	4,9200	4,5400	5,9544	5,1700	5,7633	
5,4500	5,0600	3,8400	7,3246	5,2500	5,4387	
5,4800	5,0700	3,3400	7,3004	5,8500	6,2510	
5,4800	5,0800	3,7700	7,0598	5,3400	7,6409	
5,6900	5,1000	4,0200	6,2742	4,9300	6,6332	

WT	*crb* insc	*crb* repo	*ed* insc	*ed* repo	*crb/ed* insc	
5,7000	5,1300	4,0500	5,9276	5,6400	6,1549	
5,7200	5,1500	3,4800	10,3426	5,2400	6,3416	
5,8600	5,1900	4,5600	8,6766	7,9000	4,4328	
6,0200	5,2100	4,1900	7,8453	5,9800	5,1456	
6,2500	5,2500	3,8100	6,0224	6,1600	8,6860	
5,4100	5,3100	3,6700	5,9654	7,8000	4,9795	
4,2800	5,4300	5,2200	6,8582	5,7400	5,6156	
3,7700	5,4800	3,6300	7,2378	6,6200	6,9355	
3,3500	5,4900	3,8400	7,6292	6,2100	5,6620	
4,9700	5,5000	4,2800	6,9877	6,0300	6,0723	
3,0200	5,5200	3,8400	7,4811	5,3400	5,1797	
3,9600	5,5800	5,0400	7,2453	5,0600	5,9643	
2,9500	5,6600	4,8000	5,8907	6,6800	4,9120	
4,2400	5,6900	4,0800	6,0174	5,1500	4,8593	
3,2100	5,7700	4,3100	6,1045	5,7100	5,0359	
3,7400	5,8600	3,9000	7,8063	6,0700	5,5739	
4,3300	5,8700	3,7000	5,8752	4,7500	5,3308	
4,1800	5,9500	3,9900	6,1629	6,0000	4,3539	
3,5700	5,9900	4,1500	5,1325	6,2100	6,0017	
4,6300	6,0100	3,7000	6,8510	6,7600	5,8516	
4,0800	6,0400	3,9600	5,4681	5,5600	6,0001	
4,5400	6,0700	4,1400	6,6502	4,9300	5,1139	
4,1500	6,3000	4,3500	4,4665	5,4200	5,0172	
4,6600	6,3100	4,3000	4,8590	6,9800	5,2291	
3,9500	6,4800	4,2900	4,8840	5,3200	6,0718	
2,4800	6,5000	4,2200	4,6359	4,9900	6,4601	
3,7700	6,5100	4,9600	6,6464	5,5300	4,9002	
3,9200	6,9000	4,2800	7,9381	5,5300	6,3534	
5,0400	7,1900	4,0900	6,1599	4,9900	5,8174	
3,4100	7,2200	4,4200	8,8338	4,9700	5,9203	
4,3400	7,4500	4,5100	6,7184	5,1500	4,7659	
3,5100	7,5300	3,9700	6,2063	6,6000	6,0372	
3,2100	7,9600	3,7300	6,8426	5,4400	5,5754	
4,2000	7,9700	4,5200	6,3654	5,2100	5,5616	
3,6900	8,4500	4,7700	8,2302	5,2200	6,0923	
4,3300	8,6200	4,0600	6,9088	5,8400	8,6998	
5,0000	4,4000	4,3600	6,5827	4,9700	6,8055	
4,6600	4,4500	3,7600	7,1002	5,2100	6,1477	
5,2600	4,5400	4,2800	5,1092	6,6800	4,5361	
3,9400	4,6900	4,4900	5,9518	4,5100	6,2181	
4,1300	4,6900	4,9300	10,3499	5,6300	6,2140	
4,4000	4,7700	3,6400	9,3319	5,3800	5,7498	
3,6200	4,7900	3,9200	7,6102	6,2100	6,7539	
3,6200	4,8600	7,0900	5,4916	8,9700	8,6301	
3,5200	4,8700	4,8500	5,6967	5,7100	8,3225	
5,0200	4,8900	4,6700	6,5203	6,2200	5,8960	
3,0800	5,0200	3,5300	5,8664	5,6100	5,7750	
3,6500	5,0400	4,5200	7,0423	5,0900	5,5013	
3,9000	5,3200	5,0600	7,3346	5,1600	5,1797	
3,2200	5,3400	4,1700	6,0768	4,4369	5,6326	
3,9100	5,4200	4,2900	5,1288	6,3286	5,7096	
4,5300	5,4300	5,0000	6,1983	5,1190	5,0018	
4,0000	5,4600	4,8800	6,3742	5,0674	5,3342	
4,0900	5,4700	4,7000	7,7333	4,3622	5,3036	
3,5400	5,4900	5,0100	5,5539	4,7628	6,2894	
3,7800	5,4900	4,9700	6,0008	4,6131	7,5427	
4,0500	5,5000	4,8700	6,2633	3,7406	6,6411	
3,9600	5,5300	3,5200	7,2533	4,4466	6,2660	
4,6000	5,6600	3,8700	6,2922	4,4287	6,0754	
4,6100	5,6800	4,3700	6,0096	3,4978		
4,3100	5,7400	4,8200	6,9782	4,7309		
4,1800	5,7600	3,8400	8,6425	5,2999		

WT	*crb* insc	*crb* repo	*ed* insc	*ed* repo		
4,6600	5,8400	4,4500	7,3357	5,0076		
4,3600	5,8600	4,2400	7,9508	7,0540		
4,6200	5,8600	4,6600	6,3791	5,2656		
4,5500	5,8900	4,8500	7,0230	4,0872		
4,6000	5,9500	4,3700	7,8900	4,4806		
4,0500	6,0200	4,8800	6,3479	5,3513		
3,9600	6,1300	4,7800	6,2578	3,9851		
4,3700	6,3600	5,4600	7,7723	4,0078		
4,0700	6,4700	4,8200	6,5263	3,7905		
4,1400	6,5200	4,8400	6,6281	5,6007		
3,0300	6,5300	4,0800	5,2895	4,5736		
3,9400	6,5600	4,5600	5,9724	4,4831		
3,5800	6,6000	4,8400	6,2745	4,0789		
4,4400	6,6300	4,9900	6,4222	4,1779		
2,9400	6,6900	4,4100	7,6005	5,3645		
3,4600	6,9700	3,5500	9,6620	5,9067		
3,7400	7,3000	4,4900	8,1921	6,0563		
2,9300	7,3400	5,1400	5,7071	3,8000		
3,6900	7,9400	4,6600	6,9640	6,7221		
2,8100	8,0200	4,4900	7,7347	5,4643		
3,4300	8,1400	4,1300	6,1903	4,9515		
3,2200	8,4000	4,5300	6,7480	3,6447		
2,8900	8,5500	4,9700	7,6212	4,4033		
3,4800	8,5700	4,0800	7,7487	4,5630		
3,7900	10,0900	4,5100	6,3589	6,1331		
4,7900	4,4700	4,0000	7,5423	5,7437		
4,8000	4,4900	4,9700	6,4405	5,0879		
3,1600	4,5400	4,5000	5,4089	4,4677		
3,2600	4,7400	9,5800	5,2501	6,3368		
4,4000	4,8500	6,0700	7,0966	4,9895		
3,9700	4,9000	6,5100	7,0946	4,5266		
4,2900	5,0200	5,5900	7,6522	3,7846		
3,2800	5,0800	4,6700	8,4423	3,8000		
3,7800	5,0800	4,0200	6,3850	5,8640		
4,7000	5,2600	5,7000	12,4965	5,4105		
4,7400	5,2800	5,2100	6,3379	4,9868		
4,1800	5,3400	4,0900	5,5912	4,3664		
4,3100	5,3900	4,1500	7,2556	5,1068		
4,3300	5,4000	5,2300	6,8750	4,8553		
3,1300	5,4000	6,7000	7,0460	4,8333		
3,7600	5,4200	5,7900	5,7139	4,3411		
2,7600	5,4200	4,5600	6,1835	4,7173		
3,3300	5,4500	4,6500	6,2034	5,6768		
4,2100	5,4900	4,0800	8,5368	4,2571		
2,9300	5,5100	4,4900	8,7893	4,2254		
3,3300	5,5200	4,0800	6,2890	4,1190		
3,1400	5,5700	4,2700	5,2909	3,7710		
3,1500	5,6000	5,2800	9,0890	4,8319		
3,3300	5,6000	4,7600	8,7765	5,4592		
3,2000	5,6100	6,5600	7,3962	5,3645		
4,2700	5,6200	5,3000	9,1122	4,3719		
3,4500	5,6400	4,9000	6,4249	3,8244		
3,5000	5,7300	4,3600	6,2369	5,7462		
3,8300	5,7700	5,2200	6,0286	5,4965		
3,9200	5,8100	4,7700	6,4427	5,1370		
3,4500	5,8200	4,6100	6,5439	4,9755		
2,9100	5,8700	5,3400	6,8980	3,2435		
4,4300	5,9400	4,4900	5,9237	4,3660		
3,2800	6,0700	5,8200	5,1310	5,5049		
3,8300	6,1500	4,9800	5,7431	5,0734		
3,8100	6,2600	5,9000	5,6495	5,0683		
3,8300	6,4200	4,9000	6,1517	4,9713		

WT	*crb* insc	*crb* repo	*ed* insc	*ed* repo		
2,9700	6,4800	5,1200	5,3218	4,4316		
3,8800	6,6300	5,4300	5,9090	6,4476		
4,0100	6,6400	4,3200	6,4572	5,5839		
4,4500	7,0900	4,4700	8,8949	5,7170		
3,2200	7,2700	4,8700	6,6928	3,9634		
3,9600	7,3200	4,8000	6,2092	4,1730		
3,9100	7,3500	4,4900	5,4469	5,9967		
5,1800	7,7000	5,5300	6,3486	7,1641		
3,2900	7,8500	4,0700	6,4105	5,5839		
3,8500	7,8900	4,6200	5,9550	4,4813		
4,0800	8,2200	4,1000	6,6749	4,8856		
3,9800	8,4700	5,2900	5,1683	4,1538		
3,5600	10,5900	5,4500	6,6023	3,6670		
3,5800	3,9500	4,4700	7,7147	4,9982		
3,6800	4,5200	5,9000	8,0548	5,3333		
4,3400	4,5800	3,3200	7,3150	3,9504		
4,8000	4,6600	4,6900	8,8257	4,5600		
3,0900	4,7400	4,3100	6,2365	4,2646		
4,7400	4,7600	4,4600	6,6694	5,0249		
4,1400	4,7700	4,0400	5,3925	5,0977		
3,4700	4,8800	4,4000	9,9239	4,4206		
3,6900	4,8800	5,0200	6,8410	4,3601		
3,4300	4,8800	4,1200	6,8671	4,7509		
4,3200	5,0000	4,2000	6,3862	3,8069		
4,7100	5,0000	5,0100	7,7167	5,9406		
3,8600	5,0200	4,7000	8,2583	4,1220		
4,5800	5,0500	5,2300	9,2719	4,8998		
3,6800	5,0900	5,0100	6,8864	4,6038		
3,6700	5,2200	3,9800	5,7206	4,2221		
3,5400	5,2500	5,2900	6,3535	5,3986		
4,0200	5,2500	5,2100	8,2484	5,2417		
3,6200	5,2600	5,2200	8,2219	4,7509		
4,0800	5,2600	5,2300	10,7011	5,4570		
3,5100	5,3200	3,8800	8,7967	4,8390		
5,1000	5,3200	4,6000	8,2587	5,9540		
3,4900	5,3300	4,4100	8,2481	6,1606		
4,7100	5,3900	4,3500	8,0756	4,9171		
3,4300	5,4500	4,5200	7,0259	7,1558		
3,9100	5,4900	5,1600	6,5895	4,9105		
4,1800	5,5200	4,0800	6,6982	6,4928		
3,9900	5,5700	4,0900	7,0293	6,0224		
3,8700	5,5900	3,8000	6,7540	5,0732		
3,8900	5,5900	4,1900	5,6471	5,8970		
4,1300	5,6600	4,4500	5,5979	4,5334		
3,7700	5,6600	4,4400	7,4085	4,7497		
3,2300	5,7000	4,9300	7,3678	5,5302		
5,2100	5,7100	4,6200	5,5085	4,3363		
5,7800	5,7500	4,5300	5,1425	5,5057		
3,4600	5,7800	4,8700	6,7121	5,1779		
4,0100	5,8600	4,8600	6,9087	4,4372		
3,7700	5,8900	4,2700	4,8216	4,4880		
4,0500	5,9500	4,4200	6,5621	4,8619		
5,3100	6,0200	5,4100		3,5775		
4,3200	6,0500	4,4300		5,3254		
4,3500	6,0800	5,3000		4,9960		
4,8800	6,0900	4,0600		4,0514		
4,2700	6,2300	4,7000		4,4098		
4,1300	6,3100	4,4700		4,8123		
4,6500	6,5200	4,6000		4,0845		
4,1000	6,6300	4,5500		4,1096		
4,5400	6,8600	6,4800		5,0348		
4,4800	6,9000	4,3700		3,8006		

WT	*crb* insc	*crb* repo		*ed* repo		
3,9700	7,5600	5,2900		4,7887		
4,6900	8,0900	5,4200		5,7474		
4,4300	8,8900	4,2800		5,2483		
4,6400		5,3100		7,3309		
3,8100		3,8300		5,2158		
3,7600		4,1600		5,0798		
4,7400		4,4500		4,2389		
4,0600		4,5000		6,1231		
4,2300		4,0600		5,5054		
5,1000		5,3000		4,9275		
4,1000		5,8900		4,3300		
4,1000		5,7400		3,8055		
5,2300		4,1800		4,0204		
4,2300		5,0400		4,1387		
4,3500		4,7900		3,7259		
4,8600		4,5200		6,9315		
3,2700		4,7000		5,6051		
5,4900		3,5400		5,3460		
3,5800		4,2600		4,5074		
4,5100		5,2900		4,8678		
4,9300		4,3200		5,3003		
5,0400		3,7300		4,5462		
4,1500		5,2100		4,8407		
3,4700		4,8700		5,6350		
3,1500		4,4100		5,2893		
4,7800		4,7300		4,9810		
3,9100		4,5500		4,5058		
4,8200		5,6700		3,7708		
3,4800		4,4300		5,1396		
3,8100		3,7000		5,3539		
4,4900		5,0800		4,1979		
4,3500		4,1800		4,2756		
5,1900		3,9600		3,8910		
4,4600		4,0900		4,4474		
4,7900		5,7600		4,0620		
4,4300		4,9300		5,8455		
3,7900		4,0900		5,4834		
4,2700		4,6200		5,0654		
4,0500		4,0500		5,6275		
3,5900		3,8600		5,1156		
3,4900		5,2400		5,5952		
3,8100		4,8500		4,5937		
5,0900		5,0400		5,0115		
4,1300		3,9400		4,7798		
4,0000		4,9400		4,9224		
		4,3300		6,0084		
		3,7800		6,6301		
		4,3300		5,6745		
		5,7000		5,9949		
		5,4600		6,5015		
		4,5500		5,1723		
		4,3100		6,1171		
		4,7100		5,2035		
		3,6600		5,7142		
		5,9100		5,0445		
		4,9600		4,4653		
		4,1000		4,4999		
		4,6400		4,8372		
		5,0200		6,4305		
		5,9000		4,9488		
		4,7300		4,7433		
		3,5400		5,0040		

		crb repo		*ed* repo		
		3,6300		4,3740		
		4,1600		4,5506		
		4,3000		5,7381		
		4,0600		5,1975		
		4,5100		4,6598		
		4,4600		4,5424		
		4,5700		4,8622		
		4,6300		6,2840		
		5,5600		4,7328		
		4,3600		4,2425		
		4,3400		5,9638		
		4,0000		5,1450		
		4,8600		5,3458		
		4,6200		7,3449		
		5,9200		5,5170		
		4,5600		4,4767		
		5,2000				
		4,6900				
		5,4300				
		4,2200				
		4,6700				
		3,2900				
		4,0200				
		4,3600				
		4,1000				
		3,8800				
		4,6700				
		4,8700				
		4,2700				
		5,7500				
		5,3200				
		4,6900				
		3,9100				
		4,9600				
		5,9600				
		4,0500				
		4,5800				
		4,1600				
		4,0300				
		4,3700				
		4,5600				
		4,1100				
		4,3900				
		4,4000				
		5,0000				
		4,2900				
		3,9600				
		4,7500				
		4,4500				
		4,4700				
		3,1400				
		4,0800				
		4,4300				
		5,5200				
		3,7900				
		3,9300				
		5,6900				
		4,2100				
		6,1100				
		5,7800				
		3,3200				
		4,3200				

crb repo

		4,8500				
		3,4100				
		4,6800				
		4,0800				
		4,5300				
		5,4600				
		4,4800				
		4,6700				
		4,0400				
		4,2000				
		3,9100				
		5,4200				
		4,4600				
		4,9800				
		4,0400				
		4,4600				
		3,4600				
		4,8300				
		5,4100				
		5,0500				
		4,8900				
		4,7400				
		5,0400				
		6,6600				

8.2.22 UAS-*crb*

Ectopic crb causes decreased NSC growth and proliferation.
Quantification of NSC diameters in NSC-specific prolonged expression of crb or crb/ed at 24h ALH.

WT	UAS -*crb*	UAS -*ed*	WT	UAS -*crb*	UAS -*ed*	WT	UAS -*crb*	UAS -*ed*
9,4200	7,3500	6,4300	10,4500	7,0000	7,0100	7,6600	7,7900	8,8700
7,0900	6,6400	5,9100	8,2700	5,5400	8,0100	7,4700	7,5100	6,3000
10,8000	7,1300	7,5300	8,8900	8,0200	7,3000	8,2600	6,4800	7,5700
7,6300	5,1400	6,6600	10,9600	7,1800	6,2200	9,4200	7,8800	5,2200
8,0800	5,6900	4,9300	8,9400	6,1300	5,8200	7,0900	6,6400	6,6300
8,6200	8,9000	5,5300	8,2900	6,5100	7,8300	10,8000	7,2400	5,9500
9,9700	6,5500	6,4800	10,1700	7,8200	8,1100	7,6300	6,4200	6,0900
8,9900	5,6100	5,9800	9,4400	7,6700	7,4700	8,0800	7,1800	7,5700
6,6600	5,5400	5,5900	9,3000	7,1600	6,9000	8,6200	7,1700	7,4500
9,4600	5,4300	6,8100	9,2700	7,3600	7,3200		7,0900	8,8000
9,4100	5,3900	7,4700	9,6800	7,1600	8,1900		7,3500	5,0900
8,0000	6,3200	7,0300	9,3300	6,6900	7,4500		6,9700	8,0800
6,0800	5,5400	6,6500	8,0200	7,6900	7,9700		6,5600	5,6000
6,7000	8,3700	5,7200	8,7200	6,4400	6,7900		7,3700	7,3600
9,5000	7,2100	5,5400	8,5900	6,8100	6,9300		7,4900	6,5500
9,4800	8,3000	7,1700	8,3300	7,2400	6,5700		6,5500	8,1100
9,1100	6,4600	6,0100	10,1800	7,5400	8,8500		6,5700	7,8900
11,3100	6,6700	5,4000	9,4400	6,0800	7,5700		9,4300	7,1600
10,6300	8,0600	7,8700	9,9500	6,0900	6,7700		5,8200	7,6100
9,1200	6,9800	7,2700	9,8000	7,6900	5,7000		7,1000	7,1200
8,9600	7,4200	6,3400	7,1500	6,4300	6,8400			6,8700
8,1900	5,9400	8,0500	9,9900	6,1800	6,4900			6,5300
7,6300	7,8300	7,9600	8,2700	7,1000	8,0900			6,8900
8,7900	8,2000	7,1700	8,7700	7,5800	8,0200			6,6900
10,9000	6,7100	6,0900	7,1700	7,0700	7,8500			5,0800
9,4000	6,2500	8,3200	9,8000	6,5700	7,8400			5,9500
8,3000	5,2900	8,3200	9,8800	6,9000	8,5700			5,7400
8,5200	6,6000	7,8000	8,9400	5,8800	7,5400			5,6600
8,8400	6,3300	6,8100	9,3600	7,6300	6,3600			6,1400
9,1400	8,3900	6,5800	9,1400	7,9600	6,4300			7,7000
8,5000	6,2800	7,4700	7,7300	7,9200	7,6400			7,7900
8,2400	5,2800	8,1000	7,5500	8,6800	8,8700			6,5500
7,8500	4,9800	6,2000	9,4400	7,5800	8,9100			7,2200
10,0700	6,8100	7,2600	8,6600	7,6900	8,1100			7,2000
7,1500	7,6900	7,0000	9,5100	6,2300	6,5600			5,3000
8,3200	6,2200	6,1400	7,9700	6,7600	6,5600			7,9300
7,9600	5,7600	6,0800	10,3100	6,7300	9,5000			6,6800
10,5500	7,0400	5,9300	10,8400	7,5000	5,7900			6,8200
7,9700	6,8900	6,4000	8,8700	6,8700	7,0800			8,0200
8,0700	7,3900	7,2000	10,0200	7,3700	6,8100			5,4100
8,2400	6,2600	6,4500	9,0100	6,9500	6,4300			7,0800
10,2800	6,2800	8,1400	9,7600	6,1700	8,1600			
8,8000	7,0900	6,6200	8,4000	6,3100	7,1200			
8,4000	7,4400	6,2800	7,6200	6,0000	7,3400			
9,6500	7,1700	6,8700	9,1900	9,0900	6,2500			
7,8000	4,9000	6,6100	9,6500	6,1100	7,3100			
8,4100	6,2800	6,1400	8,1300	7,5100	7,0900			
6,0700	9,3500	5,7100	9,1200	8,8400	7,3100			
7,6300	6,8300	7,3400	9,0700	6,6500	8,8100			
7,9400	5,7900	6,3100	8,7900	7,0600	8,1500			
9,5600	6,1900	7,1300	8,4100	8,7200	8,0900			
8,5600	6,5800	6,8600	10,0100	7,8100	6,4500			
9,1200	7,1100	7,3000	8,2400	8,7300	7,5100			
8,9800	6,7300	8,5400	10,1200	7,2800	5,0600			
8,6900	7,1500	6,9300	9,6600	6,5800	5,0200			
8,6400	4,9000	5,7900	8,8000	6,5400	7,7200			
9,0500	6,2700	5,8000	9,0800	7,4400	8,4100			
8,5400	8,1400	6,7500	10,4300	7,7500	6,4200			
9,2000	6,7100	5,4600	8,6900	5,9000	7,4400			
9,1400	5,0100	7,5500	8,8300	8,7200	7,3200			
10,7100	6,4800	7,8000	10,0000	6,9900	6,2600			
7,1200	6,5800	8,1600	8,4900	7,2800	6,2000			

8.2.23 *tsh*-RNAi

The transcription factor Tsh is necessary for the reactivation of larval NSCs.
Quantification of NSC diameters in *tsh*-RNAi and wild type brains at 48h ALH.

WT	*tsh*-RNAi	WT	*tsh*-RNAi		*tsh*-RNAi
13,5776	6,7215	11,7484	7,0803		8,1962
12,0335	6,0081	12,6486	7,9556		8,0817
11,4811	6,5756	10,8137	5,5964		5,0282
10,0315	5,3544	10,9285	6,1730		6,9580
10,5523	4,3163	11,1489	6,2825		6,7230
11,1578	5,0752	13,1009	7,3972		5,9484
14,3201	6,6990	10,5868	7,1946		6,8458
8,5032	5,2669	11,2838	6,7540		7,9728
10,4856	4,9311	10,7079	7,0882		6,3238
13,4831	4,9693	11,5020	6,8424		6,1399
12,3798	5,3306	13,7817	7,7629		6,1741
15,4562	4,4984	12,3002	7,9514		6,8917
10,8084	5,6231	9,7779	5,4487		5,9715
10,4915	4,5539	12,6025	7,0614		6,5029
12,7616	5,0082	11,8922	6,8874		6,7391
11,3211	3,8761	10,4259	9,5355		6,5060
9,9878	4,3473	11,5123	6,8098		7,4305
13,5994	5,8890	12,6293	7,3579		7,9933
9,1829	5,2873	12,4464	7,4839		5,4160
9,2713	5,5795	15,3499	7,6883		6,2723
10,9270	5,8137	14,8898	6,9325		6,5060
11,6649	6,0352	13,2253	6,9534		6,5276
13,3995	5,8841	13,9676	7,2204		6,0864
13,3821	7,7501	13,9497	6,1933		6,9894
11,7692	7,9261	13,1958	6,2683		5,5393
11,9119	4,7787	13,8043	6,4676		6,5824
11,7134	5,6074	9,0964	6,7897		5,8112
12,3659	6,5749	10,7268	7,8297		5,1317
7,2107	6,3909	12,5996	7,2050		
9,4138	5,7257	11,7833	6,1933		
13,2442	5,0634	11,7382	7,6546		
12,0943	5,6091	13,7874	7,3670		
8,7396	5,5782	11,5372	6,9325		
10,4856	6,2381	11,7289	5,9033		
10,6098	5,5795	13,1437	6,1346		
11,5029	5,9533		6,3311		
8,9192	5,8170		6,1187		
10,8329	5,1212		7,6108		
11,4185	5,7278		5,2885		
10,5513	4,0353		7,4705		
8,5974	4,9253		5,8428		
12,7603	5,9521		6,2992		
12,1432	6,4376		6,8081		
10,6996	5,9517		6,7581		
12,6782	7,0038		6,2006		
11,6595	6,3909		5,4478		
11,7125	5,5576		5,7470		
10,3599	4,2639		5,4290		
12,4435	5,2569		7,7971		
11,6956	5,3985		6,6588		
12,8747	5,5234		6,9235		
10,1207	5,5233		7,3990		
13,2253	7,5594		6,4387		
12,9713	6,3949		6,7685		
10,6743	5,9325		7,5708		
10,7074	5,7626		7,3035		
10,6177	7,2185		6,4628		
9,4798	6,4153		6,3588		
9,3867	7,6236		5,6625		
11,7395	6,6371		6,0729		
11,7249	6,9694		6,8334		
11,1787	6,1906		5,5477		

8.2.24 *tgi*-RNAi

Loss of Tgi in NSCs leads to premature reactivation.
Quantification of NSC diameters at 4h ALH.

WT	*tgi*-RNAi	WT	*tgi*-RNAi	WT	*tgi*-RNAi	WT	*tgi*-RNAi
5,6510	7,3545	4,6625	7,0542	4,4123	8,0066	4,6182	5,7104
5,0154	8,5701	4,6351	9,8688	4,8218	5,7889	3,7210	6,7375
5,4678	7,8930	4,5875	5,8535	4,6678	7,3611	4,5120	5,8424
4,6553	7,5952	5,9611	6,9740	3,8573	8,0852	3,9663	6,6436
5,7829	9,7946	4,9994	8,8834	4,1665	8,2979	3,9974	6,5099
3,9640	7,6497	4,9283	6,4991	3,4689	8,1411	3,8044	5,8692
5,1455	10,3574	3,9219	8,0687	4,9430	8,3317	3,3998	6,6028
5,7059	5,7461	5,4898	7,1553	4,1268	6,0910	3,6773	6,5380
5,2109	7,0157	3,9733	7,3948	5,1287	6,5098	4,0989	6,2266
3,9307	8,3065	4,8662	6,9279	4,3725	7,5997	4,1184	7,0331
5,9027	7,6055	5,2606	7,5254	3,6955	4,9644	4,5246	5,7811
3,9663	8,0645	4,7199	6,9117	4,1117	5,7002	4,1473	5,8577
4,6599	8,1615	5,1494	5,9087	4,3734	6,7731	3,5802	6,0458
4,8850	9,0215	5,1902	7,2807	3,1852	6,5060	3,7283	5,2010
4,3660	9,0257	5,3378	6,3707	4,6157	5,8702	4,7446	5,1958
4,7300	8,2320	4,8771	5,4273	4,1628	6,8305	4,8619	6,8621
5,2312	6,2767	3,8134	5,8241	5,0177	6,5597	3,9211	6,7037
5,7994	6,8494	4,1486	5,6414	3,8722	6,4283	2,9527	6,0845
5,4295	6,9562	6,2407	5,5401	4,1823	6,5982	3,8093	5,3837
4,8410	8,6195	5,0714	6,5499	4,8668	7,2399	4,3111	5,2533
6,0664	8,5897	3,9760	6,7835	4,9743	6,3932	4,3912	6,6502
5,7192	6,6518	5,1225	6,0375	4,4533	5,4430	3,7266	4,9223
4,1255	7,6872	5,5176	5,3470	5,2886	5,9082	3,5905	6,1429
4,8135	5,4222	5,2545	6,1086	4,9804	7,0194	3,5215	7,0238
4,4393	5,6573	7,1379	6,6548	4,7955	11,5802	4,3123	6,9243
4,6996	6,4728	5,7774	6,5330	4,1268	8,8651	4,1165	5,4353
5,2868	7,2866	3,8991	6,1483	4,0093	8,6079	4,9826	6,3379
7,0995	6,4709	8,6833	5,0584	4,2975	5,6439	4,2637	5,5172
5,0146	6,0872	4,9326	7,8596	4,2853	6,5654	3,9048	7,2007
5,4658	8,4637	4,6092	5,0557	4,0849	7,6009	3,3119	7,3426
4,7747	6,6720	5,9074	5,5369	3,9276	9,5273	4,1046	6,5316
5,0418	6,6292	6,5178	4,9344	4,8011	6,7416	4,6280	6,5892
8,2492	6,1658	5,6779	6,9248	5,4074	5,4874	4,1312	6,9352
4,2535	6,9657	4,2042	6,1024	4,8059	6,6069	4,9930	6,3574
4,3118	6,6061	4,1289	5,0420	4,3950	5,0669	5,7192	6,4228
5,1391	6,0123	5,6353	5,8961	5,0555	5,9231	3,9072	6,5547
4,3287	5,9502	4,7303	5,4722	4,0905	6,1476	4,4340	7,1365
4,6897	5,3759	6,1994	8,1562	5,0519	7,0982	4,3949	7,3423
5,3380	6,0040	4,2817	6,6897	4,9723	6,8817	4,3637	7,1339
4,3146	6,0949	7,3958	6,4935	4,9050	5,0618	3,5890	6,7771
6,0559	6,0749	5,0859	7,2102	4,6051	7,3313	4,4041	10,9457
5,5779	5,5475	4,0319	5,4507	5,1196	6,0616	4,0225	11,3423
4,9541	5,7711	3,7540	7,6678	5,2660	6,5563	4,5204	10,4463
4,8237	6,4925	3,7479	7,9498	6,1425	6,4946	4,5558	7,0731
3,9032	6,2067	4,4914	7,5048	5,0229	10,1253	4,1304	9,2279
4,4488	5,4227	3,9156	7,6108	5,8155	6,5758	3,9030	7,2472
4,4694	5,4606	4,3655	6,7492	4,3190	9,5082	4,2052	8,1476
3,7175	6,2340	4,1637	6,1479	4,9648	6,4083	4,0455	8,0058
4,0106	5,5486	4,3177	7,2964	5,2662	5,0583	3,7199	7,8821
4,6505	6,6236	4,3314	6,7247	4,6250	5,7418	3,5342	9,6307
4,8771	7,7464	4,4950	7,1013	4,9011	7,2874	3,8596	7,9531
4,1639	7,1104	4,2003	7,7625	4,0623	5,0419		
4,3398	7,5338	4,0311	6,9118	4,4273	6,3460		
4,4270	6,6130	4,1699	6,7493	3,2799	5,8330		
4,9578	5,8892	4,8574	7,6168	4,2003	6,1241		
3,7812	6,6941	5,0564	9,1203	5,2863	6,1657		
5,3999	6,4372	4,1268	11,3157	5,1069	6,9221		
3,7392	6,0733	4,8987	7,6733	5,1366	5,3924		
4,6880	5,4303	4,1658	10,3245	4,9677	7,0967		
4,7376	6,6294	6,1965	9,7909	4,1388	5,9298		
4,5164	7,9675	5,8020	8,7061	5,1481	6,0348		
4,7502	8,7649	4,1490	7,9732	5,3934	7,6049		

8.2.25 dm4 mutant

dMyc is necessary for NSC reactivation.
Quantification of NSC diameters of wild type brains and dm4 mutants 4h ALH.

WT	dm4	WT	dm4		dm4
8,9700	2,7900	10,7074	4,9500		6,0000
9,4600	3,5100	10,8919	4,9600		6,0000
7,7900	3,5800	10,7620	4,9700		6,0100
10,1100	3,6000	9,8790	4,9800		6,0300
10,2200	3,6000	11,0193	4,9900		6,0300
8,8700	3,8200	12,4351	5,0000		6,1200
10,1000	3,9100	12,6148	5,0100		6,1200
8,3000	3,9500	9,3061	5,0300		6,2900
8,5900	4,0000	12,0516	5,0400		6,3300
10,6600	4,0000	10,2504	5,0500		6,3300
10,3400	4,0200	14,1386	5,0500		6,3700
8,9400	4,0200	10,3213	5,0600		6,3900
11,8500	4,0300	9,8663	5,0700		6,4100
10,9200	4,0800	9,2480	5,0800		6,4800
10,8700	4,1100	12,4030	5,0900		6,5300
10,1300	4,1100	11,7713	5,1100		6,5500
9,4600	4,1200	12,8585	5,1200		6,5600
10,7700	4,1400	10,7673	5,1300		6,5600
8,2500	4,1700	11,2889	5,1400		6,5800
9,1700	4,2000	11,9013	5,1800		6,5900
8,9600	4,2100	11,9579	5,1800		6,6500
8,2800	4,2400	11,4728	5,1900		6,6700
9,3600	4,2600	11,5404	5,2000		6,6700
11,3800	4,2900	10,1080	5,2100		6,7200
8,0600	4,3100	12,8512	5,2200		6,7700
10,6500	4,3100	12,9388	5,2500		6,8200
8,9900	4,3200	11,7221	5,2700		6,8400
10,7900	4,3300	10,5184	5,2900		6,8600
10,2900	4,3300	10,4456	5,3400		6,8800
10,0300	4,3500	14,6247	5,3600		6,9900
11,2300	4,3600	10,7228	5,3800		7,0000
8,6600	4,3700	7,1607	5,3900		7,0700
10,5500	4,4400	13,4523	5,4200		7,0700
7,9500	4,4700	13,9427	5,5000		7,0800
9,3300	4,5200	11,1732	5,5100		7,0900
9,9100	4,5200	12,2900	5,5300		7,1100
11,2900	4,5500	11,3803	5,5300		7,1500
12,6300	4,5600	12,5081	5,5300		7,1600
10,1600	4,6200	11,9624	5,5700		7,1800
6,4700	4,6400	8,4032	5,5900		7,3000
7,5900	4,6400	9,0369	5,6100		7,4100
10,3400	4,6600	8,2520	5,6400		7,4400
11,6200	4,6700	8,8360	5,6500		7,4700
10,6200	4,7100	7,9064	5,6600		7,4700
10,6400	4,7200	10,6548	5,6600		7,5500
13,2700	4,7200	9,2801	5,6800		7,6200
11,1900	4,7400	11,3332	5,6900		7,7000
11,5000	4,7500		5,7000		7,7700
11,2300	4,7500		5,7500		7,8800
12,5400	4,7600		5,7500		7,8800
11,2400	4,7800		5,7600		7,9600
10,4800	4,7800		5,7800		8,1700
13,7500	4,8000		5,7800		8,3200
11,0600	4,8100		5,8000		9,2800
9,8600	4,8400		5,8300		11,1500
12,3100	4,8900		5,8800		
10,5700	4,8900		5,8900		
8,3003	4,9100		5,8900		
10,0354	4,9100		5,9200		
8,0488	4,9100		5,9300		
10,9906	4,9200		5,9700		
8,2503	4,9400		5,9800		

8.2.26 UAS-*dmyc*

Overexpression of dMyc is sufficient for NSC reactivation.
Quantification of NSC diameters of wild type type brains and UAS>*dmyc* brains at 4h ALH.

WT	UAS -*dmyc*	WT	UAS -*dmyc*	WT	UAS -*dmyc*		UAS -*dmyc*
4,3954	8,8891	4,6974	9,2594	4,2758	8,0493		6,5631
4,2092	8,3792	3,9786	8,2390	4,4637	8,0990		5,8045
4,5346	10,2349	5,3572	7,5077	4,1918	6,4125		7,4655
3,9033	8,1599	3,4241	8,1769	3,9848	7,9732		7,9311
4,6830	9,1729	4,2223	8,2348	4,1849	11,0470		7,6355
4,8371	9,7184	4,6250	9,9491	3,7800	7,1812		6,5439
4,7117	8,7862	3,8761	11,0675	4,5154	7,9078		9,4356
4,1644	6,4481	4,4013	8,7530	4,3863	11,2324		8,4515
4,2708	7,9125	4,5189	9,8720	3,0161	9,1120		7,5552
4,6974	9,2355	3,7623	8,8393	4,1163	7,4284		8,4040
4,5699	10,3532	5,2262	6,9220	4,0230	7,3591		6,6143
3,6577	10,7347	4,0701	6,8388	3,9874	10,1234		6,8912
3,9497	8,5687	4,0855	7,9836	3,3943	7,4348		8,6209
3,9305	7,0166	3,9377	7,4685	4,5289	6,4235		5,2349
4,6724	9,1098	4,1681	9,0084	3,2566	6,8328		
4,1413	7,9898	4,0866	7,9616	3,5477	7,2062		
3,7954	8,5277	4,1274	8,4358	3,8053	6,4236		
4,4283	9,9992	5,8613	7,6707	4,0450	7,8488		
4,0601	8,1020	4,2668	8,2399	4,3212	6,2396		
3,8995	10,7824	4,2668	5,9024	4,0881	6,8852		
4,7675	10,2107	6,9891	8,1214	4,4739	5,4411		
6,0847	7,9194	5,1455	8,2888	3,8610	6,9837		
7,1788	8,2378	4,6674	9,2385	5,2945	7,2357		
5,1665	7,4829	5,1847	7,2949	4,5697	6,4962		
4,8483	6,6691	4,6974	7,2390	4,0853	6,0443		
5,1455	7,2397	6,7680	6,6691	3,5607	7,9675		
4,0656	7,6297	3,9944	7,2396		10,1047		
4,7367	7,5119	4,4352	6,3722		8,0358		
4,9813	7,4478	4,7432	9,7214		9,7194		
5,9194	6,7277	4,5129	9,2385		8,7905		
6,4456	7,8337	4,9602	9,9617		10,3953		
5,1728	6,2395	4,4360	7,3663		6,5520		
3,7263	7,9915	3,9477	6,8723		12,2057		
5,6928	7,8362	4,4602	7,2378		10,4643		
6,2041	7,3074	4,1293	7,6803		5,8436		
5,3235	7,1639	4,4909	6,2461		8,6985		
5,8033	6,2379	5,2314	7,2346		6,7574		
5,7479	7,2467	5,9146	6,6124		6,1770		
4,7630	8,6879	4,7748	8,7829		8,6925		
4,2244	6,9432	4,0904	10,3637		6,9579		
4,6038	5,2687	4,6541	10,7723		10,3049		
4,4937	5,7288	4,1358	11,5793		6,2780		
5,4480	6,6601	4,0081	11,7833		6,1203		
4,4602	6,2385	4,0856	11,1029		7,8290		
6,6146	5,2766	3,5354	7,5455		9,0408		
5,1569	7,4116	2,8889	9,2784		6,9396		
4,3172	7,0468	4,4584	8,5480		9,8138		
4,6483	5,7187	3,5884	8,1136		9,2397		
5,1016	6,7490	4,2596	7,3795		10,4478		
8,2224	9,0516	4,0119	8,2390		5,7239		
4,2813	7,4238	3,9508	9,9749		9,6783		
4,3305	8,3988	3,1893	7,7333		10,1656		
4,2143	9,6120	3,8971	7,4390		10,8235		
3,8105	7,2840	3,6361	7,0812		8,5900		
4,6981	9,8402	3,9159	9,7018		8,3480		
3,8025	10,7148	3,9138	7,2594		5,9406		
4,0102	9,3168	3,6341	9,1751		6,6418		
4,8042	8,2380	3,8842	7,4192		8,1060		
4,4067	7,8617	4,1952	8,3861		9,5684		
4,4555	8,2276	3,5430	6,3087		5,9716		
4,1121	12,2385	3,8449	6,8806		8,8537		
4,4602	9,4603	4,7059	8,9608		8,4568		

9. Curriculum vitae

Name: Rouven Marian Metternich (geb. Ding)
Birthdate: 10.01.1987
Birthplace: Wolfsburg
Address: Robert Schumann Straße 3, 65428 Rüsselsheim
Nationality: German
Phone: 0176/84307136
E-Mail: dingr@uni-mainz.de / rouven-ding@web.de

Education:

1.12.2012 – 30.04.2016	Conferral of a doctorate at the Institut of Genetics, Johannes Gutenberg University Mainz
1.04.2010 – 12.10.2012	Main studies of biology at the Johannes Gutenberg University Mainz (GPA: 1.3) Diploma thesis: Identification h*tid* promoter DNA Binding proteins
1.10.2007 – 3.3.2010	Basic studies of biology at the Johannes Gutenberg University Mainz (GPA: 2.0)
2003 – 2006	Gymnasium Kreuzheide Wolfsburg, Germany
1999 – 2003	Gymnasium Vorsfelde, Germany

Awards:

- PhD Fellowship from the Stipendienstiftung Rheinland-Pfalz

Qualifications:

- Ability to coordinate working processes
- Supervision of students (Bachelor, Master)
- Self dependent intercourse and exchange of information with co-operation partners
- German Armed Forces

Past experiences:

- Max Planck Institut for brain research, Frankfurt
- University medicine Mainz, Institute of Immunology
- University medicine Mainz, Institute of medical microbiology and hygiene

Language skills:

- German (native speaker)
- English (Fluent)

PhD Thesis: Titel „ The SWH signalling as a key regulator for the maintenance of NSC quiescence in *Drosophila melanogaster* “

Methods:

- Immunhistochemistry
- Polymerase Chain Reaction (PCR)
- Gel elektrophoresis
- Quantitative Real-Time PCR (qPCR) / ddPCR
- Taqman Assay
- Western Blot
- Luciferase Assay
- Handling of confokal laser scanning mikroscopes (Leica TCS SP5, TCS SP8)
- Fluorescence Activated Cell Sorting (FACS)
- Cell culture with human and *Drosophila* Cells
- Cloning and production of expressionvectors
- Computer based analysis of neural Stem cells (Leica LAS AF Lite)
- Handling of statistical - and data anaylsis software (Adobe Photoshop CS4, Adobe Illustrator CS4, SigmaPlot 11.0)
- Dissection of diverse tissue types (*Drosophila melanogaster*)
- Transplantationsexperiments of genetically modified tissue

Publication at Nature Communications Titel: **The Hippo Signaling Pathway maintains Quiescence in *Drosophila* Neural Stem Cells**

Publication at Cell Cycle Titel: **Hippo pathway regulates neural stem cell quiescence.**

Mainz, den _____ _____

(Unterschrift)

FACHBEREICH BIOLOGIE DER JOHANNES GUTENBERG-UNIVERSITÄT MAINZ Nr. /20

Zusammenfassung der Dissertation von: Rouven Marian Metternich

Thema: The SWH signalling as a key regulator for the maintenance of NSC quiescence in *Drosophila melanogaster*

One of the challenging questions in recent stem cell biology is how stem cell behavior is regulated and how the balance between proliferation and quiescence is regulated, since deregulation of the proliferative capacity can lead to tumour formation or premature depletion of the progenitor pool (Knoblich, 2010; Cheung *et al*., 2013). To analyse one aspect of this key developmental process I studied the neural stem cells (NSCs) of the fruit fly *Drosophila melanogaster*. During my PhD work, I have made two important findings. First, the SWH signalling pathway is an important regulator of overall organ size control of the *Drosophila* CNS during larval developmental stages. The functional analysis of diverse components of the SWH pathway revealed that this signalling module is necessary for the correct maintenance of *Drosophila* NSC quiescence between embryonic and larval stages of development. Using the RNAi approach, I have identified various intracellular and extracellular regulators and downstream targets of the SWH signalling pathway in NSCs that play important roles in modulating the activity of this pathway during early larval stages. The transcriptional outcome is regulated by the main effector of this pathway, the transcriptional co-activator Yorkie (Yki), whose activity depends on DNA-binding transcription factors, like Teashirt (Tsh) (Goulev *et al*., 2008; Wu *et al*., 2008; Peng *et al*., 2009). The finding that the known Yki interaction partner Tsh (Peng *et al*., 2009) is differentially expressed in distinct NSCs across the CNS, leads to the hypothesis that Yki regulate the expression of its target genes in a cell type specific manner. The second finding revealed a highly sophisticated niche signalling to be necessary for the correct regulation of NSC quiescence. This microenvironmental signalling requires so called niche glial cells, which form the neurogenic niche in the CNS of *Drosophila melanogaster*. The processes of these glial cells as well as the NSCs itself express transmembrane proteins Crb and Ed that activate the highly conserved SWH signalling pathway in NSCs to maintain quiescence and suppress inappropriate cell growth and proliferation during this developmental stage. Taken together these data strongly suggest that *Drosophila* NSCs depend on extrinsic cues from the surrounding stem cell niche to tightly control the balance between proliferation and quiescence. Adding these far-reaching effects of the SWH pathway concerning stem cell biology and organ size control with the fact that this pathway in highly conserved, makes it a promising factor for putative cancer therapies and regenerative medicine. By way of example it was shown that the human homologs of Yki namely YAP/TAZ have the ability to reprogram terminally differentiated cells into their corresponding, tissue-specific stem cell (Panciera *et al*., 2016). As part of this effort the results of my PhD thesis shed some light on the involvement of the SWH pathway on the regulation of the activity pattern in *Drosophila* NSCs.

Genehmigt vom 1. Gutachter / Gutachterin _____

(Unterschrift)

VERSICHERUNG

für das Gesuch um Zulassung zur Promotion in den Fachbereichen 17 – 22 der Johannes Gutenberg-Universität Mainz

Name: _____

Hiermit versichere ich gemäß § 11, Abs. 3d der Promotionsordnung vom 22.12.2003:

(zutreffendes ist angekreuzt.)

☐ Ich habe die heute als Dissertation vorgelegte Arbeit selbst angefertigt und alle benutzten Hilfsmittel (Literatur, Apparaturen, Material) in der Arbeit angegeben.

☐ Ich habe oder hatte die jetzt als Dissertation vorgelegte Arbeit nicht als Prüfungsarbeit für eine staatliche oder andere wissenschaftliche Prüfung eingereicht.

☐ Ich hatte die heute als Dissertation vorgelegte Arbeit als Prüfungsarbeit für folgende Prüfung eingereicht:
Bezeichnung der Prüfung: _____

Prüfungsstelle: _____

☐ Ich hatte weder die jetzt als Dissertation vorgelegte Arbeit noch Teile einer Abhandlung bei einer anderen Fakultät bzw. einem anderen Fachbereich als Dissertation eingereicht.

☐ Ich hatte die folgende Abhandlung mit nachstehenden Ergebnis eingereicht: Titel

der Abhandlung:

_____

Fakultät bzw. Fachbereich und Hochschule:

_____

Ergebnis bzw. Beurteilung: _____

Mainz, den _____ _____

(Unterschrift)